Sulfate radical based oxidation in water treatment

Dissertation

zur Erlangung des akademischen Grades eines
Doktors der Naturwissenschaften
– Dr. rer. nat. –

vorgelegt von

Holger Lutze

geboren in Geldern

Institut für Instrumentelle Analytische Chemie
der
Universität Duisburg-Essen

2013

Die vorliegende Arbeit wurde im Zeitraum von April 2008 bis Juli 2013 im Arbeitskreis von Prof. Dr. Torsten C. Schmidt am Institut für Instrumentelle Analytische Chemie der Universität Duisburg-Essen durchgeführt.

Tag der Disputation: 20.12.2013

Gutachter:	Prof. Dr. Torsten C. Schmidt
	Prof. Dr. Urs von Gunten
Vorsitzender:	Prof. Dr. Elke Sumfleth

Abstract

In the past years sulfate radicals ($SO_4^{\bullet-}$) are increasingly discussed as an oxidizing agent for pollutant degradation in water treatment. Indeed, $SO_4^{\bullet-}$ has some unique features, such as being a very strong electron acceptor enabling the degradation of recalcitrant compounds which are refractory towards the strongest oxidant used in water treatment, i.e., the hydroxyl radical ($^{\bullet}OH$) which is formed in advanced oxidation processes (AOPs) (e.g., ozonation or photolysis of hydrogen peroxide (UV/H_2O_2). One example is perfluorinated carboxylic acids (PFCAs), which can, albeit slow, be degraded by $SO_4^{\bullet-}$, but persist in AOPs. However, important aspects related to $SO_4^{\bullet-}$ based water treatment such as energy demand and by-product formation, are hardly discussed in current literature. This point is targeted by the present study.

The influence of the water matrix on $SO_4^{\bullet-}$-based oxidation has been investigated by monitoring the behavior of model pollutants in a $SO_4^{\bullet-}$ based process. It could be shown that for two types of natural organic matter (NOM) (humic acids extracted from Leonardith layers and Suwannee River NOM) degradation of pollutants by $SO_4^{\bullet-}$ is ≈ 2-3 fold more effective than by $^{\bullet}OH$. This indicates that $SO_4^{\bullet-}$ reveals a smaller reaction rate towards NOM compared with $^{\bullet}OH$. However, some pollutants react much faster with $^{\bullet}OH$ than with $SO_4^{\bullet-}$ (e.g., *tert*-butanol: $k(^{\bullet}OH) \approx 10^8\ M^{-1}\ s^{-1}$, $k(SO_4^{\bullet-}) \approx 10^5\ M^{-1}\ s^{-1}$), counterbalancing this effect.

In the next step formation of undesired by-products was investigated. One important by-product is the potential cancerogenic compound bromate (BrO_3^-) (EU- and US-EPA drinking water standard 10 µg L^{-1}), that can be formed in ozonation. It was shown, that BrO_3^- is also formed in presence of $SO_4^{\bullet-}$ in pure water containing Br^-. However, very little amounts of organic matter effectively inhibit BrO_3^- formation. Hence, a $SO_4^{\bullet-}$ based process could principally be used as substitute for ozonation if BrO_3^- formation cannot sufficiently be controlled in the ozone based process.

The presence of Cl^- and HCO_3^-/CO_3^{2-} has far-reaching consequences on $SO_4^{\bullet-}$ based processes. $SO_4^{\bullet-}$ reacts fast with Cl^- ($\approx 10^8\ M^{-1}\ s^{-1}$). Thus, if Cl^- is present in the mM range a large fraction of $SO_4^{\bullet-}$ is involved in oxidation of Cl^- yielding chlorine atoms ($Cl^{\bullet}$). In presence of water $Cl^{\bullet}$ rapidly forms $^{\bullet}OH$ and Cl^-. Hence, $SO_4^{\bullet-}$ are converted to $^{\bullet}OH$ and the $SO_4^{\bullet-}$ based system turns into a conventional AOP. However, the fast reaction of $Cl^{\bullet}$ plus HCO_3^- competes with the turnover of $Cl^{\bullet}$ into $^{\bullet}OH$, thus diminishing the oxidation strength.

The reaction of $SO_4^{\bullet-}$ plus PFCAs has drawn a lot of attention on $SO_4^{\bullet-}$ as a potential water treatment agent. It has been proposed in the literature, that PFCAs are degraded by $SO_4^{\bullet-}$ in a step-wise process, that is, the primary product per radical attack is a PFCA shortened by one CF_2-unit, at $S_2O_8^{2-}$ doses in large excess over PFCAs (≈ 50 fold). This process, finally leads to complete mineralization yielding F^- and CO_2. The present study revealed, that at low $S_2O_8^{2-}$ concentrations (2 fold excess over PFCA) another reaction pathway sets in, leading to simultaneous formation of PFCAs shortened by up to 4 carbons. Interestingly, the fluorine balance (fluoride plus fluorine bond to PFCAs) was not complete in case of PFCAs with carbon chains > C_5. That suggests the formation of products which have not been described in the literature yet. However, the rate constants of the reaction $SO_4^{\bullet-}$ plus different PFCAs (C_2-C_8) are very small ($1\text{-}4 \times 10^4\ M^{-1}\ s^{-1}$) indicating that large amounts of energy are required for their degradation. Furthermore, perfluorinated sulfonic acids (PFSAs) are not degraded at all.

The present work has shown, that $SO_4^{\bullet-}$ can principally be used as an oxidant in water treatment. However, $SO_4^{\bullet-}$ based processes are strongly affected by the presence of main water constituents, i.e., Cl^- and HCO_3^-, which can largely affect reactions occurring in the water matrix and the efficiency of pollutant degradation. A reasonable application of $UV/S_2O_8^{2-}$ probably is restricted to boundary conditions such as low Cl^- concentration in the source water. Such kind of source waters can especially be found in areas of low population density and little industrial activities. With regard to perfluorinated compounds, however, it is questionable if a $SO_4^{\bullet-}$ based water treatment process represents a feasible tool for their degradation.

Zusammenfassung

Seit einigen Jahren wird der Einsatz von Sulfatradikalen ($SO_4^{\bullet-}$) als potenzielles Oxidationsmittel in der Wasseraufbereitung diskutiert, welches z.B. bei der Photolyse von Peroxodisulfat ($S_2O_8^{2-}$) entsteht. $SO_4^{\bullet-}$ sind starke Oxidationsmittel, die den Abbau von sehr stabilen Schadstoffen ermöglichen könnten. Ein Beispiel sind perfluorierte Carbonsäuren, die durch $SO_4^{\bullet-}$ abgebaut werden jedoch in Gegenwart hochreaktiver Hydroxylradikale ($^{\bullet}OH$), die in sog. Advanced Oxidation Processes (AOP) z.B. beim Einsatz von Ozon gebildet werden, persistieren. Allerdings sind wichtige Aspekte einer potenziellen Anwendung von $SO_4^{\bullet-}$ als Wasseraufbereitungsverfahren, wie Energieaufwand und Nebenproduktbildung, bislang kaum untersucht. Dies ist Gegenstand der vorliegenden Arbeit.
In einem ersten Schritt wurde der Einfluss von natürlichem organischem Material (NOM) auf die Effizienz des Schadstoffabbaus untersucht und mit dem Einsatz von $^{\bullet}OH$ verglichen. Dabei zeigte sich, dass $SO_4^{\bullet-}$ in Gegenwart von zwei Arten NOM (Suwannee River und aus Leonardith-Material extrahierte Huminsäuren), 2-3-fach effizienter war als in einem analogen $^{\bullet}OH$ basierten Verfahren, was auf eine geringere Reaktivität der $SO_4^{\bullet-}$ mit NOM zurückgeführt werden kann. Allerdings reagieren einige Schadstoffe deutlich langsamer mit $SO_4^{\bullet-}$ im Vergleich zu $^{\bullet}OH$ (z.B. *tert*-Butanol $k(^{\bullet}OH) \approx 10^8$ M^{-1} s^{-1}, $k(SO_4^{\bullet-}) \approx 10^5$ M^{-1} s^{-1}), was sich kompensatorisch auf diesen Effizienzgewinn auswirkt.
Im Weiteren wurde die Bildung von Bromat (BrO_3^-) untersucht. BrO_3^- ist ein wichtiges Nebenprodukt das beim Einsatz von Ozon in Gegenwart von Bromid (Br^-) entstehen kann (EU und US-EPA Trinkwassergrenzwert: 10 µg L^{-1}). Während $SO_4^{\bullet-}$ in Reinstwasser Br^- zu BrO_3^- oxidiert, führt die Gegenwart von NOM zu einer sehr effizienten Unterdrückung dieser Reaktion. Damit ist die übermäßige Bildung von BrO_3^- auch in $SO_4^{\bullet-}$ basierten Prozessen nicht zu erwarten. Bei einer übermäßigen Bildung von BrO_3^- in einem Ozon-basierten Prozess könnte ein $SO_4^{\bullet-}$ basiertes Verfahren eine günstigere Alternative darstellen.

Die Effizienz des Spurenstoffabbaus durch $SO_4^{\bullet-}$ hängt entscheidend von der Cl^- und HCO_3^-/CO_3^{2-} Konzentration ab. $SO_4^{\bullet-}$ reagieren rasch mit Cl^- ($\approx 10^8$ M^{-1} s^{-1}) wobei Chloratome ($Cl^{\bullet}$) gebildet werden, die in Wasser zu $^{\bullet}OH$ umgesetzt werden. Bei mittleren bis hohen Cl^- Konzentrationen ($\geq$ 1 mM) wird dabei ein Großteil der $SO_4^{\bullet-}$ in $^{\bullet}OH$ umgesetzt und der $SO_4^{\bullet-}$ basierte Prozess wird zu einem konventionellem AOP. In diesem System kann dabei die schnelle Reaktion von HCO_3^-/CO_3^{2-} mit $Cl^{\bullet}$ zu einer Herabsetzung der Oxidationskraft führen.
Die Möglichkeit perfluorierte Tenside durch $SO_4^{\bullet-}$ abzubauen ist in den letzten Jahren auf großes wissenschaftliches Interesse gestoßen. Die Ergebnisse der vorliegenden Arbeit deuten darauf hin, dass in Gegenwart niedriger Konzentrationen an $S_2O_8^{2-}$ wenige Angriffe des $SO_4^{\bullet-}$ bereits zu einer Mineralisierung von perfluorierten Carbonsäuren (PFCA) mit Kohlenstoffkettenlängen von < C_5 führen können. Bei größeren PFCA konnte die Fluorbilanz aus Fluorid und organisch gebundenem Fluor nicht geschlossen werden, was auf die Bildung bislang nicht identifizierter Produkte hindeutet. Die Reaktionsgeschwindigkeit der Reaktion $SO_4^{\bullet-}$ plus PFCA (C_4-C_8) ergab jedoch sehr geringe kinetische Konstanten von 1-4 × 10^4 M^{-1} s^{-1}. Dadurch ist der Energieaufwand, der für den Abbau dieser Stoffe in einem $SO_4^{\bullet-}$ basierten Prozess aufgebracht werden muss, sehr hoch. Zudem werden perfluorierte Sulfonsäuren durch $SO_4^{\bullet-}$ nicht abgebaut.
Die vorliegende Arbeit hat gezeigt, dass $SO_4^{\bullet-}$ in der Wasseraufbereitung prinzipiell als Oxidationsmittel eingesetzt werden können. Dabei hat allerdings die Zusammensetzung der Wassermatrix vor allem bezüglich der Menge an Cl^- und HCO_3^- einen sehr großen Einfluss auf die Effizienz eines $SO_4^{\bullet-}$ basierten Verfahrens. Ein sinnvoller Einsatz eines solchen Verfahrens ist vermutlich nur in Gegenwart kleiner Cl^- Konzentrationen möglich. Solche Rohwässer können in Gegenden mit geringer Bevölkerungsdichte und geringer industrieller Aktivität vorkommen. Es bleibt jedoch weiterhin fraglich, ob $SO_4^{\bullet-}$ ein geeignetes Oxidationsmittel für den Abbau von perfluorierten Verbindungen in der Wasseraufbereitung darstellt.

Table of contents

Table of contents

Table of contents

Chapter 1

-

Introduction

1.1. Preface

In the "Guidelines for drinking-water quality" of the world health organization (fourth edition) the importance of safe drinking water has been pointed out as follows:
"Access to safe drinking-water is essential to health, a basic human right and a component of effective policy for health protection (…) Water is essential to sustain life, and a satisfactory (adequate, safe and accessible) supply must be available to all. Improving access to safe drinking-water can result in tangible benefits to health. Every effort should be made to achieve drinking-water that is as safe as practicable".

The quality of drinking water is a key element for public health and a functioning society. Thus, it is of the utmost importance to apply the highest possible quality standards in drinking water production and protection of drinking water resources. The quality parameters comprise absence of pathogenic biological material and chemical pollutants. In industrial countries also esthetic requirements have to be fulfilled for compiling the demand that "drinking water should be appetizing and should entice one to enjoy it (DIN 2000)" (e.g., absence of color, taste and odor).

New pollutants are steadily released and/or regularly identified. One current example is the emerging of perfluorinated compounds (PFC) in drinking water. PFC survive most of the conventional techniques in drinking and wastewater treatment and have been detected in finished drinking in Germany, Switzerland, USA and other countries [1, 2]. This example highlights the necessity of continuous technical development in drinking water purification and environmental protection for assuring a high drinking water quality.

The present chapter 1 introduces the general principles of trace pollutant control in water treatment focusing on oxidative water treatment processes. Thereby, ozonation and photolysis of hydrogen peroxide (UV/H_2O_2) are of particular interest since in these processes the most power-full oxidant used in water treatment is formed i.e., the hydroxyl radical ($^{\bullet}OH$). Thus, these processes will be compared with the oxidative water treatment process under study in this thesis, which is based on sulfate radicals ($SO_4^{\bullet-}$). Detailed information about the fundamentals in both processes will be provided, followed by a thorough discussion of the chemical properties of $SO_4^{\bullet-}$ and $^{\bullet}OH$.

1.2. Trace pollutants in water treatment

The ongoing progress in analytical chemistry results in an increasing awareness of the number of pollutants in the environment and their large chemical diversity. This belongs to the driving forces for continuous developments in water treatment. Indeed, trace pollutants are a major issue in drinking water treatment and partly in waste water treatment due to their potential to cause adverse health effects upon long term exposure. These compounds comprise a large variety of organic and inorganic substances which can be water born or of anthropogenic origin and typically appear in the µg L^{-1} range (e.g., pharmaceuticals, pesticides, fuel additives, solvents, taste and odor compounds or toxins).
The control of pollutants in water treatment can be divided into three basic techniques:

1. Physical separation
2. Biological degradation
3. Chemical transformation

1.2.1. Physical separation

Currently, the major separation technique applied in water treatment is the use of *activated carbon* (AC) which can be dosed as slurry (powdered activated carbon (PAC)) or used as fixed bed filtration (granular activated carbon (GAC)). In these processes pollutants are adsorbed on the AC surface. Since the sorption capacity is limited AC has to be renewed regularly and pollutants may be oxidized when the sorbent is regenerated or incinerated. PAC is continuously renewed and thus, maximum adsorption capacity can be maintained. In case of GAC, sorption capacity diminishes over time due to increasing load and care has to be taken for preventing breakthrough or elution of pollutants (e.g., during episodes of elevated dissolved organic carbon (DOC) concentrations in the source water). Yet, GAC is much more common in drinking water treatment than PAC, which is due to lower operation costs.
Membrane filtration is also applied in water treatment for the removal of pollutants, albeit to a much lesser extent than AC. Membranes are physical and in some cases chemical barriers to remove particles and solutes from a fluid. In water treatment, four types of membranes are applied: microfiltration (MF), ultrafiltration (UF), nanofiltration (NF) and reverse osmosis (RO). MF and UF membranes have an average pore size in the range of 0.1-10 µm (MF) and 0.002-0.1 µm (UF) and are used to remove particles from water. The pore size distribution of NF is 0.0005-0.002 µm and of RO < 0.0005 µm.

However, as the membranes have usually a more or less broad pore size distribution, the borders between the different processes are somewhat blurred. The retardation effect of NF and RO is a combination of physical separation and chemical interactions of solutes with the membrane material. These membranes are used for the removal of dissolved compounds (e.g., pollutant control or reduction of hardness) which accumulate in the membrane concentrate [3]. Coupled with PAC also UF is used for pollutant control. A full-scale application of PAC/UF for water treatment is the CRISTAL© process (**C**ombined **R**eactors **I**ntegrating a **S**eparation by membranes and **T**reatment by **A**dsorption in **L**iquid) which is applied in Slovenia, France and Switzerland for drinking water treatment [4]. Beside sorptive removal of pollutants, the addition of PAC also reduces membrane fouling by sorption of DOC.

1.2.2 Biological degradation

Biodegradable pollutants can also be metabolized in *biological filtration* or retarded in biofilms (bio-sorption). However, the biological community needs time for adapting to the composition of source water to eventually biodegrade pollutants. Thus, biological treatment processes require stable matrices and constant load of pollutants to achieve the optimal performance. Spontaneous episodes such as seasonal occurrence of taste and order compounds or agricultural agents such as pesticides in surface waters (e.g., in summer/autumn) might rather require a more flexible tool such as PAC or oxidative treatment (see below).

1.2.3 Chemical transformation

Chemical transformation leads to a change in the molecular structure of a pollutant with the aim to reduce its undesired effect and can be divided into oxidation and reduction processes. However, the latter process is applied in only few cases of ground water remediation (e.g., for transformation of halogenated solvents). Oxidation is widely-used in water treatment with ozone (O_3) representing one of the most common and important oxidants. Ozonation is applied in drinking water treatment for more than a century for disinfection, color removal, oxidation of reduced iron and manganese species and belongs to the most efficient methods for pollutant control [5]. It will also be shown that in some cases of drinking water treatment other oxidative treatment options such as photolysis of hydrogen peroxide (UV/H_2O_2) yielding highly reactive $^{\bullet}OH$ (such kind of processes are also called advanced oxidation process (AOP) [6]) are more applicable.

For assessing the feasibility of new oxidative treatment options these treatment methods give a very important point of reference in the question of potential advantages and applicability. Thus, basic principles as well as the potential and limitations of ozonation and UV/H_2O_2 are provided in the following.

1.2.4 Ozone based processes

O_3 reacts fast with compounds revealing double bonds, activated aromatic systems, reduced sulfur containing groups and deprotonated amines [7]. O_3 refractory compounds (e.g., most X-ray contrast media, pesticides such as triazine herbicides and fuel additives e.g., MTBE) are still degraded in ozone based processes due to the intrinsic formation of hydroxyl radicals $^{\bullet}OH$ [7]. In conventional ozonation $^{\bullet}OH$ are formed in a side reaction of O_3 with electron rich moieties of dissolved organic matter (DOM), i.e., free amines and activated aromatic compounds [8-10]. In these reactions (see below) O_3 undergoes electron transfer yielding $O_3^{\bullet-}$ (reaction 6). $O_3^{\bullet-}$ is in equilibrium with $O^{\bullet-}$ and O_2. However, protonation of $O^{\bullet-}$ inhibits the reverse reaction since $^{\bullet}OH$ does not react with O_2 [5] (p*K*a ($^{\bullet}OH$) = 11.8 [5]) (reaction 7 and 8).

The slow reaction of O_3 plus OH^- may also yield $^{\bullet}OH$ at pH > 8 (reaction 1 and 2; note that reaction 1 might be initiated by formation of HO_4^- which rapidly decomposes into $O_2^{\bullet-}$ and $HO_2^{\bullet}$ [11]). Considering hydraulic retention times in ozone reactors ranging between 10 and 30 minutes and assuming an O_3 depletion of 90% this corresponds to an average O_3 degradation rate of 0.013 – 0.038 s^{-1}. At pH 8.5, O_3 depletion *via* reaction 1 reveals an observed degradation rate of 0.0002 s^{-1}. Hence, even at elevated pH the contribution of reaction 1 to O_3 depletion (and $^{\bullet}OH$ formation) is small (≈ 5-18 %; note that at pH 8 the fraction of O_3 reacting with OH^- already drops down to ≈ 2-5 % in the present example).

$O_3 + OH^-$	→	$O_2^{\bullet-} + HO_2^{\bullet}$	$k = 70\ M^{-1} s^{-1}$	(reaction 1) [11]
$O_2^{\bullet-} + O_3$	→	$O_3^{\bullet-} + O_2$	$k = 1.6 \times 10^6\ M^{-1} s^{-1}$	(reaction 2) [12]
$HO_2^- + O_3$	→	HO_5^-	$k = 2.8 \times 10^6\ M^{-1} s^{-1}$	(reaction 3) [5]
HO_5^-	→	$HO_2^{\bullet} + O_3^{\bullet-}$		(reaction 4) [5]
HO_5^-	→	$2\ ^3O_2 + OH^-$		(reaction 5) [5]
$O_3 + DOM$	→	$O_3^{\bullet-} + DOM^{+\bullet}$		(reaction 6) [5]
$O_3^{\bullet-}$	⇄	$O^{\bullet-} + O_2$	$k_+ = 1.4 \times 10^3\ s^{-1}$	
			$k_- = 3.5 \times 10^3\ M^{-1} s^{-1}$	(reaction 7) [5]
$O^{\bullet-} + H_2O$	→	$^{\bullet}OH + OH^-$	$k = 10^8\ s^{-1}$	(reaction 8) [5]

In some cases H_2O_2 is dosed along with O_3 for enhancing the formation of $^{\bullet}OH$ (reaction 3-5 and 7-8). Corresponding reactions have been revised by Fischbacher et al. [13] and Merényi et al., [14] ensuing a 50% smaller yield of $^{\bullet}OH$ as assumed previously (0.5 instead of 1 mol of $^{\bullet}OH$ per mol of O_3 [15]). It is currently assumed that both pathways of HO_5^- decomposition (reaction 3 and 4) are similar fast, thus, only 50 % of HO_5^- yields $O_3^{\bullet-}$ [5]. Reactions of $^{\bullet}OH$ with organic matter can further enhance O_3 decomposition. This process is called "propagation" and is driven by release of $HO_2^{\bullet}/O_2^{\bullet-}$ which could react with O_3 in reaction 2, thus giving rise of $^{\bullet}OH$ in reaction 7 and 8 [7]. This chain reaction is terminated in reactions of $^{\bullet}OH$, which do not yield $O_2^{\bullet-}$ (scavenging; e.g., reaction of $^{\bullet}OH$ with HCO_3^-) [7].

A major draw-back in ozonation is the formation of bromate (BrO_3^-) (potential cancerogen; EU and US-EPA drinking water standard of 10 µg L^{-1} [19]). BrO_3^- is the final product in Br^- oxidation involving both O_3 and $^{\bullet}OH$ [16-18]. This reaction can be somewhat suppressed by addition of H_2O_2 which is reducing HOBr/OBr^- yielding Br^-. However, this does not completely prevent BrO_3^- formation. In presence of both, O_3 and $^{\bullet}OH$, another albeit less pronounced route of BrO_3^- formation is possible and BrO_3^- may be formed without HOBr being a requisite intermediate [19]. Thus, at high O_3 doses and high concentrations of Br^- (e.g., 100 µg L^{-1}), BrO_3^- could also be formed in significant levels in the peroxone process. Figure 1 shows the formation of BrO_3^- in surface water containing 80 µg L^{-1} Br^- during ozonation and in presence of various concentration of H_2O_2 (experimental procedure is analogous to ozonation experiments described in chapter 6 and 7).

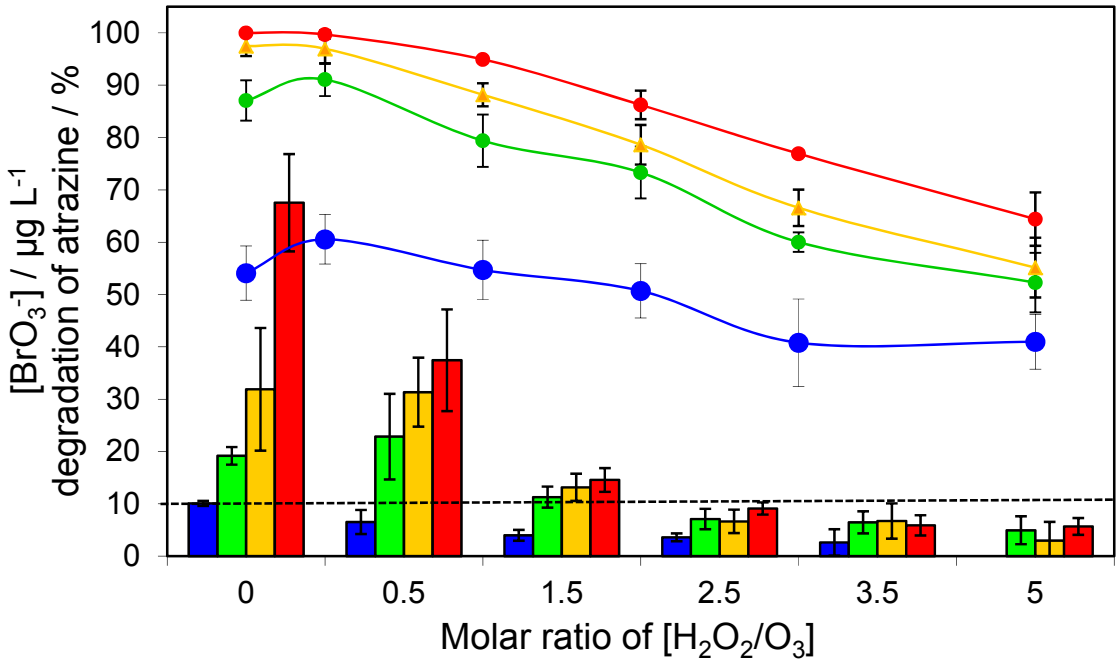

Figure 1: Degradation of atrazine (lines) and BrO_3^- formation (columns) in surface water in ozone based oxidation at different molar ratios of H_2O_2 towards O_3 (0 means no addition of H_2O_2); $[Br^-]_0$ = 80 µg L^{-1}, [DOC] = 1.5 mg L^{-1}, $[HCO_3^-] \approx 0.4$ mM, pH = 7 (buffered with 20 mM borate), T = 20-25 °C; O_3 dose (columns and lines (mg L^{-1})): blue 1, green 2, orange 3, red 5; the horizontal dashed black line indicates the BrO_3^- drinking water standard of 10 µg L^{-1}, error bars mark the standard deviation (number of replicates = 3)

It can be seen, that at elevated Br^- concentrations (80 µg L^{-1}) BrO_3^- formation becomes problematic in conventional ozonation even at a moderate dose of 1 mg L^{-1} O_3. However, at the raw water condition of the present example an H_2O_2 dose corresponding to a molar ratio of 0.5 H_2O_2 towards O_3 can reduce the formation of BrO_3^- to a tolerable level at that O_3 dose. In this surface water 1 mg L^{-1} O_3 suffices for degradation of pollutants with moderate to fast kinetics towards O_3 (i.e., > 100 M^{-1} s^{-1}). Yet, a higher O_3 dose has to be applied in case O_3 recalcitrant compounds such as atrazine ($k(O_3)$ = 6 M^{-1} s^{-1} [20]) have to be degraded to an extent above 50% which results in massive BrO_3^- formation. Thus, higher molar ratios of H_2O_2 towards O_3 (i.e., 2.5-3.5) are required, which is problematic since H_2O_2 can also contribute to scavenging of $^{\bullet}OH$, hence, mitigating the oxidation strength. This is reflected by the decrease of the level of atrazine degradation at constant O_3 dose and increasing molar ratio of H_2O_2 towards O_3. Figure 2 pools the data of Figure 1 in one function of BrO_3^- formation vs. atrazine degradation. Maximal ≈ 80 % of atrazine can be degraded without exceeding the BrO_3^- drinking water standard. A further increase of the O_3 dose would require a higher ratio of $[H_2O_2]/[O_3]$ rendering the ozonation process more inefficient. If H_2O_2 is added in large excess, ozonation becomes very inefficient

since the product of the reaction $^{\bullet}OH$ plus H_2O_2 yields $HO_2^{\bullet}$ which in turn initiates O_3 decomposition (reaction 2) [5].

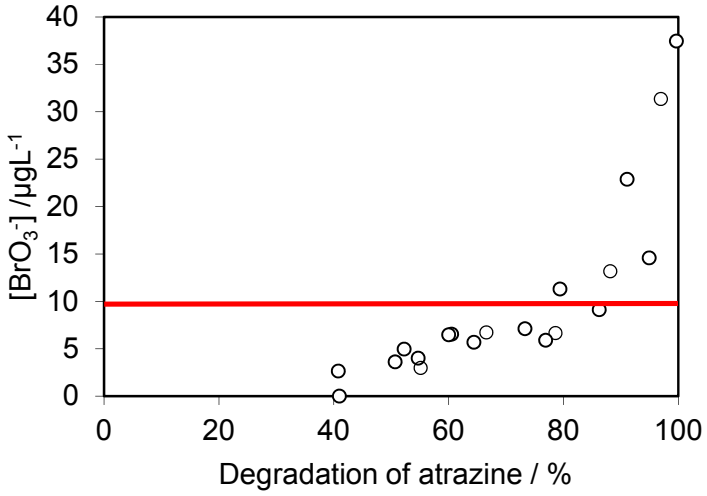

Figure 2: Formation of BrO_3^- vs. degradation of atrazine in ozone based oxidation of a surface water at conditions of figure 1; The red line marks the EU and US-EPA BrO_3^- drinking water standard

1.2.5 Photolysis of hydrogen peroxide

In case BrO_3^- formation cannot be sufficiently controlled in ozone based processes UV/H_2O_2 represents a feasible alternative. In UV/H_2O_2, Br^- is exclusively oxidized by $^{\bullet}OH$ and $HOBr/OBr^-$ is a requisite intermediate [18]. Thus, reduction of $HOBr/OBr^-$ by H_2O_2 effectively prevents BrO_3^- formation [18]. Table 1 lists UV/H_2O_2 full scale applications which are already in operation.

Table 1: Full-scale plants for UV/H_2O_2 treatment in drinking water purification

Location	Contaminants	Flow rate / $m^3\,day^{-1}$	Ref.
Aurora Reservoir Water Purification Facility, Aurora, CO, USA	NDMA and other nitrosamines	Bench scale experiments	[21]
City of Cornwall, ON, Canada	MIB and geosmin	9.99×10^4	
Orange County Water District, CA, USA (potable reuse application)	NDMA, 1,4-dioxane	3.79×10^4	
PWN Treatment Plant Andijk, PWN Treatment Plant Andijk	80% reduction of various micro-pollutants	9.46×10^4	
Salt Lake City Department of Public, Utilities, UT, USA	PCE	1.64×10^4	
San Gabriel Valley Water Company, CA, USA	NDMA, 1,4-dioxane	4.24×10^4	
Stockton, CA, USA	1,4-dioxane	Under construction	
The La Puente Valley County Water, District, CA, USA	NDMA, 1,4-dioxane	1.36×10^4	
Valley County Water District, CA, USA	NDMA, 1,4 Dioxane	4.24×10^4	
West Basin Municipal Water District, CA, USA	NDMA	4.73×10^4	
Region of Peel, ON, Canada	MIB, Geosmin	2.00×10^5	[22]

If UV/H_2O_2 is applied for pollutant degradation it normally also provides sufficient disinfection power. In the work of Katsoyiannis et al., the fluence for 90% degradation of atrazine in Lake Zurich water was found to be ≈ 9000 J m^{-2} at 254 nm, applying a dose of H_2O_2 of 0.2 mM [23] (note that this low H_2O_2 dose results in an negligible molar absorption (254 nm) of 0.04 $M^{-1}\,cm^{-1}$ ($\varepsilon(H_2O_2)_{254nm}$ = 18.6 $M^{-1}cm^{-1}$ [23]). Thus, the UV fluence in this processes is much larger than recommended for disinfection (i.e., 400 J m^{-2} [24]). A large disadvantage of UV/H_2O_2 is the elevated demand of energy compared with ozonation (ca. factor 10 [23]).

The high energy demand in UV/H_2O_2 belongs to the reasons why in waste water treatment, ozonation (and PAC treatment) is much more in the focus as a potential tertiary treatment for pollutant degradation than is UV/H_2O_2, since a waste water standard for BrO_3^- does not exist (note that the strong UV absorption in wastewater further increases the energy demand of photochemical processes).

There are many other options to generate $^{\bullet}OH$ such as photolysis of O_3, photo excitation of titanium dioxide (UV/TiO_2), and the Fenton reaction (i.e., reduction of H_2O_2 by Fe(II) at low pH) which have currently been reviewed by von Sonntag [25]. However, since most of these processes are of minor importance in drinking water treatment their further detailed discussion exceeds the scope of the present work.

1.3 Comparison of sulfate radical based oxidation with hydroxyl radical based oxidation

In the past years the sulfate radical ($SO_4^{\bullet-}$) has been increasingly discussed as an oxidizing agent for pollutant degradation. Indeed, $SO_4^{\bullet-}$ has some unique features, such as being a very strong electron acceptor enabling reaction pathways which are not possible in case of $^{\bullet}OH$ (see below). Oxidation processes involving $SO_4^{\bullet-}$ are already applied in ground water remediation [26] and the potential of $SO_4^{\bullet-}$ is increasingly investigated in the context of water treatment [27-36]. As will be shown below, the generation of $SO_4^{\bullet-}$ resembles an AOP based on H_2O_2 in that a similar radical precursor can be used for generation of $SO_4^{\bullet-}$ (i.e., $S_2O_8^{2-}$). This might enable retrofitting existing AOPs based on H_2O_2 by dosing of $S_2O_8^{2-}$. Experience with regard to building and operating such kind of plants, would further facilitate implementing $SO_4^{\bullet-}$ chemistry into water treatment chains. In the following, the conventional AOP is compared with principles of $SO_4^{\bullet-}$ based oxidation.

1.4 Peroxodisulfate and hydrogen peroxide as radical precursors

For studying radical reactions the use of $S_2O_8^{2-}$ and H_2O_2 is convenient, since both peroxides normally do not interfere by direct reactions. Even though H_2O_2 and $S_2O_8^{2-}$ reveal high oxidation potentials ($S_2O_8^{2-}$: 2.01 V [37] and H_2O_2: 1.776 V [26]) their reactions with organic compounds are considered to be very slow [26] (e.g., the reaction of $S_2O_8^{2-}$ with different phenols (Elbs reaction) has been reported to be in the range of $\approx 2 \times 10^{-3}$ to 0.34 $M^{-1} s^{-1}$ at 30 °C and in presence of 1.7 M KOH [38]). The peroxide bond of $S_2O_8^{2-}$ and H_2O_2 can be broken by UV-radiation, thermal radiation or in the reaction with a suitable nucleophile reductant (chemical reduction) [35, 39, 40].

1.4.1 Photolysis

The photochemistry of H_2O_2 and $S_2O_8^{2-}$ is very similar. The bond dissociation energy needed for cleaving the peroxide-bond is quite low (120 kJ mol^{-1} ($S_2O_8^{2-}$) and 210 kJ mol^{-1} (H_2O_2) [41]), thus electro-magnetic radiation in the visible range (i.e., < 500 nm) would principally provide enough energy for their cleavage. However, both peroxides do not significantly absorb visible light but reveal a distinctive absorption in the UV range (molar absorption at 254 nm = 18.6 (H_2O_2) $M^{-1} cm^{-1}$ [23] and 22 ($S_2O_8^{2-}$) $M^{-1} cm^{-1}$ [42]). The quantum yield of $S_2O_8^{2-}$ (1.4 mol $SO_4^{\bullet-}$ $Einstein^{-1}$ [39, 43]) is much larger than that of H_2O_2 (1 mol $^{\bullet}OH$ $Einstein^{-1}$ [44]). This difference in quantum yield could be related to the

rate of recombination of $^{\bullet}OH$ (5.5×10^{9} M^{-1} s^{-1} [45]) and $SO_4^{\bullet-}$ (1.6×10^{8} M^{-1} s^{-1} [39]). After photolytic cleavage of the peroxide bond, the radicals are hold together in a solvent cage and recombination competes for formation of free radicals. Since the rate of $SO_4^{\bullet-}$ recombination is much smaller (around one order of magnitude) than of $^{\bullet}OH$ the chance of $SO_4^{\bullet-}$ to escape from the solvent cage upon photolysis of the peroxide is greater.

1.4.2 Reduction by transition-metals

H_2O_2 and $S_2O_8^{2-}$ readily react with inorganic nucleophiles such as reduced metals (e.g., Fe^{2+}, Co^{+}, Zn^{+} and Cd^{+}) or sulfide. Thereof, the reaction of H_2O_2 with Fe^{2+} is well known as Fenton reaction. In this reaction H_2O_2 replaces a water molecule in the Fe^{2+}-hexa-aquo complex yielding $Fe(H_2O)_5OOH^{+}$ [25]. In an acid catalyzed reaction this complex decomposes giving rise to either $^{\bullet}OH$ or FeO^{2+} as reactive species. At neutral pH probably no $^{\bullet}OH$ but FeO^{2+} is formed, which is a selective oxidant [25]. Information about this reactive iron species, such as yields and reactivity, is largely lacking [25]. H_2O_2 also undergoes complexes with Fe^{3+} which slowly decompose yielding Fe^{2+} and $HO_2^{\bullet}$ thus, redelivering reduced iron species for feeding the Fenton reaction. The reduction of Fe^{3+} is accelerated in presence of light (< 500 nm) (photo-Fenton) [25]. It has to be mentioned that the present description of Fenton is a strong simplification. In corresponding chemistry of $S_2O_8^{2-}$, yet, major gaps in knowledge do not allow a detailed mechanistic insight. Anipsitakis et al. [35] investigated the reaction of H_2O_2, $S_2O_8^{2-}$ and Caro´s acid (HSO_5^{-}) with different transition metals revealing that the reaction of Fe^{2+} with $S_2O_8^{2-}$ yields $SO_4^{\bullet-}$ at acidic conditions and indicated that a reaction of $S_2O_8^{2-}$ with Fe^{3+} does not happen to occur [35]. This might be explained by the evidence, that $S_2O_8^{2-}$ is a weaker reductant than H_2O_2 because of its higher oxidation potential (see above).

H_2O_2 reacts with Fe^{2+} (as $Fe(H_2O)_6^{2+}$) at a reaction rate of 40-80 M^{-1} s^{-1} at pH < 3 [46]. A much lower reaction rate for the reaction of Fe^{2+} plus $S_2O_8^{2-}$ (8.3 $M^{-1}s^{-1}$) has been reported by Petri et al. [26].

The presence of reduced transition metals introduces an additional radical scavenging and degradation efficiency might be reduced, since the reductant is typically present in excess over the (trace-) pollutant.

1.4.3 Thermolysis

For studying $SO_4^{\bullet-}$ reactions thermal activation of $S_2O_8^{2-}$ is quite convenient, since moderate temperatures (i.e., > 40 °C) [47] are sufficient for rupturing the peroxide bond. Under such conditions

H_2O_2 is stable due to the higher bond dissociation energy (BDE) of its peroxide bond (see above) [48]. $S_2O_8^{2-}$ may also yield small steady state concentrations of $SO_4^{\bullet-}$ at room temperature (i.e., 20 °C). This process hampers a differentiation between direct reactions of $S_2O_8^{2-}$ (such as the reaction with phenols (Elbs reaction [49])) and indirect pathways *via* $SO_4^{\bullet-}$. The few reaction rates available for direct $S_2O_8^{2-}$ reactions indicate very slow reaction kinetics and low concentrations of $SO_4^{\bullet-}$ possibly interfere. In case $S_2O_8^{2-}$ is used as a radical source, precautions have to be considered for preventing reactions by $SO_4^{\bullet-}$ formed during storage time (see chapter 3).

1.4.4 Kinetics and mechanisms in the reaction of hydroxyl radicals and sulfate radicals

The oxidation potentials of $SO_4^{\bullet-}$ (2.43 V [50]) and $^{\bullet}OH$ (2.73 V [50]) are similar. However, these often cited values are of limited information since reactions are rather driven by kinetics than by thermodynamics, which has been discussed for $^{\bullet}OH$ [5] and may also apply for $SO_4^{\bullet-}$. In the reaction with toluene, for example, $^{\bullet}OH$ react predominantly *via* addition to the ring and not by H-abstraction at the methyl group [51], although the latter reaction is thermodynamically favored [5]. Another example is electron transfer which principally could be fast due to the high oxidation potential of $^{\bullet}OH$ [5]. Even though electron transfer is energetically feasible $^{\bullet}OH$ reacts rather *via* addition (examples are the reactions of $^{\bullet}OH$ with phenols or transition metals [5]). In fact the main reaction pathways of $^{\bullet}OH$ in the reaction with organic compounds are addition to C-C, C-N and C-S double bonds and H-abstraction [48] which will be discussed briefly.

The kinetics of most $^{\bullet}OH$ addition reactions are close to diffusion controlled, whereas in H-abstraction kinetics depend on the BDE of the corresponding H-bond [5]. Thiolic and thiophenolic groups belong to the weakest H-bonds and kinetics of H-abstraction driven by $^{\bullet}OH$ is also diffusion controlled [5]. In C-H bonds the reaction rate decreases in the order tertiary ($R\text{-}CH_2\text{-}H$) > secondary ($R_2\text{-}CH\text{-}H$) > primary carbon ($R_3\text{-}C\text{-}H$) [5] in both, $^{\bullet}OH$ and $SO_4^{\bullet-}$. The dependency of reaction rates on C-H BDE is demonstrated in Figure 3 (reaction rate constants have been taken from: [52-55] ($SO_4^{\bullet-}$ reactions) and [45, 56-61] ($^{\bullet}OH$ reactions); BDE have been taken from [5], note that the dependency of log(*k*) vs. BDE of C-H in $^{\bullet}OH$-reactions is much weaker, compared with $SO_4^{\bullet-}$ for the given set of compounds). Since most organic compounds reveal structural moieties which allow addition and H-abstraction, $^{\bullet}OH$ react fast with a large variety of compounds (i.e., > 10^9 M^{-1} s^{-1}) [45].

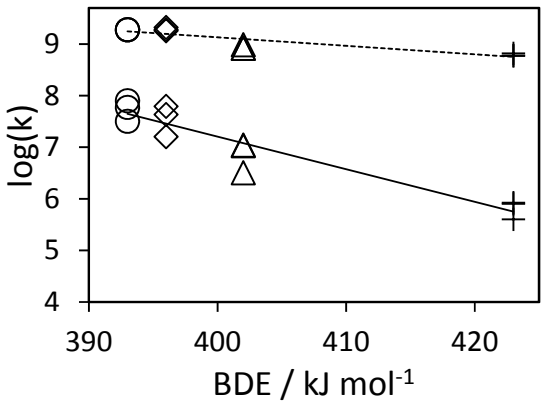

Figure 3: Correlation of bond dissociation energy of different C-H bonds and log(*k*) of the reaction with $^{\bullet}OH$ (dashed line) and $SO_4^{\bullet-}$ (continuous line); circles: isopropanol, diamonds: ethanol, triangles: methanol, crosses: *tert*-butanol

In contrast to $^{\bullet}OH$, $SO_4^{\bullet-}$ reacts more selectively by electron transfer [61] and addition as well as H-abstraction is mostly slower compared to corresponding reactions with $^{\bullet}OH$. The pattern of kinetics in H-abstraction is similar to $^{\bullet}OH$ (Figure 3). However, the dependency of the reaction rate on the BDE is much more pronounced and the reaction rates of H-abstraction (e.g., reaction with saturated organic acids or alcohols) typically are in the order of 10^7-10^8 M^{-1} s^{-1} (one exception is *tert*-butanol (*k*(*tert*-butanol + $SO_4^{\bullet-}$ = 4-9 × 10^5 $M^{-1}s^{-1}$ [61] (Figure 3). Compounds containing double bonds react in the range of 10^8-10^9 M^{-1} s^{-1} [61]. In both reactions the kinetic constants are around one order of magnitude below corresponding reaction rates of $^{\bullet}OH$ [45, 61].

As for $^{\bullet}OH$ the reaction rates of $SO_4^{\bullet-}$ plus aromatic compounds depend on the nature of the substituents, albeit the reaction mechanism might be different ($^{\bullet}OH$ reacts *via* addition and $SO_4^{\bullet-}$ *via* electron transfer). Both radicals display a linear correlation in a Hammett plot (log(*k*) vs. Hammett constants (σ) of the substituents (note that the slope is designated as ρ, a negative value indicates that the reactive species is an electrophile, a positive value indicates a nucleophile). This dependency is much more distinctive in $SO_4^{\bullet-}$ reactions (ρ = -2.4 [62]) compared with $^{\bullet}OH$ (ρ = -0.5 [62]) and aromatic compounds with strongly deactivating substituents (e.g., 4-nitrobenzoic acid) are nearly inert towards $SO_4^{\bullet-}$ (≤ 10^6 M^{-1} s^{-1} [62]) but still react fast with $^{\bullet}OH$ (2.6 × 10^9 M^{-1} s^{-1} [45]). With regard to water treatment it can be concluded, that $SO_4^{\bullet-}$ tends to react at a similar rate or slower with most pollutants compared with $^{\bullet}OH$.

However, $SO_4^{\bullet-}$ also reveals the potential of degrading pollutants which are refractory against $^{\bullet}OH$. A case in point are perfluorinated carboxylic acids (PFCAs) [63]. The reaction of $^{\bullet}OH$ with PFCAs is not favored because H-abstraction is impossible and electron transfer hampered by reduction of the electron density in the carboxylic group by the fluorine atoms attached on the α-C atom. Abstraction of a fluorine atom is thermodynamically disfavored since the F-OH bond has a much lower BDE (216 kJ mol^{-1} [64]) compared to the C-F bond (R-CF_2-F 352 kJ mol^{-1}, R,R´CF-F 508 kJ mol^{-1} [64]). However, the degradation of PFCAs in a $SO_4^{\bullet-}$ based process has been observed in several studies under various conditions [65]. The second order reaction rate for the reaction of $SO_4^{\bullet-}$ plus trifluoroacetic acid has been determined by laser-flash photolysis (1.6×10^4 M^{-1} s^{-1} [66]) and reaction rates for other short chain PFCAs have been estimated (perfluoropropionic acid (1.4×10^4 M^{-1} s^{-1}) and perfluorobutyric acid (1.3×10^4 M^{-1} s^{-1}) [32]. As one can see, even $SO_4^{\bullet-}$, which is a stronger electron acceptor than $^{\bullet}OH$ reacts with very slow kinetics and it is doubtful if a $SO_4^{\bullet-}$-based oxidation is feasible for the degradation of PFCAs especially in presence of a natural water matrix (e.g., natural organic matter (NOM) and alkalinity) which leads to scavenging of $SO_4^{\bullet-}$ (see below and chapter 5 and 7). Furthermore, the behavior of perfluorinated sulfonates in presence of $SO_4^{\bullet-}$ has not yet been investigated.

It has to be mentioned that, several compounds are hardly degraded by $SO_4^{\bullet-}$ such as deactivated aromatic compounds (4-nitrobenzoic acid) and H-abstraction at methyl groups (*tert*-butanol) which is remarkably slow (see above).

1.4.5 Reaction with matrix components

In oxidative water treatment processes, usually most of the oxidation strength is consumed by the main matrix constituents i.e., alkalinity and NOM. The influence of these matrix compounds in $^{\bullet}OH$-based and $SO_4^{\bullet-}$ based processes is discussed in the following. The reaction of $SO_4^{\bullet-}$ and $^{\bullet}OH$ with HCO_3^-/CO_3^{2-} yields the carbonate radical ($CO_3^{\bullet-}$) which is a rather mild oxidant [61] and in most cases not important in the degradation of pollutants. The reaction rates of $^{\bullet}OH$ and $SO_4^{\bullet-}$ are in the same range in case of HCO_3^- ($k(HCO_3^- + {}^{\bullet}OH) = 0.85\text{-}1 \times 10^7$ M^{-1} s^{-1} [45], recommended value : 1×10^7 M^{-1} s^{-1}[67], $k(HCO_3^- + SO_4^{\bullet-}) = 2.8\text{-}9.1 \times 10^6$ M^{-1} s^{-1} [55, 68]), but $SO_4^{\bullet-}$ is less reactive towards CO_3^{2-} ($k(CO_3^{2-} + {}^{\bullet}OH) = 3.2\text{-}4.2 \times 10^8$ M^{-1} s^{-1} [45], recommended value: 4×10^8 M^{-1} s^{-1}[67], $k(CO_3^{2-} + SO_4^{\bullet-}) = 4.1 \times 10^6$ M^{-1} s^{-1} [69])). However, the latter species is of minor importance in the typical pH range of natural waters (pH 6-8), thus, it can be expected, that the effect of alkalinity is the same for both $^{\bullet}OH$- and $SO_4^{\bullet-}$- based oxidation. However, in its reaction with organic compounds $SO_4^{\bullet-}$ is

probably much more selective (see above), thus scavenging by NOM might be much weaker than in case of $^{\bullet}OH$. Since the efficiency in pollutant degradation depends on both, the reaction kinetics as well as the life time of the oxidant, pollutants reacting at similar rates with both $SO_4^{\bullet-}$ and $^{\bullet}OH$ (e.g., atrazine ($k(^{\bullet}OH)$ and $k(SO_4^{\bullet-}) = 3 \times 10^9\ M^{-1}\ s^{-1}$ [20, 33, 70]) could be more efficiently degraded in $SO_4^{\bullet-}$ driven oxidation. Under typical conditions of water treatment compounds with a reaction rate of $< 10^8\ M^{-1}\ s^{-1}$ probably survive $^{\bullet}OH$ based treatment if an economically feasible energy demand is applied. Yet, this threshold value might be somewhat lower in $SO_4^{\bullet-}$ based oxidation due to a weaker scavenging by matrix constituents. This has already been indicated in a study of Mendez-Diaz et al., [71] in which the degradation of dodecylbenzene sulfonate in presence of organic matter during UV/$S_2O_8^{2-}$ and UV/H_2O_2 has been compared. Thereby, UV/$S_2O_8^{2-}$ was more effective which has been attributed to a weaker scavenging of $SO_4^{\bullet-}$ compared with $^{\bullet}OH$. However, the current literature does not provide a more detailed and quantitative view on the influence of water components in pollutant degradation based on $SO_4^{\bullet-}$.

1.5 Secondary reactions in radical based oxidation

The reaction of a radical on a substrate (e.g., a pollutant) again yields reactive species. Due to their large influence on subsequent reactions and final products, it is important to understand the nature of these intermediates. In that regard carbon centered radicals are mostly formed upon radical attack, which is illustrated in Figure 4.

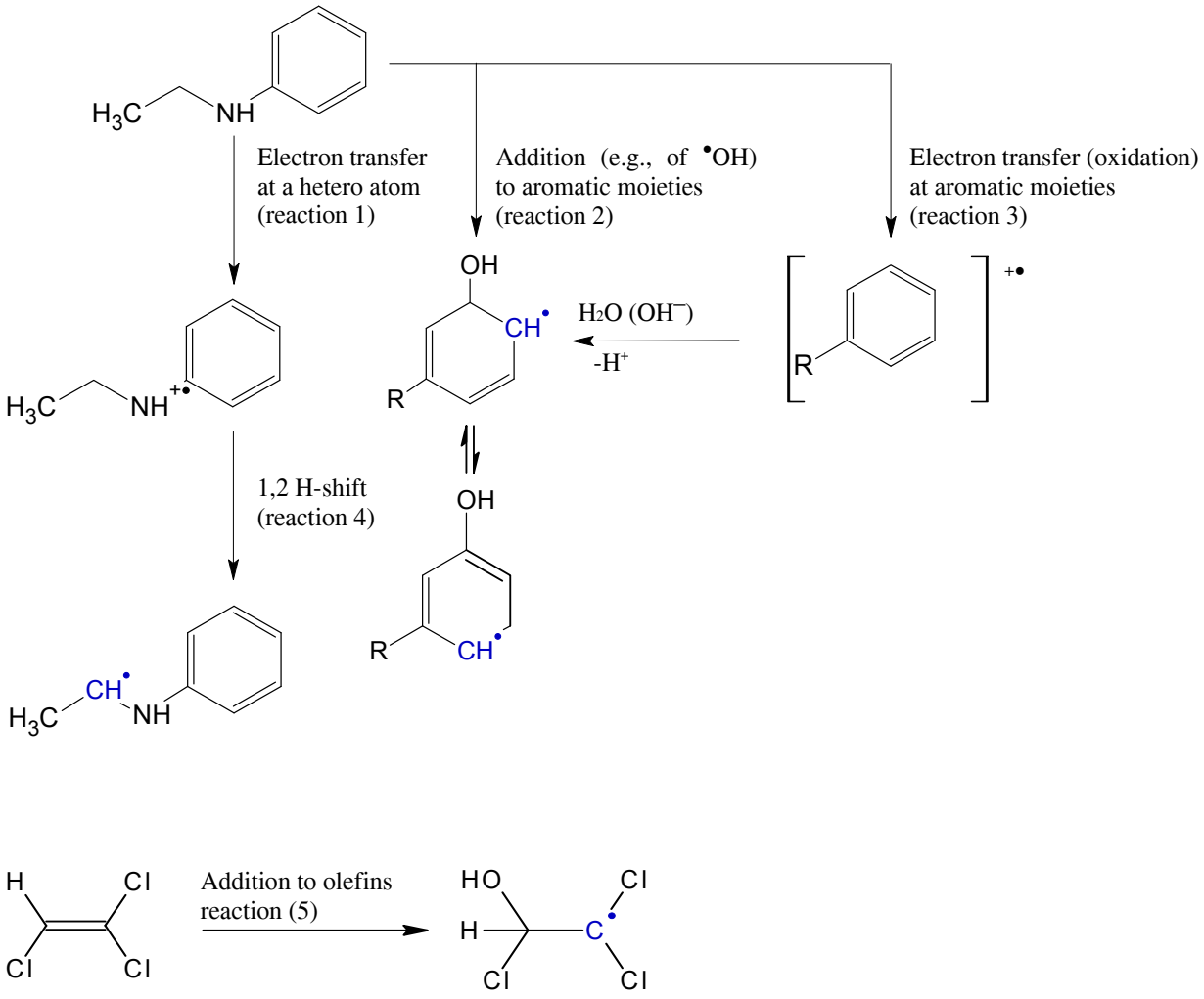

Figure 4: Formation of carbon centered radicals in oxidation processes; C•R represents carbon centered radicals

Electron transfer at a hetero atom (reaction 1) results in a radical cation which may deprotonate and undergo a 1,2-H-shift resulting in a carbon centered radical. Analogous reactions have already been documented for alkoxyl radicals [72].

The first intermediate in addition reactions of •OH to C-C double bonds (reaction 2 and 5) is a π-complex which may collapse into a sigma complex [5]. A case in point is the addition of •OH to

benzene yielding hydroxy-cyclohexadienyl radicals (reaction 2) [73]. Electron transfer from benzene to an appropriate electron acceptor (reaction 3) yields a radical cation (e.g., in case of $SO_4^{\bullet-}$ plus benzene [74]) which is also giving rise to an hydroxy-cyclohexadienyl radical in its reaction with water [74].
The carbon centered radicals add O_2 at diffusion controlled rates [5] or may react with H_2O_2 or $S_2O_8^{2-}$. In air saturated solutions these radicals likely react with O_2 yielding organic peroxy radicals. The chemistry of peroxy radicals has been explained in detail by Mertens [75] as well as by von Sonntag and von Gunten [5], which will be summarized in the following. The unimolecular decomposition of aliphatic hydroxy-peroxyl radicals yields superoxide ($O_2^{\bullet-}$) or perhydroxyl radicals ($HO_2^{\bullet}$) and an aldehyde. In the bimolecular decomposition a tetroxide is formed which can liberate O_2 (Russel mechanism) or H_2O_2 (Bennett mechanism) yielding aldehydes, alcohols, organic peroxides or highly reactive organic oxyl radicals. Aromatic carbon centered radicals also add O_2 and undergo hydroxylation (e.g., by liberating $HO_2^{\bullet}$) [73]. Carbon centered radicals that have a hydroxyl or amino group on the same carbon as the unpaired electron have reduction potentials in the range of -1 to -2 V vs. SHE (standard hydrogen electrode) [76] and can principally also be oxidized by O_3, H_2O_2 or $S_2O_8^{2-}$ yielding an organic radical cation [5, 48]. This can induce a chain reaction since the reduction of $S_2O_8^{2-}$ and H_2O_2 yields $SO_4^{\bullet-}$ [35] and $^{\bullet}OH$ [46], respectively. In absence of O_2, O_3, $S_2O_8^{2-}$ and H_2O_2, carbon centered radicals probably undergo termination reactions *via* dimerization [5].

Chapter 1 demonstrates the large complexity of oxidative water treatment processes. The research of the past decades enables assessing efficiency of pollutant degradation and formation of by-products in AOPs to a certain extent. A case in point is UV/H_2O_2 which can be described fairly well on basis of simple source water parameters (DOC, alkalinity and pH) and the amount of UV-light available for photochemical reactions (further description will be provided in chapter 3). Also the efficiency of disinfection and pollutant degradation in ozonation can be assessed by few simple experiments for calibrating the matrix influence on O_3 demand and formation of $^{\bullet}OH$ [77, 78]. However, the lack of information related to the interaction of the matrix components on $SO_4^{\bullet-}$ currently does not allow such kind of estimates. However, understanding the role of the water matrix, including the potential to form undesired by-products is a key element for assessing the feasibility of $SO_4^{\bullet-}$ based oxidation.

1.6 Literature

1. Rayne, S. and K. Forest, *Perfluoroalkyl sulfonic and carboxylic acids: A critical review of physicochemical properties, levels and patterns in waters and wastewaters, and treatment methods.* Journal of Environmental Science and Health - Part A Toxic/Hazardous Substances and Environmental Engineering, 2009. **44**(12): p. 1145-1199.
2. Rumsby, P.C., C.L. McLaughlin, and T. Hall, *Perfluorooctane sulphonate and perfluorooctanoic acid in drinking and environmental waters.* Philosophical Transactions of the Royal Society A: Mathematical, Physical and Engineering Sciences, 2009. **367**(1904): p. 4119-4136.
3. Van Der Bruggen, B., C. Vandecasteele, T. Van Gestel, W. Doyen, and R. Leysen, *A review of pressure-driven membrane processes in wastewater treatment and drinking water production.* Environmental Progress, 2003. **22**(1): p. 46-56.
4. Rovel, J.M., ed. *Water Treatment Handbook.* 2007, Degremont: Frankreich.
5. von Sonntag, C. and U. von Gunten, eds. *Chemistry of ozone in water and wastewater treatment*. 2012, IWA Publishing.
6. Glaze, W.H., J.-W. Kang, and D.H. Chapin. *Chemistry of water treatment processes involving ozone, hydrogen peroxide and ultraviolet radiation*. 1987. Amsterdam, Netherlands.
7. von Gunten, U., *Ozonation of drinking water: Part I. Oxidation kinetics and product formation.* Water Research, 2003. **37**(7): p. 1443-1467.
8. Buffle, M.O. and U. von Gunten, *Phenols and amine induced HO• generation during the initial phase of natural water ozonation.* Environmental Science and Technology, 2006. **40**(9): p. 3057-3063.
9. Pocostales, J.P., M.M. Sein, W. Knolle, C. Von Sonntag, and T.C. Schmidt, *Degradation of ozone-refractory organic phosphates in wastewater by ozone and ozone/hydrogen peroxide (peroxone): The role of ozone consumption by dissolved organic matter.* Environmental Science and Technology, 2010. **44**(21): p. 8248-8253.
10. Nöthe, T., H. Fahlenkamp, and C. Von Sonntag, *Ozonation of wastewater: Rate of ozone consumption and hydroxyl radical yield.* Environmental Science and Technology, 2009. **43**(15): p. 5990-5995.
11. Merényi, G., J. Lind, S. Naumov, and C.V. Sonntag, *The reaction of ozone with the hydroxide ion: Mechanistic considerations based on thermokinetic and quantum chemical calculations and the role of HO_4^- in superoxide dismutation.* Chemistry - A European Journal, 2010. **16**(4): p. 1372-1377.
12. Bühler, R.E., J. Staehelin, and J. Hoigné, *Ozone decomposition in water studied by pulse radiolysis. 1. HO_2/O_2^- and HO_3/O_3^- as intermediates.* Journal of Physical Chemistry, 1984. **88**(12): p. 2560-2564.
13. Fischbacher, A., J. von Sonntag, C. von Sonntag, and T.C. Schmidt, *The $^{\bullet}OH$ radical yield in the $H_2O_2 + O_3$ (peroxone) reaction.* Environmental Science and Engineering, submitted.
14. Merényi, G., J. Lind, S. Naumov, and C.V. Sonntag, *Reaction of ozone with hydrogen peroxide (peroxone process): A revision of current mechanistic concepts based on thermokinetic and quantum-chemical considerations.* Environmental Science and Technology, 2010. **44**(9): p. 3505-3507.
15. Staehelin, J. and J. Hoigné, *Decomposition of ozone in water: Rate of initiation by hydroxide ions and hydrogen peroxide.* Environmental Science and Technology, 1982. **16**(10): p. 676-681.
16. Haag, W.R. and J. Hoigné, *Ozonation of bromide-containing waters: Kinetics of formation of hypobromous acid and bromate.* Environmental Science and Technology, 1983. **17**(5): p. 261-267.

17. von Gunten, U. and J. Hoigne, *Bromate formation during ozonation of bromide-containing waters: Interaction of ozone and hydroxyl radical reactions.* Environmental Science and Technology, 1994. **28**(7): p. 1234-1242.
18. von Gunten, U. and Y. Oliveras, *Advanced oxidation of bromide-containig waters: Bromate formation mechanisms.* Environmental Science and Technology, 1998. **32**(1): p. 63-70.
19. von Gunten, U., *Ozonation of drinking water: Part II. Disinfection and by-product formation in presence of bromide, iodide or chlorine.* Water Research, 2003. **37**(7): p. 1469-1487.
20. Acero, J.L., K. Stemmler, and U. von Gunten, *Degradation kinetics of atrazine and its degradation products with ozone and OH radicals: A predictive tool for drinking water treatment.* Environmental Science and Technology, 2000. **34**(4): p. 591-597.
21. Pantin, S., *Impacts of UV-H_2O_2 treatment for taste and odor control on secondary disinfection*, in *Department of Civil Engineering*. 2009, University of Toronto: Toronto.
22. Trojan Technologies Inc. *TrojanUV Case studies - taste and ordor treatment with UV-oxidation: Mississauga, Ontario Canada*. 2012 [cited 2012 23.7.2012]; Available from: http://trojanuv.com/resources/trojanuv/casestudies/ECT/LornePark_CaseStudy_FINAL.pdf.
23. Katsoyiannis, I.A., S. Canonica, and U. von Gunten, *Efficiency and energy requirements for the transformation of organic micropollutants by ozone, O_3/H_2O_2 and UV/H_2O_2.* Water Research, 2011. **45**(13): p. 3811-3822.
24. *DVGW 1997. W 294. UV-Desinfektionsanlagen für die Trinkwasserversorgung - Anforderungen und Prüfung.*
25. von Sonntag, C., *Advanced oxidation processes: Mechanistic aspects.* Water Science and Technology, 2008. **58**: p. 1015-1021.
26. Siegrist, R.L., M. Crimi, and T.J. Simpkin, eds. *In sito chemical oxidation for groundwater remediation*. 2011: New York Heidelberg Dordrecht London.
27. Liang, C., C.F. Huang, and Y.J. Chen, *Potential for activated persulfate degradation of BTEX contamination.* Water Research, 2008. **42**(15): p. 4091-4100.
28. Liang, C., Z.S. Wang, and C.J. Bruell, *Influence of pH on persulfate oxidation of TCE at ambient temperatures.* Chemosphere, 2007. **66**(1): p. 106-113.
29. Hori, H., E. Hayakawa, H. Einaga, S. Kutsuna, K. Koike, T. Ibusuki, H. Kiatagawa, and R. Arakawa, *Decomposition of environmentally persistent perfluorooctanoic acid in water by photochemical approaches.* Environmental Science and Technology, 2004. **38**(22): p. 6118-6124.
30. Hori, H., Y. Nagaoka, M. Murayama, and S. Kutsuna, *Efficient decomposition of perfluorocarboxylic acids and alternative fluorochemical surfactants in hot water.* Environmental Science and Technology, 2008. **42**(19): p. 7438-7443.
31. Hori, H., A. Yamamoto, E. Hayakawa, S. Taniyasu, N. Yamashita, S. Kutsuna, H. Kiatagawa, and R. Arakawa, *Efficient decomposition of environmentally persistent perfluorocarboxylic acids by use of persulfate as a photochemical oxidant.* Environmental Science and Technology, 2005. **39**(7): p. 2383-2388.
32. Kutsuna, S. and H. Hori, *Rate constants for aqueous-phase reactions of SO_4^- with $C_2F_5C(O)O^-$ and $C_3F_7C(O)O^-$ at 298 K.* International Journal of Chemical Kinetics, 2007. **39**(5): p. 276-288.
33. Manoj, P., K.P. Prasanthkumar, V.M. Manoj, U.K. Aravind, T.K. Manojkumar, and C.T. Aravindakumar, *Oxidation of substituted triazines by sulfate radical anion ($SO_4^{\bullet-}$) in aqueous medium: A laser flash photolysis and steady state radiolysis study.* Journal of Physical Organic Chemistry, 2007. **20**(2): p. 122-129.
34. Anipsitakis, G.P. and D.D. Dionysiou, *Degradation of organic contaminants in water with sulfate radicals generated by the conjunction of peroxymonosulfate with cobalt.* Environmental Science and Technology, 2003. **37**(20): p. 4790-4797.
35. Anipsitakis, G.P. and D.D. Dionysiou, *Radical generation by the interaction of transition metals with common oxidants.* Environmental Science & Technology, 2004. **38**(13): p. 3705-3712.

36. Anipsitakis, G.P., D.D. Dionysiou, and M.A. Gonzalez, *Cobalt-mediated activation of peroxymonosulfate and sulfate radical attack on phenolic compounds. Implications of chloride ions.* Environmental Science and Technology, 2006. **40**(3): p. 1000-1007.
37. House, D.A., *Kinetics and mechanism of oxidations by peroxydisulfate.* Chemical Reviews, 1962. **62**: p. 185-203.
38. Behrman, E.J., *Studies on the mechanism of the elbs peroxydisulfate oxidation.* Journal of the American Chemical Society, 1963. **85**(21): p. 3478-3482.
39. Herrmann, H., *On the photolysis of simple anions and neutral molecules as sources of O˙7OH, $SO_x^-$and Cl in aqueous solution.* Physical Chemistry Chemical Physics, 2007. **9**(30): p. 3935-3964.
40. Kolthoff, I.M. and I.K. Miller, *The chemistry of persulfate. I. The kinetics and mechanism of the decomposition of the persulfate ion in aqueous medium.* Journal of the American Chemical Society, 1951. **73**(7): p. 3055-3059.
41. Brusa, M.A., M.S. Churio, M.A. Grela, S.G. Bertolotti, and C.M. Previtali, *Reaction volume and reaction enthalpy upon aqueous peroxodisulfate dissociation: $S_2O_8^{2-} \rightarrow 2SO_4^{\cdot-}$.* Physical Chemistry Chemical Physics, 2000. **2**(10): p. 2383-2387.
42. Heidt, L.J., *The photolysis of persulfate.* The Journal of Chemical Physics, 1942. **10**(5): p. 297-302.
43. Mark, G., M.N. Schuchmann, H.P. Schuchmann, and C. von Sonntag, *The photolysis of potassium peroxodisulphate in aqueous solution in the presence of tert-butanol: a simple actinometer for 254 nm radiation.* Journal of Photochemistry and Photobiology A, 1990. **55**(2): p. 157-168.
44. Legrini, O., E. Oliveros, and A.M. Braun, *Photochemical processes for water treatment.* Chemical Reviews, 1993. **93**(2): p. 671-698.
45. Buxton, G.V., C.L. Greenstock, W.P. Helman, and A.B. Ross, *Critical review of rate constants for reactions of hydrated electrones, hydrogen-atoms and hydroxyl radicals (˙OH/O˙⁻) in aqueous solution.* Journal of Physical and Chemical Reference Data, 1988. **17**(2): p. 513-886.
46. Pignatello, J.J., E. Oliveros, and A. MacKay, *Advanced oxidation processes for organic contaminant destruction based on the fenton reaction and related chemistry.* Critical Reviews in Environmental Science and Technology, 2006. **36**(1): p. 1-84.
47. Liang, C. and C.J. Bruell, *Thermally activated persulfate oxidation of trichloroethylene: Experimental investigation of reaction orders.* Industrial and Engineering Chemistry Research, 2008. **47**(9): p. 2912-2918.
48. von Sonntag, C., ed. *Free-radical-induced DNA damage and its repair- A chemical perpesctive*. 2005, Springer Berlin Heidelberg.
49. Behrman, E.J., *The Elbs and Boyland-Sims peroxydisulfate oxidations.* Beilstein Journal of Organic Chemistry, 2006. **2**.
50. Wardman, P., *Reduction potentials of one-electron couples involving free-radicals in aqueous-solution*. Vol. 18 1989. 1637-1755.
51. Christensen, H.C., K. Sehested, and E.J. Hart, *Formation of benzyl radicals by pulse radiolysis of toluene in aqueous solutions.* The Journal of Physical Chemistry, 1973. **77**(8): p. 983-987.
52. Redpath, J.L. and R.L. Willson, *Chain reactions and radiosensitization: model enzyme studies.* International Journal of Radiation Biology, 1975. **27**(4): p. 389-398.
53. Eibenberger, H., S. Steenken, P. O'Neill, and D. Schulte-Frohlinde, *Pulse radiolysis and electron spin resonance studies concerning the reaction of SO4-˙ with alcohols and ethers in aqueous solution [1].* Journal of Physical Chemistry, 1978. **82**(6): p. 749-750.
54. Clifton, C.L. and R.E. Huie, *Rate constants for hydrogen abstraction reactions of the sulfate radical, $SO_4^{\cdot-}$. Alcohols.* International Journal of Chemical Kinetics, 1989. **21**(8): p. 677-687.
55. Dogliotti, L., *Flash photolysis of persulfate ions in aqueous solutions. Study of the sulfate and ozonide radical ions.* Journal of Physical Chemistry, 1967. **71**(8): p. 2511-2516.

56. Neta, P. and L.M. Dorfman, *Pulse radiolysis studies. 13. Rate constants for reaction of hydroxyl radicals with aromatic compounds in aqueous solution.* Advances in Chemistry Series, 1968(81).
57. Willson, R.L., C.L. Greenstock, G.E. Adams, R. Wageman, and L.M. Dorfman, *The standardization of hydroxyl radical rate data from radiation chemistry.* International Journal for Radiation Physics and Chemistry, 1971. **3**(3): p. 211-220.
58. Buxton, G.V., *Pulse radiolysis of aqueous solutions. Rate of reaction of OH with OH.* Transactions of the Faraday Society, 1970. **66**: p. 1656-1660.
59. Thomas, J.K., *Rates of reaction of the hydroxyl radical.* Transactions of the Faraday Society, 1965. **61**: p. 702-707.
60. Elliot, A.J. and A.S. Simsons, *Rate constants for reactions of hydroxyl radicals as a function of temperature.* Radiation Physics and Chemistry, 1984. **24**(2): p. 229-231.
61. Neta, P., R.E. Huie, and A.B. Ross, *Rate constants for reactions of inorganic radicals in aqueous solution.* Journal of Physical and Chemical Reference Data, 1988. **17**(3): p. 1027 - 1040.
62. Neta, P., V. Madhavan, H. Zemel, and R.W. Fessenden, *Rate constants and mechanism of reaction of sulfate radical anion with aromatic compounds.* Journal of the American Chemical Society, 1977. **99**(1): p. 163-164.
63. Plumlee, M.H., K. McNeill, and M. Reinhard, *Indirect photolysis of perfluorochemicals: Hydroxyl radical-initiated oxidation of N-ethyl perfluorooctane sulfonamido acetate (N-EtFOSAA) and other perfluoroalkanesulfonamides.* Environmental Science and Technology, 2009. **43**(10): p. 3662-3668.
64. Tsang, W., D.R. Burgess Jr, and V. Babushok, *On the incinerability of highly fluorinated organic compounds.* Combustion Science and Technology, 1998. **139**(1): p. 385-402.
65. Vecitis, C.D., H. Park, J. Cheng, B.T. Mader, and M.R. Hoffmann, *Treatment technologies for aqueous perfluorooctanesulfonate (PFOS) and perfluorooctanoate (PFOA).* Frontiers of Environmental Science and Engineering in China, 2009. **3**(2): p. 129-151.
66. Maruthamuthu, P., S. Padmaja, and R.E. Huie, *Rate Constants for Some Reactions of Free Radicals with Haloacetates in Aqueous Solution.* International Journal of Chemical Kinetics, 1995. **27**: p. 605-612.
67. Schwarzenbach, R.P., P.M. Gschwend, and D.M. Imboden, eds. *Environmental organic chemistry*. John Wiley & Sons, Inc. ISBN 0-47 1-35750-2. 2003.
68. Huie, R.E. and C.L. Clifton, *Temperature dependence of the rate constants for reactions of the sulfate radical, SO_4^-, with anions.* Journal of Physical Chemistry, 1990. **94**(23): p. 8561-8567.
69. Padmaja, S., P. Neta, and R.E. Huie, *Rate constants for some reactions of inorganic radicals with inorganic ions. Temperature and solvent dependence.* International Journal of Chemical Kinetics, 1993. **25**(6): p. 445-455.
70. Tauber, A. and C. von Sonntag, *Products and kinetics of the OH-radical-induced dealkylation of atrazine.* Acta Hydrochimica et Hydrobiologica, 2000. **28**(1): p. 15-23.
71. Mendez-Diaz, J., M. Sanchez-Polo, J. Rivera-Utrilla, S. Canonica, and U. von Gunten, *Advanced oxidation of the surfactant SDBS by means of hydroxyl and sulphate radicals.* Chemical Engineering Journal, 2010. **163**(3): p. 300-306.
72. Konya, K.G., T. Paul, S. Lin, J. Lusztyk, and K.U. Ingold, *Laser flash photolysis studies on the first superoxide thermal source. First direct measurements of the rates of solvent-assisted 1,2-hydrogen atom shifts and a proposed new mechanism for this unusual rearrangement.* Journal of the American Chemical Society, 2000. **122**(31): p. 7518-7527.
73. Pan, X.M., M.N. Schuchmann, and C. Von Sonntag, *Oxidation of benzene by the OH radical. A product and pulse radiolysis study in oxygenated aqueous solution.* Journal of the Chemical Society, Perkin Transactions 2, 1993(3): p. 289-297.

74. Norman, R.O.C., P.M. Storey, and P.R. West, *Electron spin resonance studies. Part XXV. Reactions of the sulphate radical anion with organic compounds.* Journal of the Chemical Society B: Physical Organic, 1970: p. 1087-1095.
75. Mertens, R., ed. *Photochemie und Strahlenchemie von organischen Chlorverbindungen in wäßriger Lösung*. Dissertation. 1994: Mülheim an der Ruhr.
76. Neta, P., J. Grodkowski, and A.B. Ross, *Rate constants for reactions of aliphatic carbon-centered radicals in aqueous solution.* Journal of Physical and Chemical Reference Data, 1996. **25**(3): p. 709-988.
77. Elovitz, M.S. and U. von Gunten, *Hydroxyl radical/ozone ratios during ozonation processes. I. The R(ct) concept.* Ozone: Science and Engineering, 1999. **21**(3): p. 239-260.
78. Elovitz, M.S., U. von Gunten, and H.P. Kaiser, *Hydroxyl radical/ozone ratios during ozonation processes. II. The effect of temperature, pH, alkalinity, and DOM properties.* Ozone: Science and Engineering, 2000. **22**(2): p. 123-150.

Chapter 2

-

Scope

Trace pollutants belong to the major issues in drinking water treatment and partly in wastewater treatment and are suspected to cause adverse health effects upon long term exposure. One option for pollutant control is oxidative water treatment. However, the increasing number of pollutants and their large chemical diversity request a continuous development in oxidative water treatment. As highly reactive species sulfate radicals ($SO_4^{\bullet-}$) are principally capable of degrading a large range of pollutants. Thus, $SO_4^{\bullet-}$ based oxidation is frequently discussed as an alternative oxidative treatment option for pollutant control in water treatment. Indeed, due to the different nature of $^{\bullet}OH$ and $SO_4^{\bullet-}$, $SO_4^{\bullet-}$ may have a potential to overcome limitations of conventional AOP. A $SO_4^{\bullet-}$ based oxidation process could be realized by using existing plants designed for advanced oxidation processes based on H_2O_2 (e.g., Fenton or UV/H_2O_2), since formation of $SO_4^{\bullet-}$ works in a similar way on basis of $S_2O_8^{2-}$.
Even though the chemistry of $S_2O_8^{2-}$ and $SO_4^{\bullet-}$ has been studied since nearly one century, major gaps of knowledge regarding chemical processes related to water treatment hardly allow any estimate about the feasibility of such a process.
The present work provides a systematic survey of the potential of UV/$S_2O_8^{2-}$ as a water treatment option. In that regard oxidation efficiency and by-product formation in presence of typical main constituents of natural waters have been investigated. The experimental approach is based on comparing the new process UV/$S_2O_8^{2-}$ with applied treatment options as a reference (i.e., UV/H_2O_2 and ozonation). This allows a direct comparison with standard treatment options in addition to a literature based analysis.

For studying $SO_4^{\bullet-}$ chemistry using $S_2O_8^{2-}$ as a radical precursor several precautions have to be taken into account. Main aspects are the high reactivity of $SO_4^{\bullet-}$ with buffers and halides and the presence of distinctive steady state concentrations of $SO_4^{\bullet-}$ during storage of samples containing $S_2O_8^{2-}$. To our knowledge, chapter 3 provides a first compilation of precautions mandatory for avoiding interferences in studying $SO_4^{\bullet-}$ chemistry.

Atrazine has been used as one of the model compounds in the present study and thus, its reaction with $SO_4^{\bullet-}$ along with other triazine herbicides has been characterized with regard to reaction kinetics and product formation (chapter 4). The results have been compared with $^{\bullet}OH$ reactions revealing similarities in both, reaction kinetics and product pattern.

In water treatment the life time of an oxidant largely depends on its reactivity towards main water constituents (i.e., alkalinity and organic matter). While reaction rates of $SO_4^{\bullet-}$ plus HCO_3^- and CO_3^{2-}

are already known hardly any quantitative information about the reactivity of $SO_4^{\bullet-}$ towards organic matter of natural waters is reported in the literature. In chapter 5 the kinetics of the reaction $SO_4^{\bullet-}$ plus different types of humic acids are determined and compared with corresponding reactions of $^{\bullet}OH$.

The formation of by-products is another important key parameter in oxidative water treatment. One of the notorious by-products is bromate (BrO_3^-) which is one reason to switch from ozonation to UV/H_2O_2 where no BrO_3^- is formed. In the discussion of UV/$S_2O_8^{2-}$ as an alternative process to UV/H_2O_2 the BrO_3^--formation potential has to be carefully investigated. Since $SO_4^{\bullet-}$ react very fast with Br^-, BrO_3^- formation is possible in principle. The complex reactions in the oxidation of Br^- by $SO_4^{\bullet-}$ were studied and a model of BrO_3^- was developed in Chapter 6. The reaction of $SO_4^{\bullet-}$ plus Br^- was investigated in pure water as well as in presence of natural matrices.

Main constituents of the water matrix largely influence the efficiency of oxidative water treatment. In that regard the complex interactions of chloride, alkalinity and NOM in UV/$S_2O_8^{2-}$ were investigated and a kinetic model for predicting the degradation of pollutants was developed in Chapter 7. Understanding the reactions that happen in natural matrices during UV/$S_2O_8^{2-}$ is helpful for assessing the energy efficiency of pollutant degradation, which belongs to the crucial points in water treatment. The efficiency of pollutant degradation in UV/$S_2O_8^{2-}$ has been investigated for a surface water used for drinking water production (River Ruhr water) and compared with standard methods in oxidative water treatment (i.e., UV/H_2O_2 and ozonation). That allows estimating the feasibility of UV/$S_2O_8^{2-}$ as a water treatment process for pollutant control.

The degradation of perfluorinated carboxylic acids by $SO_4^{\bullet-}$ has been frequently cited as a potential water treatment option. However, a critical study about the feasibility of a $SO_4^{\bullet-}$ based process for degrading these compounds is yet lacking. Furthermore, the reaction of perfluorinated sulfonic acids plus $SO_4^{\bullet-}$ has not yet been investigated. Chapter 8 provides some mechanistic and kinetic data with regard to the degradation of perfluorinated carboxylic acids and perfluorinated sulfonic acids in their reaction with $SO_4^{\bullet-}$. These data have been used for estimating if $SO_4^{\bullet-}$ could be a suitable agent for their degradation in drinking or waste water treatment.

The data revealed in Chapter 3-8 enable a first assessment of the feasibility of UV/$S_2O_8^{2-}$ as a water treatment process contrasting potential advantages and disadvantages with regard to standard treatment options. Furthermore, the approach developed in the present study for studying $SO_4^{\bullet-}$ based oxidation as

a water treatment option can also be used for investigating the feasibility of other oxidative treatment options.

Chapter 3

New concepts in peroxodisulfate chemistry

-

experimental aspects

3.1 Introduction

Even though $S_2O_8^{2-}$ chemistry has been investigated since more than one century, aspects regarding experimental procedures still need further elucidation. This applies e.g., for storage of samples containing $S_2O_8^{2-}$ which can be very instable. Nevertheless, such aspects are hardly addressed in the current literature. In the present chapter some of these gaps are closed and a set of precautions is developed which is very important for preventing bias in using $S_2O_8^{2-}$ for studying reactions of $SO_4^{\bullet-}$. Furthermore, one emphasis of the thesis is photochemistry. Thus, photochemical concepts applied are also explained in the present chapter.

3.2 Material and methods

3.2.1 Chemicals

Following chemicals have been used as received:
Acetonitrile (≥ 99.9%) Sigma Aldrich, *Atrazine* (≥97.4%) Riedel-de Haën, *acetonitrile 4-chlorobenzoic acid* (≥ 99%) Sigma-Aldrich, *ethanol* (99.9%) VWR, *hydrochloric acid* (37% in water, p.a.) Merck, *hydrogen peroxide* (30%) Sigma Aldrich *methanol* (≥ 99.9%) Applichem and (≥ 99.9%) VWR, *potassium chloride* (≥ 99.5%) Riedel-de Haën, *sodium hydroxide* (≥ 99%) VWR, *sodium peroxodisulfate* (≥ 99%) Riedel-de Haën, *sulfuric acid* (95-97%) Applichem and (> 95%) Fischer Chemical, *terbuthylazine* (≥ 98.8%), Fluka, *thiosulfate* (≥ 99.8%) Sigma-Aldrich

3.2.2 Experimental procedures

General aspects: $SO_4^{\bullet-}$ were generated by thermal activation of $S_2O_8^{2-}$ at different temperatures (scavenger tests: 60°C, competition kinetics 40, 50 and 60°C). The pH of the solutions was adjusted with NaOH or sulfuric acid (depending on the initial pH of the solution). In experiments involving $SO_4^{\bullet-}$, samples may slowly acidify, e.g., due to their reaction with chloride (chapter 1 and chapter 7). Yet, no buffers were used due to their potential interference in $SO_4^{\bullet-}$-based reactions (see below). However, in studying $SO_4^{\bullet-}$ reactions speciation of every reactant has to be controlled, since it may influence both, reaction pathway and reactivity. Thus, pH was measured over the whole time span of an experiment. A threshold value of the pH has been defined to be one pH unit above the p*K*a values of all

reactants. In case the pH dropped below this threshold value, the corresponding experiment was aborted or samples were no longer used for data interpretation.

Analytics. The triazine herbicides and pCBA were determined by following HPLC instruments (Shimadzu): Liquid chromatograph LC 20-AT equipped with UV/Vis detector SPD 20A, Auto sampler SIL 20A, Degasser DGU-20A$_5$, communication bus module CBM 20A and column oven CTO-10AS vp and Liquid chromatograph LC-10AT vp equipped with an diode array detector SPD M10A vp, auto sampler SIL 10 AD vp, degasser DGU 14A, system controller SCL-10A vp and column oven CTO-10AS vp. For separation of the analytes a reversed phase column (ProntoSIL C-18; 5 µm particle size 250 × 4.0 mm, Bischoff) has been used and following methods applied:

Determination of atrazine in presence and absence of methanol or ethanol:
Flow rate: 0.5 mL min^{-1}; injection volume: 50 µL; detected wavelength: 220 nm; isocratic eluent (50 % methanol / 50 % water (pH not controlled)); retention time: 34 min

Simultaneous determination of pCBA and atrazine: Flow rate 0.7 ml min^{-1}; detected wavelengths 220 nm & 234 nm. Following eluent program has been applied (acetonitrile/water (pH 2, adjusted with HCl) (%)):0-1 min, isocratic at 10/90, 1-21 min gradient to 100/0, 25-26 min isocratic at 100/0, 26-36 min gradient to 10/90; Retention times pCBA: 19.2 min, atrazine: 20.0 min

Determination of terbutylazine: Flow rate: 1 ml min^{-1}; injection volume: 50 µL; detected wavelength range: 200-400 nm; retention-time of terbuthalyzine (14.9 min):
Eluent program (acetonitrile/water (%) (pH not controlled)): 0-3 min: isocratic at 8/92,
3-7 min: gradient to 70/30, 7-30 min: isocratic at 70/30, 30-31 min: gradient to 08/92, 31-40 min: isocratic at 08/92

Determination of chloride:
Chloride has been determined by the following ion chromatograph (Metrohm): 883 Basic IC plus equipped with an conductivity detector and chemical ion suppression, an anion separation column (250 × 4.0 mm, Metrosep Asup 4) and an 863 compact auto-sampler. Following method has been applied: Flow rate 1 ml min^{-1}; injection volume: 20 µL; Eluent: 1.8 mM Na_2CO_3 and 1.6 mM $NaHCO_3$ mixed with acetonitrile (ratio 7:3) (note that addition of acetonitrile reduces the retention time of $S_2O_8^{2-}$. This

is important since the presence of $S_2O_8^{2-}$ can cause acquisition times of several hours); retention time of chloride: 3.8 min

3.4 Storage of samples containing persulfate

The thermal rupture of the peroxide bond in $S_2O_8^{2-}$ yields low steady state concentrations of $SO_4^{\bullet-}$ even at ambient temperature (e.g., 20 °C). Thus, aqueous solutions of compounds which are reactive towards $SO_4^{\bullet-}$ may not be stable over time in presence of $S_2O_8^{2-}$. This is of particular importance when $S_2O_8^{2-}$ is present in excess over a substrate, which can apply in case $S_2O_8^{2-}$ is used as a radical source (e.g., UV/$S_2O_8^{2-}$). If storage of samples obtained from such kind of experiments lasts for more than one day $SO_4^{\bullet-}$ formation has to be suppressed. Principally one possibility is chemical quenching of $S_2O_8^{2-}$, thus removing the radical source from the reaction system. However, direct reactions of $S_2O_8^{2-}$ are often slow and hampered by formation of free radicals in the reaction of $S_2O_8^{2-}$ with a reducing agent (e.g., reduced transition metals [1]). Another possibility is the addition of an appropriate $SO_4^{\bullet-}$ scavenger.

Such kind of a scavenger has to fulfill following prerequisites:

1. Sufficiently fast reaction with $SO_4^{\bullet-}$
2. Good solubility in water
3. Products formed in the reaction of $SO_4^{\bullet-}$ with the scavenger must not cause interferences
4. Further sample preparation (e.g., derivatization) must not be adversely affected

Short chain alcohols (i.e., C_1-C_4) react moderately fast with $SO_4^{\bullet-}$ (> 10^7 $M^{-1}s^{-1}$ [2]) and are mixable with water thus, no limitation with regard to solubility has to be considered. In experiments regarding degradation of organic compounds such as chlorotriazine herbicides, high dosages of aliphatic alcohols (i.e., methanol or ethanol) effectively suppress triazine degradation at room temperature (Figure 1).

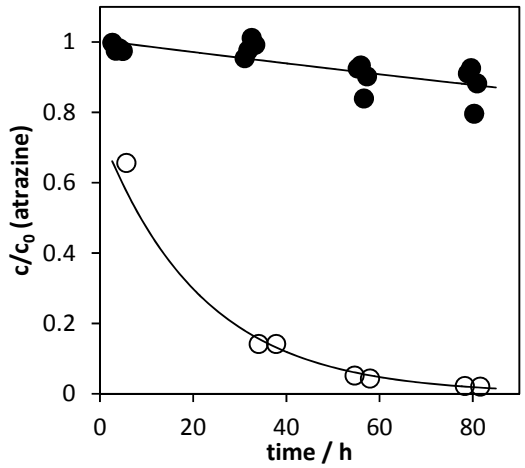

Figure 1: Degradation of atrazine in solutions containing $S_2O_8^{2-}$ at room temperature in presence of ethanol or methanol (0.5 and 1 M) (filled symbols) and in absence of a radical scavenger (open symbols); $[S_2O_8^{2-}]_0$ = 1 mM, $[atrazine]_0$ = 5 µM, T = 20-25°C, pH not controlled

Even in presence of these short chain alcohols a long storage time (i.e., > 2 days) has to be avoided since little changes in the composition of the sample can hardly be prevented, albeit these interferences are further suppressed by storage in the refrigerator or cooling chamber. Thus, samples were measured as soon as possible after performing the experiment. Furthermore, $S_2O_8^{2-}$ has also been added as the last reagent for initiating the reaction. Furthermore, the performance of calibrations as well as measurements of control samples withdrawn right before addition of $S_2O_8^{2-}$ allowed recognizing changes during storage time related to $S_2O_8^{2-}$ chemistry.

Alternatively to the organic scavengers mentioned above, inorganic scavengers such as thiosulfate ($S_2O_3^{2-}$) can be applied in principle. Using $S_2O_3^{2-}$ as a $SO_4^{\bullet-}$ scavenger revealed an optimal dose of around 0.125 mM. If higher concentrations of $S_2O_3^{2-}$ are added, the degradation rates of the chlorotriazine herbicides increase, albeit they are still slower compared with experiments lacking any radical scavenger (Figure 2). This indicates that a direct reaction of $S_2O_8^{2-}$ and $S_2O_3^{2-}$ activates the peroxide yielding $SO_4^{\bullet-}$. However, $SO_4^{\bullet-}$ are also scavenged by $S_2O_3^{2-}$, thus lowering the overall oxidation capacity. The chemistry of these reactions is very complex and is probably still not sufficiently understood [3, 4]. However, this topic exceeds the scope of the present study and will not be discussed in more detail.

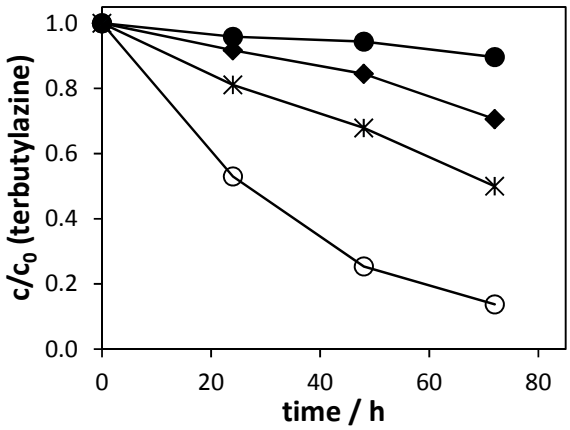

Figure 2: Degradation of terbuthylazine (20 µM) in presence of $S_2O_8^{2-}$ (1 mM) at room temperature and different concentrations of thiosulfate (0.125 M (closed circles), 0.25 M (diamonds), 0.5 M (stars), no $S_2O_3^{2-}$ (open circles); pH not controlled

Furthermore, preliminary experiments revealed that $S_2O_3^{2-}$ may inhibit derivatization of aldehydes using dinitrophenylhydrazine (for more information about use of hydrazine reagents in environmental analysis see review of Vogel et al. [5]). In that regard aliphatic alcohols also have to be carefully used, since they may yield aldehydes in their reaction with $SO_4^{\bullet-}$, which would contaminate the samples. However, the latter kind of interference can be avoided by choosing a suitable alcohol (e.g., methanol cannot yield other aldehydes than formaldehyde or acids than formic acid). Finally, methanol and ethanol have been chosen for "preserving" samples containing $S_2O_8^{2-}$. These alcohols are comfortable in use (easy preparation of stock solution, can be stored over long periods of time) and do not lead to adverse effects on analytical procedures used in the present work.

3.5 Effect of chloride and other inorganic ions

In 1990, McElroy described the reaction of $SO_4^{\bullet-}$ with Cl^- in atmospheric droplets yielding $^{\bullet}OH$ at neutral pH [6]. Thus, in experiments involving $SO_4^{\bullet-}$ chemistry the presence of Cl^- has to be controlled carefully. However, complete avoidance of Cl^- in the samples is extremely difficult and mostly one has to deal with fluctuating concentrations in the lower µM range. Important sources of Cl^- are the conventional pH electrode using KCl as electrolyte, impurities in reagents and the lab air. In our experiments the Cl^- concentration ranged from 2 – 30 µM which is problematic in case other reactants are present in similar concentrations (e.g., due to limitations in solubility). In fact the presence of Cl^- might be a more important source of $^{\bullet}OH$ in $SO_4^{\bullet-}$ based systems than the frequently cited reaction of $SO_4^{\bullet-}$ with OH^-. Interferences by Cl^- can affect product yields and reaction kinetics and thus, bias the experimental results silently. One strategy for preventing effects of Cl^- is addition of *tert*-butanol. *tert*-

butanol can act as a selective scavenger for $^{\bullet}OH$ because it reacts ≈ 1000 times faster with $^{\bullet}OH$ (6×10^8 M^{-1} s^{-1} [7]) compared to $SO_4^{\bullet-}$ (4-9.1 × 10^5 M^{-1} s^{-1} [2]). *tert*-butanol has been used for scavenging of $^{\bullet}OH$ in case of the determination of reaction rate constants by competition kinetics for triazine herbicides (Chapter 4) (typical composition of the reaction solution was: 5 µM of an triazine herbicide (e.g., atrazine $k(^{\bullet}OH) = 3 \times 10^9$ $M^{-1}s^{-1}$ [8, 9]; $k(SO_4^{\bullet-}) = 3 \times 10^9$ $M^{-1}s^{-1}$ [10], 5 µM of a competitor (e.g., pCBA $k(^{\bullet}OH) = 5 \times 10^9$ $M^{-1}s^{-1}$, $k(SO_4^{\bullet-}) = 3.6 \times 10^8$ $M^{-1}s^{-1}$ [11]), 1 mM $S_2O_8^{2-}$ and *tert*-butanol (see below). Every experimental run has been performed in presence of 1 and 10 mM *tert*-butanol. With kinetic data given above, scavenging of $^{\bullet}OH$ and $SO_4^{\bullet-}$ by *tert*-butanol can be calculated. Thereby, 1 mM *tert*-butanol results in 94% scavenging of $^{\bullet}OH$ and 10% scavenging of $SO_4^{\bullet-}$ and 10 mM *tert*-butanol leads to 99% scavenging of $^{\bullet}OH$ and 53% scavenging of $SO_4^{\bullet-}$. Under such conditions interferences by $^{\bullet}OH$ can be ruled out.

3.6 Competition kinetics at elevated temperatures

Reaction rate constants of $SO_4^{\bullet-}$ have been determined by competition kinetics in analogy to Peter and von Gunten, [12]. Thereby, the observed degradation rate of a probe compound under investigation is related to the observed degradation rate of a reference compound (note that both compounds have to experience the same exposure of the oxidant, e.g., by their simultaneous degradation in one reaction system). The slope of a plot such as shown in Figure 3 yields the ratio of the reaction rates of probe and reference compound, from which the unknown reaction rate can be obtained (further detailed information about competition kinetics is provided by von Sonntag and von Gunten [13]).

$SO_4^{\bullet-}$ has been generated by thermolysis of $S_2O_8^{2-}$ at 60°C. It is important to point out that the reaction rate determined under such condition corresponds to the temperature at which the reaction rate of the competitor has been determined (typically 20-25°C). This is due to the fact that the activation energies in the reaction with radicals such as $SO_4^{\bullet-}$ and $^{\bullet}OH$ hardly differ between different reaction partners. This has been verified by comparing the observed degradation rates of atrazine and 4-chlorobenzoic acid in their degradation with $SO_4^{\bullet-}$ generated by thermal activation of $S_2O_8^{2-}$ at different temperatures. This couple of compounds is suited well for this kind of test, since corresponding reaction rates differ by nearly one order of magnitude, thus, representing a worst case scenario with regard to difference in activation energies. Figure 3 shows the first order degradation rate of pCBA vs. atrazine during thermal activation of $S_2O_8^{2-}$ at 40, 50, and 60°C.

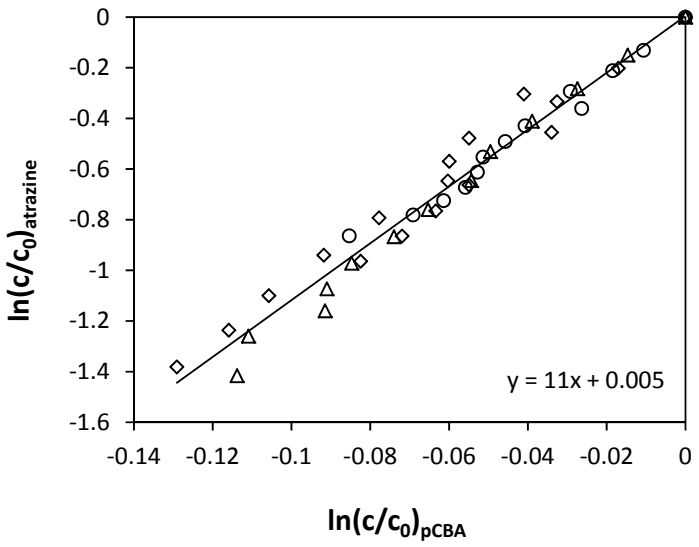

Figure 3: Degradation of pCBA vs. atrazine during thermal activation of $S_2O_8^{2-}$ at 40 °C (circles), 50 °C (triangles) and 60 °C (diamonds); $[pCBA]_0$ = 4.71 ± 0.02 µM, $[atrazine]_0$ = 4.63 ± 0.12 µM; $[S_2O_8^{2-}]_0$ = 1 mM; initial pH: 7

It can be seen, that data obtained from thermal activation at all temperatures lie on one line indicating that differences in activation energy can be neglected. From this plot a reaction rate for atrazine of 4.0×10^9 M^{-1} s^{-1} can be obtained which fairly well matches the value of Manoj determined by laser flash photolysis (3×10^9 M^{-1} s^{-1} [10]).

3.7 Use of buffers

In $S_2O_8^{2-}$ chemistry changes in pH easily happen. This is mainly due to electron transfer reactions of $SO_4^{\bullet-}$ with e.g., Cl^- (note that $Cl^\bullet$ yields H^+ and $^\bullet OH$ in the reaction with water [6]) and to a minor extent with OH^- (k = 4.6-8.3 × 10^7 $M^{-1}s^{-1}$). Furthermore, H-abstraction by $SO_4^{\bullet-}$ yields HSO_4^- which may give rise to H^+ upon its dissociation. In many cases changes in pH are not desirable and buffers have to be dosed for maintaining a certain pH. However, the reactivity of buffer ions towards $SO_4^{\bullet-}$ limits the dose to be applied. Such kind of reactions have to be avoided since other inorganic radicals are probably formed which could lead to interferences (e.g., $HPO_4^{\bullet-}$ in case phosphate is used as buffer). This could even happen in case corresponding kinetics are slow (e.g., $k(SO_4^{\bullet-} + HPO_4^-)$ = 1.2 × 10^6 M^{-1} s^{-1}) since high doses of buffers have to be applied (e.g., for studying the oxidation of Br^- phosphate has to be added in the upper mM level). The reactivity of buffers has to be kept in mind before a buffer system is used.

3.8 Photochemical calculations

The degradation of pollutants in UV/H_2O_2 or UV/$S_2O_8^{2-}$ can be modeled based on the average flux of photons penetrating a sample (fluence rate). The fluence rate can be determined by monitoring the degradation of a photo-sensitive probe compound (actinometer), if the corresponding quantum yield and absorption coefficient at the wavelength emitted by the radiation source is known (e.g., 254 nm in case Hg-low pressure lamps equipped with a filter for the emission band at 185 nm are used)). It has to be assured, that the actinometer does not lead to a significant change in absorption upon its degradation. This can be achieved by either using very high concentrations (total absorption e.g., $A > 2$ cm^{-1}) or very low concentration (vanishing absorption $A < 0.1$ cm^{-1}). In the first method very low turnovers are achieved, thus > 95% of photons are absorbed during the whole time span of the experiment. Thereby the incident fluence rate is determined. This method requires the determination of a product formed in the photochemical reaction. At vanishing absorption < 10% of the photons are absorbed by the photo-sensitive compound. In this case the degradation of the actinometer does not affect the absorption of the sample. Actinometry at vanishing absorption of the actinometer can also be used in presence of other compounds (e.g., NOM) for taking the UV-absorption of the water matrix into account. Furthermore the average fluence rate of non-optimal reactor geometries can be determined since the UV-light penetrates the whole optical path length. Since in most experiments of the present work the samples distinctively absorbed UV-radiation (e.g., 0.2 cm^{-1} at 254 nm) actinometry has been performed at vanishing absorption applying the experimental procedure described by Canonica at al., [14]. Thereby, the average fluence rate can be obtained from the first order degradation rate of an actinometer (e.g., atrazine) (Figure 5).

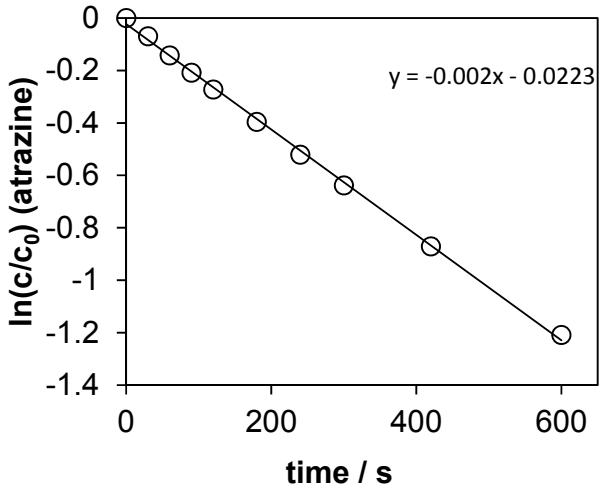

Figure 4: Photo-degradation of atrazine in River Ruhr water; [DOC] = 2.45 mgL^{-1}, [HCO_3^-] = 2.07 mM; $[atrazine]_0$ = 5 µM, A_{254nm} = 0.058 cm^{-1}, radiation source: low pressure mercury arc (185 nm band suppressed); pH= 7.2, T = 25°C

The slope in Figure 4 is proportional to the fluence rate (Equation 1).

$$E_{\lambda}^{avg} = \frac{k(photolysis\ \ of\ \ atrazine)}{2.303 \times \phi_{atrazine} \times \varepsilon_{atrazine}} = 45 \times 10^{-6}\ Einstein\ m^{-2} s^{-1} \qquad \text{(Equation 1)}$$

E_{λ}^{avg} = Fluence rate in presence of NOM (Einstein m^{-2} s^{-1})

k(photolysis of atrazine) = First order degradation rate of atrazine (s^{-1})

$\phi_{atrazine}$ = Quantum yield of atrazine (0.045 mol $Einstein^{-1}$ at 254 nm [14])

$\varepsilon_{atrazine}$ = Molar absorption coefficient of atrazine (386 mol^{-1} m^2 at 254 nm)

However, the inner filter effect caused by e.g., NOM can also be calculated by using the Morrowitz correction (Equation 2) which will be explained in the following (see also Katsoyiannis et al. [15]). In this calculation the fluence rate determined at negligible absorption (i.e., in pure water at 254 nm) can be corrected for another solution revealing a higher absorption. This helps confirming the results of the internal actinometer.

$$E_{\lambda}^{avr} = S_{\lambda} \times E_{\lambda} = \frac{1-10^{-A_{\lambda}}}{2.303 A_{\lambda}} E_{\lambda} \quad \text{(Equation 2)}$$

E_{λ}^{avg} = Fluence rate in presence of NOM (Einstein $m^{-2} s^{-1}$)

S_{λ} = Morrowitz correction coefficient

E_{λ} = Fluence rate in pure water without significant absorption (Einstein $m^{-2} s^{-1}$)

A_{λ} = Absorbance of the water matrix (cm^{-1})

The absorbance (A_{λ}) can be calculated for the quartz tubes as follows:

$$A_{\lambda} = a_{\lambda} \times l^{avg} \quad \text{(Equation 3)}$$

A_{λ} = Absorbance at wavelength λ

l^{avg} = Average optical path length

The fluence rate was used for calculating the radical formation rate $k^{+}(radical)$ by using Φ and ϵ of the radical precursor (e.g., H_2O_2: Φ = 1 mol Einstein^{-1} [16] , ϵ = 18.6 cm^{-1} [15]) or $S_2O_8^{2-}$: 1.4 mol Einstein^{-1} [17, 18], ϵ = 22 cm^{-1} [19]) (Equation 4).

$$k[radical]^{+} = E_{\lambda}^{avg} \times \varepsilon \times \phi \times [peroxide] \quad \text{(Equation 4)}$$

As mentioned above, most of the radicals react with matrix compounds of the water (mainly DOM and HCO_3^-/CO_3^{2-}) thus, the radical steady state concentration can be calculated by dividing the radical formation rate by the scavenger rate (reaction rate of corresponding reaction (k_i(radical$_i$ + scavenger$_i$)) multiplied by the concentration of the scavenger [scavenger]$_i$) (Equation 5).

$$[radical]_{steady\,state} = \frac{k[radical]^{+}}{\sum k_i (radical + scavenger) \times [scavenger]_i} \quad \text{(Equation 5)}$$

The product of [radical]$_{steady\ state}$ and time yields the radical exposure (integral of radical concentration over time ($\int [radical] dt$)) which can be used for predicting the concentration of a pollutant (P) at a defined reaction time. However, this requests that the reaction rate constant of P with the corresponding

radical (k (radical + P)) is known (Equation 6). Note that direct photo-oxidation (k(photolysis of P) has also to be taken into account.

$$[P] = [P]_0 \times e^{-k(radical+P)\times\int[radical]dt - k(photolysis\ of\ P)} \qquad \text{(Equation 6)}$$

This approach allows an easy and fast description of pollutant degradation in UV/H_2O_2 and UV/$S_2O_8^{2-}$ systems since most reactions affecting pollutant degradation are irreversible. However, if the reaction system is more complex with various equilibria a suitable software tool has to be used. For this purpose kintecus [20] has been applied.

The photochemical experiments have been conducted in a merry-go-round type photo-reactor (Figure 5). This reactor was equipped with an Hg-low pressure arc located in the center of the rotating disk fixating samples tubes made of standard quartz glass. The radiation source was placed into a vessel which could be thermostatted by an external water cycle. Both, the vessel of the radiation source and the sample tubes were merged in deionized water allowing to control the temperature of the samples.

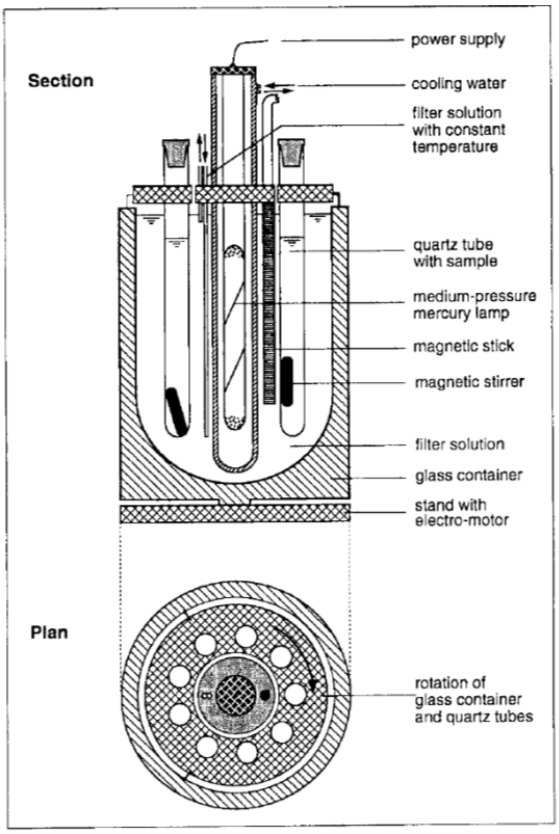

Figure 5: Merry-go-round photo-apparatus (figure taken from Wegelin et al., [21])

3.9 Use of model compounds

For characterization of $SO_4^{\bullet-}$ based processes in natural matrices a set of model compounds has been used (i.e., 4-chloro benzoic acid (pCBA), 4-nitrobenzoic acid (pNBA) and atrazine). Since these compounds behave very differently in photochemical systems such as UV/$S_2O_8^{2-}$ and UV/H_2O_2 their degradation pattern allows characterizing the mechanisms of pollutant degradation in these processes (see below). Table 1 summarizes reaction rate constants and photochemical features of the model compounds used in the present study. The quantum yields of pNBA and pCBA have been obtained by determining their observed rate of direct photolysis at a known fluence rate (Figure 6). Note, that pNBA and pCBA was dosed in small concentrations (0.5 µM). Thus, their contribution on the overall absorption can be neglected. Solving equation 1 for quantum yield can then be used to calculate the quantum yields of pNBA and pCBA.

Table 1: Reaction rate constants, absorption coefficients and quantum yields of atrazine, pNBA and pCBA, a) this study

Model compound	$k(SO_4^{\bullet-})$ / $M^{-1} s^{-1}$	$k(^{\bullet}OH)$ / $M^{-1} s^{-1}$	A_{254} / cm^{-1}	Φ / $Einstein^{-1}$
Atrazine	1.4×10^9 [22] 3×10^9 [10]	3×10^9 [8, 9] 1.2×10^9 [22]	3860 [23]	0.05[23]
pNBA	$\leq 10^6$ [11]	2.6×10^9 [7]	11750 [24]	< 0.0003[a)]
pCBA	3.6×10^8 [11]	5×10^9 [7]	4670 [24]	0.008[a)]

Atrazine represents persistent pollutants which react similar fast with $SO_4^{\bullet-}$ and $^{\bullet}OH$. This allows comparing radical yields and exposures in processes such as UV/$S_2O_8^{2-}$ and UV/H_2O_2. Furthermore, the high molar absorption and the distinctive quantum yield at 254 nm enables determining the fluence rate in photo-reactors using a low pressure Hg-arc as a radiation source (mainly emitting 254 nm, see above) according to Canonica et al., [14] (see above). pCBA and pNBA, however, are far less sensitive towards UV-radiation. This is illustrated in Figure 6.

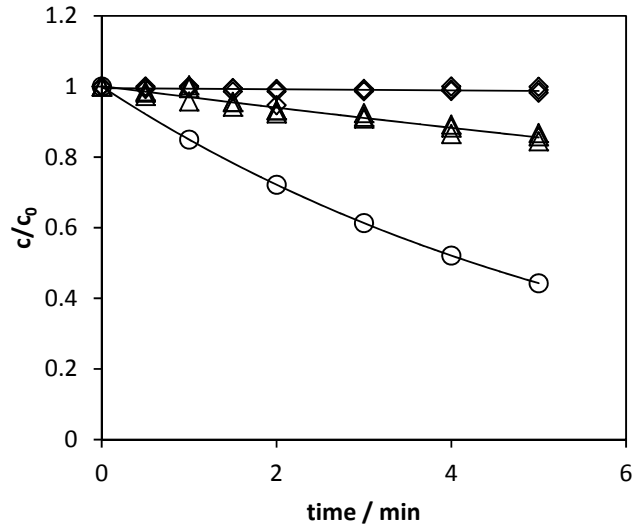

Figure 6: Direct photolysis of pNBA (diamonds), pCBA (triangles) and atrazine (circles) in aqueous solution. [pCBA] = [pNBA] = 0.5 µM, [phosphate] = 10 m; Fluence rate = 61 ± 3 µEinstein (n=11); pH 7.2, T = 25°C; observed degradation rates: pCBA: 0.0005 s^{-1}, pNBA: < 0.0005 s^{-1}; Note that the degradation of atrazine has been calculated on basis of the fluence rate determined for the merry-go-round apparatus in pure water

Even though pCBA and pNBA absorb UV-light at 254 nm much stronger than atrazine, direct photolysis is hampered by their low quantum yields (see above) and can often be neglected.

However, a further discussion on the photochemical features is beyond the scope of the present study.

With regard to radical reactions, pCBA represents compounds with a moderate reaction rate towards $SO_4^{\bullet-}$ and a high reactivity towards $^{\bullet}OH$, whereas pNBA hardly reacts with $SO_4^{\bullet-}$. Hence, the degradation pattern of these three compounds can be used as a specific finger print pointing to main reactants present in the photochemical systems under study. The degradation of pNBA for instance, suggests that the system under study is based on another reactive species than $SO_4^{\bullet-}$, since $SO_4^{\bullet-}$ hardly reacts with pNBA. Furthermore, a ratio of first order degradation rates of pNBA vs. pCBA of ca. 0.52 points to $^{\bullet}OH$-radical based reactions since it corresponds to the ratio of their second order rate constants with $^{\bullet}OH$ ($k(^{\bullet}OH + pNBA)/k(^{\bullet}OH + pCBA) = 0.52$ (Table 1). A $SO_4^{\bullet-}$ based system, however, is indicated if pNBA survives the oxidative treatment.

Describing the degradation of these compounds at different conditions applying the model approaches shown above helps understanding the chemistry of a radical based process. Furthermore, application oriented aspects can also be covered, such as energy demand required for a certain degree of pollutant degradation. By using this set of model compounds important information can be obtained for studying the feasibility of new processes such as UV/$S_2O_8^{2-}$.

3.10 Literature

1. Anipsitakis, G.P. and D.D. Dionysiou, *Radical generation by the interaction of transition metals with common oxidants.* Environmental Science & Technology, 2004. **38**(13): p. 3705-3712.
2. Neta, P., R.E. Huie, and A.B. Ross, *Rate constants for reactions of inorganic radicals in aqueous solution.* Journal of Physical and Chemical Reference Data, 1988. **17**(3): p. 1027 - 1040.
3. House, D.A., *Kinetics and mechanism of oxidations by peroxydisulfate.* Chemical Reviews, 1962. **62**: p. 185-203.
4. Indelli, A., V. Bartocci, F. Ferranti, and M.G. Lucarelli, *Salt effects in the reaction of peroxydisulfate with thiosulfate.* The Journal of Chemical Physics, 1966. **44**(5): p. 2069-2075.
5. Vogel, M., A. Büldt, and U. Karst, *Hydrazine reagents as derivatizing agents in environmental analysis - A critical review.* Fresenius' Journal of Analytical Chemistry, 2000. **366**(8): p. 781-791.
6. McElroy, W.J., *A laser photolysis study of the reaction of SO_4^- with Cl^- and the subsequent decay of Cl_2^- in aqueous solution.* Journal of Physical Chemistry, 1990. **94**(6): p. 2435-2441.
7. Buxton, G.V., C.L. Greenstock, W.P. Helman, and A.B. Ross, *Critical review of rate constants for reactions of hydrated electrones, hydrogen-atoms and hydroxyl radicals ($^{\bullet}OH/O^{\bullet-}$) in aqueous solution.* Journal of Physical and Chemical Reference Data, 1988. **17**(2): p. 513-886.
8. Acero, J.L., K. Stemmler, and U. von Gunten, *Degradation kinetics of atrazine and its degradation products with ozone and OH radicals: A predictive tool for drinking water treatment.* Environmental Science and Technology, 2000. **34**(4): p. 591-597.
9. Tauber, A. and C. von Sonntag, *Products and kinetics of the OH-radical-induced dealkylation of atrazine.* Acta Hydrochimica et Hydrobiologica, 2000. **28**(1): p. 15-23.
10. Manoj, P., K.P. Prasanthkumar, V.M. Manoj, U.K. Aravind, T.K. Manojkumar, and C.T. Aravindakumar, *Oxidation of substituted triazines by sulfate radical anion ($SO_4^{\bullet-}$) in aqueous medium: A laser flash photolysis and steady state radiolysis study.* Journal of Physical Organic Chemistry, 2007. **20**(2): p. 122-129.
11. Neta, P., V. Madhavan, H. Zemel, and R.W. Fessenden, *Rate constants and mechanism of reaction of sulfate radical anion with aromatic compounds.* Journal of the American Chemical Society, 1977. **99**(1): p. 163-164.
12. Peter, A. and U. von Gunten, *Oxidation kinetics of selected taste and odor compounds during ozonation of drinking water.* Environmental Science and Technology, 2007. **41**(2): p. 626-631.
13. von Sonntag, C. and U. von Gunten, eds. *Chemistry of ozone in water and wastewater treatment*. 2012, IWA Publishing.
14. Canonica, S., L. Meunier, and U. von Gunten, *Phototransformation of selected pharmaceuticals during UV treatment of drinking water.* Water Research, 2008. **42**(1-2): p. 121-128.
15. Katsoyiannis, I.A., S. Canonica, and U. von Gunten, *Efficiency and energy requirements for the transformation of organic micropollutants by ozone, O_3/H_2O_2 and UV/H_2O_2.* Water Research, 2011. **45**(13): p. 3811-3822.
16. Legrini, O., E. Oliveros, and A.M. Braun, *Photochemical processes for water treatment.* Chemical Reviews, 1993. **93**(2): p. 671-698.
17. Mark, G., M.N. Schuchmann, H.P. Schuchmann, and C. von Sonntag, *The photolysis of potassium peroxodisulphate in aqueous solution in the presence of tert-butanol: a simple actinometer for 254 nm radiation.* Journal of Photochemistry and Photobiology A, 1990. **55**(2): p. 157-168.

18. Herrmann, H., *On the photolysis of simple anions and neutral molecules as sources of O⁻/OH, SO_x^- and Cl in aqueous solution.* Physical Chemistry Chemical Physics, 2007. **9**(30): p. 3935-3964.
19. Heidt, L.J., *The photolysis of persulfate.* The Journal of Chemical Physics, 1942. **10**(5): p. 297-302.
20. Ianni, J.C., *Kintecus Version 3.95.* www.kintecus.com, 2008.
21. Wegelin, M., S. Canonica, K. Mechsner, T. Fleischmann, F. Pesaro, and A. Metzler, *Solar water disinfection: Scope of the process and analysis of radiation experiments.* Aqua: Journal of Water Supply Research and Technology, 1994. **43**(4): p. 154-169.
22. Azenha, M.E.D.G., H.D. Burrows, L.M. Canle, R. Coimbra, M.I. Fernández, M.V. García, A.E. Rodrigues, J.A. Santaballa, and S. Steenken, *On the kinetics and energetics of one-electron oxidation of 1,3,5-triazines.* Chemical Communications, 2003. **9**(1): p. 112-113.
23. Nick, K., H.F. Schöler, T. Söylemez, M.S. Akhlaq, H.P. Schuchmann, and C. von Sonntag, *Degradation of some triazine herbicides by UV radiation such as used in the UV disinfection of drinking water* J. Water SRT - Aqua, 1992. **41**: p. 82-87.
24. Talrose, V., A.N. Yermakov, A.A. Usov, A.A. Goncharova, A.N. Leskin, N.A. Messineva, N.V. Trusova, and M.V. Efimkina, eds. *UV/Visible Spectra*. NIST Chemistry WebBook, NIST Standard Reference Database, ed. P.J. Linstrom and W.G. Mallard. Vol. 69. 2013.

Chapter 4

-

Degradation of chlorotriazine pesticides by sulfate radicals

4.1 Abstract

Triazine herbicides such as atrazine and propazine have frequently been used in agriculture and thus are a potential drinking water contaminant. These persistent compounds can be degraded by hydroxyl radicals ($^{\bullet}OH$), which are produced in advanced oxidation processes. The herbicides atrazine, propazine and terbuthylazine react also very fast with sulfate radicals ($SO_4^{\bullet-}$) (2.0 - 4.3 × 10^9 M^{-1} s^{-1}). Dealkylation decreases the reaction rates to 1.5 × 10^8 M^{-1} s^{-1} for the completely dealkylated chlorotriazine-diamine (desethyl-desisopropyl-atrazine (DEDIA). The high reactivity of chlorotriazine herbicides is largely given by the ethyl or isopropyl group. While desisopropyl-atrazine (DIA) still reacts fast (k = 2 × 10^9 M^{-1} s^{-1}), desethyl-atrazine (DEA) reacts noticeably slower (k = 9.6 × 10^8 $M^{-1}s^{-1}$). The *tert*-butyl group has no rate enhancing effect and desethyl-terbuthylazine (DET) and DEDIA react slowly ($k \approx 10^8$ M^{-1} s^{-1}). In atrazine degradation by $SO_4^{\bullet-}$, one important pathway is dealkylation (63%), whereby deethylation dominates largely over deisopropylation (9:1).

4.2 Introduction

Sulfate radical ($SO_4^{\bullet-}$) based oxidation finds increasing interest in oxidative water treatment. $SO_4^{\bullet-}$ is a strong one-electron oxidant, but it also readily reacts by addition to C═C double bonds and by H-abstraction. Thus, it is capable of degrading a large number of pollutants such as chlorinated solvents, trichloroethene [1] and *tert*-butylmethylether [2]. $SO_4^{\bullet-}$ can be produced by photolysis [3, 4], thermolysis [5], or reduction of peroxodisulfate ($S_2O_8^{2-}$) by transition metals in their low oxidation states [6-9]. Reaction mechanisms of $SO_4^{\bullet-}$ reactions differ somewhat from those of $^{\bullet}OH$. $SO_4^{\bullet-}$ reacts more readily by electron transfer than $^{\bullet}OH$, but slower by H-abstraction and addition [10, 11]. Thus, reactivity, product patterns, and energy efficiency of $SO_4^{\bullet-}$-based oxidation may also be different from $^{\bullet}OH$-based oxidation. For example, perfluorinated carboxylic acids are inert towards $^{\bullet}OH$ but can be degraded by $SO_4^{\bullet-}$ [12, 13]. This indicates that $SO_4^{\bullet-}$-based oxidation may complement more common ($^{\bullet}OH$-based) advanced oxidation processes (AOPs).

The reaction of $SO_4^{\bullet-}$ with atrazine has been described to be very fast, k(atrazine + $SO_4^{\bullet-}$) = 3 × 10^9 M^{-1} s^{-1} [14], which is similar to the reaction rate of $^{\bullet}OH$, k(atrazine + $^{\bullet}OH$) = 2.4-3.0 × 10^9 M^{-1} s^{-1} [15-17]. The herbicide is readily dealkylated by $^{\bullet}OH$, however, the triazine ring system seems also to be attacked, but products have not been identified [17]. In the European Union a drinking water standard of 0.1 µg L^{-1} has been defined for a particular pesticide and 0.5 µg L^{-1} for the sum of all pesticides. Chlorotriazine pesticides continue to be an issue for the water suppliers and public health. Although the use of atrazine as herbicide is banned in the European Union since March 2004 (commission decision 2004/248/EC &

commission decision 2004/247/EC), atrazine has been frequently found in European ground waters even in the year 2010. The same study reports also the detection of terbuthylazine [18].
The mechanism of the $^{\bullet}OH$ reaction with atrazine has already been investigated in quite some detail [15, 17]. However, hardly any information on the mechanism in $SO_4^{\bullet-}$- based oxidation is available. The present study provides a first insight into this reaction.

4.3 Material and methods

4.3.1 Chemicals

All chemicals were commercially available and used as received. *Acetaldehyde* (p.a.) from (Sigma-Aldrich), *acetone* (p.a.) from KMF Laborchemie Handels GmbH, *acetanilide* (≥ 99.5%) from Fluka, *acetonitrile* (≥ 99.9%) Sigma Aldrich *argon* (5.0) Air liquid, *atrazine* (97.4%) Sigma-Aldrich; *4-chlorobenzoic acid (pCBA)* (99%) from Aldrich, *desethyl-atrazine (DEA)* (99%) from Sigma Aldrich, *desethyl-desisopropyl-atrazine (DEDIA)* (97.8%) from Sigma-Aldrich, *desisopropyl-atrazine (DIA)* (95.4%) from Sigma-Aldrich, *2,4-dinitrophenyl-hydrazine* (50% in water, p.a.) (DNPH) from Merck, *Ethanol* (≥ 99.8 vol. %) from Sigma-Aldrich, *humic acids* (Depur) (45-70%) from Carl Roth; *hydrochloric acid* (37% in water, p.a.) from Merck, *methanol* (p.a.) from Sigma-Aldrich, *perchloric acid* (60,4% in water, p.a.) from J.T. Baker, *simazine* (99%) from Sigma-Aldrich, *sodium hydroxide* (≥ 99.9%, p.a.) from Sigma-Aldrich, *sodium peroxodisulfate* (p.a.) from Sigma-Aldrich, *sulfuric acid* (98%, p.a.) from Merck, *tert-butyl alcohol* (≥ 99%) from Merck, *terbuthylazine* (98.8%) from Sigma Aldrich, *desethyl-terbuthylazine* (97.4%) from Sigma-Aldrich.

4.3.2 Experimental procedures

$SO_4^{\bullet-}$ rate constants for atrazine and the other chlorotriazines (terbuthylazine, propazine, desethyl-atrazine (DEA), desisopropyl-atrazin (DIA), desethyl-desisopropyl-atrazine (DEDIA), desethyl-terbuthylazine (DET) have been determined by competition kinetics [19] using 4-chlorobenzoic acid, k(pCBA + $SO_4^{\bullet-}$) = 3.6×10^8 M^{-1} s^{-1} [20], acetanilide k(acetanilide + $SO_4^{\bullet-}$) = 3.6×10^9 M^{-1} s^{-1} [20] and atrazine, k(atrazine + $SO_4^{\bullet-}$)= 3×10^9 M^{-1} s^{-1} [14] as competitors. The caption of Table 1 indicates the choice of competitors for determining the different rate constants. $SO_4^{\bullet-}$ was generated by

thermolysis of peroxodisulfate ($S_2O_8^{2-}$) at 60°C. The reaction solutions were adjusted to pH 7 with sodium hydroxide. Unless otherwise specified, no buffers were added because they can also react with $SO_4^{\bullet-}$ (e.g., $k(HPO_4^{2-} + SO_4^{\bullet-}) = 1.2 \times 10^6$ M^{-1} s^{-1} [11]). This reaction leads to the formation of $HPO_4^{\bullet-}$ which could also react with the chlorotriazines but at a different rate. Similar problems may arise with other buffers.

In a $SO_4^{\bullet-}$ based process, solutions can slowly acidify due to possible formation of sulfuric acid (e.g., in case $SO_4^{\bullet-}$ reacts *via* H-abstraction) and reaction of $SO_4^{\bullet-}$ with Cl^- (see chapter 7). This can be problematic since protonation of the substrates may change both, reaction kinetics and mechanism. Thus, it has been assured, that the pH remains at least 1 pH unit above the highest p*K*a value of corresponding substrates. In the present experiments the reaction time was short enough that the pH did not drop below this value. After heating up the sample, $S_2O_8^{2-}$ was added to a final concentration of 1 mM to initiate the reaction. After different reaction times, aliquots were withdrawn and chilled on ice. Methanol was immediately added (1 M in the sample ≈ 4% (v/v)) for scavenging $SO_4^{\bullet-}$ that could be formed at low rates during storage time. For preventing the influence of $^{\bullet}OH$ arising from the reaction of $SO_4^{\bullet-}$ plus Cl^- *tert*-butanol has been added in case competition kinetics has been performed. In case of the product studies *tert*-butanol was not added for preventing interferences in the product pattern. However, the substrates have been added in higher concentrations thus, suppressing the reaction of $SO_4^{\bullet-}$ with Cl^-.

All compounds were separated by HPLC-UV on a C-18 reversed phase column and detected by UV absorption. The following HPLC-systems have been used:

Shimadzu: Liquid chromatograph LC 20-AT, UV/Vis detector SPD 20A, Auto sampler SIL 20A, Degasser DGU-20A$_5$, communication bus module CBM 20A, column oven CTO-10AS vp

Shimadzu: Liquid chromatograph LC-10AT vp, diode array detector SPD M10A vp, auto sampler SIL 10 AD vp, degasser DGU 14A, system controller SCL-10A vp, column oven CTO-10AS vp

Agilent 1100 Series: Quaternary pump G1311A, UV-Vis detector VWD G1314A, Autosampler ALS G1313A, Degasser G1379A, column oven Colom G1316A)

As separation columns reversed phase C-18 (5 µm particle size 250 × 4.6 mm from Knauer or Bischoff) have been used. As mobile phase various isocratic mixtures and gradients of water and methanol as well as water and acetonitrile have been used. All compounds have been determined by UV absorption at their maxima (chlorotriazine herbicides 210-225 nm, pCBA 235-239 nm, acetanilide 224 nm).

Acetone and acetaldehyde were derivatized with 2,4-dinitrophenylhydrazine [21] and the hydrazones quantified by HPLC-UV. Most experiments were carried out in air-saturated solution. For studying the

reaction of $SO_4^{\bullet-}$ with atrazine in the absence of O_2, experiments were carried out in Ar-saturated solution as will be explained in the following. The design of these experiments is shown in Figure 1.

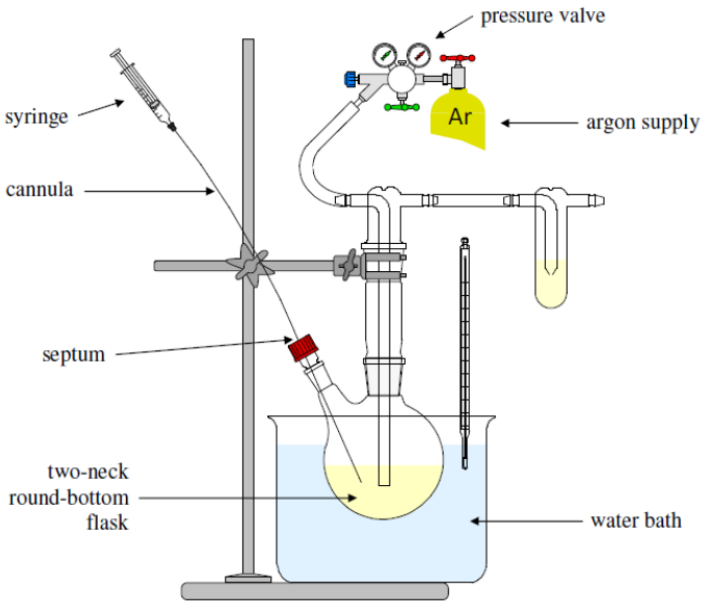

Figure 1: Design of the experiments in argon-saturated solution

The reaction solution containing $S_2O_8^{2-}$ (1 mM), pCBA (5 µM) and atrazine (5 µM) was filled into a two-neck round-bottom flask and heated in a water bath to 60 °C. During the experiment, the solution was continuously purged with argon. The samples have been withdrawn by a glass syringe which was connected to the reaction solution by a stainless steel cannula.

4.4 Results and Discussion

4.4.1 Kinetics.

The rate constants for the reaction of $SO_4^{\bullet-}$ and $^{\bullet}OH$ with the investigated triazine herbicides and their dealkylation products are compiled in Table 1.

Table 1: Rate constants for the reaction of $SO_4^{\bullet-}$ and $^{\bullet}OH$ with *s*-triazines; competitors: a) pCBA, b) atrazine, c) acetanilide, σ = standard deviation, n = number of replicates

Compound	$SO_4^{\bullet-}$ / $M^{-1} s^{-1}$	$^{\bullet}OH$ / $M^{-1} s^{-1}$
Atrazine 6-Chloro-2-ethylamino-4-isopropylamino-1,3,5-triazine	$4.2 \pm 0.20 \times 10^{9}$ a) n = 4 [this study] $4.7 \pm 0.10 \times 10^{9}$ c) n = 4 [this study] Average: $4.5 \pm 0.30 \times 10^{9}$ [this study] 3×10^{9} [14] 1.4×10^{9} [22]	$(2.4 – 3) \times 10^{9}$ [15-17]
Desisopropyl-atrazine (DIA) 6-Chloro-2-ethylamino-4-amino-1,3,5-triazine	$2.0 \pm 0.57 \times 10^{9}$ a) n = 4 [this study]	1.9×10^{9} [16]
Desethyl-atrazine (DEA) 6-Chloro-2-amino-4-isopropylamino-1,3,5-triazine	$9.6 \pm 0.17 \times 10^{8}$ a) n = 4 [this study]	1.2×10^{9} [16]
Desethyl-desisopropyl-atrazine (DEDIA) 6-Chloro-2,4-amino-1,3,5-triazine	$1.5 \pm 0.08 \times 10^{8}$ a) n = 4 [this study]	$< 5 \times 10^{7}$ [16]
Terbuthylazine 6-Chloro-2-ethylamino-4-terbutylamino-1,3,5-triazine	3.0×10^{9} b) $\pm 5.2 \times 10^{7}$ n = 4	Not available
Propazine 6-Chloro-2,4-isopropylamino -1,3,5-triazine	$2.2 \pm 0.05 \times 10^{9}$ b) n = 6 [this study]	Not available
Desethyl-terbuthylazine (DET) 6-Chloro-2-amino-4-terbutylamino-1,3,5-triazine	$3.6 \pm 0.23 \times 10^{8}$ a) n = 6 [this study]	Not available
s-Triazine	8.1×10^{7} [14]	9.6×10^{7} [17]
3,4,6-Trimethoxy-*s*-triazine	5.1×10^{7} [14]	Not available
2,4-Dioxohexahydo-1,3,5-triazine	4.6×10^{7} [14]	Not available

The reaction rate of atrazine plus $SO_4^{\bullet-}$ reported in the literature ranges between 1.4 and 3×10^{9} $M^{-1} s^{-1}$ (Table 1). Thus the error margin of the present study ($4.5 \pm 0.3 \times 10^{9}$ $M^{-1}s^{-1}$) and the literature values ($2.2 \pm 1.6 \times 10^{9}$ $M^{-1}s^{-1}$) nearly overlap, albeit the values determined by competition kinetics are somewhat larger. In the present study atrazine has also been used as a competitor for determination of rate constants (terbuthylazine and propazine). For calculating corresponding rate constants the average of reaction rates for the reaction $SO_4^{\bullet-}$ plus atrazine (i.e., 3×10^{9} $M^{-1}s^{-1}$) has been used.

Comparing the reactions $SO_4^{\bullet-}$ plus atrazine, propazine and DIA reveals very similar rate constants. However, the reaction of $SO_4^{\bullet-}$ plus DEA displays a decrease in the reaction rate, albeit it is still near 10^{9} $M^{-1} s^{-1}$. Furthermore, DET and DEDIA drop in their reactivity down by a factor ≈ 10. Yet, substitution of

an isopropyl- by a *tert*-butyl group shows no significant effect as long as one ethyl or isopropyl group remains attached on the triazine ring system. The reaction rates of the desethylated chloro-triazines (DIA, DEA and DET) decrease in the order ethyl- > isopropyl- >> *tert*-butyl group attached to the triazine ring. This indicates that *N*-ethyl and to a somewhat lesser extent the *N*-isopropyl group is a key factor in the reactivity of $SO_4^{\bullet-}$ towards *s*-triazine herbicides. In that it finds its analogy in $^{\bullet}OH$ reactions, albeit $SO_4^{\bullet-}$ displays a more distinct prevalence for the ethyl group.

Interestingly, $SO_4^{\bullet-}$ react remarkably faster with DEDIA than $^{\bullet}OH$, which might enable its degradation in $SO_4^{\bullet-}$ based processes.

4.4.2 Product formation

The reaction of $SO_4^{\bullet-}$ with atrazine leads to dealkylation thereby giving rise to DEA and DIA as well to the corresponding products, acetaldehyde and acetone (Figure 2).

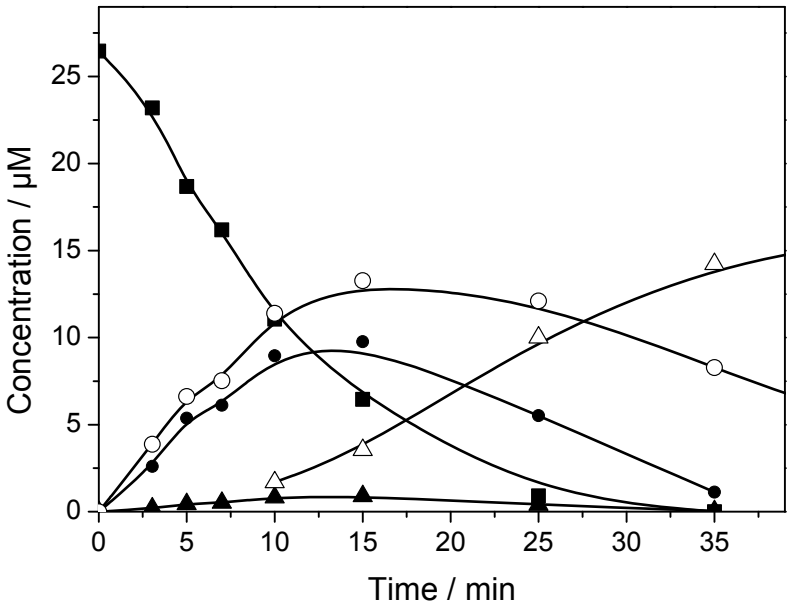

Figure 2: Degradation of atrazine by $SO_4^{\bullet-}$ and product formation in air-saturated aqueous solution; initial pH = 7; $[S_2O_8^{2-}]$ = 1 mM; T = 60°C; Atrazine (squares), acetaldehyde (open circles), DEA (filled circles), DIA (filled triangles), acetone (open triangles)

A plot of atrazine degradation vs. product formation allows quantifying product yields by a linear regression as illustrated in Figure 3 (the slope represents the product yield, which is DEA in the example below)

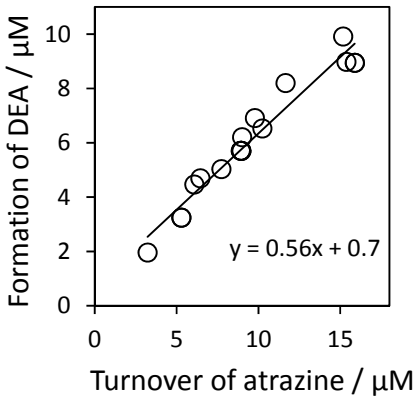

Figure 3: Formation of DEA vs. degradation of atrazine in thermal activation of $S_2O_8^{2-}$, initial pH: 7, T = 60°C, $[S_2O_8^{2-}]$ = 1 mM [atrazine] = 26 µM; pooled data of three individual experiments

By that means, the product yields of every individual experiment were calculated and averaged. The corresponding data are compiled in Table 2. The small deviation between the calculations shown in Table 2 and the linear regression of the pooled data shown in Figure 3 can be explained by slightly uneven weighting factors of the individual experiments in the linear regression, since the data points derived from these experiments are not equidistant.

The formation of the DEA, DIA, acetaldehyde and acetone has also been observed as a result of $^{\bullet}OH$-induced degradation of atrazine [17], corresponding yields are summarized in Table 2. There is, however, a remarkable difference. In case of $^{\bullet}OH$, the DEA to DIA ratio is 2.6, while with $SO_4^{\bullet-}$ it is 9.5 (Table 2). Acetone at low turnovers was too uncertain to be reported due to a fluctuating background of acetone in the samples. At higher turnovers, acetone is mainly formed as a secondary product from the $SO_4^{\bullet-}$-induced dealkylation of the major product DEA (Figure 2).

In contrast to $SO_4^{\bullet-}$, acetone is formed substantially in primary reactions of $^{\bullet}OH$ with atrazine [17] (Table 2).

Table 2: Primary product yields in % of educt degradation in the $SO_4^{\bullet-}$ and $^{\bullet}OH$ reactions with *s*-triazines. NA = Not applicable, *detected but not quantified, due to fluctuating contamination from the lab air

Product	Atrazine		DEA	DIA
	$SO_4^{\bullet-}$	$^{\bullet}OH$ [17]	$SO_4^{\bullet-}$	
Acetaldehyde	63 %	53 %	NA	91 %
Acetone	*	20 %	73 %	NA
Formaldehyde	NA	NA	NA	NA
DEA	57 %	51 %	NA	NA
DIA	6 %	20 %	NA	NA
DEDIA	NA	NA	80 %	91 %
Mass balance	63 % (DEA+DIA)	71 % (DEA+DIA)	73-80%	91 %
Ratio DEA:DIA	9.5	2.6	NA	NA

Desisopropylation occurs to a minor extent in primary reactions of atrazine (ca. 6 %), reflecting the low concentration of DIA during atrazine degradation (Figure 2). The cleavage of the *N*-ethyl group is largely favored over the cleavage of the *N*-isopropyl group.

Product yields shown in Table 2 indicate that ≈ 40% of the $SO_4^{\bullet-}$ reactions give rise to unidentified products. Such an incomplete mass balance has also been reported for $^{\bullet}OH$ reactions with atrazine [17] and in purine free-radical chemistry [10]. In the purines, *N*-centered and *O*-centered radicals that do not react with O_2 play a major role, and it is envisaged that these give rise to a large number of dimers that escaped detection. In the present system, radical cations are also likely intermediates, and it is conceivable that the missing fraction is due to such dimers. With three ring nitrogens and two exocyclic nitrogens, the number of potential dimers is very large, that is, each individual dimer may be formed in a very low yield only.

In analogy with the $SO_4^{\bullet-}$ reaction of atrazine, DEA and DIA yield DEDIA as well as acetone and acetaldehyde, respectively. This confirms the formation of DEDIA and the major fraction of acetone as secondary product of atrazine degradation.

4.4.3 Reaction mechanism

In the reaction of $SO_4^{\bullet-}$ with electron-rich aromatic compounds such as methoxy derivatives of benzene, the corresponding radical cations are generated by electron transfer as primary short-lived intermediates [23]. With aromatic carboxylic acids, the formation of phenyl radicals is observed by ESR pointing to a decarboxylation of the primarily formed radical cations [23]. With benzene lacking electron-donating groups hydroxycyclohexadienyl radicals have been observed [24]. A rapid reaction of water with primarily formed radical cations may account for this. For all electron-rich aromatic compounds, $SO_4^{\bullet-}$ rate constants are $\geq 1 \times 10^9$ M^{-1} s^{-1}. With strongly electron-withdrawing substituents, the reaction becomes noticeably slower (k(benzonitrile + $SO_4^{\bullet-}$) = 1.2×10^8 M^{-1} s^{-1}), and the reaction with nitrobenzene is too slow to be measured by pulse radiolysis ($k < 10^6$ M^{-1} s^{-1}) [20]. The triazines have been suggested to react with $SO_4^{\bullet-}$ by electron transfer as well [14] and based on this a mechanism can be proposed resulting in dealkylation along with formation of carbonylic compounds and free amines. In the first step electron transfer yields a radical cation (reaction 1).

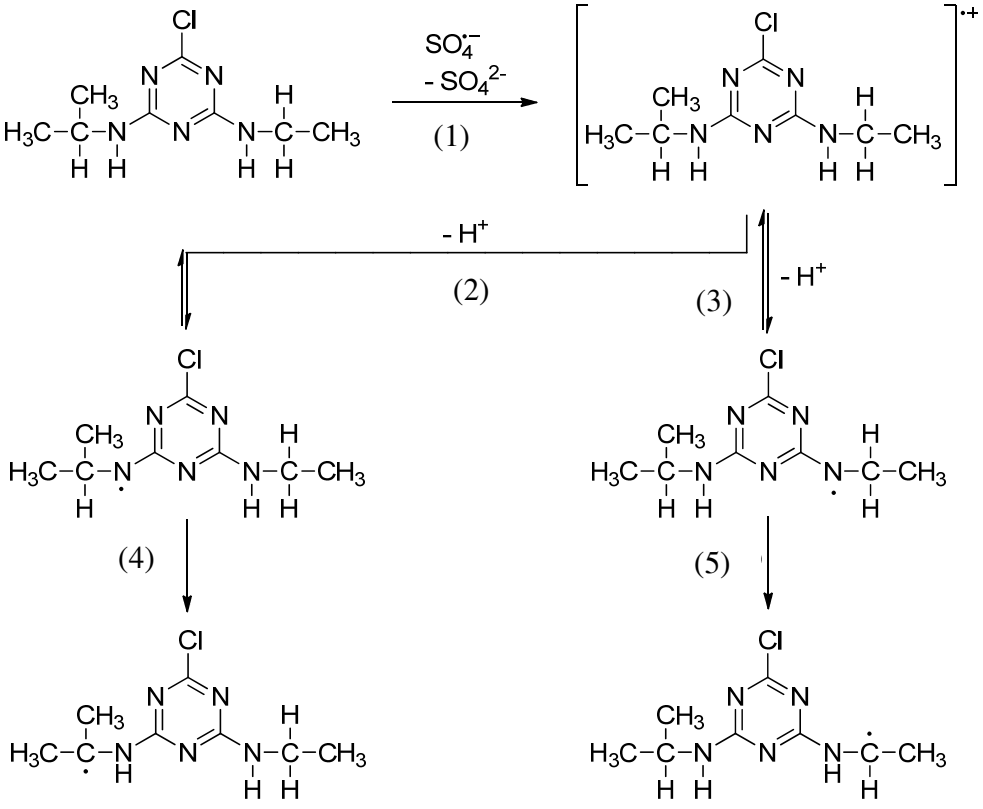

This primary radical cation will be in equilibrium with the corresponding N-centered radicals (reactions 2 and 3). The N-H bond at the *N*-ethyl group is more acidic than that at the *N*-isopropyl group and

deprotonation will occur more preferably at the H–*N*-ethyl site (reaction 3). In accordance with this, the energy difference between these two N-centered radicals has been calculated to be 21 kJ mol^{-1}. The N-centered radicals are expected to undergo a (water-catalyzed) 1,2-H shift in analogy to the well-documented 1,2-H shift of alkoxyl radicals [25]. Thereby C-centered radicals are formed. These are at lower energies than the N-centered radicals by 80 kJ mol^{-1} (reaction 4) and 66 kJ mol^{-1} (reaction 5). For DEA, the corresponding energy gain has been calculated at 57 kJ mol^{-1}. The N-centered radicals do not react with O_2, but the C-centered ones react rapidly (reaction 6, $k = 3 \times 10^9$ M^{-1} s^{-1}) [17].

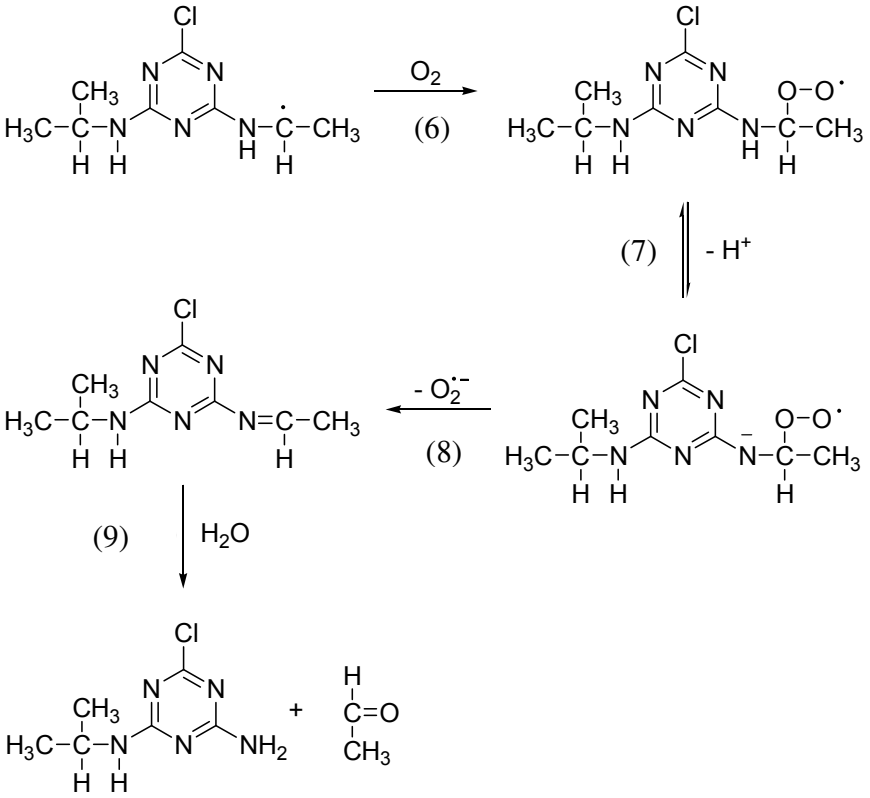

The resulting peroxyl radical subsequently loses $O_2^{\bullet-}$ (reactions 7 and 8). Details of the kinetics have been studied by pulse radiolysis [17]. The subsequent hydrolysis of the imine (reaction 9) is base and acid catalysed [15, 17].

The above mechanistic considerations can explain why in $SO_4^{\bullet-}$-induced dealkylation of atrazine, formation of DEA plus acetaldehyde is so largely favored over the formation of DIA plus acetone (preferred deprotonation at the N-ethyl group upon formation of a radical cation). Yet, in the $^{\bullet}OH$-induced reaction, such a preference is also observed, albeit to a smaller extent [17]. This requires that $^{\bullet}OH$ preferably abstract hydrogen at the α–C of the ethyl side group over attacking the isopropyl group. Why this is so, is not yet understood.

The main reaction pathway of $^{\bullet}OH$ is abstraction of a hydrogen located at the α-position of the alkyl groups (preferably at the ethyl group), thus resulting in a carbon centered radical which is formed in reaction 4 and 5. $SO_4^{\bullet-}$ could principally also react *via* H-abstraction, which would explain the sharp drop in reaction rate observed in the kinetics of the reaction $SO_4^{\bullet-}$ plus DET. In fact this observation contradicts electron transfer since the electron density in the aromatic system of DET is similar compared to DEA, thus, large differences in reaction rates are not to be expected in case of electron transfer. On the other hand, reaction rates of H-abstractions by $SO_4^{\bullet-}$ typically range between 10^7-10^8 M^{-1} s^{-1}. Hence, the reaction rates of atrazine, DIA, terbuthylazine and propazine (> 10^9 M^{-1} s^{-1}) would be unusually high for an H-abstraction reaction. Yet, the present data do not allow a clear distinction between both pathways.
Imines (notation: imine at the ethyl group = ethyl-imine, imine at the isopropyl group = isopropyl-imine) are proposed to appear in both pathways and in fact ethyl-imine has been observed in HPLC-diode array detection (HPLC-DAD) measurements. If the analysis is started with a short time delay between the experiment and start of the analysis (i.e., ≤ 2 hours) ethyl-imine elutes as a dominant product peak with a retention time in between atrazine and DEA (Figure 4).

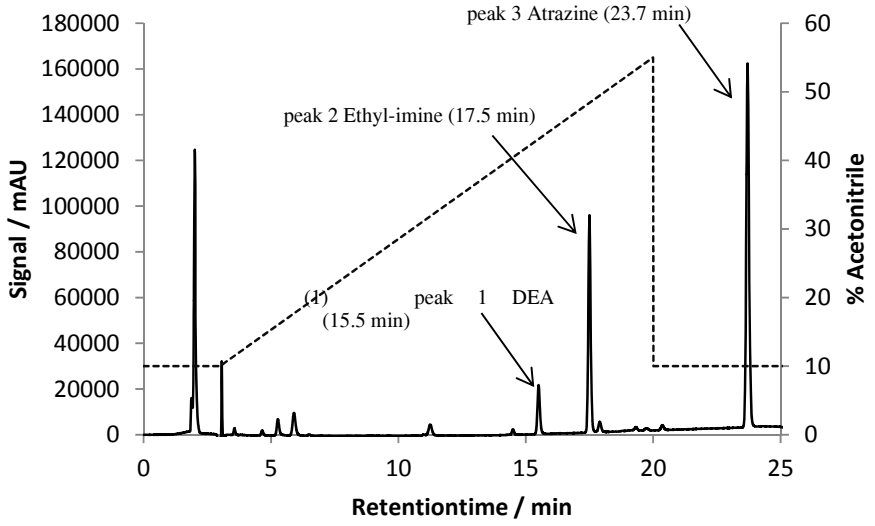

Figure 4 Chromatogram of atrazine and products formed upon its reaction by $SO_4^{\bullet-}$, 60°C; reaction time = 8 min, initial pH = 7; eluent acetonitrile/water (pH6-7)

For a quantitative view on the evolution of ethyl-imine its response factor has to be determined. This has been done in an experiment where upon hydrolysis of ethyl-imine DEA formation has been monitored over time (half-life time of ethyl-imine was ≈ 7 h (Figure 5b)). Assuming a 100% yield of DEA arising from hydrolysis of ethyl-imine the DEA formation corresponds to the amount of the hydrolyzed ethyl-

imine. Thus, a plot of the ethyl-imine peak area vs. concentration of formed DEA yields the required response factor of ethyl-imine (≈ 99000 mAU × min μM^{-1} (213 nm)) (Figure 5a). This response is very similar compared to DEA (≈ 91000 mAU × min μM^{-1} , 213 nm).

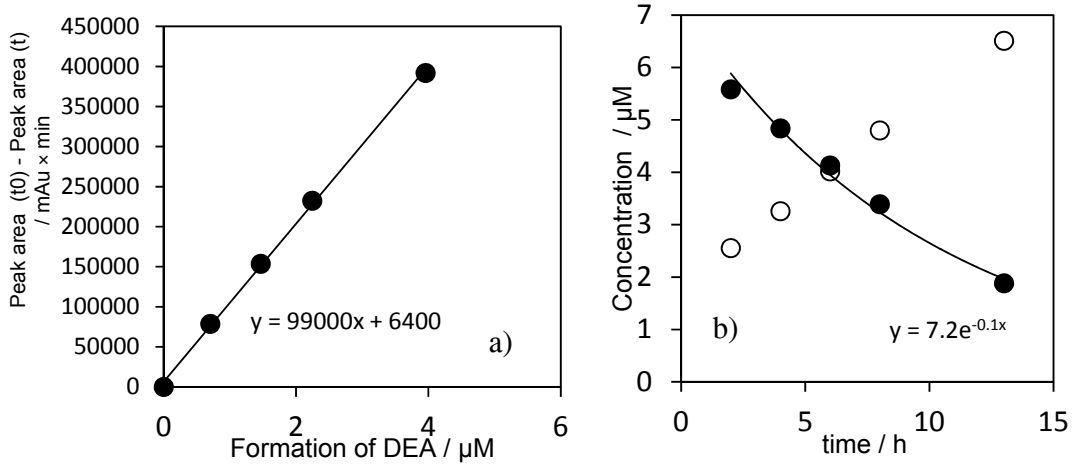

Figure 5 : a) Calibration of ethyl-imine; the signal of atra-imine which is hydrolysed (i.e., difference of initial peak area to a peak area at a certain time (t) is plotted vs. the concentration of DEA formed; hydrolysis of ethyl-imine (b): closed symbols = ethyl-imine, open symbols = DEA; pH ≈ 7, T = 20-25°C

Furthermore, the UV-spectra of atrazine, ethyl-imine and DEA obtained from the DAD, do hardly differ (Figure 6).

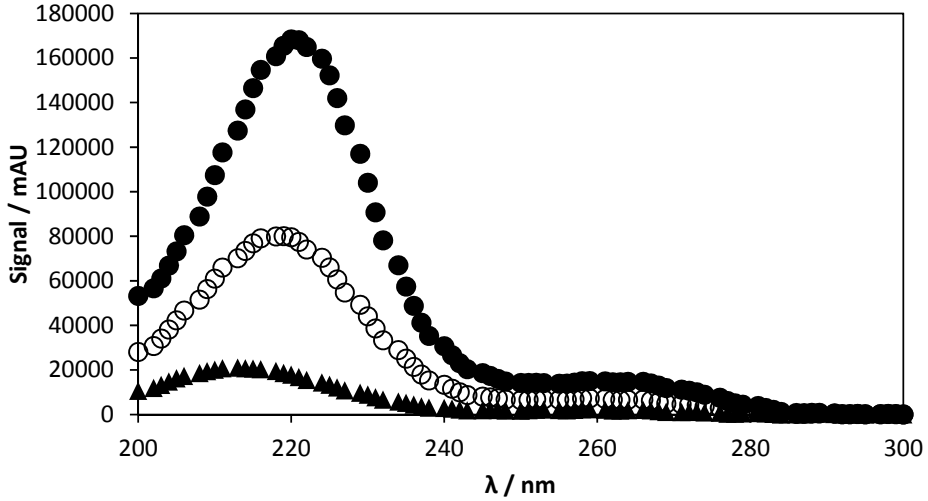

Figure 6 UV-spectra of atrazine (closed circles), ethyl-imine (open circles) and DEA (closed triangles)

It can be concluded that calibration of DEA at 213 nm fairly works for ethyl-imine. Acero et al. [15] also based their quantification of ethyl-imine on the calibration of DEA assuming similar UV-absorption. This approach is herewith further corroborated.

The evolution of ethyl-imine in atrazine degradation can now be quantified (Figure 7). Even though ethyl-imine has been considered being the precursor of DEA, the latter compound appears in all samples. This can be explained by hydrolysis of the ethyl-imine before HPLC-determination was started (ca. 2-3 h delay between the experiment and the analysis). The full yield of DEA has also been determined after complete turnover of ethyl-imine (i.e., after ≈ 72 h). The sum of ethyl-imine and DEA corresponds to the DEA yield after 72 h (Figure 7, inset).

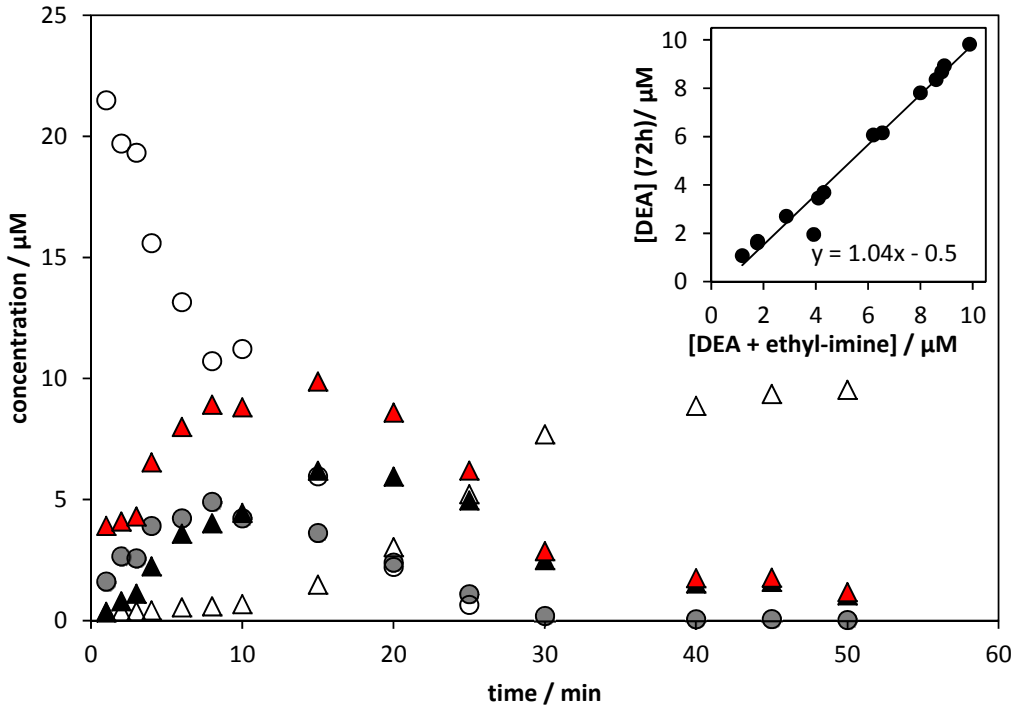

Figure 7 degradation of atrazine (open circles) and formation of products; DEA-imine (grey circles), DEA (black triangles) and DEDIA (open triangles); red triangles: formation of DEA after 72 h, thermal activation of $S_2O_8^{2-}$, T = 60°C, initial pH 7, $[atrazine]_0$ =25 µM, $[S_2O_8^{2-}]_0$ = 1 mM, inset: correlation of the sum of ethyl-imine and DEA of the first measurement vs. DEA formation after 72 h

The hydrolysis of the isopropyl-imine is much faster and right after the reaction DIA is present in full yield. This explains why in contrast to the ethyl-imine, no isopropyl-imine could be detected in HPLC analysis. Yet, the reason for the differences of the two Schiff bases is not fully understood.

It has been shown above that one key reaction in the degradation of atrazine is the oxidation of carbon centered radicals by O_2. However, $S_2O_8^{2-}$ might also be able to oxidize these radicals, which in fact is indicated by the outcome of experiments in argon saturated solutions. Figure 8 shows that the absence of O_2 even increases the overall degradation rate of atrazine.

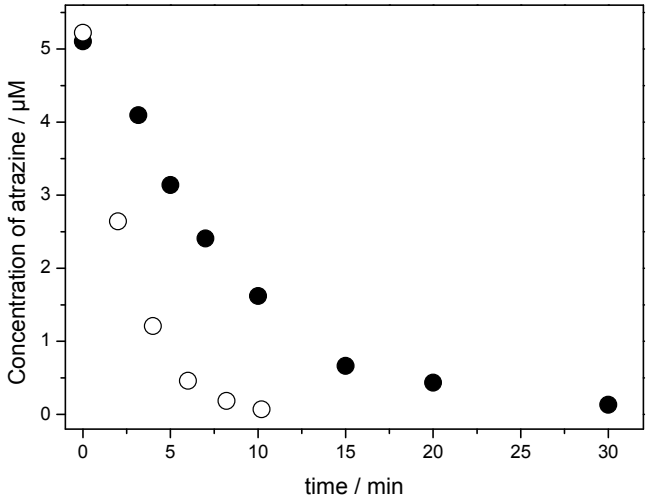

Figure 8: Degradation of atrazine (5 µM) in presence of 4-chlorbenzoic acid (5 µM) in air-saturated solution (closed circles) and in argon-saturated solution (open circles); $[S_2O_8^{2-}]$ = 1 mM, initial pH = 7, T = 60°C

This suggests that $S_2O_8^{2-}$ may indeed oxidize the strongly reducing *N*-alkyl-substituted carbon-centered radicals, leading to the formation of $SO_4^{\bullet-}$ and SO_4^{2-}. This reaction induces a chain reaction accelerating atrazine degradation. The potentially somewhat less reducing α-hydroxyalkyl radicals also undergo such a reaction [26].

The present study has shown that a transformation of chlorotriazine herbicides in $SO_4^{\bullet-}$ resembles $^{\bullet}OH$ based oxidation. In both cases the degradation yields DEDIA which is much less reactive towards $SO_4^{\bullet-}$ and $^{\bullet}OH$ compared to its precursors. DEDIA presumably persists $^{\bullet}OH$ attack in AOPs. DEDIA reacts with $^{\bullet}OH$ at a very low rate, if at all (k ($^{\bullet}OH$) ≤ 5×10^7 M^{-1} s^{-1} [16]), whereas it is surely reactive towards

$SO_4^{\bullet-}$ ($k = 1.5 \times 10^8$ M^{-1} s^{-1}, Table 1). This might enable a radical based pathway of its degradation in an $SO_4^{\bullet-}$ based process. However, the degradation of pollutants depends on kinetics of the oxidant plus pollutant and oxidant plus matrix compounds as well. The influence of the matrix is complex especially in case of $SO_4^{\bullet-}$ based oxidation since chlorine chemistry is part of the reaction system.

4.5 Literature

1. Liang, C., I.L. Lee, I.Y. Hsu, C.P. Liang, and Y.L. Lin, *Persulfate oxidation of trichloroethylene with and without iron activation in porous media.* Chemosphere, 2008. **70**(3): p. 426-435.
2. George, C., H. El Rassy, and J.M. Chovelon, *Reactivity of selected volatile organic compounds (VOCs) toward the sulfate radical ($SO_4^{\bullet-}$).* International Journal of Chemical Kinetics, 2001. **33**(9): p. 539-547.
3. Herrmann, H., *On the photolysis of simple anions and neutral molecules as sources of O^-/OH, SO_x^- and Cl in aqueous solution.* Physical Chemistry Chemical Physics, 2007. **9**(30): p. 3935-3964.
4. Mark, G., M.N. Schuchmann, H.P. Schuchmann, and C. von Sonntag, *The photolysis of potassium peroxodisulphate in aqueous solution in the presence of tert-butanol: a simple actinometer for 254 nm radiation.* Journal of Photochemistry and Photobiology A, 1990. **55**(2): p. 157-168.
5. Liang, C. and H.W. Su, *Identification of sulfate and hydroxyl radicals in thermally activated persulfate.* Industrial and Engineering Chemistry Research, 2009. **48**(11): p. 5558-5562.
6. Anipsitakis, G.P. and D.D. Dionysiou, *Degradation of organic contaminants in water with sulfate radicals generated by the conjunction of peroxymonosulfate with cobalt.* Environmental Science and Technology, 2003. **37**(20): p. 4790-4797.
7. Anipsitakis, G.P., D.D. Dionysiou, and M.A. Gonzalez, *Cobalt-mediated activation of peroxymonosulfate and sulfate radical attack on phenolic compounds. Implications of chloride ions.* Environmental Science and Technology, 2006. **40**(3): p. 1000-1007.
8. Anipsitakis, G.P., E. Stathatos, and D.D. Dionysiou, *Heterogeneous activation of oxone using Co_3O_4.* Journal of Physical Chemistry B, 2005. **109**(27): p. 13052-13055.
9. Anipsitakis, G.P. and D.D. Dionysiou, *Radical generation by the interaction of transition metals with common oxidants.* Environmental Science & Technology, 2004. **38**(13): p. 3705-3712.
10. von Sonntag, C., *Free-radical-induced DNA damage and its repair- A chemical perpesctive.* Springer Verlag Berlin Heidelberg, ISBN: 3-540-26120-6, 2005.
11. Neta, P., R.E. Huie, and A.B. Ross, *Rate constants for reactions of inorganic radicals in aqueous solution.* Journal of Physical and Chemical Reference Data, 1988. **17**(3): p. 1027 - 1040.
12. Hori, H., E. Hayakawa, H. Einaga, S. Kutsuna, K. Koike, T. Ibusuki, H. Kiatagawa, and R. Arakawa, *Decomposition of environmentally persistent perfluorooctanoic acid in water by photochemical approaches.* Environmental Science and Technology, 2004. **38**(22): p. 6118-6124.
13. Schröder, H.F. and R.J.W. Meesters, *Stability of fluorinated surfactants in advanced oxidation processes - A follow up of degradation products using flow injection-mass spectrometry, liquid chromatography-mass spectrometry and liquid chromatography-multiple stage mass spectrometry.* Journal of Chromatography A, 2005. **1082**(1 SPEC. ISS.): p. 110-119.
14. Manoj, P., K.P. Prasanthkumar, V.M. Manoj, U.K. Aravind, T.K. Manojkumar, and C.T. Aravindakumar, *Oxidation of substituted triazines by sulfate radical anion ($SO_4^{\bullet-}$) in aqueous medium: A laser flash photolysis and steady state radiolysis study.* Journal of Physical Organic Chemistry, 2007. **20**(2): p. 122-129.
15. Acero, J.L., K. Stemmler, and U. von Gunten, *Degradation kinetics of atrazine and its degradation products with ozone and OH radicals: A predictive tool for drinking water treatment.* Environmental Science and Technology, 2000. **34**(4): p. 591-597.
16. De Laat, J., N. Chramosta, M. Dore, H. Suty, and M. Pouillot, *Rate constants for reaction of hydroxyl radicals with some degeradation by-products of atrazine by O_3 or O_3/H_2O_2.* Environmental Technology, 1994. **15**(5): p. 419-428.
17. Tauber, A. and C. von Sonntag, *Products and kinetics of the OH-radical-induced dealkylation of atrazine.* Acta Hydrochimica et Hydrobiologica, 2000. **28**(1): p. 15-23.

18. Loos, R., G. Locoro, S. Comero, S. Contini, D. Schwesig, F. Werres, P. Balsaa, O. Gans, S. Weiss, L. Blaha, M. Bolchi, and B.M. Gawlik, *Pan-European survey on the occurrence of selected polar organic persistent pollutants in ground water.* Water Research, 2010. **44**(14): p. 4115-4126.
19. Peter, A. and U. von Gunten, *Oxidation kinetics of selected taste and odor compounds during ozonation of drinking water.* Environmental Science and Technology, 2007. **41**(2): p. 626-631.
20. Neta, P., V. Madhavan, H. Zemel, and R.W. Fessenden, *Rate constants and mechanism of reaction of sulfate radical anion with aromatic compounds.* Journal of the American Chemical Society, 1977. **99**(1): p. 163-164.
21. Vogel, M., A. Büldt, and U. Karst, *Hydrazine reagents as derivatizing agents in environmental analysis - A critical review.* Fresenius' Journal of Analytical Chemistry, 2000. **366**(8): p. 781-791.
22. Azenha, M.E.D.G., H.D. Burrows, L.M. Canle, R. Coimbra, M.I. Fernández, M.V. García, A.E. Rodrigues, J.A. Santaballa, and S. Steenken, *On the kinetics and energetics of one-electron oxidation of 1,3,5-triazines.* Chemical Communications, 2003. **9**(1): p. 112-113.
23. O'Neill, P., S. Steenken, and D. Schulte-Frohlinde, *Formation of radical cations; of methoxylated benzenes by reaction with OH radicals, Tl^{2+}, Ag^{2+}, and $SO4^{\bullet-}$ in aqueous solution. An optical and conductometric pulse radiolysis and in situ radiolysis electron spin resonance study.* Journal of Physical Chemistry, 1975. **79**(25): p. 2773-2779.
24. Norman, R.O.C., P.M. Storey, and P.R. West, *Electron spin resonance studies. Part XXV. Reactions of the sulphate radical anion with organic compounds.* Journal of the Chemical Society B: Physical Organic, 1970: p. 1087-1095.
25. Konya, K.G., T. Paul, S. Lin, J. Lusztyk, and K.U. Ingold, *Laser flash photolysis studies on the first superoxide thermal source. First direct measurements of the rates of solvent-assisted 1,2-hydrogen atom shifts and a proposed new mechanism for this unusual rearrangement.* Journal of the American Chemical Society, 2000. **122**(31): p. 7518-7527.
26. Schuchmann, H.P. and C. von Sonntag, *The oxidation of methanol and 2-propanol by potassium peroxodisulphate in aqueous solution: Free-radical chain mechanisms elucidated by radiation-chemical techniques.* Radiation Physics and Chemistry, 1988. **32**(2): p. 149-156.

Chapter 5

-

Reaction of sulfate radicals with organic matter

5.1 Introduction

For characterizing oxidative water treatment the influence of the water matrix on the stability of corresponding oxidants is very important. In that regard the most relevant matrix components are dissolved organic carbon (DOC) and alkalinity (HCO_3^- and CO_3^{2-}). The kinetics of $SO_4^{\bullet-}$ plus HCO_3^- and CO_3^{2-} has already been determined (Chapter 1). Yet, no reaction rate of $SO_4^{\bullet-}$ plus DOC is available. The present work provides a first estimate of corresponding kinetics which will be helpful for assessing the effectiveness of a $SO_4^{\bullet-}$ based water treatment process.

5.2 Material and methods

5.2.1 Chemicals

Following chemicals were commercially available and used as received: *Atrazine* (97.4%) from Sigma Aldrich, *humic acids* (Depur) (45-70%) from Carl Roth, *hydrogen peroxide* (30%) Sigma Aldrich, *methanol* (p.a.) from Sigma-Aldrich, *$NaHCO_3$* (99%) KMF optichem, *phosphoric acid* (≥ 85%) Merck, *sodium hydroxide* (≥ 99.9%, p.a.) from Sigma-Aldrich, *sodium peroxodisulfate* (p.a.) from Sigma-Aldrich, *sulfuric acid* (98%, p.a.) from Merck; *Suwannee River NOM* (reverse osmosis concentrate) (International Humic Substances Society),

5.2.2 Experimental procedures

Analytical instruments

Atrazine was analyzed by HPLC-UV on a C-18 reversed phase column (5 µm particle size 250 × 4.6 mm, Bischoff) and detected by UV absorption (220 nm). The following HPLC-system purchased from Shimadzu has been used:

Liquid chromatograph LC 20-AT, UV/Vis detector SPD 20A, Auto sampler SIL 20A, Degasser DGU-$20A_5$, communication bus module CBM 20A, column oven CTO-10AS vp. As eluent a mixture of 60% methanol and 40% water has been used.

Setup of photochemical experiments

For photochemical experiments a merry-go-round apparatus has been used (Hans und Thomas Schneider Glasapparatebau, Kreuwertheim). This apparatus was equipped with a low pressure mercury arc lamp from Heraeus Noble Light (GPH303T5L/4, 15 W). This radiation source emits nearly monochromatic light at 254 nm. The quartz glass of this radiation source is not transparent for the minor

emission at 185 nm and a water filter with an optical path length of ca. 0.5 cm served as an additional safeguard. Thus, effects by 185 nm radiation can be neglected. Methanol was added after sampling (1 M in the sample ≈ 4% (v/v)) for scavenging $SO_4^{\bullet-}$ during storage time (Chapter 3).

Determination of fluence rate

For taking the UV-absorption of the water matrix into account the fluence rate has been derived from direct photolysis of atrazine in presence of humic acids analogous to Canonica et al. [1] (see also Chapter 3). Following photochemical parameters have been applied: quantum yield of direct atrazine photolysis (254 nm): 0.046 mol Einstein^{-1}, molar absorption of atrazine (254 nm): 386 m^2 mol^{-1} [1, 2].

Use of buffers

For preventing speciation of the humic acids, which could cause changes in the reactivity towards $SO_4^{\bullet-}$ and $^{\bullet}OH$, buffering of pH was necessary (pH = 7.2). Therefore 1.25-2.5 mM phosphate has been added. Due to the high concentration of humic acids (7.5-15 mgC L^{-1}) only a minor fraction of $SO_4^{\bullet-}$ is expected to react with the phosphate species and interferences by phosphate radicals can be neglected as will be explained below. The reaction rates of $SO_4^{\bullet-}$ with phosphate species are low ($k(HPO_4^{2-} + SO_4^{\bullet-})$ = 1.2 × 10^6 M^{-1}s^{-1} [3] $k(H_2PO_4^- + SO_4^{\bullet-}) \leq 7.4 \times 10^4$ M^{-1}s^{-1} [4]). Due to the high DOC concentration, the reaction rate of $SO_4^{\bullet-}$ plus DOC has to be below 1000 L mg^{-1}C s^{-1} for enabling a > 10% fraction of $SO_4^{\bullet-}$ reacting with phosphate. Yet, for the $SO_4^{\bullet-}$ being similar reactive as $^{\bullet}OH$ a reaction rate < 1000 L mg^{-1}C s^{-1} is unlikely (average reaction rate $k(^{\bullet}OH + DOC)$ = 2.5 × 10^4 L mg^{-1}C s^{-1} [5, 6]). Hence, the above assumption is justified.

5.2.3 Determination of reaction rate constants for $SO_4^{\bullet-}$ and $^{\bullet}OH$ with DOC

The reaction rate constants of DOC plus $SO_4^{\bullet-}$ and $^{\bullet}OH$ have been determined as will be described in the following.

In the present system $SO_4^{\bullet-}$ and $^{\bullet}OH$ are mainly scavenged by DOC competing for the degradation of atrazine. Since $k(SO_4^{\bullet-})$ and $k(^{\bullet}OH)$ of atrazine are known, the reaction rates of $^{\bullet}OH$ and $SO_4^{\bullet-}$ plus DOC can be calculated on basis of the fluence rate and first order degradation of atrazine. The corresponding relationship is shown in equation 1.

Equation (1)

$$k'(atrazine) = \frac{2.303 \times \varepsilon_{peroxide} \times \phi_{peroxide} \times E_\lambda \times [peroxide] \times (k(atrazine + radical) - k(photolysis\ of\ atrazine))}{[DOC] \times k(DOC + radical)}$$

$k'(atrazine)$: First order degradation rate of atrazine / s^{-1}

$\varepsilon_{peroxide}$: Molar absorption of H_2O_2 or $S_2O_8^{2-}$ / mol m^{-2}

$\phi_{peroxide}$: Quantum yield of H_2O_2 or $S_2O_8^{2-}$ / mol $Einstein^{-1}$

E_λ : Fluence rate / Einstein m^{-2} s^{-1}

$[peroxide]$: Concentration of H_2O_2 or $S_2O_8^{2-}$ / M

$k(atrazine + radical)$: Second order rate constant of atrazine plus $^{\bullet}OH$ or $SO_4^{\bullet-}$ / M^{-1} s^{-1}

$k(photolysis\ of\ atrazine)$: Rate of atrazine photolysis / s^{-1}

$[DOC]$: Concentration of DOC / mgC L^{-1}

$k(DOC + radical)$: Rate constant of the reaction $^{\bullet}OH$ or $SO_4^{\bullet-}$ plus DOC / $Lmg^{-1}C$ s^{-1}

As the only unknown, *k* (DOC + radical) can either be derived by calculating the first order degradation rate of atrazine (experimental data) and solving the above equation for *k*(DOC + radical), or by adjusting *k*(DOC + radical) arriving at the best fit for the experimentally determined degradation of atrazine. The latter method has been used in the present study for different DOC and peroxide concentrations.

Following reaction parameters have been applied:

- quantum yield of H_2O_2 (254 nm, radical formation) : 1 mol $Einstein^{-1}$ [7]
- quantum yield of $S_2O_8^{2-}$ (254 & 248 nm, radical formation) : 1.4 mol $Einstein^{-1}$ [8, 9]
- molar absorption of H_2O_2 at 254 nm :1.86 m^2 mol^{-1} [10]
- molar absorption of $S_2O_8^{2-}$ at 254 nm : 2.2 m^2 mol^{-1} [11]
- second order rate constant of atrazine plus $SO_4^{\bullet-}$ and $^{\bullet}OH$: 3×10^9 M^{-1} s^{-1} (see chapter 4).

5.3 Results and Discussion

Figure 1 shows the degradation of atrazine in presence of humic acids by direct photolysis and in UV/H_2O_2, and UV/$S_2O_8^{2-}$. It can be seen that the degradation in UV/$S_2O_8^{2-}$ treatment is most efficient.

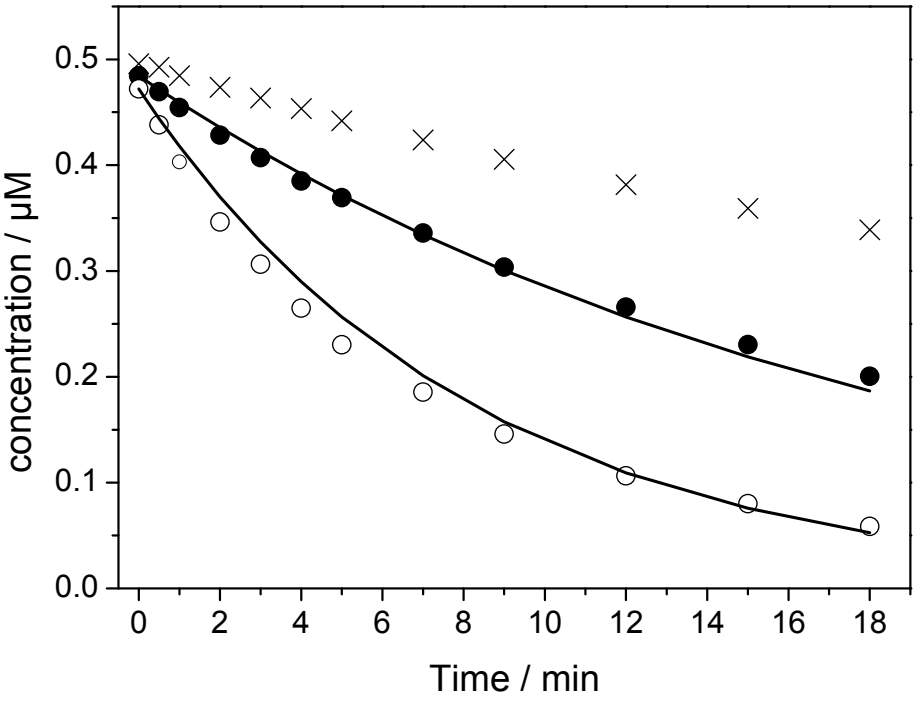

Figure 1: Photochemical degradation of atrazine (0.5 µM) in presence of humic acids (15 mgC L^{-1}); [$S_2O_8^{2-}$] = [H_2O_2] = 1 mM; [phosphate] = 2.5 mM; pH = 7.2; radiation source: low pressure mercury arc (15 W); Fluence rate (254 nm) = 58 µEinstein m^{-2} s^{-1} in pure water and 8.7 µEinstein m^{-2} s^{-1} in presence of humic acids (A_{254}:1.65 cm^{-1}); Direct photolysis (crosses); UV/H_2O_2 (closed circles); UV/$S_2O_8^{2-}$ (open circles); Lines represent modeled data (according to equation 1), symbols measured data; Observed degradation kinetics of atrazine: UV/$S_2O_8^{2-}$: 2.0×10^{-3} s^{-1}; UV/H_2O_2: 8.8×10^{-4} s^{-1}; UV: 3.6×10^{-4} s^{-1}.

According to equation 1 the degradation of atrazine now allows calculating the reaction rate of $SO_4^{\bullet-}$ and $^{\bullet}OH$ with humic acids. Following rate constants have been derived from three individual experiments:

- $k(SO_4^{\bullet-}$ + humic acids) = $6.6 \pm 0.4 \times 10^3$ L mgC^{-1} s^{-1}
- $k(^{\bullet}OH$ + humic acids) = $1.4 \pm 0.2 \times 10^4$ L mgC^{-1} s^{-1}

The value determined for $^{\bullet}OH$ is in accordance to a value determined for Suwannee River humic acids ($k = 1.9 \times 10^4$ L mgC^{-1} s^{-1} [12]). This confirms the experimental concept used. Beside the lower reaction rate of $SO_4^{\bullet-}$ towards DOC the higher molar absorption coefficient of $S_2O_8^{2-}$ and the higher quantum yield for radical formation (see above) further increase the efficiency of atrazine degradation in UV/$S_2O_8^{2-}$.

Figure 2 compares the first order degradation rates of atrazine in UV/H_2O_2 with UV/$S_2O_8^{2-}$ in presence of humic acids at different concentrations of HCO_3^- (2.5-10 mM). Atrazine is degraded twice as fast in UV/$S_2O_8^{2-}$ than in UV/H_2O_2 regardless of the presence of HCO_3^-. This independency from alkalinity is further illustrated in Figure 2 b) showing that the ratios of degradation rates in both processes do not correlate with the HCO_3^- concentration. This is in accordance to the similar reaction rates of the reactions $^{\bullet}OH$ and $SO_4^{\bullet-}$ plus HCO_3^- reported in the literature (($k(^{\bullet}OH + HCO_3^-) = 0.85\text{-}1\times10^7$ M^{-1}s^{-1} [13], recommended value 1×10^7 M^{-1}s^{-1}[5], $k(SO_4^{\bullet-} + HCO_3^-) = 2.8\text{-}9.1\times10^6$ M^{-1}s^{-1} [14, 15]), cancelling the influence of HCO_3^- out.

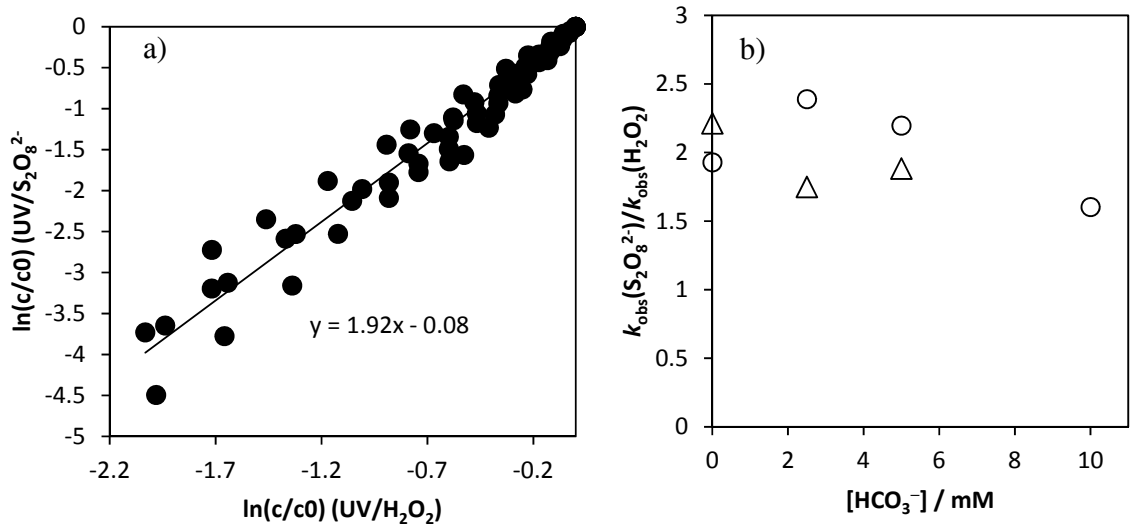

Figure 2: a) Observed degradation rates of atrazine in UV/H_2O_2 and UV/$S_2O_8^{2-}$ in presence of humic acids and different concentration of [HCO_3^-]; b) Ratio of first order degradation rates for atrazine vs. HCO_3^- concentration (derived from a)); circles: 15 mgC L^{-1}, triangles 7.5 mgC L^{-1}; [HCO_3^-] = 0, 2.5, 5 and 10 mM, [phosphate] = 2.5 mM in case of experiments with 15 mgC L^{-1}, 1.25 mM in case of experiments with 7.5 mgC L^{-1}, pH = 7.2, T = 25 °C

In presence of Suwannee River organic matter UV/$S_2O_8^{2-}$ was even 3 fold more efficient than UV/H_2O_2 (Figure 3). The reaction rate constant of $SO_4^{\bullet-}$ plus DOC (Suwannee River) has been estimated to be ≈ 3.8×10^3 L mg^{-1} C. This is ca. 3 times lower compared with the reported value determined for $^{\bullet}OH$ in the present system 1.14×10^4 L mg^{-1} C. (Note that the value determined for $^{\bullet}OH$ in UV/H_2O_2 is in fair agreement with a value reported in the literature 1.9×10^4 L $mg^{-1}C$ s^{-1} [12]).

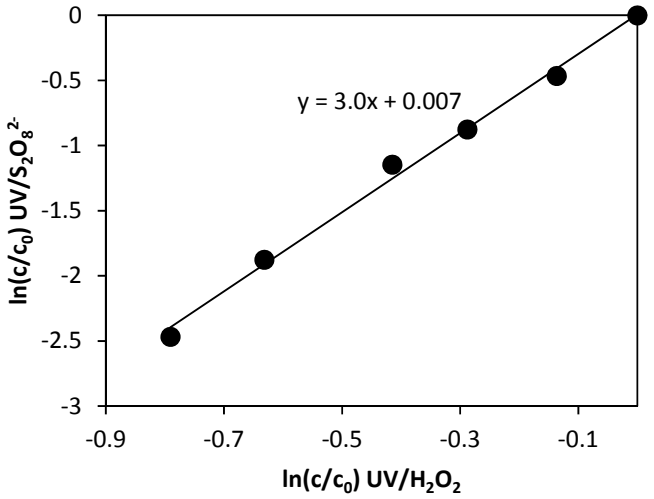

Figure 3: Observed degradation rates of atrazine in UV/H_2O_2 and UV/$S_2O_8^{2-}$ in presence of Suwannee River DOC 10 mgC L^{-1}, [HCO_3^-] = 0 mM, [phosphate] = 5 mM; pH = 7.2, T = 25 °C

The lower reactivity of the organic matter in $SO_4^{\bullet-}$ reactions can be explained by the fact that H-abstraction reactions are mostly slow. The reactions of several alcohols, alkanes and ethers with $SO_4^{\bullet-}$ proceed *via* H-abstraction, with reaction rates in the range of 10^7-10^8 M^{-1} s^{-1} [16, 17]). In contrast, H-abstraction is fast in $^{\bullet}OH$ reactions. Thus, saturated moieties of the organic matter might react fast with $^{\bullet}OH$ but not with $SO_4^{\bullet-}$. This leads to a weaker scavenging of radicals which could improve the degradation efficiency.

The results show, that the $SO_4^{\bullet-}$ reacts much more selective with natural organic carbon than $^{\bullet}OH$ does and that degradation of pollutants with a comparable kinetics towards $SO_4^{\bullet-}$ and $^{\bullet}OH$ can be more efficient in UV/$S_2O_8^{2-}$ compared with UV/H_2O_2. However, as will be shown in following chapters, the influence of DOC on $SO_4^{\bullet-}$ in natural waters is diminished by Cl^- driven scavenging of $SO_4^{\bullet-}$. A deeper discussion of the behavior of $SO_4^{\bullet-}$ in real water matrix will be provided in corresponding Chapter 7.

5.4 Literature

1. Canonica, S.; Meunier, L.; von Gunten, U., Phototransformation of selected pharmaceuticals during UV treatment of drinking water. *Water Res.*, **2008**. *42*(1-2): 121-128.
2. Nick, K.; Schöler, H.F.; Söylemez, T.; Akhlaq, M.S.; Schuchmann, H.P.; von Sonntag, C., Degradation of some triazine herbicides by UV radiation such as used in the UV disinfection of drinking water *J. Water SRT - Aqua*, **1992**. *41*: 82-87.
3. Neta, P.; Huie, R.E.; Ross, A.B., Rate constants for reactions of inorganic radicals in aqueous solution. *J. Phys. Chem. Ref. Data*, **1988**. *17*(3): 1027 - 1040.
4. Maruthamuthu, P.; Neta, P., Phosphate radicals. Spectra, acid-base equilibriums, and reactions with inorganic compounds. *J. Phys. Chem.*, **1978**. *82*(6): 710-713.
5. Schwarzenbach, R.P.; Gschwend, P.M.; Imboden, D.M., eds. *Environmental organic chemistry*. John Wiley & Sons, Inc. ISBN 0-47 1-35750-2. 2003.
6. von Sonntag, C., Advanced oxidation processes: Mechanistic aspects. *Water Sci. Technol.*, **2008**. *58*: 1015-1021.
7. Legrini, O.; Oliveros, E.; Braun, A.M., Photochemical processes for water treatment. *Chem. Rev.*, **1993**. *93*(2): 671-698.
8. Herrmann, H., On the photolysis of simple anions and neutral molecules as sources of O^{-}/OH, $SO_x^{-}$and Cl in aqueous solution. *Phys. Chem. Chem. Phys.*, **2007**. *9*(30): 3935-3964.
9. Mark, G.; Schuchmann, M.N.; Schuchmann, H.P.; von Sonntag, C., The photolysis of potassium peroxodisulphate in aqueous solution in the presence of tert-butanol: a simple actinometer for 254 nm radiation. *J. Photochem. Photobiol., A*, **1990**. *55*(2): 157-168.
10. Katsoyiannis, I.A.; Canonica, S.; von Gunten, U., Efficiency and energy requirements for the transformation of organic micropollutants by ozone, O_3/H_2O_2 and UV/H_2O_2. *Water Res.*, **2011**. *45*(13): 3811-3822.
11. Heidt, L.J., The photolysis of persulfate. *J. Chem. Phys.*, **1942**. *10*(5): 297-302.
12. Goldstone, J.V.; Pullin, M.J.; Bertilsson, S.; Voelker, B.M., Reactions of hydroxyl radical with humic substances: Bleaching, mineralization, and production of bioavailable carbon substrates. *Environ. Sci. Technol.*, **2002**. *36*(3): 364-372.
13. Buxton, G.V.; Greenstock, C.L.; Helman, W.P.; Ross, A.B., Critical review of rate constants for reactions of hydrated electrones, hydrogen-atoms and hydroxyl radicals ($^{\bullet}OH/O^{\bullet-}$) in aqueous solution. *J. Phys. Chem. Ref. Data*, **1988**. *17*(2): 513-886.
14. Huie, R.E.; Clifton, C.L., Temperature dependence of the rate constants for reactions of the sulfate radical, SO_4^{-}, with anions. *J. Phys. Chem.*, **1990**. *94*(23): 8561-8567.
15. Dogliotti, L., Flash photolysis of persulfate ions in aqueous solutions. Study of the sulfate and ozonide radical ions. *J. Phys. Chem.*, **1967**. *71*(8): 2511-2516.
16. Clifton, C.L.; Huie, R.E., Rate constants for hydrogen abstraction reactions of the sulfate radical, SO4-. Alcohols. *Int. J. Chem. Kinet.*, **1989**. *21*(8): 677-687.
17. Huie, R.E.; Clifton, C.L., Rate constants for hydrogen abstraction reactions of the sulfate radical, SO4-. Alkanes and ethers. *Int. J. Chem. Kinet.*, **1989**. *21*(8): 611-619.

Chapter 6

-

Formation of bromate in sulfate radical based oxidation

6.1 Abstract

Sulfate radical based oxidation is discussed being a potential alternative to hydroxyl radical based oxidation for pollutant control in water treatment. However, formation of undesired by-products, has been hardly addressed in the current literature, which is an issue in other oxidative processes such as bromate formation in ozonation of bromide containing water (US-EPA and EU drinking water standard of bromate: 10 µg L^{-1}). Sulfate radicals react fast with bromide ($k = 3.5 \times 10^9$ M^{-1} s^{-1}) which could also yield bromate as final product. The mechanism of bromate formation in aqueous solution in presence of sulfate radicals has been investigated in the present paper. Further experiments have been performed in presence of humic acids and in surface water for investigating the relevance of bromate formation in context of pollutant control.

6.2 Introduction

Oxidative water treatment based on highly reactive hydroxyl radicals ($^{\bullet}OH$) is referred to as advanced oxidation processes (AOP) and often used for degrading recalcitrant pollutants such as pesticides, X-ray contrast media and fuel additives (e.g., MTBE) [1]. $^{\bullet}OH$ can be generated in various ways e.g., by photolysis of hydrogen peroxide (UV/H_2O_2) [2] or in ozonation [1]. Beside $^{\bullet}OH$, sulfate radicals ($SO_4^{\bullet-}$) are frequently investigated as potential alternative oxidants for water treatment [3-12] and have already been applied in ground water remediation [13]. $SO_4^{\bullet-}$ can be formed in various ways using $S_2O_8^{2-}$ as a radical precursor. One possibility is its photolysis by UVC-radiation (UV/$S_2O_8^{2-}$) which is in analogy to UV/H_2O_2. A major drawback in oxidative water treatment is the formation of undesired by-products. For example ozone based processes can be limited by the formation of bromate (BrO_3^-) a potential carcinogen (US-EPA and EU drinking water standard: 10 µg L^{-1}) arising from the oxidation of Br^- [14]. Thereby, formation of BrO_3^- can be driven by O_3 and/or $^{\bullet}OH$. Corresponding mechanisms of these reactions have been investigated in detail [14-17]. For reactions in which solely O_3 or $^{\bullet}OH$ are involved, hypobromous acid (HOBr) is a requisite intermediate. Under typical conditions of water treatment HOBr can effectively be reduced by hydrogen peroxide (H_2O_2) to give rise to Br^- [18]. This instance is used for mitigating bromate formation in ozone applications by adding H_2O_2 [14]. In most $^{\bullet}OH$ based processes H_2O_2 is used as a radical source (e.g., UV/H_2O_2), thus preventing BrO_3^- formation. UV/TiO_2 is known to not require H_2O_2 addition for formation of $^{\bullet}OH$. However, studies indicated that BrO_3^- is not formed in this process [19]. Also Gamma radiolysis which is discussed being a potential water treatment option for both disinfection [20] and pollutant degradation [21-23] might oxidize Br^-

yielding BrO_3^-. In analogy to $^{\bullet}OH$ the reaction of $SO_4^{\bullet-}$ plus Br^- ($k = 3.5 \times 10^9\ M^{-1}s^{-1}$ [24]) yield BrO_3^- [25]. In the recent work of Fang and Shang [25] an empirical model has been established, which was used for describing the formation of HOBr/OBr^- and BrO_3^-. However, this model approach does not allow a decent mechanistic insight into the reaction pathway. That is targeted in the present Chapter. Therefore, a reaction mechanism has been established based on reactions and kinetics available in the literature and used for developing a kinetic model of $SO_4^{\bullet-}$ driven formation of BrO_3^-. This model has been used to describe the product pattern in BrO_3^- formation which was experimentally determined in the present study at various conditions. Furthermore, the bromate formation potential in natural matrices has been determined which was contrasted to the oxidation strength available for pollutant control.

6.3 Material and Methods

6.3.1 Chemicals

All chemicals were commercially available and used as received.

Acetonitrile (≥ 99.9%) Sigma Aldrich, *atrazine* (≥ 97.4%) Riedel-de Haën, *4-chlorobenzoic acid (pCBA)* (99%) Aldrich, *hydrochloric acid* (37% in water, p.a.) Merck, *hydrogen peroxide* (30%) Sigma Aldrich, *methanol* (p.a.) Sigma-Aldrich, *4-nitrobenzoic acid* (pNBA) (≥ 97.4%) Sigma Aldrich, *oxygen* (≥ 99.9%) Liquid Air, *phosphoric acid* (≥ 85%) Merck, *potassium bromate* (99.5 %) Fluka, *potassium chloride* (≥ 99.5%) Riedel-de Haën, *pure water* has been prepared by treating deionized water with a pure lap ultra instrument (Elga) (electrical resistance 18.6 MΩ), *sodium bicarbonate* (≥ 99.5%) KMF optichem, *sodium bromate* (99%) Fluka, *sodium carbonate* (≥ 99.8%) Riedel-de Haën, *sodium hydroxide* (≥ 99.9%, p.a.) VWR, *sodium peroxodisulfate* (p.a.) Sigma-Aldrich, *sulfuric acid* (95-97%) Applichem International, *Suwannee River NOM* (reverse osmosis concentrate) International Humic Acid Society, *Uridine* (≥ 99%) Sigma

6.3.2 Experimental procedures

Sulfate radicals have been generated by photolysis of peroxodisulfate (UV/$S_2O_8^{2-}$) in a merry-go-round apparatus equipped with a low pressure mercury lamp. This radiation source emits monochromatic light at 254 nm (Heraeus Noble Light GPH303T5L/4, 15 W, (185 nm band suppressed)). The fluence rate has

been determined by uridine actinometry according to [26]. Solutions have been buffered with phosphate. Even though $SO_4^{\bullet-}$ reacts with HPO_4^{2-} with a considerable rate (k = 1.2 × 10^6 M^{-1} s^{-1}) ($H_2PO_4^-$ is nearly inert (k < 7 × 10^4 M^{-1} s^{-1})) the reactions under study are faster by several orders of magnitudes (k($SO_4^{\bullet-}$ plus Br^-) = 3.5 × 10^9 M^{-1} s^{-1}). This allows addition of phosphate buffer in excess over bromide (e.g., factor 100), which is necessary for keeping pH constant (experimental details can be found in the caption of corresponding figures). pH-adjustments have been done by addition of sulfuric acid or sodium hydroxide, respectively. Methanol has been added to the samples (1 M in the sample) for scavenging low levels of $SO_4^{\bullet-}$ which may be formed during storage time by thermolysis of $S_2O_8^{2-}$. BrO_3^- and Br^- have been analyzed by ion chromatography (Metrohm 883 basic) equipped with a conductivity detector coupled with ion suppression (anion separation column with quaternary ammonium groups: Metrosep A Supp 4 - 250/4.0 mm, particle size 9 µm; eluent HCO_3^- (1.7 mM), CO_3^{2-} (1.8 mM) mixed with acetonitrile (30% (v/v)); flow: 1 mL min^{-1}; retention times: Br^- : 3.6 min, BrO_3^-: 4.4 min). For determining bromate and bromide at concentrations in the µM range a different IC system has been used coupled with ion and subsequent CO_2-suppression (881 Compact IC plus), equipped with a high capacity anion separation column (Metrosep A Supp 5 – 250/4.0, particle size 5 µm) which was necessary for separation of chloride and bromate (Eluent: 3.2 mM Na_2CO_3 and 1.0 mM $NaHCO_3$, flow: 0.7 mL min^{-1}; retention times: BrO_3^-: 8.0 min, Cl^-= 8.7 min , Br^- = 13.0 min). Atrazine, 4-chlorobenzoic acid (pCBA) and 4-nitrobenzoic acid (pNBA) have been determined by HPLC with UV-detection (Shimadzu) (C18 reversed phase separation column: Bischoff, NUCLEOSIL 100, 250/4.0 mm, particle size: 5.0 µm). As eluent a gradient of methanol/water has been used (gradient program (methanol content (v/v)): 0-3 min: gradient 20%-50%, 3-25 min: gradient 50%-75%; 25-30 min: gradient 75%-20%, 30-38 min: isocratic 20%; flow 0.6 mL min^{-1}; retention times/measured wave length: pNBA: 20.6 min/262 nm; atrazine: 25.8 min/234 nm, pCBA: 26.5 min/234 nm). HOBr has been determined by UV-absorption as OBr^- at 329 nm (ε(OBr^-) = 332 M^{-1} cm^{-1} [27]) by adjusting the solution to pH 11. Model calculations have been performed by using the software tool Kintecus [28].

Experiments in presence of humic acids where performed for simulating bromate formation in a real water during UV/$S_2O_8^{2-}$. Beside Br^-, probe compounds have been added for two purposes:

1. As model compound for simulating the degradation of pollutants, atrazine has been added (k(atrazine + $SO_4^{\bullet-}$) = 3 × 10^9 M^{-1} s^{-1} [9])

2. As indication for $^{\bullet}OH$ which may be formed in the reaction of $SO_4^{\bullet-}$ with Cl^- [29]. For this purpose pNBA has been chosen because it is inert in presence of $SO_4^{\bullet-}$ (k($SO_4^{\bullet-}$ + pNBA) ≤ 10^6 M^{-1} s^{-1} [30]) and UV radiation under present experimental conditions. However, it reacts fast with $^{\bullet}OH$ (k($^{\bullet}OH$ + pNBA) = 2.6 × 10^9 M^{-1} s^{-1} [31]). Thus, it is a sensitive indicator for the presence of $^{\bullet}OH$.

These compounds have been added in low concentrations (0.5 µM) for assuring that their contribution in scavenging of $SO_4^{\bullet-}$/$^{\bullet}OH$ is below 10%. In this situation these radicals react largely with the main water constituents (e.g., DOC), which is normal in water treatment.

As another matrix for simulating real water treatment conditions River Ruhr water (RWW, Mülheim a.d. Ruhr) has been used. The water has been filtered with cellulose acetate/cellulose nitrate filters with a pore size of 0.45 µm (Whatman).

Ozonation experiments have been performed as follows. An aqueous O_3 stock solution was prepared purging an O_3 enriched gas through ice cooled pure water. At stationary conditions a steady state concentration of ozone of 1 mM O_3 could be achieved. This solution was used to dose specific amounts of O_3 to samples under study. Therefore glass syringes with stainless steel cannulas haven been used. For maintaining a constant O_3 concentration, continuous purging with the ozone enriched gas ozone was necessary. Ozone has been generated by an ozone generator purchased from BMT Messtechnik Berlin (Philaqua 802x) with oxygen as feed gas.

6.4 Results and discussion

6.4.1 Oxidation of bromide in pure water

The reaction of $SO_4^{\bullet-}$ with Br^- leads to the formation of BrO_3^- in aqueous solution (Figure 1). The product pattern is in good agreement with the study of Fang and Shang [25] in that they observed a complete turnover of Br^- *via* HOBr/OBr^- to BrO_3^-. Furthermore, in their study Fang and Shan reported HOBr/OBr^- evolving to a peak concentration corresponding to 25 % of the initial Br^- concentration, which fairly matches the value of the present study (20 %, Figure 1 b), horizontal line). This supports the experimental results of both studies. The chemistry of bromine is well documented in the literature and sufficient reactions including their kinetics have been reported for describing the oxidation of Br^- by $SO_4^{\bullet-}$ as will be explained below. Bromine atoms formed as primary products (reaction 1) may induce a cascade of reactions (Table 1) yielding HOBr and BrO_3^- as main products. The HOBr yield displays a distinctive dependency on the pH-value, which has also been observed in the reaction of $^{\bullet}OH$, where HOBr has been proposed to be a requisite intermediate [17]. The influence of the pH-value on the yield of HOBr can be explained by HOBr speciation (p*K*a 8.8-9 [15, 16]), which may largely affect the rates of its consecutive degradation by $Br^{\bullet}$ which predominantly reacts with hypobromite (OBr^-) [17]. In analogy to mechanistic considerations in $^{\bullet}OH$ driven formation of BrO_3^- the present mechanism has

been modeled with equations shown in Table 1 (modeled data: lines in Figure 1). For determining the reaction rates in reactions involving HOBr a p*K*a of 8.8 has been used, which was suggested for solutions with an ionic strength of > 0.15 M [15] that suits our experimental conditions (ionic strength > 0.250 M). The good agreement of the model with the experimental results indicates a similar reaction mechanism compared to that proposed by von Gunten and Oliveras for $^{\bullet}OH$-based BrO_3^- formation [17].

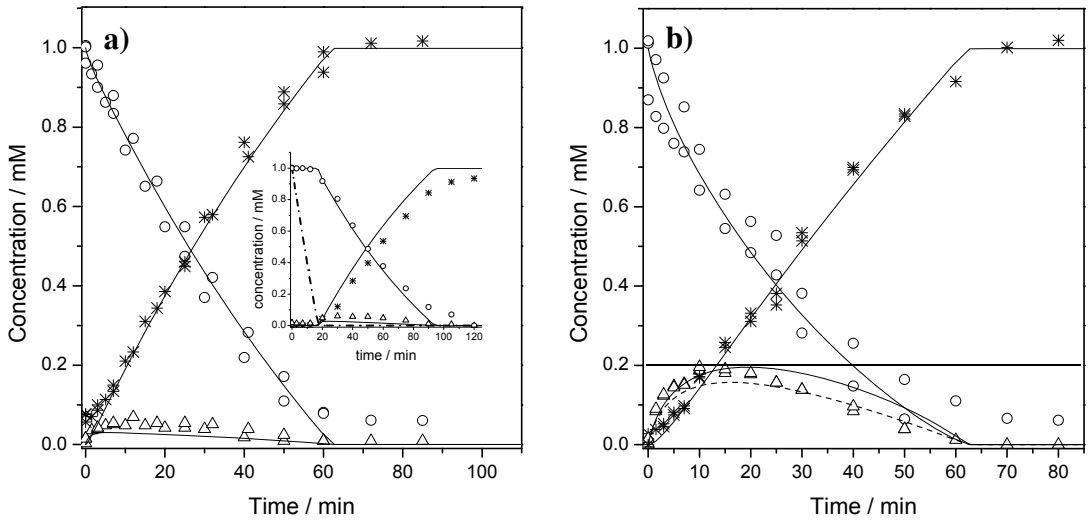

Figure 1: Product formation in the reaction of $SO_4^{\bullet-}$ with Br^-. Reaction conditions: [Br^-]: 1 mM, [$S_2O_8^{2-}$] 10 mM, [phosphate]: 100 mM, T: 25°C, a) Initial pH 8.0-8.1 (gradual decrease to pH 7.6 within a reaction time of 60 min), inset: bromate formation in presence of 1 mM H_2O_2, dotted-dashed line (inset) model calculation of H_2O_2 consumption; b) Initial pH 7.0 (gradual decrease to pH 6.8 within a reaction time of 90 min); circles: Br^-, triangles: HOBr/OBr^-; stars: BrO_3^-, solid lines model calculations, dashed line model of HOBr including the reaction of $Br^{\bullet}$ plus HOBr (*k*: 5×10^7 M^{-1} s^{-1}) (not shown in a), see below), horizontal line marks the peak concentration of HOBr/OBr^-.

However, the model does not fit well to the experimental results of bromate formation at pH 6 (data not shown). At pH 6 the formation of HOBr/OBr^- formation is largely overestimated, indicating that oxidative species may also react with HOBr/OBr^-, which has not been taken into account in the model calculations (Table 1). A good agreement with the HOBr concentration pattern can be achieved by taking a reaction of the bromine atom with HOBr into account assuming a reaction rate of 5×10^7 M^{-1} s^{-1}. This rate constant is around 2 orders of magnitude smaller compared with the reaction rate of $Br^{\bullet}$ plus OBr^-. This seems to be a realistic value which can also be found for other acid base couples in their

reaction with $Br^{\bullet}$ such as hydrogen cyanide (HCN) ($k = 1 \times 10^7$ M^{-1} s^{-1}) and cyanide (CN^-) ($k = 8 \times 10^8$ M^{-1} s^{-1}) [32]. Furthermore, this reaction does not change the other model calculations for lower pH values significantly (dashed line in Figure 1 b), because the reaction $Br^{\bullet}$ plus OBr^- is largely dominating (note that at pH 8 this effect must be even weaker (calculations not shown in Figure 1 a)). A contribution of $SO_4^{\bullet-}$ on oxidizing HOBr is not likely to happen. Included in the model, this reaction affects the outcome only if a very high rate constant is assumed for both species OBr^- and HOBr ($k(SO_4^{\bullet-}$ + HOBr/OBr^- (10^{10} M^{-1} s^{-1}). Such a rate constant would be much higher than that for the reaction with Br^- (3.5×10^9 M^{-1} s^{-1} [24]), which is most unlikely.

Table 1: Reactions occurring in UV/$S_2O_8^{2-}$ of bromide-containing aqueous solutions

No.	Reaction	$k_{forward}$, $k_{backward}$, *or* p*K*a	Ref.
(1)	$Br^- + SO_4^{\bullet-} \rightarrow Br^{\bullet} + SO_4^{2-}$	3.5 x 10^9 M^{-1} s^{-1}	[24]
(2)	$Br^{\bullet} + Br^- \rightleftarrows Br_2^{\bullet-}$	1 x 10^{10} M^{-1} s^{-1}, 1 x 10^5 s^{-1}	[33]
(3)	$Br_2^{\bullet-} + Br_2^{\bullet-} \rightarrow Br^- + Br_3^-$	1.8 x 10^9 M^{-1} s^{-1}	[34]
(4)	$Br_3^- \rightleftharpoons Br^- + Br_2$	1 x 10^7 s^{-1}, 1.5 x 10^9 M^{-1} s^{-1}	[35]
(5)	$Br_2 + H_2O \rightleftharpoons HOBr + Br^- + H^+$	97 s^{-1}, 1.6 x 10^{10} M^{-2} s^{-1}	[35]
(6)	$HOBr \rightleftharpoons BrO^- + H^+$	pKa: 8.8	[15]
(7)	$BrO^- + Br_2^{\bullet-} \rightarrow BrO^{\bullet} + 2Br^-$	8 ± 0.7 x 10^7 M^{-1} s^{-1}	[36]
(8)	$BrO^- + Br^{\bullet} \rightarrow BrO^{\bullet} + Br^-$	4.1 x 10^9 M^{-1} s^{-1}	[37]
(9)	$2BrO^{\bullet} + H_2O \rightarrow BrO^- + BrO_2^- + 2H^+$	4.9 ± 1 x 10^9 M^{-1} s^{-1}	[36]
(10)	$BrO_2^- + BrO^{\bullet} \rightarrow BrO^- + BrO_2^{\bullet}$	3.4 ± 0.7 x 10^8 M^{-1} s^{-1}	[36]
(11)	$BrO_2^- + Br_2^{\bullet-} \rightarrow Br^- + BrO^{\bullet} + BrO^-$	8.0 ± 0.8 x 10^7 M^{-1} s^{-1}	[36]
(12)	$2BrO_2^{\bullet} \rightleftharpoons Br_2O_4$	1.4 x 10^9 M^{-1} s^{-1}, 7.4 x 10^7 s^{-1}	[36]
(13)	$2BrO_2^{\bullet} + H_2O \rightarrow BrO_2^- + BrO_3^- + 2H^+$	4.2 x 10^7 M^{-1} s^{-1}	[36]

In the current model the formation of HOBr/BrO^- has been considered to be a requisite intermediate. This has been confirmed by experiments in presence of H_2O_2, which reduces HOBr/OBr^- to give rise to Br^- and thus suppressing the formation of BrO_3^-. This effect is shown in Figure 1 a) (inset), where 1 mM H_2O_2 has been added before irradiation, which led to a delay in BrO_3^- formation of ca. 20 min. This has been modeled by including the reduction of HOBr/OBr^- *via* H_2O_2 in the model (reaction 14/15, see below; note that the reaction rate is pH-dependent ($k = 1.96 \times 10^5$ M^{-1} s^{-1} at pH 8) [18]). Taking this rate constant into account the delay in bromate formation can be described by the model (Figure 1 a (inset)).

$OBr^- + H_2O_2 \rightarrow Br^- + H_2O + O_2$ (14)

$HOBr + HO_2^- \rightarrow Br^- + H_2O + O_2$ (15)

Both, experimental data and the model outcome revealed that the presence of H_2O_2 effectively suppresses the Br^- turnover (note, that the photochemical degradation of H_2O_2 is largely overwhelmed by its reaction with OBr^-/HOBr). This is a strong evidence for HOBr being a requisite intermediate.

6.4.2 Oxidation of bromide in presence of organic matter

DOC and bromide concentration have been varied to achieve different proportions of $SO_4^{\bullet-}$ reacting with bromide ([DOC] = 1, 3, and 10 mg L^{-1}, [Br^-] = 1 µM). The reaction rate of $SO_4^{\bullet-}$ plus the humic acids used has been determined to be $k(SO_4^{\bullet-}$ plus humic acids) = 6.6×10^3 L mg^{-1} s^{-1} (Chapter 5). The ratios of [Br^-]/[DOC] range from 0.1-0.5 µM L mg^{-1}, covering the range found in natural waters such as river Ruhr ([DOC] = 1.9 mg L^{-1}, [Br^-] = 0.54 µM (see caption of Figure 4), Br^-/DOC = 0.28 µM L mg^{-1}). Within a reaction time sufficient for degrading > 90 % of pNBA and atrazine neither bromide degradation nor bromate formation has been observed ([$S_2O_8^{2-}$] = 0.5 mM, reaction time = 2, 6 and 25 min for [DOC] = 1, 3, 10 mg L^{-1}). Even an increase of bromide concentration in presence of 10 mg L^{-1} DOC from 1 µM to 50 µM did not reveal any formation of BrO_3^- within a reaction time of 50 min, even though the proportion of $SO_4^{\bullet-}$ reacting with Br^- increased largely. Note that under these conditions atrazine degradation is mainly driven by photolysis (Figure 2).

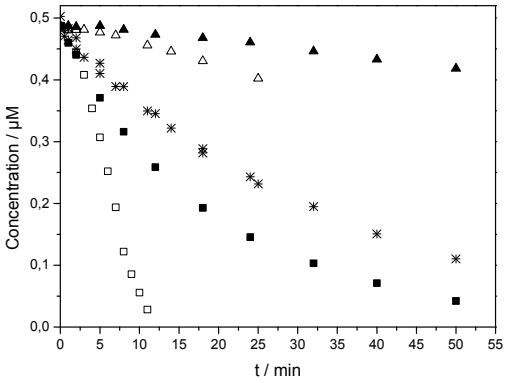

Figure 2: Degradation of atrazine (squares) and pNBA (triangles) in UV/$S_2O_8^{2-}$ in presence of humic acids and Br^-; [Br^-] = 1 µM (open symbols), 50 µM (filled symbols), stars: direct photo degradation of atrazine, [DOC] = 9.8-10.0 mg L^{-1}, [phosphate] = 2.5 mM, [Cl^-] = 9.1 – 11.5 µM, pH: 7.1-7.2

The humic acids used in the present study contain small amounts of Cl^-, which cannot be avoided without changing the chemical composition of the organic matter. Furthermore, Cl^- can be introduced by several means such as pH-measurements and contaminated reagents. IC measurements reveal a concentration of 9.05 – 11.47 µM for the experiments in presence of 9-10 mg L^{-1} DOC and a Cl^- content of 1.2 ± 0.3 µM per mg L^{-1} DOC as average value for all experiments in presence of humic acids.

The slow degradation of pNBA might be related to the presence of $Cl^\bullet$ and $^\bullet OH$. However, their contribution to the transformation of probe compounds or Br^- is negligible as will be explained below.

The reaction of $Cl^\bullet$ with water is fast (2500 s^{-1}) and yields $ClOH^-$ as short-lived intermediate [29]. At pH 7 the back reaction ($ClOH^- \rightarrow Cl^\bullet + OH^-$) is rather slow ($k = 2 \times 10^3$ s^{-1}) and the $ClOH^-$ adduct may largely decompose en route of $^\bullet OH$ formation ($ClOH^- \rightarrow Cl^- + {}^\bullet OH$; $k = 6.9 \times 10^9$ s^{-1}) [29]. The reaction rate of $^\bullet OH$ plus pNBA ($k = 2.6 \times 10^9$ M^{-1} s^{-1} [31]) is similar fast as for atrazine ($k = 3 \times 10^9$ M^{-1} s^{-1} [38, 39]) and only a bit slower than for Br^- (10^{10} M^{-1} s^{-1} [40]) (a detailed discussion of the interaction of Cl^- and $SO_4^{\bullet-}$ is given in chapter 7). Since pNBA displays a very slow apparent degradation rate, the contribution of $^\bullet OH$ arising from Cl^- oxidation probably hardly affects atrazine or Br^- degradation.

Analogous experiments have been performed in river Ruhr water, which is used for drinking water purification. The Br^- content of this water is 40-50 µg L^{-1}, which may already lead to an exceedance of the drinking water standard for bromate in ozonation under certain treatment conditions [14]. River Ruhr water also contains Cl^- in the mM range (0.78 ± 0.02 mM) that leads to a large proportion of $SO_4^{\bullet-}$ reacting with Cl^- (> 90%) yielding $^\bullet OH$ [29] (see Chapter 7). This does not necessary prevent BrO_3^- formation because BrO_3^- can also be formed in the reactions with $^\bullet OH$ as mentioned above [17]. However, BrO_3^- has not been formed in UV/$S_2O_8^{2-}$ in River Ruhr water. Variation of the HCO_3^- concentration (0-2 mM) also did not lead to a detectable formation of BrO_3^-. This is illustrated in

Figure 3 a) showing the concentration of bromide in different photochemical processes. It can be observed, that the bromide concentrations in UV/$S_2O_8^{2-}$ are near the Br^- level of the original River Ruhr water (red line) and resembles that of UV/H_2O_2 and UV which are both known to not form BrO_3^- in presence of Br^- (the differences in case of UV and UV/H_2O_2 at 0 mM HCO_3^- are probably related to an analytical issues). This suggests, that no turnover of Br^- happened to appear, while the oxidation power achieved in UV/$S_2O_8^{2-}$ suffices for > 95 % degradation of atrazine and up to 95% degradation of pNBA (Figure 3 b)) (note that pNBA is degraded by $^{\bullet}OH$ formed in the reaction of $SO_4^{\bullet-}$ plus Cl^-, see Chapter 7). The mechanisms behind the tendency of pNBA to be less degraded with increasing concentration of HCO_3^- (Figure 3 b) will be discussed in Chapter 7.

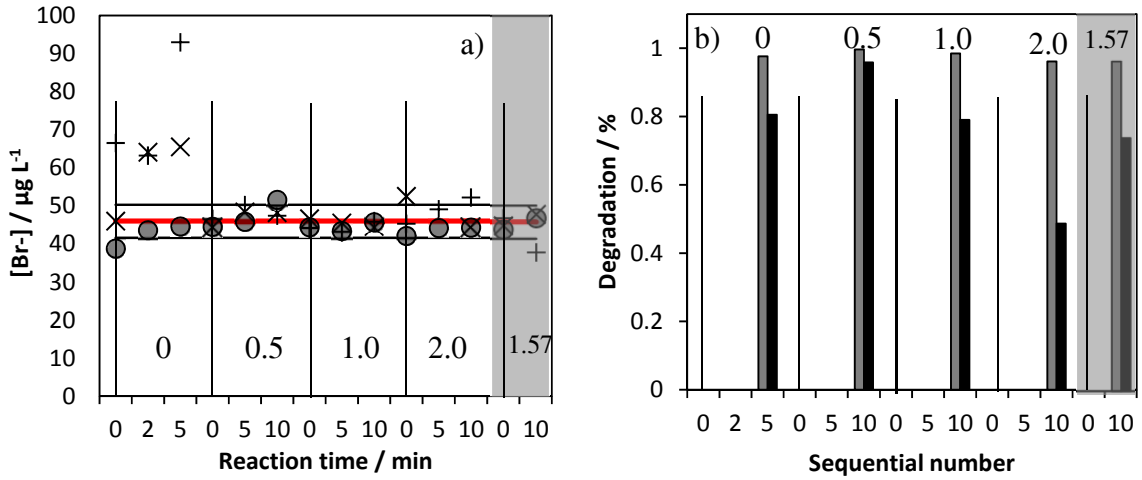

Figure 3: a) Concentration of bromide in River Ruhr water at different alkalinities in photochemical treatment; UV/$S_2O_8^{2-}$ (circles), UV/H_2O_2 (triangles), UV (crosses), vertical lines indicate initial conditions, the following points represent subsequent samples after different reaction times given at the x-axis; red line: concentration of bromide in untreated River Ruhr water, horizontal black lines: upper and lower range of the Br^- concentration in untreated River Ruhr; b) Degradation of organic compounds in the experiments of a); grey = atrazine, black = pCBA; a) and b) numbers indicate the concentration of HCO_3^-; shaded area = original River Ruhr water (no adjustment of alkalinity); $[S_2O_8^{2-}]_0 = [H_2O_2]_0$; T 25°C, pH 7.2, [DOC] = 1.9 mg/L, $[HCO_3^-]$ = 0-2 mM

For comparing these experimental results with ozonation, ozone has been dosed to the unmodified river Ruhr water. As shown in Figure 4 ozonation leads to a quantitative turnover of Br^- to BrO_3^- (complete mass balance). However, a dose of 3 mg L^{-1} O_3 is needed for achieving the same extent of pNBA and atrazine degradation as achieved in UV/$S_2O_8^{2-}$. At that dose 16 ± 0.1 µg L^{-1} BrO_3^- is formed which is largely exceeding the EU and USEPA drinking water standard of 10 µg L^{-1} [14] (Figure 4).

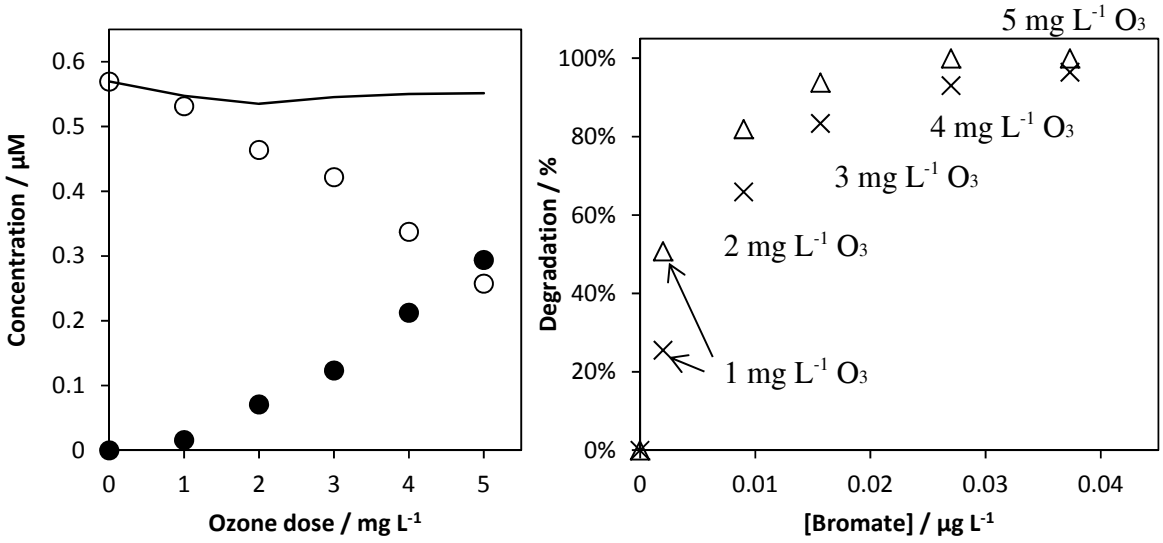

Figure 4: a) turnover of bromide (open circles) to bromate (closed circles) after different ozone doses, the black line indicates the sum of Br^- and BrO_3^- ; b) Degradation of atrazine (triangles) and pNBA (crosses) vs. bromate formation in river Ruhr water. Ozone doses are noted in the figure; pH 7.2, [DOC] = 1.9 mg L^{-1}, [HCO_3^-] = 1.57 mM, [Br^-] = 43 ± 0.3 µg L^{-1}

The lack of BrO_3^- formation in UV/$S_2O_8^{2-}$ can be explained by the formation of superoxide anion ($O_2^{\bullet-}$) that has been reported to occur in reactions of $SO_4^{\bullet-}$ with organic matter in presence of oxygen [41-43]. With few exceptions $O_2^{\bullet-}$ is considered to be a mild reducing radical [41-43]. However, its reaction rate constants with inorganic bromine species are fast and can reduce several intermediates such as HOBr/BrO^- (reactions 16 to 20).

(16) $HOBr + O_2^{\bullet-} \xrightarrow{Br^-} O_2 + OH^- + Br_2^{\bullet-}$ $3.5 \times 10^9\ M^{-1}\ s^{-1}$ [44]

(17) $BrO^- + O_2^{\bullet-} \xrightarrow{Br^-, H_2O} O_2 + 2OH^- + Br_2^{\bullet-}$ $< 2 \times 10^8\ M^{-1}\ s^{-1}$ [44]

(18) $Br_2^{\bullet-} + O_2^{\bullet-} \rightarrow O_2 + Br^- + Br^-$ $1.7 \times 10^8\ M^{-1}\ s^{-1}$ [45]

(19) $Br_2^{\bullet-} + Br_2^{\bullet-} \rightarrow Br^- + Br_3^-$ $1.8 \times 10^9\ M^{-1}\ s^{-1}$ [34]

(20) $Br_3^{\bullet-} + O_2^{\bullet-} \rightarrow O_2 + Br^- + Br_2^-$ $1.5 \times 10^9\ M^{-1}\ s^{-1}$ [46]

$O_2^{\bullet-}$ is formed in the reaction of $^{\bullet}OH$ with benzene at high yields (69 % of $^{\bullet}OH$ attacks yield $O_2^{\bullet-}$ [47]). The reaction of $SO_4^{\bullet-}$ with benzene leads to the formation of a radical cation which subsequently reacts with water to give rise to the hydroxycyclohexadienyl radical [48]. That radical is also formed in the primary attack of $^{\bullet}OH$ on benzene (addition). The subsequent steps are the same for both $^{\bullet}OH$, and $SO_4^{\bullet-}$. Thus, a similar high yield of $O_2^{\bullet-}$ can be expected in the reactions of $SO_4^{\bullet-}$ with aromatic compounds. The constant concentration of $Br^{\bullet}$ in UV/$S_2O_8^{2-}$ of River Ruhr water (Figure 3a) corroborates a reductive pathway resulting in a reformation of Br^- (reaction 16-20). Any other sink of $Br^{\bullet}$, $Br_2^{\bullet-}$ or HOBr/OBr^- such as bromination of phenolic moieties of the DOC would result in a deficient Br^- balance.

Considering following rate constants of $k(^{\bullet}OH \text{ plus DOC}) = 2.5 \times 10^4$ L mg^{-1} s^{-1} [49] and $k(^{\bullet}OH \text{ plus } Br^-) = 1 \times 10^{10}$ M^{-1} s^{-1} [40] and the concentrations of DOC ≈ 1.9 mg L^{-1} and of Br^- ≈ 0.6 µM in River Ruhr water, it can be calculated that ca. nine $^{\bullet}OH$ react with DOC per reaction with Br^-. Since most aromatic moieties of the organic matter (e.g., alkyl phenols) react fast with $^{\bullet}OH$ and $SO_4^{\bullet-}$ it is likely that $O_2^{\bullet-}$ is formed in excess over $Br^{\bullet}$, thus providing sufficient reducing power for preventing the formation of BrO_3^- *via* reaction 16 to 20.

Since Fang and Shang [25] also performed experiments in presence of NOM their work will be discussed below. The authors reported a suppression of bromate formation in presence of natural matrices (Shatin Water Treatment Works in Hong Kong and Suwannee River NOM). However, their explanation that this suppression is due to scavenging of reactive bromine species by NOM, has been ruled out in the present study by the complete Br^- balance (Figure 3) as explained above. The authors further compared the formation of BrO_3^- with the degradation of pCBA and observed a suppression of BrO_3^- formation at a very high Br^- to NOM ratio of 20 µM L mg^{-1}, while pCBA was largely degraded. However, at higher Br^- to NOM ratios of 50 and 100, BrO_3^- formation set in while pCBA degradation was incomplete (80% and 40% degradation of pCBA). Yet, even in such extreme scenarios pCBA was degraded to an extent of > 90% without exceedance of the EU and US-EPA BrO_3^- drinking water standard (10 µg L^{-1} [14]). It has to be noted that the very large concentrations of both pCBA (20 µM) and Br^- (20 µM) Fang and Shang applied diminishes the fraction of $SO_4^{\bullet-}$ reacting with NOM (0.1-1 mg L^{-1}) to below 10 %, while Br^- and pCBA comprise the main reactants.

Despite this small fraction of the reaction NOM plus $SO_4^{\bullet-}$, BrO_3^- formation is effectively suppressed confirming that the inhibition of BrO_3^- is very sensitive towards NOM. It has to be pointed out, that pCBA does probably not interfere by yielding $O_2^{\bullet-}$ in its reaction with $SO_4^{\bullet-}$, since the reaction of pCBA plus $SO_4^{\bullet-}$ led to no distinctive suppression of BrO_3^-.

In ozonation the situation is somewhat different, because under typical conditions of water purification ozone exposures are much higher compared with radical exposures in any AOP or related processes. Furthermore ozone competes with the bromine intermediates for $O_2^{\bullet-}$ with a fast reaction ($k = 1.6 \times 10^9$ M^{-1} s^{-1} [50]) yielding $^{\bullet}OH$ [50]. Both factors favor the formation of BrO_3^-. However, the present work indicated that it seems to be effectively suppressed in oxidative water treatment processes exclusively based on radical reactions including those processes where H_2O_2 dosage is not necessary (e.g., UV/TiO_2 or gamma radiolysis) [51].

6.5 Literature

1. von Gunten, U., *Ozonation of drinking water: Part I. Oxidation kinetics and product formation.* Water Research, 2003. **37**(7): p. 1443-1467.
2. Legrini, O., E. Oliveros, and A.M. Braun, *Photochemical processes for water treatment.* Chemical Reviews, 1993. **93**(2): p. 671-698.
3. Liang, C., C.F. Huang, and Y.J. Chen, *Potential for activated persulfate degradation of BTEX contamination.* Water Research, 2008. **42**(15): p. 4091-4100.
4. Liang, C., Z.S. Wang, and C.J. Bruell, *Influence of pH on persulfate oxidation of TCE at ambient temperatures.* Chemosphere, 2007. **66**(1): p. 106-113.
5. Hori, H., E. Hayakawa, H. Einaga, S. Kutsuna, K. Koike, T. Ibusuki, H. Kiatagawa, and R. Arakawa, *Decomposition of environmentally persistent perfluorooctanoic acid in water by photochemical approaches.* Environmental Science and Technology, 2004. **38**(22): p. 6118-6124.
6. Hori, H., Y. Nagaoka, M. Murayama, and S. Kutsuna, *Efficient decomposition of perfluorocarboxylic acids and alternative fluorochemical surfactants in hot water.* Environmental Science and Technology, 2008. **42**(19): p. 7438-7443.
7. Hori, H., A. Yamamoto, E. Hayakawa, S. Taniyasu, N. Yamashita, S. Kutsuna, H. Kiatagawa, and R. Arakawa, *Efficient decomposition of environmentally persistent perfluorocarboxylic acids by use of persulfate as a photochemical oxidant.* Environmental Science and Technology, 2005. **39**(7): p. 2383-2388.
8. Kutsuna, S. and H. Hori, *Rate constants for aqueous-phase reactions of SO_4^- with $C_2F_5C(O)O^-$ and $C_3F_7C(O)O^-$ at 298 K.* International Journal of Chemical Kinetics, 2007. **39**(5): p. 276-288.
9. Manoj, P., K.P. Prasanthkumar, V.M. Manoj, U.K. Aravind, T.K. Manojkumar, and C.T. Aravindakumar, *Oxidation of substituted triazines by sulfate radical anion ($SO_4^{\bullet-}$) in aqueous medium: A laser flash photolysis and steady state radiolysis study.* Journal of Physical Organic Chemistry, 2007. **20**(2): p. 122-129.
10. Anipsitakis, G.P. and D.D. Dionysiou, *Degradation of organic contaminants in water with sulfate radicals generated by the conjunction of peroxymonosulfate with cobalt.* Environmental Science and Technology, 2003. **37**(20): p. 4790-4797.
11. Anipsitakis, G.P. and D.D. Dionysiou, *Radical generation by the interaction of transition metals with common oxidants.* Environmental Science & Technology, 2004. **38**(13): p. 3705-3712.
12. Anipsitakis, G.P., D.D. Dionysiou, and M.A. Gonzalez, *Cobalt-mediated activation of peroxymonosulfate and sulfate radical attack on phenolic compounds. Implications of chloride ions.* Environmental Science and Technology, 2006. **40**(3): p. 1000-1007.
13. Siegrist, R.L., M. Crimi, and T.J. Simpkin, eds. *In sito chemical oxidation for groundwater remediation*. 2011: New York Heidelberg Dordrecht London.
14. von Gunten, U., *Ozonation of drinking water: Part II. Disinfection and by-product formation in presence of bromide, iodide or chlorine.* Water Research, 2003. **37**(7): p. 1469-1487.
15. Haag, W.R. and J. Hoigné, *Ozonation of bromide-containing waters: Kinetics of formation of hypobromous acid and bromate.* Environmental Science and Technology, 1983. **17**(5): p. 261-267.
16. von Gunten, U. and J. Hoigne, *Bromate formation during ozonation of bromide-containing waters: Interaction of ozone and hydroxyl radical reactions.* Environmental Science and Technology, 1994. **28**(7): p. 1234-1242.
17. von Gunten, U. and Y. Oliveras, *Advanced oxidation of bromide-containig waters: Bromate formation mechanisms.* Environmental Science and Technology, 1998. **32**(1): p. 63-70.

18. von Gunten, U. and Y. Oliveras, *Kinetics of the reaction between hydrogen peroxide and hypobromous acid: Implication on water treatment and natural systems.* Water Research, 1997. **31**(4): p. 900-906.
19. Tercero Espinoza, L.A. and F.H. Frimmel, *Formation of brominated products in irradiated titanium dioxide suspensions containing bromide and dissolved organic carbon.* Water Research, 2008. **42**(6-7): p. 1778-1784.
20. de Souza, G.S.M.B., L.A. Rodrigues, W.J. de Oliveira, C.A.L. Chernicharo, M.P. Guimaraes, C.L. Massara, and P.A. Grossi, *Disinfection of domestic effluents by gamma radiation: Effects on the inactivation of Ascaris lumbricoides eggs.* Water Research, 2011. **45**(17): p. 5523-5528.
21. Dessouki, A.M., H.F. Aly, and H.H. Sokker, *The use of gamma radiation for removal of pesticides from waste water.* Czechoslovak Journal of Physics, 1999. **49**: p. 521-533.
22. Tahri, L., D. Elgarrouj, S. Zantar, M. Mouhib, A. Azmani, and F. Sayah, *Wastewater treatment using gamma irradiation: Tetouan pilot station, Morocco.* Radiation Physics and Chemistry, 2010. **79**(4): p. 424-428.
23. Getoff, N., *Factors influencing the efficiency of radiation-induced degradation of water pollutants.* Radiation Physics and Chemistry, 2002. **65**(4-5): p. 437-446.
24. Redpath, J.L. and R.L. Willson, *Chain reactions and radiosensitization: model enzyme studies.* International Journal of Radiation Biology, 1975. **27**(4): p. 389-398.
25. Fang, J.Y. and C. Shang, *Bromate formation from bromide oxidation by the UV/persulfate process.* Environmental Science and Technology, 2012. **46**(16): p. 8976-8983.
26. von Sonntag, C. and H.P. Schuchmann, *UV disinfection of drinking water and by-product formation - some basic considerations.* J Water SRT - Aqua, 1992. **41**(2): p. 67-74.
27. Troy, R.C. and D.W. Margerum, *Non-metal redox kinetics: Hypobromite and hypobromous acid reactions with iodide and with sulfite and the hydrolysis of bromosulfate.* Inorganic Chemistry, 1991. **30**(18): p. 3538-3543.
28. Ianni, J.C., *Kintecus Version 3.95.* www.kintecus.com, 2008.
29. McElroy, W.J., *A laser photolysis study of the reaction of SO_4^- with Cl^- and the subsequent decay of Cl_2^- in aqueous solution.* Journal of Physical Chemistry, 1990. **94**(6): p. 2435-2441.
30. Neta, P., V. Madhavan, H. Zemel, and R.W. Fessenden, *Rate constants and mechanism of reaction of sulfate radical anion with aromatic compounds.* Journal of the American Chemical Society, 1977. **99**(1): p. 163-164.
31. Buxton, G.V., C.L. Greenstock, W.P. Helman, and A.B. Ross, *Critical review of rate constants for reactions of hydrated electrones, hydrogen-atoms and hydroxyl radicals ($^{\bullet}OH/O^{\bullet-}$) in aqueous solution.* Journal of Physical and Chemical Reference Data, 1988. **17**(2): p. 513-886.
32. NIST. *National institut of standards and technology - data base of reaction rate constants*. [cited 2013]; Available from: http://kinetics.nist.gov/solution/SearchForm.
33. Zehavi, D. and J. Rabani, *Oxidation of aqueous bromide ions by hydroxyl radicals. Pulse radiolytic investigation.* The Journal of Physical Chemistry, 1972. **76**(3): p. 312-319.
34. Cercek, B., M. Ebert, M. Gilbert and A.J. Swallow, *Pulse radiolysis of aerated aqueous potassium bromide solutions.* in Pulse Radiolysis academic press New York, 1965. p. 83-98.
35. Beckwith, R.C., T.X. Wang, and D.W. Margerum, *Equilibrium and kinetics of bromine hydrolysis.* Inorganic Chemistry, 1996. **35**(4): p. 995-1000.
36. Buxton, G.V. and F.S. Dainton, *Radiolysis of aqueous solutions of oxybromine compounds - Spectra and reactions of BrO and BrO_2.* Proceedings of the Royal Society of London Series a-Mathematical and Physical Sciences, 1968. **304**(1479): p. 427-439.
37. Klaning, U.K. and T. Wolff, *Laser flash-photolysis of HClO, ClO^-, HBrO, and BrO^- in aqueous-solution - Reactions of Cl atoms and Br atoms.* Berichte Der Bunsen-Gesellschaft-Physical Chemistry Chemical Physics, 1985. **89**(3): p. 243-245.

38. Acero, J.L., K. Stemmler, and U. von Gunten, *Degradation kinetics of atrazine and its degradation products with ozone and OH radicals: A predictive tool for drinking water treatment.* Environmental Science and Technology, 2000. **34**(4): p. 591-597.
39. Tauber, A. and C. Von Sonntag, *Products and kinetics of the OH-radical-induced dealkylation of atrazine.* Acta Hydrochimica et Hydrobiologica, 2000. **28**(1): p. 15-23.
40. Zehavi, D. and J. Rabani, *The oxidation of aqueous bromide ions by hydroxyl radicals. A pulse radiolytic investigation.* Journal of Physical Chemistry, 1972. **76**(3): p. 312-319.
41. Peyton, G.R., *The free-radical chemistry of persulfate-based total organic-carbon analyzers.* Marine Chemistry, 1993. **41**(1-3): p. 91-103.
42. Siegrist, R.L.C., M.; Simpkin, T. J., *In situ chemical oxidation for groundwater remediation*. 2011: Springer Science +Business Media LLC.
43. Furman, O.S., A.L. Teel, and R.J. Watts, *Mechanism of base activation of persulfate.* Environmental Science & Technology, 2010. **44**(16): p. 6423-6428.
44. Schwarz, H.A. and B.H.J. Bielski, *Reactions of hydroperoxo and superoxide with iodine and bromine and the iodide (I_2^-) and iodine atom reduction potentials.* The Journal of Physical Chemistry, 1986. **90**(7): p. 1445-1448.
45. Wagner, I. and H. Strehlow, *On the flash-photolysis of bromide ions in aqueous-solutions.* Berichte Der Bunsen-Gesellschaft-Physical Chemistry Chemical Physics, 1987. **91**(12): p. 1317-1321.
46. Schwarz, H.A. and B.H.J. Bielski, *Reactions of HO2 and O2- with iodine and bromine and the I2- and I atom reduction potentials.* Journal of Physical Chemistry, 1986. **90**(7): p. 1445-1448.
47. Pan, X.M., M.N. Schuchmann, and C. Von Sonntag, *Oxidation of benzene by the OH radical. A product and pulse radiolysis study in oxygenated aqueous solution.* Journal of the Chemical Society, Perkin Transactions 2, 1993(3): p. 289-297.
48. Norman, R.O.C., P.M. Storey, and P.R. West, *Electron spin resonance studies. Part XXV. Reactions of the sulphate radical anion with organic compounds.* Journal of the Chemical Society B: Physical Organic, 1970: p. 1087-1095.
49. Schwarzenbach, R.P., P.M. Gschwend, and D.M. Imboden, eds. *Environmental organic chemistry*. John Wiley & Sons, Inc. ISBN 0-47 1-35750-2. 2003.
50. Bühler, R.E., J. Staehelin, and J. Hoigné, *Ozone decomposition in water studied by pulse radiolysis. 1. HO_2/O_2^- and HO_3/O_3^- as intermediates.* Journal of Physical Chemistry, 1984. **88**(12): p. 2560-2564.
51. von Sonntag, C., *Advanced oxidation processes: Mechanistic aspects.* Water Science and Technology, 2008. **58**: p. 1015-1021.

Chapter 7

-

Influence of chloride & alkalinity in sulfate radical based oxidation

7.1 Abstract

Sulfate radical ($SO_4^{\bullet-}$) based oxidation is discussed being a potential water treatment option and is already used in ground water remediation. However, the complex $SO_4^{\bullet-}$ chemistry in natural matrices is hardly understood. In that regard the fast reaction of $SO_4^{\bullet-}$ plus Cl^- is of high importance since Cl^- belongs to main constituents in the aqueous environment. This reaction yields chlorine atoms ($Cl^\bullet$) as primary products. $Cl^\bullet$ initiates a cascade of subsequent reactions with a pH dependent product pattern. At low pH (< 5) formation of chlorine derived oxidation products such as chlorate (ClO_3^-) is favored. This is undesired because ClO_3^- may reveal adverse effects on the environment and human health. At pH > 5 $Cl^\bullet$ mainly reacts with water yielding hydroxyl radicals ($^\bullet OH$). These reactions are important in the context of $SO_4^{\bullet-}$ based water treatment, since $^\bullet OH$ can be formed by other processes already applied in water treatment and potential advantages of $SO_4^{\bullet-}$ then do not apply anymore. The energy efficiency has been investigated for photolysis of peroxodisulfate (UV/$S_2O_8^{2-}$), photolysis of H_2O_2 (UV/H_2O_2) and ozonation. UV/$S_2O_8^{2-}$ and UV/H_2O_2 are similar efficient in degrading atrazine in River Ruhr water (≈ 0.9 kWh m^{-3} for 90% degradation), even though quantum yield (Φ) and absorption coefficient of $S_2O_8^{2-}$ (Φ = 1.4 mol $Einstein^{-1}$, 22 $M^{-1}cm^{-1}$) is higher than of H_2O_2 (Φ = 1.0 mol $Einstein^{-1}$, 20 $M^{-1}cm^{-1}$). This is mainly due to scavenging of $Cl^\bullet$ by HCO_3^-.

7.2 Introduction

As highly reactive species sulfate radicals ($SO_4^{\bullet-}$) are principally capable of oxidizing pollutants such as, trichloroethene [1], *tert*-butylmethylether [2], chlorinated ethenes [3] and phenols [4]. Thus, $SO_4^{\bullet-}$ based oxidation is frequently discussed as an alternative oxidative treatment option for pollutant control in water treatment. Conventional radical based processes are based on nonselective hydroxyl radicals ($^\bullet OH$) (Advanced oxidation process (AOP)). Due to the different nature of $^\bullet OH$ and $SO_4^{\bullet-}$, $SO_4^{\bullet-}$ may have a potential to overcome limitations of conventional AOP. A case in point are perfluorinated compounds which are inert towards $^\bullet OH$ [5-7] but slightly reactive towards $SO_4^{\bullet-}$ [5].

As mentioned in Chapter 1 $^\bullet OH$ and $SO_4^{\bullet-}$ are formed in the photolysis of H_2O_2 and $S_2O_8^{2-}$, respectively and both peroxides have similar photochemical features such as molar absorption ($\varepsilon_{254}(H_2O_2)$ = 20 cm^{-1} [8], $\varepsilon_{254}(S_2O_8^{2-})$ = 22 cm^{-1} [9]) and quantum yield of radical formation $\Phi_{254}(H_2O_2)$ = 1 mol $einstein^{-1}$ [10], $\Phi_{254}(S_2O_8^{2-})$ = 1.4 mol $einstein^{-1}$ [11, 12]. Thus, reactor design for photolysis of H_2O_2 (UV/H_2O_2) which is already applied in water treatment would principally suit for UV/$S_2O_8^{2-}$ and investment costs might be justifiable. However, additional efforts have to be considered such as establishing of a drinking water standard for continuous use of $S_2O_8^{2-}$ and investigation of effects on subsequent water treatment.

Main constituents of source water, i.e., dissolved organic carbon (DOC), and inorganic ions such as HCO_3^-/CO_3^{2-} largely affect the efficiency of radical based water treatment. In that regard Méndez-Diaz et al. described a remarkably different behavior of $SO_4^{\bullet-}$ compared with $^\bullet OH$ in presence of DOC. The authors indicated that in presence of fulvic acids, dodecylbenzenesulfonate is degraded faster in $UV/S_2O_8^{2-}$ than in UV/H_2O_2, which has been explained by a weaker scavenging of $SO_4^{\bullet-}$ compared with $^\bullet OH$ [13]. However, a systematic investigation regarding the influence of main constituents in natural waters is hardly available with respect to $SO_4^{\bullet-}$ based oxidation. One important reaction is $SO_4^{\bullet-}$ plus Cl^- ($k = 2.8 \times 10^8$ $M^{-1}s^{-1}$ [14]), since Cl^- is typically present in concentrations in the mM range in natural waters. The fraction of $SO_4^{\bullet-}$ reacting with Cl^- can be calculated if the rate constants for reactions with other main constituents are known. The reaction rates of HCO_3^- and CO_3^{2-} have already been determined (k (HCO_3^-) = 2.8-9.1 $\times 10^6$ M^{-1} s^{-1} [15, 16], k (CO_3^{2-}) = 4.1 $\times 10^6$ M^{-1} s^{-1} [17]) . It can be assumed, that the reaction rate of $SO_4^{\bullet-}$ plus DOC is somewhat similar if not smaller than k($^\bullet OH$ plus DOC) (2.5 $\times 10^4$ $Lmg^{-1}s^{-1}$ [18]) since $SO_4^{\bullet-}$ is more selective than $^\bullet OH$ [19]. This is has been supported by the reaction rate for $SO_4^{\bullet-}$ plus humic acids of 5.4 $\times 10^3$ L mg^{-1} s^{-1} Chapter 5 (note that corresponding reaction rate for $^\bullet OH$ plus humic acids (same lot) a value of 1.4 $\times 10^4$ L mg^{-1} s^{-1} has been determined, which ≈ 2.5 times higher). However, using a very high reaction rate for $SO_4^{\bullet-}$ plus DOC of 2.5 $\times 10^4$ L mg^{-1} s^{-1} may be sufficient for a rough estimation of the minimal fraction of $SO_4^{\bullet-}$ reacting with Cl^-. A typical raw water in drinking water purification may contain 2 mg L^{-1} DOC, 3 mM HCO_3^- and 1 mM Cl^-. In such a water ≈ 80% of $SO_4^{\bullet-}$ react with Cl^-, thus direct reactions of $SO_4^{\bullet-}$ plus pollutants are strongly diminished. However, this reaction gives rise to chlorine atoms ($Cl^\bullet$) as primary products that induce a sequence of reactions involving water and Cl^- as main reactants. Corresponding equilibria have been investigated in detail [14, 20, 21] revealing that $^\bullet OH$ are formed in these reactions. Beside $^\bullet OH$ the reactions might also yield ClO_3^-, especially at acidic conditions. The presence of ClO_3^- is undesired in drinking water, since it is classified as being harmful to human health and ecosystems (EU regulation 1907/2006; note that Switzerland established a drinking water standard of 200 μgL^{-1} [22] and WHO recommended a maximum value of 700 μgL^{-1} (WHO/SDE/WSH/05.08/86)).

For deciding if $UV/S_2O_8^{2-}$ is a useful option in water treatment the influence of Cl^- is a very important issue and has to be carefully investigated. The present study comprises a thorough investigation of ClO_3^- formation in $UV/S_2O_8^{2-}$ in pure water including a model of its formation. Furthermore, the influence of Cl^- and alkalinity in $UV/S_2O_8^{2-}$ treatment of surface waters was characterized with regard to degradation of pollutants.

7.3 Material and Methods

7.3.1 Chemicals

Acetonitrile (≥ 99.9%) Sigma Aldrich, *atrazine* (≥ 97.4%) Riedel-de Haën, *4-chlorobenzoic acid (pCBA)* (99%) Aldrich, *hydrochloric acid* (37% in water, p.a.) Merck, *hydrogen peroxide* (30%) Sigma Aldrich, *methanol* (p.a.) Sigma-Aldrich, *4-nitrobenzoic acid* (pNBA) (≥ 97.4%) Sigma Aldrich, *oxygen* (≥ 99.9%) Liquid Air, *phosphoric acid* (≥ 85%) Merck, *potassium chlorate* (99%) Merck, *potassium chloride* (≥ 99.5%) Riedel-de Haën, *pure water* has been prepared by treating deionized water with a pure lap ultra instrument (Elga) (electrical resistance 18.6 MΩ), *sodium bicarbonate* (≥ 99.5%) KMF optichem, *sodium carbonate* (≥ 99.8%) Riedel-de Haën, *sodium hydroxide* (≥ 99.9%, p.a.) VWR, *sodium peroxodisulfate* (p.a.) Sigma-Aldrich, *sulfuric acid* (95-97%) Applichem International, *Suwannee River NOM* (reverse osmosis concentrate) International Humic Acid Society

7.3.2 Experimental procedure

Sulfate radicals were generated by photolysis of peroxodisulfate ($UV/S_2O_8^{2-}$) in a merry-go-round apparatus equipped with a low pressure mercury lamp. This radiation source emits monochromatic light at 254 nm (Heraeus Noble Light GPH303T5L/4, 15 W). The reactions were buffered with phosphate (0.5 or 10 mM, see caption of corresponding figures). pH adjustments were done by addition of sulfuric acid or sodium hydroxide, respectively. Methanol was added to the samples (1 M in the sample) for scavenging low levels of $SO_4^{\bullet-}$ which could be formed during storage time as explained in Chapter 3. River Ruhr water (RWW, Mülheim a.d. Ruhr) and solutions of humic acids were used as a model waters for simulating real conditions. The water was filtered with cellulose acetate/cellulose nitrate filters of a pore size of 0.45 µm (Whatman). In some of the experiments HCO_3^-/CO_3^{2-} was removed by acidification (pH = 2) and purging with oxygen prior performing the experiments. Furthermore, Suwannee River NOM has been used to simulate a real water matrix. To that end, aqueous solutions of Suwannee River NOM have been prepared by dissolving the Suwannee River NOM in pure water. This solution has been filtered and on a cellulose-acetate membrane filter (pore size 0.45 µm, Schleicher and Schüell) followed by determination of the concentration of DOC by a TOC-Analyzer (TOC 5000A Shimadzu). Alkalinity was determined by titration of acid capacity. Cl^- was analyzed by ion chromatography (Metrohm 883 basic) equipped with a conductivity detector coupled with ion suppression (anion separation column with quaternary ammonium groups: Metrosep A Supp 4 - 250/4.0 mm, particle size 9 µm; eluent: a solution of HCO_3^- (1.7 mM), CO_3^{2-} (1.8 mM) was mixed with

acetonitrile (70% aqueous buffer : 30 % acetonitrile); flow: 1 mL min^{-1}; retention time 3.8 min). Atrazine, 4-chlorobenzoic acid (pCBA) and 4-nitrobenzoic acid (pNBA) were determined by HPLC with UV-detection (Shimadzu) (C18 reversed phase separation column: Bischoff, NUCLEOSIL 100, 250/4.0 mm, particle size: 5.0 µm). As eluent a gradient of methanol/water was used (gradient program (methanol content): 0-3 min: gradient 20% - 50%, 3-25 min: gradient 50%-75%; 25-30 min: gradient 75%-20%, 30-38 min: isocratic 20%; flow 0.6 $mLmin^{-1}$; retention times/measured wave lengths: pNBA: 20.6 min/262 nm; atrazine: 25.8 min/234 nm, pCBA: 26.5 min/234 nm).

The overall fluence rate of the photo reactor has been determined by chemical actinometry using uridine [23] in pure water. Thereby a value of 61 µEinstein m^{-2} s^{-1} was obtained. For determining the apparent fluence rate, atrazine has been used as actinometer in analogy to Canonica et al [24] in presence of corresponding natural water. This allows taking the inner filter effect of the water matrix (organic matter) into account. The quartz tubes were turned over a few times before sampling and the average fluence rate was obtained. By that means a value of 48-51 µEinstein m^{-2} s^{-1} was determined which is around 17% below fluence rate in pure water (see above). A similar value can be calculated by using the Morowitz correction factor [25] (48-50 µEinstein m^{-2} s^{-1} (path length ≈ 1.5 cm; UV-Absorption of River Ruhr water = 0.058-0.046 cm^{-1})). In case of experiments in presence of Suwannee River NOM a fluence rate of 36 ± 2 µEinstein m^{-2} s^{-1} has been obtained (10 mg L^{-1} DOC). Ozonation experiments have been performed as follows. An aqueous O_3 stock solution was prepared purging an O_3 enriched gas through ice cooled pure water. At stationary conditions a steady state concentration of ozone of 1 mM O_3 could be achieved. This solution was used to dose specific amounts of O_3 to samples under study. Therefore glass syringes with stainless steel cannulas have been used. For maintaining a constant O_3 concentration, continuous purging with the ozone enriched gas ozone was necessary. Ozone has been generated by an ozone generator purchased from BMT Messtechnik Berlin (Philaqua 802x) with oxygen as feed gas.

7.4 Results and discussion

7.4.1 Oxidation of chloride in pure water

Figure 1 shows a comparison of determined and modeled product patterns in the oxidation of Cl^- during UV/$S_2O_8^{2-}$ in pure water. Model calculations are based on reactions given in Table 1. During the experiment the solution acidifies, which is included in the model calculations. In the investigated system no Cl^- turnover can be observed at pH ≥ 6. However, at lower pH values Cl^- is oxidized yielding ClO_3^- nearly quantitatively. The corresponding mechanism can be proposed as follows:

$SO_4^{\bullet-}$ reacts with Cl^- giving rise to SO_4^{2-} and $Cl^\bullet$ (reaction 1). It has been suggested that $Cl^\bullet$ forms complexes with water ($H_2OCl^\bullet$) [14, 26, 27], which may act as an oxygen acid (p*K*a 5.1 [28]), and deprotonate yielding $^\bullet OH$ (reaction 4 and 9). At a Cl^- concentration of 1 mM, a substantial amount of $Cl^\bullet$ may also react with Cl^- and $Cl_2^{\bullet-}$ is formed (reaction 3). $Cl_2^{\bullet-}$ may react with water (reaction 6) giving rise to $HClO^{\bullet-}$, the precursor of $^\bullet OH$ or $Cl^\bullet$ (reaction 8 and 9). Formation of $^\bullet OH$ is predominant at neutral pH whereas $Cl^\bullet$ concentration increases at low pH values (see below). $Cl_2^{\bullet-}$ may also recombine yielding Cl_2 and Cl^- (reaction 7). It is worth mentioning, that $Cl_3^{\bullet-}$ probably is no product in reaction 7 [29] (note that $Br_3^{\bullet-}$ is indeed proposed to be formed in the analogous reaction of dibromine radicals (2 $Br_2^{\bullet-}$ → $Br_3^{\bullet-}$ + Br^- (chapter 6). This has been explained by hindrance of adduct formation due to the like charge of the reactants. Thus, outer sphere electron transfer might be feasible [29]. It is presently proposed that $Cl_3^{\bullet-}$ may, however, appear in the reaction Cl_2 plus Cl^- at very high Cl^- concentrations (above 1 M) [29]. Cl_2 ensuing reaction 7 hydrolyses to form HOCl/OCl^- (reaction 10) which will be further oxidized by $^\bullet OH$ or $Cl^\bullet$ giving rise to ClO_3^- (reaction 12-15). In this sequence of reactions the formation of Cl_2 largely depends on the steady state concentration of $Cl^\bullet$. The concentration of $Cl^\bullet$ in turn is related to the apparent equilibrium in reaction 4. With decreasing pH this equilibrium is shifted towards $Cl^\bullet$ thus enhancing ClO_3^- formation. At a pH-value of ≈ 3.4 the Cl^- turnover approaches the maximum rate (Figure 1).

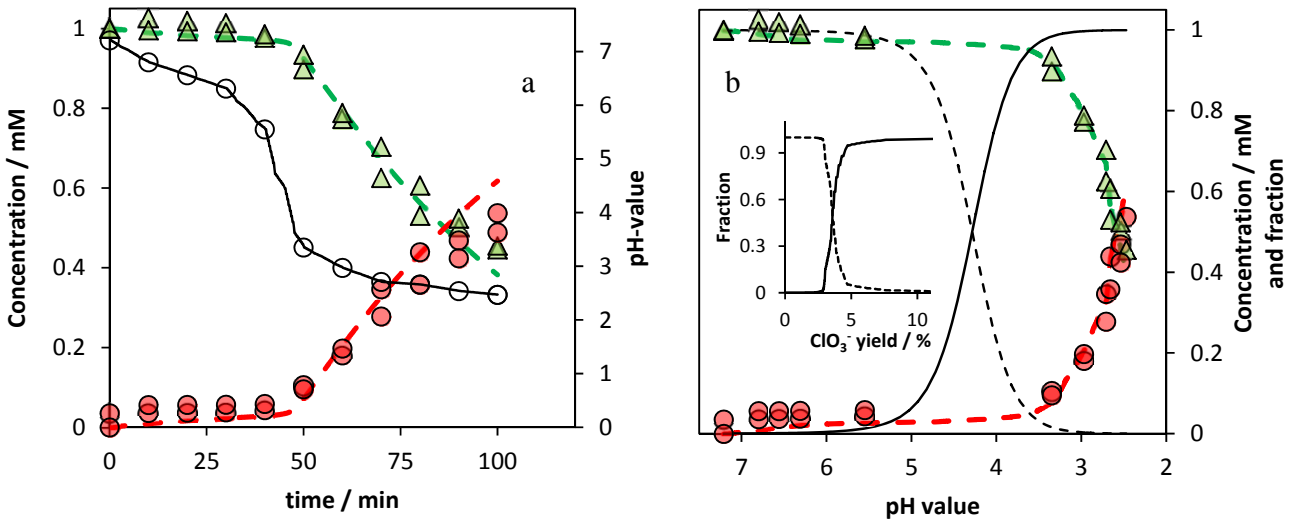

Figure 1: Oxidation of Cl^- in $SO_4^{\bullet-}$ based oxidation at decreasing pH value; pure water; Cl^-: green triangles, ClO_3^-: red circles; a) concentration of Cl^- and ClO_3^- as well as pH (open circles) vs. time, model predictions: dashed line; b) concentration of Cl^- and ClO_3^- vs. pH value; black lines give the fractions of $^{\bullet}OH$ (dashed) and $Cl^{\bullet}$ (solid) involved in oxidation of $HOCl/OCl^-$; inset: fraction of $^{\bullet}OH$ (dashed) and $Cl^{\bullet}$ (solid) involved in oxidation of HOCl/OCl vs. ClO_3^- yield; $[Cl^-]_0 = 1$ mM, $[S_2O_8^{2-}] = 10$ mM, [phosphate] = 10 mM; fluence rate = 61 ± 3 µEinstein $m^{-2}\,s^{-1}$

However, at pH ≥ 6 no consumption of Cl^- or formation of ClO_3^- has been observed in UV/$S_2O_8^{2-}$. Figure 1b shows the fraction of $^{\bullet}OH$ and $Cl^{\bullet}$ reacting with $HOCl/OCl^-$ as a function of pH which has been derived from the model calculations. It can be seen, that $^{\bullet}OH$ possibly contribute in the oxidation of $HOCl/OCl^-$ at pH values > 4. However, at lower pH values this reaction is suppressed by speciation since HOCl largely dominates over OCl^- and has been considered being not reactive towards $^{\bullet}OH$ in the model calculations. The model well reflects the experimental data neglecting the reaction $^{\bullet}OH$ plus HOCl, indicating that the corresponding reaction indeed plays a minor role. $Cl^{\bullet}$ reacts with both HOCl and OCl^- at a similar rate (Table 1), thus the reaction with $HOCl/OCl^-$ is nearly independent of pH. Since formation of $HOCl/OCl^-$ is favored at acidic conditions below its p*K*a value, oxidation of $HOCl/OCl^-$ is mainly driven by $Cl^{\bullet}$. After a Cl^- turnover into ClO_3^- of 5% the fraction of the reaction $^{\bullet}OH$ plus $HOCl/OCl^-$ is negligible (< 5%) (see inset of Figure 1b). Oxidation of $HOCl/OCl^-$ by $Cl^{\bullet}$ (or $^{\bullet}OH$) gives $ClO^{\bullet}$ (reaction 12, 19 and 20) which disproportionates in its reaction with water yielding ClO^- and ClO_2^- (reaction 13). The oxidation of ClO_2^- may be driven by $^{\bullet}OH$ yielding the final product ClO_3^- (reaction 14,15). Some additional reactions are also included in the model calculation. H_2O_2 could be formed by recombination of $^{\bullet}OH$ (reaction 16). H_2O_2 might act as a $^{\bullet}OH$ radical scavenger

giving rise to the reducing radical $HO_2^{\bullet}$ (reaction 17). In fact this radical rapidly reacts with $Cl_2^{\bullet-}$ giving rise to Cl^- (reaction 18) which could reduce the ClO_3^- formation rate. However, model calculations are not significantly influenced by reaction 18. The rate of some reactions involved in oxidation of Cl^- might also depend on the ion strength of the reaction system. A case in point is reaction 4 and 7 which are reported to change with the ion strength. Thereby reaction 4 slows down ($\approx 2.5 \times 10^{10}$ M^{-1} s^{-1} (ionic strength = 0), $\approx 1.4 \times 10^{10}$ M^{-1} s^{-1} (ionic strength = 1)), reaction 7 is accelerated with increasing ion strength ($\approx 0.8 \times 10^{9}$ M^{-1} s^{-1} (ionic strength = 0), $\approx 2.5 \times 10^{9}$ M^{-1} s^{-1} (ionic strength = 1)) [29]. However, model calculations were not affected by changing these reaction rate within the range mentioned above. That can be explained by equilibrium 4 representing the rate limiting step, what is in accordance with the large pH dependency of ClO_3^- formation.

Table 1: Reactions involved in the oxidation of Cl^- during UV/$S_2O_8^{2-}$

No.	Reaction	Reaction rate forward	Unit	Ref.		Reaction rate backward	Unit	Ref.
(1)	$SO_4^{\bullet-} + Cl^- \rightleftarrows Cl^{\bullet} + SO_4^{2-}$	$k = 2.7 \times 10^8$	$M^{-1}s^{-1}$	[14]		$k = 2.5 \times 10^8$	$M^{-1}s^{-1}$	[30]
(2)	$2\ SO_4^{\bullet-} \rightarrow S_2O_8^{2-}$	$k = 4.4 \times 10^8$	$M^{-1}s^{-1}$	[31]				
(3)	$Cl^{\bullet} + Cl^- \rightleftarrows Cl_2^{\bullet-}$	$k = 8 \times 10^9$	$M^{-1}s^{-1}$	[32]		$k = 4.7 \times 10^4$	s^{-1}	[14]
(4)	$Cl^{\bullet} \rightleftarrows HOCl^{\bullet-} + H^+$	$k = 2.5 \times 10^5$	$M^{-1}s^{-1}$	[20]		$k = 2.1 \times 10^{10}$	$M^{-1}s^{-1}$	[33]
(5)	$Cl^{\bullet} + OH^- \rightarrow {}^{\bullet}OH + Cl^-$	$k = 1.8 \times 10^{10}$	$M^{-1}s^{-1}$	[34]				
(6)	$Cl_2^{\bullet-} + H_2O \rightarrow HOCl^{\bullet-} + Cl^- + H^+$	$k = 1.3 \times 10^3$	s^{-1}	[35]				
(7)	$Cl_2^{\bullet-} + Cl_2^{\bullet-} \rightarrow Cl_2 + 2Cl^-$	$k = 2.1 \times 10^9$	$M^{-1}s^{-1}$	[36]				
(8)	$Cl_2^{\bullet-} + OH^- \rightarrow ClOH^- + Cl^-$	$k = 4.5 \times 10^7$	$M^{-1}s^{-1}$	[36]				
(9)	$ClOH^{\bullet-} \rightleftarrows {}^{\bullet}OH + Cl^-$	$k = 6.1 \times 10^9$	s^{-1}	[33]		$k = 4.3 \times 10^9$	$M^{-1}s^{-1}$	[33]
(10)	$Cl_2 + H_2O \rightarrow HOCl + Cl^- + H^+$	$k = 5.5$	s^{-1}	[37]				
(11)	$HOCl \rightleftarrows H^+ + OCl^-$	p*K*a 7.42		[38]				
(12)	$ClO^- + {}^{\bullet}OH \rightarrow ClO^{\bullet} + OH^-$	$k = 9 \times 10^9$	$M^{-1}s^{-1}$	[39]				
(13)	$2\ ClO^{\bullet} + H_2O \rightarrow ClO^- + ClO_2^- + 2H^+$	$k = 2.5 \times 10^9$	$M^{-1}s^{-1}$	[28]				
(14)	$ClO_2^- + {}^{\bullet}OH \rightarrow ClO_2^{\bullet} + OH^-$	$k = 4.2 \times 10^9$	$M^{-1}s^{-1}$	[40]				
(15)	$ClO_2^{\bullet} + {}^{\bullet}OH \rightarrow ClO_3^- + H^+$	$k = 4 \times 10^9$	$M^{-1}s^{-1}$	[40]				
(16)	${}^{\bullet}OH + {}^{\bullet}OH \rightarrow H_2O_2$	$k = 5.5 \times 10^9$	$M^{-1}s^{-1}$	[41]				
(17)	$H_2O_2 + {}^{\bullet}OH \rightarrow HO_2^{\bullet} + H_2O$	$k = 2.7 \times 10^7$	$M^{-1}s^{-1}$	[42]				
(18)	$HO_2^{\bullet} + Cl_2^{\bullet-} \rightarrow 2Cl^- + O_2 + H^+$	$k = 4.5 \times 10^9$	$M^{-1}s^{-1}$	[43]				
(19)	$Cl^{\bullet} + ClO^- \rightarrow ClO^{\bullet} + Cl^-$	$k = 8.0 \times 10^9$	$M^{-1}s^{-1}$	[28]				
(20)	$Cl^{\bullet} + HOCl \rightarrow ClO^{\bullet} + Cl^- + H^+$	$k = 3.0 \times 10^9$	$M^{-1}s^{-1}$	[28]				

The presented results indicate that under typical conditions of water treatment (pH > 6) formation of ClO_3^- is not likely to happen. However, in remediation of ground waters where $S_2O_8^{2-}$ finds increasing application, residence time might be sufficient to cause a considerable acidification in turn of reactions of $SO_4^{\bullet-}$ with Cl^- or other reactions releasing protons. This might lead to favorable conditions of chlorate formation and mobilization of metals. Furthermore, formation of chlorinated compounds might

be enhanced due to elevated levels of reactive chlorine species at acidic conditions. However, this might be of less importance in case of ground waters and soils revealing a high buffer capacity.

7.4.2 Influence of chloride and alkalinity on sulfate radical based oxidation in water treatment

The presence of Cl^- has also a substantial effect on UV/$S_2O_8^{2-}$ at typical conditions of drinking water treatment, since it may turn $SO_4^{\bullet-}$ into $^\bullet OH$. This has been confirmed by performing a competition kinetic experiment (for further information about competition kinetics see the Supporting Information of Dodd et al. [44]). In these experiments, degradation of pNBA and pCBA in UV/$S_2O_8^{2-}$ (in presence of 1 mM Cl^-) and UV/H_2O_2 (in absence of Cl^-), has been compared. UV/H_2O_2 is hardly affected by Cl^- at a neutral pH because the reaction of $^\bullet OH$ plus Cl^- (reaction 9 (reverse)) has a fast back reaction, thus steady state concentration of $HOCl^{\bullet-}$ is low. Furthermore, decomposition of $HOCl^{\bullet-}$ (reaction 4) yields very low $Cl^\bullet$ steady state concentrations at pH ≈ 7. Taking both reactions into account the observed reaction rate for oxidation of Cl^- by $^\bullet OH$ at pH 7 has been calculated to be ca. 10^3 M^{-1} s^{-1} [22]. Thus, it can only become important at a pH below 3, because the equilibrium in reaction 4 is than shifted towards $Cl^\bullet$ [22]. This is in agreement with Ershov who mentioned that the oxidation of Cl^- by $^\bullet OH$ requires acidic conditions [29].

pNBA and pCBA are very different in their reactions with $SO_4^{\bullet-}$ and $^\bullet OH$. pNBA is inert towards $SO_4^{\bullet-}$ but readily reacts with $^\bullet OH$ (k = 2.6 × 10^9 $M^{-1}s^{-1}$ [41]) and pCBA reacts with both $SO_4^{\bullet-}$ and $^\bullet OH$, but at different rates ($k(SO_4^{\bullet-})$ = 3.6 × 10^8 $M^{-1}s^{-1}$ [45], $k(^\bullet OH)$ = 5 × 10^9 $M^{-1}s^{-1}$ [41]). It can be seen in Figure 2, that the competition plot reveals the same slope for both UV/$S_2O_8^{2-}$ in presence of Cl^- and UV/H_2O_2 indicating that in both processes $^\bullet OH$ are the major reactive species (note that a $SO_4^{\bullet-}$ based process would not reveal any correlation of ln(c/c_0) (pNBA) vs. ln(c/c_0) (pCBA), since pNBA is hardly degraded). The good agreement of the slopes in UV/$S_2O_8^{2-}$ and UV/H_2O_2 and the good accordance to the theoretical slope of $k(^\bullet OH + p\text{NBA})/k(^\bullet OH + \text{pCBA})$ of 0.52 further corroborate this conclusion.

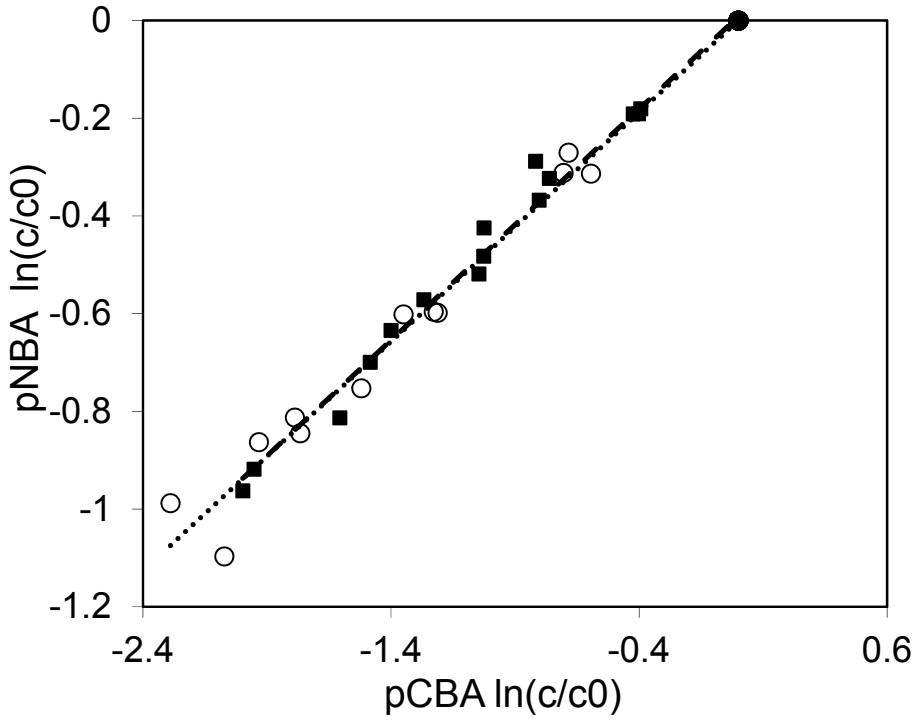

Figure 2: competition plot ln(c/c0) of pCBA vs. pNBA; dotted line and circles UV/$S_2O_8^{2-}$ (slope 0.47; intercept 0.0081), dashed line and squares UV/H_2O_2 (slope 0.47; intercept 0.0001); $[pCBA]_0 = [pNBA]_0 = 0.5$ µM; $[S_2O_8^{2-}] = [H_2O_2] = 0.1$ mM, $[Cl^-] = 1$ mM (UV/$S_2O_8^{2-}$), no addition of Cl^- in UV/H_2O_2; pH = 7.2; [phosphate] = 10 mM; T = 25°C

The formation of $^{\bullet}OH$ in UV/$S_2O_8^{2-}$ in natural waters which can contain Cl^- in large quantities can be expected. This has been investigated by measuring the degradation of pNBA, pCBA and atrazine, which have been added to river Ruhr water containing 0.8-1.3 mM Cl^- (Figure 3). Since $Cl^{\bullet}$ are effectively scavenged by HCO_3^- ($k = 2.2 \times 10^8$ $M^{-1}s^{-1}$) and CO_3^{2-} ($k = 5 \times 10^8$ $M^{-1}s^{-1}$) [46], the carbonate species have been removed by acidification and purging with oxygen. Afterwards, the pH was readjusted to the original value. This largely simplifies the system because oxidative species are exclusively scavenged by dissolved organic matter ([DOC] = 2.45 mg L^{-1}). Degradation of atrazine, pCBA and pNBA, has been modeled by using reactions given in Table 1, the reactions involving the probe compounds and radical scavenging by DOC (k(atrazine + $^{\bullet}OH$) = 3×10^9 M^{-1} s^{-1}, k(atrazine + $SO_4^{\bullet-}$) = 3×10^9 M^{-1} s^{-1} [47], k($^{\bullet}OH$ + DOC) = 2.5×10^4 L $mg^{-1}s^{-1}$ [48], k($SO_4^{\bullet-}$ + DOC) = 5.4×10^3 L mg^{-1} s^{-1} (own measurements determined for humic acids (Chapter 5), rate constants for pCBA and pNBA see above). The overall radical formation has been calculated by using the fluence rate determined by atrazine actinometry and photochemical features of $S_2O_8^{2-}$ as described in Chapter 3. It is worth to note, that the fair agreement of the model data and the experimental values corroborate the quantum yield used for

$S_2O_8^{2-}$ (i.e., 1.4 mol $SO_4^{\bullet-}$ per Einstein) and contradicts the frequently cited quantum yield ($S_2O_8^{2-}$) of 2 moles $SO_4^{\bullet-}$ per Einstein (e.g., Yu et al. and references therein [36]).

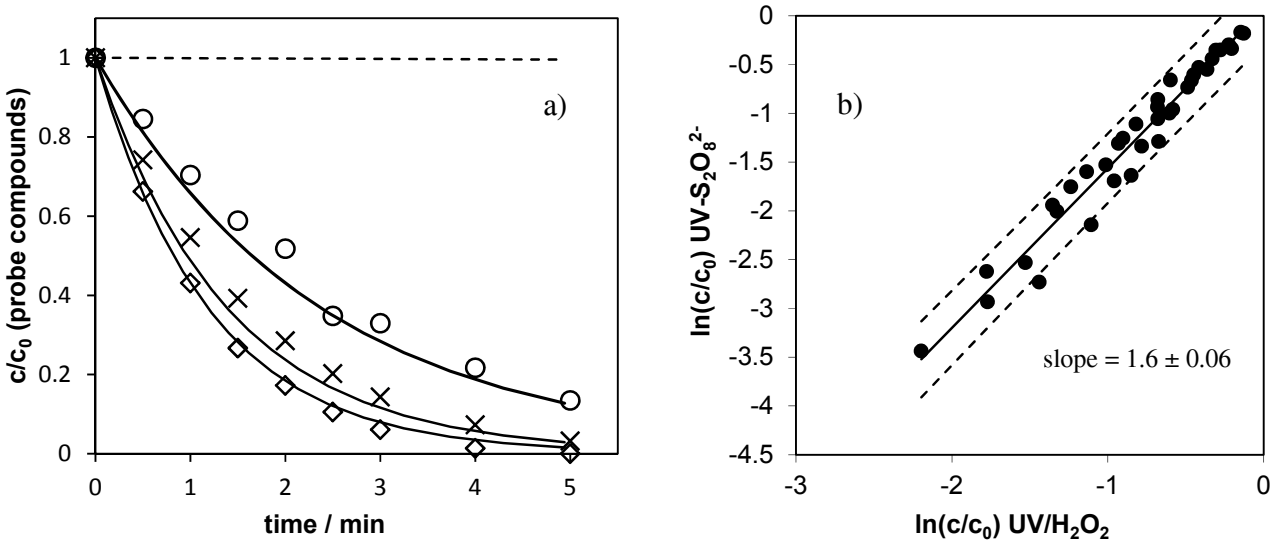

Figure 3: a) Degradation of pNBA (open circles), pCBA (open diamonds) and atrazine (crosses) in river Ruhr water during UV/$S_2O_8^{2-}$ treatment; solid lines modeled data; dashed line: modeled degradation of pNBA in absence of Cl^-; T = 25 °C, [DOC] = 2.45 mg L^{-1}, [Cl^-] = 1.05 mM; [$S_2O_8^{2-}$] = [H_2O_2] = 0.5 mM; [phosphate] = 0.5 mM; HCO_3^- has been removed (see experimental); b) Degradation in UV/$S_2O_8^{2-}$ vs. degradation in UV/H_2O_2, circles: pooled data of all model compounds from experiments performed in two River Ruhr water samples, solid line: linear regression, dashed lines: 95 % confidence interval; experimental conditions: one River Ruhr sample is identical with that used in a), the other differed as follows, DOC = 1.9 mg/L, Cl^- = 0.84 mM

Since > 80% of $SO_4^{\bullet-}$ react with Cl^- it is largely transformed into $^{\bullet}OH$, thus, UV/$S_2O_8^{2-}$ is converted into a conventional $^{\bullet}OH$ based process. Atrazine is degraded at a similar rate compared to pCBA even though it reacts considerably slower with $^{\bullet}OH$ (nearly factor 2). This accounts for the substantial degree of direct photolysis, which is much weaker in case of pCBA and pNBA (molar absorption coefficient and quantum yields at 254 nm are summarized in Chapter 3). Especially the good agreement in pNBA degradation demonstrates a large involvement of $^{\bullet}OH$ since it would hardly be degraded in a $SO_4^{\bullet-}$ based process (dashed line in Figure 3). Figure 3 b) compares the degradation of the probe compounds during UV/$S_2O_8^{2-}$and UV/H_2O_2. Corresponding experiments have been performed using River Ruhr water from two different sampling events. A plot of ln(c/c0) of UV/$S_2O_8^{2-}$ vs. ln(c/c0) of UV/H_2O_2 reveals a linear function and the data points of all compounds fall on one line. Since a contribution of

$SO_4^{\bullet-}$ in UV/$S_2O_8^{2-}$ would result in different functions for every probe compound due to the different ratio of $k(SO_4^{\bullet-})/k(^{\bullet}OH)$ the plot indicates that $^{\bullet}OH$ is the major reactive species in both processes. The slope of the function (1.6) shows that at present conditions UV/$S_2O_8^{2-}$ is more efficient with regard to degrading the probe compounds. This can be explained by the higher quantum yield and absorption coefficient of $S_2O_8^{2-}$ compared with H_2O_2 (see above and chapter 1 and 3) which leads to a higher radical formation rate in UV/$S_2O_8^{2-}$ by the same factor (difference in quantum yield multiplied by difference in absorption (1.4 × 1.1 = 1.54)). A distinctive involvement of $Cl^{\bullet}$ in degrading the model compounds is unlikely since beside the reaction with water $Cl^{\bullet}$ is scavenged by Cl^- (reaction 3), largely diminishing the steady state concentration of $Cl^{\bullet}$ and yielding the milder oxidant $Cl_2^{\bullet-}$. Beside formation of $^{\bullet}OH$ and ClO_3^- the formation of halogenated organic compounds has also to be addressed. If the fraction of reactions $Cl^{\bullet}$ or $Cl_2^{\bullet-}$ plus DOC would be large, a distinctive deviation of the modeled data from the experimental data (Figure 3) would be observed, which not the case was. Thus, the fraction of $Cl^{\bullet}$ reacting with DOC in the river Ruhr water seems to be of minor importance.

The influence of HCO_3^-/CO_3^{2-} was also studied. Figure 4 shows observed first order degradation rates (k_{obs}) of the model compounds, atrazine and pNBA in UV/$S_2O_8^{2-}$ and UV/H_2O_2 in river Ruhr water at different HCO_3^- concentrations. For taking variations of the fluence rate into account k_{obs} has been divided by the respective fluence rate determined in every experiment by atrazine actinometry (see experimental).

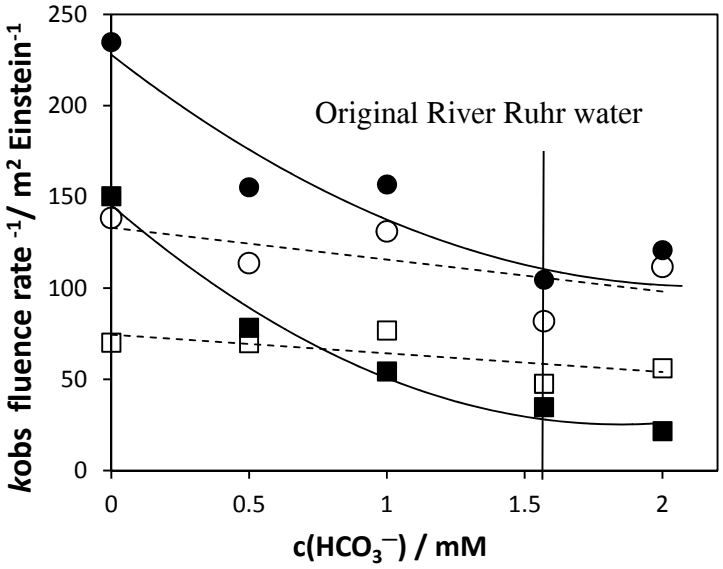

Figure 4: Degradation efficiency in UV/$S_2O_8^{2-}$ and UV/H_2O_2; closed symbols: UV/$S_2O_8^{2-}$, open symbols UV/H_2O_2, circles: atrazine degradation, squares pNBA-degradation, pH = 7.2, T = 25 °C, DOC = 1.92 mg L^{-1}, Cl^- = 0.84 mM, [pNBA] = [atrazine] = 0.5 µM, [$S_2O_8^{2-}$] = [H_2O_2] = 0.5 mM, [phosphate] = 0.5 mM, lines: polynomic regression in UV/$S_2O_8^{2-}$ (continuous) and UV/H_2O_2 (dashed), vertical line marks alkalinity in original River Ruhr water

Alkalinity diminishes the efficiency of pollutant degradation in UV/$S_2O_8^{2-}$ to a much higher extent than in UV/H_2O_2, which is hardly affected. This results in similar oxidation efficiencies under conditions of original River Ruhr water (≈ 1.6 mM HCO_3^-). Scavenging of $^{\bullet}OH$ by HCO_3^-, which happens in both processes, seems to be of minor importance. However, $Cl^{\bullet}$ react fast with HCO_3^- and CO_3^{2-} (reaction 23 and 24, see below) and might be efficiently scavenged, thus the oxidation strength of the photochemical system is largely directed into alkalinity.

This assumption has been verified by including reactions 21-24 in the previous model calculations used for predicting the degradation of the model compounds.

Reaction 21 $^{\bullet}OH + HCO_3^- \rightarrow CO_3^{\bullet-} + OH^- + H^+$ $k = 1\times10^7\ M^{-1}s^{-1}$ [18]

Reaction 22 $SO_4^{\bullet-} + HCO_3^- \rightarrow CO_3^{\bullet-} + SO_4^{2-} + H^+$ $k = 9.1\times10^6\ M^{-1}s^{-1}$ [16]

Reaction 23 $Cl^{\bullet} + HCO_3^- \rightarrow CO_3^{\bullet-} + Cl^- + H^+$ $k = 2.2\times10^8\ M^{-1}s^{-1}$ [46]

Reaction 24 $Cl_2^{\bullet-} + HCO_3^- \rightarrow CO_3^{\bullet-} + 2\ Cl^- + H^+$ $k = 1.5\times10^6\ M^{-1}s^{-1}$ (assumed)

The reaction of HCO_3^- plus $Cl_2^{\bullet-}$ (reaction 24) has not been described in literature yet, however, it is likely that this reaction is important in the present system. If this reaction is not included in the model, the calculations overestimate the degradation rates (Figure 5c).

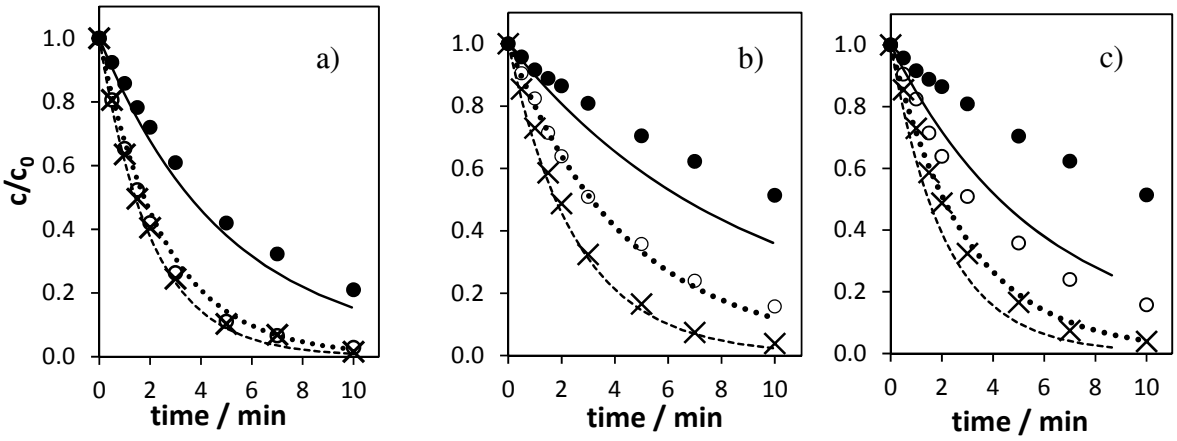

Figure 5: Degradation of atrazine (experimental data: crosses; model calculation: dashed line), pCBA (experimental data: open circles; model calculation: dotted line) and pNBA (experimental data: closed circles; model calculation: continuous line) in River Ruhr water containing HCO_3^-; a) HCO_3^- = 1 mM, b) HCO_3^- = 2 mM, c) HCO_3^- = 2 mM without reaction 24; $[pCBA]_0 = [pNBA]_0$ = 0.5 µM, $[S_2O_8^{2-}] = [H_2O_2]$ = 0.5 mM, pH = 7.2-7.8, T = 25°C, DOC = 1.92 mgL^{-1}, Cl^- = 0.84 mM

Very little information is available about reactions of dihalogen radicals with CO_3^{2-} or HCO_3^-. The only reaction rate currently available is $k(CO_3^{2-} + Br_2^{\bullet-}) = 1.1\times10^5$ M^{-1} s^{-1} [30]. Considering that $Cl_2^{\bullet-}$ is much more reactive than $Br_2^{\bullet-}$ [19] a value of 1.5×10^6 M^{-1} s^{-1} for HCO_3^- is realistic, even though $Cl_2^{\bullet-}$ could react with HCO_3^- at a lower rate than with CO_3^{2-}. However, the current lack of knowledge about reaction kinetics of dihalogen radicals does not allow a more decent discussion and should be addressed in future work.

Since direct reactions of $SO_4^{\bullet-}$ are largely suppressed by its reaction with Cl^- (reaction 1) scavenging of this radical by HCO_3^- (reaction 22) is of minor importance. The main loss in oxidation capacity results from scavenging of $Cl^{\bullet}$ (reaction 23). In original River Ruhr water ≈ 60% of $Cl^{\bullet}$ are scavenged by HCO_3^- leading to formation of $CO_3^{\bullet-}$. Compared to $^{\bullet}OH$ and $SO_4^{\bullet-}$, $CO_3^{\bullet-}$ reveals a much smaller reactivity towards many compounds [19]. However, the capability of $CO_3^{\bullet-}$ to degrade pollutants also depends on its stability in natural matrices. $CO_3^{\bullet-}$ reacts very selectively and it can be expected that its

reactivity towards DOC largely varies. The two values available in literature are a good demonstration (40 L mg^{-1} s^{-1} [49] and 280 ± 90 L mg^{-1} s^{-1} [50]). In case of $k(CO_3^{\bullet-} + DOC)$ = 40 L mg^{-1} s^{-1} atrazine is degraded by $^{\bullet}OH$ and $CO_3^{\bullet-}$ at a similar rate since the high exposure of $CO_3^{\bullet-}$ compensates the low reaction rate of $k(CO_3^{\bullet-} + atrazine) = 3.7 \times 10^6$ M^{-1} s^{-1} [50]. With $k(CO_3^{\bullet-} + DOC)$ = 280 ± 90 L mg^{-1} s^{-1}, however, the oxidation strength is reduced by ≈ 80% (calculations made for 1 mg L^{-1} DOC and 1 mM HCO_3^-; note that $CO_3^{\bullet-}$ is probably not affected by alkalinity, since the reaction of $CO_3^{\bullet-}$ plus HCO_3^- again yields $CO_3^{\bullet-}$). A reaction rate $k(CO_3^{\bullet-} + DOC)$ ≈ 280 probably applies for River Ruhr water, since computed data agree well with experimental data without taking the reaction of $CO_3^{\bullet-}$ plus atrazine into account.

7.4.3 Variation of chloride concentration in presence of Suwannee River DOC

In the above experimental setup $SO_4^{\bullet-}$ were nearly quantitatively converted to $^{\bullet}OH$ *via* Cl^-. At lower concentrations Cl^-, however, $SO_4^{\bullet-}$ and $^{\bullet}OH$ coexist. This has been investigated by monitoring the degradation of atrazine, pCBA and pNBA in presence of Suwannee River NOM and different concentrations of Cl^-.

Figure 6 shows the first order degradation rates of these compounds plotted vs. the concentration of Cl^- (note that ≈ 4 µM of Cl^- is present per mg L^{-1} DOC in the Suwannee River NOM extract). It can be observed that the degradation rate of atrazine decreases with the Cl^- concentration. This trend is supported by the present model calculations also shown in Figure 6 and can be explained as follows. With increasing concentration of Cl^- the fraction of the reaction $SO_4^{\bullet-}$ plus Cl^- raises, yielding $Cl^{\bullet}$ resulting in an enhanced turnover into $^{\bullet}OH$ *via* reactions 3, 4, 6 and 9 (Table 1). The conversion of $SO_4^{\bullet-}$ to $^{\bullet}OH$ diminishes the degradation rate of atrazine, since the scavenging by Suwannee River NOM is faster in case of $^{\bullet}OH$ compared with $SO_4^{\bullet-}$ ($k(SO_4^{\bullet-}) \approx 3.8 \times 10^3$ L mg^{-1} s^{-1}, $k(^{\bullet}OH) \approx 1.14 \times 10^4$ L mg^{-1} s^{-1} (see Chapter 5); note, that atrazine reacts at a similar rate with both radicals (i.e., $\approx 3 \times 10^9$ M^{-1} s^{-1} [47, 51, 52]).

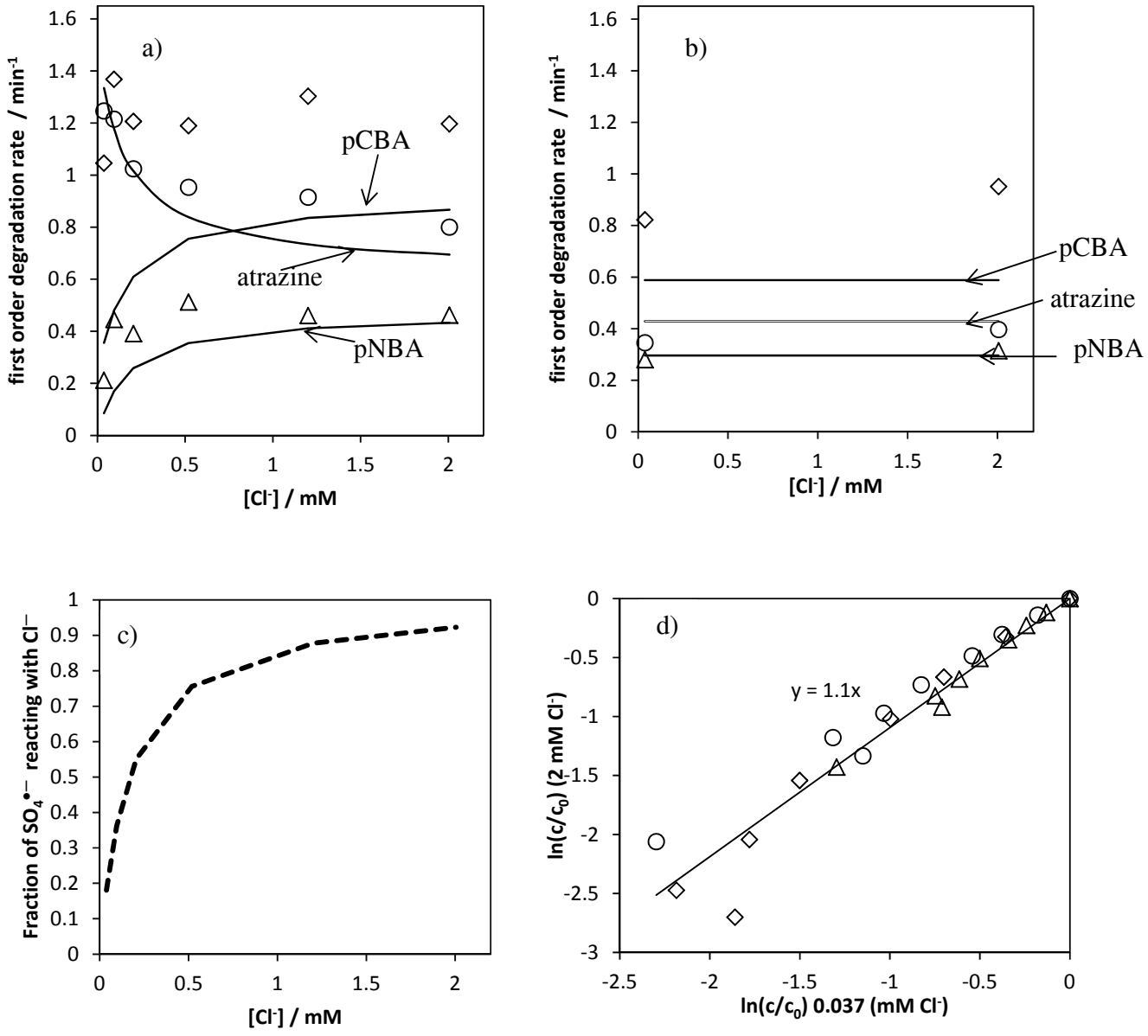

Figure 6: a) First order degradation rate of atrazine (circles), pCBA (diamonds) and pNBA (triangles) in UV/$S_2O_8^{2-}$ in presence of Suwannee River NOM and different concentrations of Cl^-; b) Same as a) in UV/H_2O_2; Lines represent model calculations; c) calculated fractions of $SO_4^{\bullet-}$ reacting with Cl^-, d) Comparison of first order degradation rates in UV/H_2O_2 at 0.037 mM Cl^- and 2 mM Cl^-; Experimental conditions for a)-d): $[atrazine]_0 = [pCBA]_0 = [pNBA]_0 =$ 0.5 µM, $[S_2O_8^{2-}] = [H_2O_2] = 2$ mM, [phosphate] = 5 mM, [DOC] = 10 mg L^{-1}, pH = 7.2, T = 25°C

pNBA displays a very different behavior. Its observed degradation rate increases with increasing Cl^- concentration since the $^\bullet OH$ formed react fast with pNBA ($k = 2.6 \times 10^9$ M^{-1} s^{-1}), whereas $SO_4^{\bullet-}$ hardly degrades pNBA ($k(SO_4^{\bullet-} + pNBA) \leq 10^6$ M^{-1} s^{-1}). At 37 µM a distinctive degradation of pNBA can be observed indicating the presence of $^\bullet OH$ (for enabling a comparison with other natural systems the Cl^-

can be normalized by DOC; in this case revealing: 3.7 µM Cl^- per mg L^{-1} DOC). At that condition already 20 % of $SO_4^{\bullet-}$ react with Cl^- (Figure 6 c). A gradual increase of Cl^- concentration leads to a further increase in the degradation rate of pNBA reaching a plateau at 0.5 mM Cl^- (50 µM Cl^- per mg L^{-1} DOC). This indicates that at a concentration of 50 µM per mg L^{-1} DOC the system is largely converted to a $^\bullet OH$ radical based process (note that the fraction of the reaction $SO_4^{\bullet-}$ plus Cl^- has been calculated to be ≈ 80% resulting in a transformation of $SO_4^{\bullet-}$ into $^\bullet OH$ (Figure 6 c)). The Cl^- concentration in natural waters displays a large range (e.g., several Canadian lakes and rivers 0.8-10 mg L^{-1} (0.024-0.3 mM) [53] and rivers in the UK 11-42 mg L^{-1} (0.32-1.5 mM [54]). Hence, the efficiency as well as the nature of the main oxidant ($SO_4^{\bullet-}$ and/or $^\bullet OH$) in UV/$S_2O_8^{2-}$ might also be very different depending on the composition of the source water. It has to be noted that UV/$S_2O_8^{2-}$ could reveal certain advantages over UV/H_2O_2 if the source water reveals a low Cl^- concentration leading to a low conversion of $SO_4^{\bullet-}$ into $^\bullet OH$ *via* oxidation of Cl^- (e.g., ≤ 3 µM per mg L^{-1} DOC). Indeed this kind of waters may be found in areas with low population density and low industrial activity (e.g., the lakes of the experimental lakes area (ELA) in the Kenora District of Ontario, Canada [53])

In UV/H_2O_2 Cl^- has no significant effect on the degradation rates of pollutants which is supported by the model calculations (Figure 6 b)) and further illustrated by Figure 6 d) plotting ln(c/c_0) of atrazine, pNBA and pCBA in UV/H_2O_2 in presence of 2 mM Cl^- vs. in presence of 0.037 mM Cl^-. The degradation rates of all compounds fall in one line revealing a slope of 1.1 ± 0.07, which is near the ideal slope of 1 (the standard deviation of the slope has been derived from analysis of the linear regression). This can be explained by the low observed second order rate constant of $^\bullet OH$ plus Cl^- at pH 7 ($k = 10^3$ M^{-1} s^{-1} [22]) as discussed above.

It has to be noted, that the observed degradation of pCBA is distinctively underestimated by the model approach in case of both reaction systems UV/$S_2O_8^{2-}$ and UV/H_2O_2. The reason for this discrepancy between model calculation and experimental data in case of pCBA, whereas pNBA and atrazine reveal a fair agreement with the model, cannot be explained, yet.

7.4.4 Energy demand

As mentioned above, pollutant degradation in UV/$S_2O_8^{2-}$ and UV/H_2O_2 does not significantly differ in River Ruhr water, thus the demand of electrical energy for operating a UV-radiation source is similar in both processes.

The overall energy demand including production of the peroxides has been calculated for River Ruhr water in analogy to Katsoyiannis et al, 2011 [25] (Table 2).

Table 2: Energy demand for 90% degradation of pollutants in river Ruhr water; DOC = 2.45 mg L^{-1}, alkalinity = 2.07 mM; pH = 7.2, [Cl^-] = 1.05 mM for the UV-based processes the optical path length was set to 1 cm, [H_2O_2] = [$S_2O_8^{2-}$] = 0.5 mM; values in brackets have been taken from literature for Lake Zurich water

	Ozonation / kWh	UV/H_2O_2 / kWh	UV/$S_2O_8^{2-}$/ kWh
Atrazine	0.06; 4 mgL^{-1} O_3 (0.05) [25]	0.9 (0.98) [25]	0.9
pNBA	0.06; 4 mgL^{-1} O_3	2.4	2.8

For H_2O_2 production, a value of 0.34 kWh M^{-1} (10 kWh kg^{-1} [55]) has been suggested. The energy demand for $S_2O_8^{2-}$ production varies (0.25-0.38 kWh M^{-1} (1.3-2 kWh kg^{-1} [56], note that costs for sulfuric acids or sulfate metal salts, which are substrates in persulfate production are not taken into account) but is in the same range as for H_2O_2 (lowest value has been used in the calculations). At the present conditions the energy demand for 90% degradation of atrazine or pNBA is not distinctively different in both UV-based processes, albeit the energy demand for pNBA degradation is slightly higher in UV/$S_2O_8^{2-}$ (≈14%). As already mentioned, direct photo-oxidation largely contributes to atrazine degradation, which is reflected in much lower energy costs compared with pNBA (factor > 2), despite their similar reactivity towards $^{\bullet}OH$. However, both UV-based processes require much more energy than ozonation (factor > 10) which is in good agreement with the results of Katsoyiannis et al. [25] given in Table 2 (it will be discussed below that, the energy demand of the photochemical processes can hardly be improved by varying the peroxide dose, see below). It has to be mentioned that the ozone dose of 4 mg L^{-1} is very high in context of drinking water treatment and the potential for elevated formation of bromate (potential carcinogen; US-EPA and EU drinking water standard 10 µgL^{-1} [22]) has to be considered. One strategy for mitigating formation of bromate in ozonation is the addition of H_2O_2 (peroxon process; detailed information are provided by reviews of von Gunten [22, 48] and the book of von Sonntag and von Gunten [57]). However, the typical dose of H_2O_2 is 0.5 µM per µM of O_3 [22] will not increase the energy demand to a level comparable with the UV-based processes (ozone dose of 4

mgL^{-1} (83 µM) corresponds to a dose of 42 µM of H_2O_2 leading to an additional energy demand of 0.014 kWh). It has to be mentioned hat, the addition of H_2O_2 in ozonation may also lead to disadvantages such as a reduced disinfection strength due to destabilization of ozone (note that $^{\bullet}OH$ is less efficient in disinfection than O_3 [22]). A further limitation of H_2O_2 addition is that it can also scavenge $^{\bullet}OH$ thus, reducing the oxidation strength of the ozone based process (see Chapter 1).

It might now be thought, that one could optimize the above photochemical water treatment options by proper adjustment of the peroxide dose. However as will be explained below, this is hardly possible in the present systems. Figure 7 shows the dependency of peroxide dose vs. energy demand for 90% degradation of atrazine (note that corresponding scenarios are based on model calculations and no experimental data). It can be seen that the function of energy demand vs. peroxide dose has a hyperbolic shape. This is due to the fact that the two factors influencing the energy demand that is, operation of the UV-radiation source and peroxide production (figure 7, dotted lines), compensates each other. An increase of the peroxide dose accelerates the degradation rate of a pollutant and thus, reduces the fluence, which has to be applied for achieving a certain degree of degradation. This saving in energy costs is however counterbalanced by an increased energy demand for peroxide production. In the present system the optimum of pollutant degradation rate and peroxide costs in UV/H_2O_2 and $UV/S_2O_8^{2-}$ arrives at 0.5 - 1 mM of H_2O_2 or $S_2O_8^{2-}$. If these peroxides are dosed outside this range the energy demand of the UV-based process will probably increase. However, it has to be mentioned that the optimum of peroxide dose is shifted in dependency to the reaction rate of a pollutant with $^{\bullet}OH$ or $SO_4^{\bullet-}$. Thereby, the optimal peroxide dose will be higher in case of pollutants with a lower reactivity towards the oxidants or in case of a stronger scavenging by the water matrix. The reason is, that in those cases the energy requirements for operating the UV radiation source will get a stronger weighting while the costs for peroxide production remain constant. This also applies in the reverse case (higher reactivity of a pollutant and weaker scavenging reduces the optimal peroxide dose).

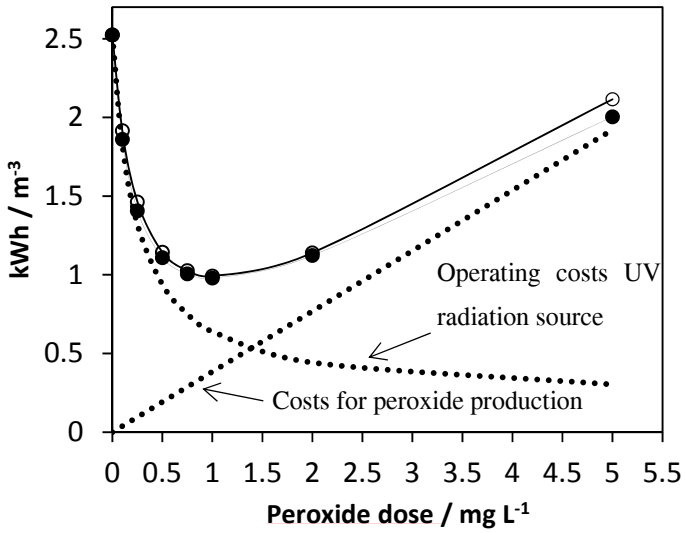

Figure 7: Energy demand for 90 % degradation of atrazine in UV/$S_2O_8^{2-}$ and UV/H_2O_2 at different peroxide concentrations; Calculated for River Ruhr water and a fluence rate of 48 µEinstein m^{-2} s^{-1}; solid lines: sum of energy costs for operating the UV radiation source and energy costs for producing $S_2O_8^{2-}$ respectively H_2O_2 (open symbols UV/$S_2O_8^{2-}$, closed symbols UV/H_2O_2), dotted lines single entries of energy costs

This has to be kept in mind, while optimizing the energy efficiency in UV/H_2O_2 and UV/$S_2O_8^{2-}$. However, the model calculation developed in the present study can be used for assessing roughly the optimal peroxide dose for a certain pollutant and defined water quality of the source water in both processes UV/H_2O_2 and UV/$S_2O_8^{2-}$.

The present study has shown, that if waters such as River Ruhr are used as source water for water treatment, $SO_4^{\bullet-}$-based oxidation reveals hardly any benefit over $^{\bullet}OH$-based oxidation, neither in degrading compounds which are refractory against $^{\bullet}OH$ nor in energy demand. Furthermore, UV/$S_2O_8^{2-}$ and probably also other $SO_4^{\bullet-}$-based processes reveal disadvantages compared to conventional AOP:

1. Lack of experience in operation (e.g., fate of $S_2O_8^{2-}$ in other treatment steps and the distribution system)
2. Possible acidification of the water to be purified (e.g., in the reaction of $SO_4^{\bullet-}$ with Cl^-)
3. Literature information about $SO_4^{\bullet-}$ chemistry revealed from studies conducted in pure water can only partly be transferred to an application.

However UV/$S_2O_8^{2-}$ might be a reasonable alternative to UV/H_2O_2 in case source waters contain very low levels of Cl^- such as 3 µM per mg L^{-1} DOC. Than $SO_4^{\bullet-}$ might indeed belong to the major reactive

species and advantages from its unique features (e.g., lower reactivity towards NOM) can be drawn. Furthermore, the strong impact of alkalinity on the oxidation capacity as well as acidification driven by $Cl^{\bullet}$ (reaction 6 and 4) will be far less pronounced. However, the feasibility of UV/$S_2O_8^{2-}$ and other $SO_4^{\bullet-}$-based processes has to be carefully scrutinized for every individual water composition.

7.5 Literature

1. Liang, C., I.L. Lee, I.Y. Hsu, C.P. Liang, and Y.L. Lin, *Persulfate oxidation of trichloroethylene with and without iron activation in porous media.* Chemosphere, 2008. **70**(3): p. 426-435.
2. George, C., H. El Rassy, and J.M. Chovelon, *Reactivity of selected volatile organic compounds (VOCs) toward the sulfate radical ($SO_4^{\bullet-}$).* International Journal of Chemical Kinetics, 2001. **33**(9): p. 539-547.
3. Waldemer, R.H., P.G. Tratnyek, R.L. Johnson, and J.T. Nurmi, *Oxidation of chlorinated ethenes by heat-activated persulfate: Kinetics and products.* Environmental Science and Technology, 2007. **41**(3): p. 1010-1015.
4. Lin, Y.T., C. Liang, and J.H. Chen, *Feasibility study of ultraviolet activated persulfate oxidation of phenol.* Chemosphere, 2011. **82**(8): p. 1168-1172.
5. Hori, H., E. Hayakawa, H. Einaga, S. Kutsuna, K. Koike, T. Ibusuki, H. Kiatagawa, and R. Arakawa, *Decomposition of environmentally persistent perfluorooctanoic acid in water by photochemical approaches.* Environmental Science and Technology, 2004. **38**(22): p. 6118-6124.
6. Schröder, H.F. and R.J.W. Meesters, *Stability of fluorinated surfactants in advanced oxidation processes - A follow up of degradation products using flow injection-mass spectrometry, liquid chromatography-mass spectrometry and liquid chromatography-multiple stage mass spectrometry.* Journal of Chromatography A, 2005. **1082**(1 SPEC. ISS.): p. 110-119.
7. von Sonntag, C., *Advanced oxidation processes: Mechanistic aspects.* Water Science and Technology, 2008. **58**: p. 1015-1021.
8. Nick, K., H.F. Schöler, T. Söylemez, M.S. Akhlaq, H.P. Schuchmann, and C. von Sonntag, *Degradation of some triazine herbicides by UV radiation such as used in the UV disinfection of drinking water* J. Water SRT - Aqua, 1992. **41**: p. 82-87.
9. Heidt, L.J., *The photolysis of persulfate.* The Journal of Chemical Physics, 1942. **10**(5): p. 297-302.
10. Legrini, O., E. Oliveros, and A.M. Braun, *Photochemical processes for water treatment.* Chemical Reviews, 1993. **93**(2): p. 671-698.
11. Herrmann, H., *On the photolysis of simple anions and neutral molecules as sources of $O^{\bullet-}/OH$, $SO_x^{\bullet-}$ and Cl in aqueous solution.* Physical Chemistry Chemical Physics, 2007. **9**(30): p. 3935-3964.
12. Mark, G., M.N. Schuchmann, H.P. Schuchmann, and C. von Sonntag, *The photolysis of potassium peroxodisulphate in aqueous solution in the presence of tert-butanol: a simple actinometer for 254 nm radiation.* Journal of Photochemistry and Photobiology A, 1990. **55**(2): p. 157-168.
13. Mendez-Diaz, J., M. Sanchez-Polo, J. Rivera-Utrilla, S. Canonica, and U. von Gunten, *Advanced oxidation of the surfactant SDBS by means of hydroxyl and sulphate radicals.* Chemical Engineering Journal, 2010. **163**(3): p. 300-306.
14. McElroy, W.J., *A laser photolysis study of the reaction of SO_4^- with Cl^- and the subsequent decay of Cl_2^- in aqueous solution.* Journal of Physical Chemistry, 1990. **94**(6): p. 2435-2441.
15. Huie, R.E. and C.L. Clifton, *Temperature dependence of the rate constants for reactions of the sulfate radical, SO_4^-, with anions.* Journal of Physical Chemistry, 1990. **94**(23): p. 8561-8567.
16. Dogliotti, L., *Flash photolysis of persulfate ions in aqueous solutions. Study of the sulfate and ozonide radical ions.* Journal of Physical Chemistry, 1967. **71**(8): p. 2511-2516.
17. Padmaja, S., P. Neta, and R.E. Huie, *Rate constants for some reactions of inorganic radicals with inorganic ions. Temperature and solvent dependence.* International Journal of Chemical Kinetics, 1993. **25**(6): p. 445-455.
18. Schwarzenbach, R.P., P.M. Gschwend, and D.M. Imboden, eds. *Environmental organic chemistry*. John Wiley & Sons, Inc. ISBN 0-47 1-35750-2. 2003.
19. Neta, P., R.E. Huie, and A.B. Ross, *Rate constants for reactions of inorganic radicals in aqueous solution.* Journal of Physical and Chemical Reference Data, 1988. **17**(3): p. 1027 - 1040.
20. Buxton, G.V., M. Bydder, and G.A. Salmon, *Reactivity of chlorine atoms in aqueous solution: Part 1.* Journal of the Chemical Society - Faraday Transactions, 1998. **94**(5): p. 653-657.
21. Buxton, G.V., M. Bydder, G.A. Salmon, and J.E. Williams, *The reactivity of chlorine atoms in aqueous solution. Part III. The reactions of $Cl^{\bullet}$ with solutes.* Physical Chemistry Chemical Physics, 1999. **2**(2): p. 237-245.

22. von Gunten, U., *Ozonation of drinking water: Part II. Disinfection and by-product formation in presence of bromide, iodide or chlorine.* Water Research, 2003. **37**(7): p. 1469-1487.
23. von Sonntag, C. and H.P. Schuchmann, *UV disinfection of drinking water and by-product formation - some basic considerations.* J Water SRT - Aqua, 1992. **41**(2): p. 67-74.
24. Canonica, S., L. Meunier, and U. von Gunten, *Phototransformation of selected pharmaceuticals during UV treatment of drinking water.* Water Research, 2008. **42**(1-2): p. 121-128.
25. Katsoyiannis, I.A., S. Canonica, and U. von Gunten, *Efficiency and energy requirements for the transformation of organic micropollutants by ozone, O_3/H_2O_2 and UV/H_2O_2.* Water Research, 2011. **45**(13): p. 3811-3822.
26. Sevilla, M.D., S. Summerfield, I. Eliezer, J. Rak, and M.C.R. Symons, *Interaction of the chlorine atom with water: ESR and ab initio MO evidence for three-electron (σ 2σ* 1) bonding.* Journal of Physical Chemistry A, 1997. **101**(15): p. 2910-2915.
27. Roeselová, M., G. Jacoby, U. Kaldor, and P. Jungwirth, *Relaxation of chlorine anions solvated in small water clusters upon electron photodetachment.: The three lowest potential energy surfaces of the neutral Cl·H2O complex.* Chemical Physics Letters, 1998. **293**(3-4): p. 309-316.
28. Kläning, U.K. and T. Wolff, *Laser flash-photolysis of HClO, ClO-, HBrO, and BrO^- in aqueous-solution - reactions of Cl-atoms and Br-atoms.* Berichte der Bunsen-Gesellschaft Physical Chemistry Chemical Physics, 1985. **89**(3): p. 243-245.
29. Ershov, B.G., *Kinetics, mechanism and intermediates of some radiation-induced reactions in aqueous solutions.* Russian Chemical Reviews, 2004. **73**(1): p. 101-113.
30. Huie, R.E., C.L. Clifton, and P. Neta, *Electron transfer reaction rates and equilibria of the carbonate and sulfate radical anions.* Radiation Physics and Chemistry, 1991. **38**(5): p. 477-481.
31. Huie, R.E. and C.L. Clifton, *Kinetics of the self-reaction of hydroxymethylperoxyl radicals.* Chemical Physics Letters, 1993. **205**(2-3): p. 163-167.
32. Nagarajan, Y. and R.W. Fessenden, *Flash photolysis of transient radicals. 1. X^{2-} with X = Cl, Br, I, and SCN.* Journal of Physical Chemistry, 1985. **89**(11): p. 2330-2335.
33. Jayson, G.G., B.J. Parsons, and A.J. Swallow, *Some simple, highly reactive, inorganic chlorine derivatives in aqueous solution. Their formation using pulses of radiation and their role in the mechanism of the Fricke dosimeter.* Journal of the Chemical Society, Faraday Transactions 1, 1973. **69**: p. 1597-1607.
34. Kläning, U.K. and T. Wolff, *Laser flash-photolysis of HClO, ClO, HBrO, and BrO^- in aqueous solution - reactions of Cl atoms and Br atoms.* Berichte der Bunsen-Gesellschaft Physical Chemistry Chemical Physics, 1985. **89**(3): p. 243-245.
35. Buxton, G.V., M. Bydder, and G.A. Salmon, *Reactivity of chlorine atoms in aqueous solution: Part 1. The equilibrium $Cl^· + Cl^- \rightleftharpoons Cl_2$.* Journal of the Chemical Society - Faraday Transactions, 1998. **94**(5): p. 653-657.
36. Yu, X.Y., Z.C. Bao, and J.R. Barker, *free radical reactions involving Cl, Cl_2^-, and SO_4^- in the 248 nm photolysis of aqueous solutions containing $S_2O_8^{2-}$ and Cl.* Journal of Physical Chemistry A, 2004. **108**(2): p. 295-308.
37. Lifshitz, A. and B. Perlmutter-Hayman, *The kinetics of the hydrolysis of chlorine. I. Reinvestigation of the hydrolysis in pure water.* Journal of Physical Chemistry, 1960. **64**(11): p. 1663-1665.
38. Haag, W.R. and J. Hoigne, *Ozonation of water containing chlorine or chloramines. Reaction products and kinetics.* Water Research, 1983. **17**(10): p. 1397-1402.
39. Buxton, G.V. and M.S. Subhani, *Radiation chemistry and photochemistry of oxychlorine ions. Part 2. Photodecomposition of aqueous solutions of hypochlorite ions.* Journal of the Chemical Society, Faraday Transactions 1, 1972. **68**: p. 958-969.
40. Kläning, U.K., K. Sehested, and J. Holcman, *Standard Gibbs energy of formation of the hydroxyl radical in aqueous solution. Rate constants for the reaction $ClO_2^- + O_3 \rightleftarrows O_3^- + ClO_2$.* Journal of Physical Chemistry, 1985. **89**(5): p. 760-763.
41. Buxton, G.V., C.L. Greenstock, W.P. Helman, and A.B. Ross, *Critical review of rate constants for reactions of hydrated electrones, hydrogen-atoms and hydroxyl radicals ($^•OH/O^{•-}$) in aqueous solution.* Journal of Physical and Chemical Reference Data, 1988. **17**(2): p. 513-886.
42. Merényi, G. and J.S. Lind, *Role of a peroxide intermediate in the chemiluminescence of luminol. A mechanistic study.* Journal of the American Chemical Society, 1980. **102**(18): p. 5830-5835.

43. Gilbert, C.W., R.B. Ingalls, and A.J. Swallow, *Pulse irradiation of aqueous solutions containing ferrous and chloride ions: Reaction between Cl_2^- and HO_2.* Radiation Physics and Chemistry, 1977. **10**(4): p. 221-225.
44. Dodd, M.C., M.O. Buffle, and U. Von Gunten, *Oxidation of antibacterial molecules by aqueous ozone: Moiety-specific reaction kinetics and application to ozone-based wastewater treatment.* Environmental Science & Technology, 2006. **40**(6): p. 1969-1977.
45. Neta, P., V. Madhavan, H. Zemel, and R.W. Fessenden, *Rate constants and mechanism of reaction of sulfate radical anion with aromatic compounds.* Journal of the American Chemical Society, 1977. **99**(1): p. 163-164.
46. Mertens, R. and C. von Sonntag, *Photolysis (λ = 354 nm) of tetrachloroethene in aqueous solutions.* Journal of Photochemistry and Photobiology A, 1995. **85**(1-2): p. 1-9.
47. Manoj, P., K.P. Prasanthkumar, V.M. Manoj, U.K. Aravind, T.K. Manojkumar, and C.T. Aravindakumar, *Oxidation of substituted triazines by sulfate radical anion ($SO_4^{\bullet-}$) in aqueous medium: A laser flash photolysis and steady state radiolysis study.* Journal of Physical Organic Chemistry, 2007. **20**(2): p. 122-129.
48. von Gunten, U., *Ozonation of drinking water: Part I. Oxidation kinetics and product formation.* Water Research, 2003. **37**(7): p. 1443-1467.
49. Larson, R.A. and R.G. Zepp, *Environmental chemistry. Reactivity of the carbonate radical with aniline derivatives.* Environmental Toxicology and Chemistry, 1988. **7**(4): p. 265-274.
50. Canonica, S., T. Kohn, M. Mac, F.J. Real, J. Wirz, and U. Von Gunten, *Photosensitizer method to determine rate constants for the reaction of carbonate radical with organic compounds.* Environmental Science and Technology, 2005. **39**(23): p. 9182-9188.
51. Acero, J.L., K. Stemmler, and U. von Gunten, *Degradation kinetics of atrazine and its degradation products with ozone and OH radicals: A predictive tool for drinking water treatment.* Environmental Science and Technology, 2000. **34**(4): p. 591-597.
52. Tauber, A. and C. von Sonntag, *Products and kinetics of the OH-radical-induced dealkylation of atrazine.* Acta Hydrochimica et Hydrobiologica, 2000. **28**(1): p. 15-23.
53. *Department of National Health and Welfare - Canada; Guidelines for Canadian drinking water quality. Supporting documentation*. 1978 April 1979 [cited 2013; Available from: http://www.hc-sc.gc.ca/index-eng.php.
54. Fawell, J.K., U. Lund, and B. Mintz, *Chloride in Drinking-water Background document for development WHO Guidelines for Drinking-water Quality*, in *Guidelines for drinking-water quality - Health criteria and other supporting information*, M. Sheffer, Editor. 2003, World Health Organization: Geneva, Switzerland.
55. Rosenfeldt, E.J., K.G. Linden, S. Canonica, and U. von Gunten, *Comparison of the efficiency of $^{\bullet}OH$ radical formation during ozonation and the advanced oxidation processes O_3/H_2O_2 and UV/H_2O_2.* Water Research, 2006. **40**(20): p. 3695-3704.
56. Thiele, W., H.-J. Kramer, and H.J. Forster, *Method for producing peroxodisulfates in aqueous solution*, U.s.p.a. publication, Editor. 2007: USA. p. 1-5.
57. von Sonntag, C. and U. von Gunten, eds. *Chemistry of ozone in water and wastewater treatment*. 2012, IWA Publishing.

Chapter 8

-

Degradation of perfluorinated compounds by sulfate radicals

8.1 Abstract

Advanced Oxidation Processes (AOP) are based on the oxidation power of highly reactive hydroxyl radicals and are used in water treatment for pollutant control. These radicals react with most organic and inorganic compounds with nearly diffusion controlled rates. In spite of the high oxidation strength of hydroxyl radicals, some compounds are stable under AOP-conditions such as perfluorooctanoic acid (PFOA). PFOA and other perfluorchemicals (PFC) accumulate in the environment and are ubiquitary distributed. The potential of PFC being harmful to human health, requires options the control of these chemicals in water treatment. In this context the generation of sulfate radical ($SO_4^{\bullet-}$) by photolysis of peroxodisulfate ($S_2O_8^{2-}$) has appeared to be effective in decomposing PFOA in pure water systems. However, with regard to both, kinetics and reaction mechanism major gaps still exist. The present study has shown, that perfluorinated carboxylic acids (PFCAs) can be partly mineralized in a chain reaction initiated by $SO_4^{\bullet-}$. However, the kinetics of the reaction $SO_4^{\bullet-}$ plus PFCAs with chain length of C_4-C_8 revealed very slow reaction rates ($\approx 10^4$ M^{-1} s^{-1}). Thus, the energy demand required for generation $SO_4^{\bullet-}$ in a potential water treatment option such as photolysis of $S_2O_8^{2-}$ is very high (the energy demand for operating a Hg low pressure lamp has been estimated to be 47 kWh m^{-3} to achieve a degradation of 10 % PFOA).

8.2 Introduction

The distribution, environmental behavior, human health risk and emission routes of perfluorinated compounds (PFC) are intensively discussed in science as well as on a political level. Due to the potential harm for human health the US-EPA proposed an advisory drinking water standard for perfluorooctanoic acid (PFOA) and perfluorooctane sulfonic acid (PFOS) of 0.4 µg L^{-1} [1]. An advisory threshold value for the sum of PFOA and PFOS has also been set by the German drinking water commission (0.3 µg L^{-1}) [2]. The ongoing discussion about micro-pollutant control suggests that a regulation for PFC in domestic waste water treatment will be set in the near future. Very little is known about the consequences of elevated perfluorochemical concentrations in the environment and how this is connected with health and economical risks. This is aggravated by the high persistence of these compounds in the environment and the tendency for bioaccumulation especially of long chain PFC such as PFOA and PFOS [3]. Due to the high mobility of especially low-molecular PFC and the ubiquitous occurrence of PFC, the remediation of contaminated sites is very difficult. Thus the prevention of PFC release is important that is partly achieved by the development and usage of alternative agents. However, the unique features of perfluorinated organics are still important for some applications such as

fire-fighting foams [3] and the production of semiconductors [4] and thus renders replacement difficult. In addition to drinking water, other routes of exposure have also to be taken into account. Drinking water is probably not the main source for PFC exposure to humans whereas domestic dust, food and textiles probably play a more important role within this context [5].

Perfluoro-chemicals are present in the environment and have been detected all over the globe, [6-14] whereby fluorotelomer alcohols may act as highly mobile precursors for perfluorinated carboxylic acids [8]. PFC are present in drinking water resources, where they probably persist for a long time due to their high environmental stability. Thus, drinking water suppliers have to deal with the possibility of elevated PFC concentrations in their raw water and thereby need to consider treatment strategies as barriers for PFC.

Perfluorinated compounds survive most of the conventional techniques in drinking and wastewater treatment and are found in finished drinking water in Germany, Switzerland, USA and other countries [13, 15]. In some of these cases, the PFC concentrations exceeded the advisory drinking water standard suggested by the German and US-EPA drinking water commission.

In particular, treatment techniques based on the structural change of the target molecules such as ozonation or advanced oxidation fail due to the high chemical stability of these compounds [16]. Separation methods such as ion exchange and sorption on activated carbon as well as nanofiltration and reverse osmosis, appear to be effective to remove PFC from water. The waste produced is enriched with the pollutants and needs to be treated further which can be done *via* incineration.

Sulfate radical anions ($SO_4^{\bullet-}$) are strong oxidizing agents for which a reduction potential in the range of 2.5-3.1 V has been reported [17, 18]. As already mentioned, these radicals can be generated in various ways such as UV-photolysis and reduction of peroxodisulfate ($S_2O_8^{2-}$) or peroxomonosulfate (HSO_5^-) by transition metals as well as thermolysis of $S_2O_8^{2-}$ ($T > 40°C$) [19, 20]. In contrast to the reaction with $^{\bullet}OH$, perfluorocarboxylic acids of chain length between C_2-C_{11} have been degraded by $SO_4^{\bullet-}$ in pure water systems (UV/$S_2O_8^{2-}$ and thermolysis of $S_2O_8^{2-}$) [21-25]. A second order rate constant has been determined for trifluoroacetic acid (1.6×10^4 M^{-1} s^{-1} [26]) and estimated for PFCAs with carbon chain length of C_3 (1.4×10^4 M^{-1} s^{-1}) and C_4 (1.3×10^4 M^{-1} s^{-1}) [25]. The rate constants for the reaction of $SO_4^{\bullet-}$ with short chain PFCAs are very low. However, this may be partly counterbalanced by the longer lifetime of $SO_4^{\bullet-}$ in presence of persulfate compared to $^{\bullet}OH$ in presence of H_2O_2 ($k(SO_4^{\bullet-} + S_2O_8^{2-}) = 5.5 \times 10^5$ M^{-1} s^{-1} [27], $k(^{\bullet}OH + S_2O_8^{2-}) = 2.4 \times 10^7$ M^{-1} s^{-1}) ([28]).

However, some aspects are still unclear, which are important for assessing the feasibility of PFCA degradation by $SO_4^{\bullet-}$, such as reaction rates of PFCAs beyond chain length of C_4. Furthermore, some

mechanistic aspects in the degradation mechanism of PFCAs as well as the reactivity of perfluorinated sulfonic acids are targeted in the present study.

8.3 Material and Methods

8.3.1 Chemicals

Following chemicals have been used as received.

Acetone (99.5%) AppliChem, *acetonitrile* (≥ 99.9%) Sigma-Aldrich, a*rgon* (99.99%) Air liquide, *perfluorobutyric acid* (PFBA) (98%) Sigma-Aldrich, *perfluoroheptanoic acid* (PFHpA) (99%) Sigma Aldrich, *perfluorooctanoic acid* (PFOA) (96%) Sigma-Aldrich, *perfluoropentanoic acid* (PFPeA) (97%) Sigma-Aldrich*, pentafluoropropionic acid* (PFPrA) (97%) Sigma-Aldrich, *sodium bicarbonate* (p.a.) Riedel de Haën, *sodium carbonate* (pure) Applichem and Merck*, sodium fluoride* (p.a.) Merck, *sodium peroxodisulfate* ($S_2O_8^{2-}$) (99%) Sigma-Aldrich, *sodium sulfate* (pure) Merck, *sulfuric acid* (95-97%) AppliChem, *trifluoroacetic acid (TFA)* (≥ 97%) Sigma-Aldrich*, trifluoromethane sulfonic acid (TFMS)* (≥99%) Aldrich.

8.3.2 Experimental procedures

Solutions have been prepared in water purified by an ultra-pure water production system (Purelab ultra from ELGA). $SO_4^{\bullet-}$ have been generated by thermolysis and photolysis of $S_2O_8^{2-}$. Thermolysis has been performed at 60-80 °C in a shaking water bath (GFL Gesellschaft für Labortechnik mbH). The reaction was stopped by chilling the solutions in an ice bath after different time intervals. The solutions were closed gas-tight with a screw cap and PTFE sealing. For photochemical experiments a merry-go-round photo-apparatus as described previously (Chapter 3) has been used. As radiation source a Hg-low pressure arc (TNN 15/32, 15 W Hans und Thomas Schneider Glasapparatebau) has been installed. The body of this radiation source (suprasil quartz glass) is transparent for the 185 nm emission line. However, the recirculating cooling water in the cooling finger acts as an effective spectral filter (A(185 nm) ≈ 200 cm^{-1}, path length ≈ 0.5 cm). It is important to mention that the radiation source has to be run in a protective atmosphere (i.e., in absence of oxygen) to prevent the formation of ozone. Thus, the inner part of the cooling finger containing the radiation source has been continuously purged with argon. These experiments have been conducted at 25 °C and if not otherwise mentioned the pH of the solution was monitored but not adjusted or buffered. However, during the experimental run the pH

never reached a value which would lead to a significant change in speciation of any compound present in the sample solutions. Since most of the solutions had a low conductivity and buffer strength the pH was determined by a special electrode used for solutions with low ion concentration (serial number 6.0253.100; Metrohm). For other solutions a regular pH electrode has been used (serial number 6.0234.100; Metrohm). For determining rate constants, competition kinetics have been applied (see Chapter 3). TFA has been used as a reference compound, because it reacts with comparable kinetics as the other PFCAs ($k(SO_4^{\bullet-}) = 1.6 \times 10^4\ M^{-1}\ s^{-1}$ [26]). It has to be mentioned that other compounds with such a low reactivity towards $SO_4^{\bullet-}$ can hardly be found. TFA is a potential product in PFCA degradation. However, the TFA yield in the degradation of C_6-C_8 is below 5 % (see below) and can thus be neglected. In case of PFCAs with lower carbon chain length considerable yields of TFA have been observed ($C_5 \approx 10$ %, $C_4 \approx 30$ % yield of TFA). In those cases of competition kinetics experiments the determined concentration of TFA has been corrected by subtracting the theoretical TFA yields per degraded PFCA determined in separate experiments in which no TFA has been added (i.e., the TFA concentration in these competition kinetics experiments was subtracted by the TFA yield multiplied by the turnover of PFPeA/PFBA).

All compounds have been determined by an ion chromatograph coupled with ion suppression and conductivity detector (883 IC Basic plus and 881 compact IC Pro (with additional CO_2 suppressor unit), Metrohm). equipped with an anion separation column (Metrosep A Supp 4; 250 × 4.0 mm; particle size 8 µm, guard column Metrosep A Supp 4/5 guard 4.0) and an auto-sampler (863 Compact Autosampler and 814 USB Sample Processor, Metrohm). Two sample loops were used (20 and 50 µL). With a regular IC lacking the option to run a solvent gradient or to switch between different columns, the analysis of samples containing $S_2O_8^{2-}$ is hampered by the long retention time of $S_2O_8^{2-}$. The elution of $S_2O_8^{2-}$ can be accelerated by addition of acetonitrile, which also suppresses hydrophobic interactions of PFCAs with carbon chain length of > C_3. Currently, the mechanisms of how organic solvents interact in IC largely lack a systematic investigation).

In the following the eluents which have been used for separating the PFCAs (C_8-C_2) will be described.

The eluent was based on HCO_3^- and CO_3^{2-} to enable reducing the background conductivity by chemical suppression by an acidic cation exchanger. The eluent used for 883 IC Basic plus was composed as follows: 0.65 mM Na_2CO_3 dissolved in an aqueous solution containing 17.6 % v/v acetonitrile.

In order to reduce the analysis time the eluent flow was changed during the measurement as follows:

Time / min	Flow rate / mL min^{-1}	remarks
0 – 40	1	constant flow rate
40 – 41.3	1.5	increase of the flow rate
41.3 – 158.66	1.5	constant flow rate
158.66 –169.66	1	decrease of the flow rate
169.66 – 180	1	constant flow rate

Retention times / min: F^-: 5.3, TFA (C_2): 8.1 min, PFPrA (C_3): 9.2, PFBA (C_4): 10.4, PFPeA (C_5): 12.5, PFHxA (C_6): 18.5, PFHpA (C_7): 25.2, PFOA: 36.1, SO_4^{2-}: 40.1, $S_2O_8^{2-}$ ca. 150

The following method has been used for determining TFA and trifluoro methane sulfonic acid (TFMS) in the photochemical experiments

Eluent: 2.52 mM Na_2CO_3, 2.38 mM $NaHCO_3$, 30% (v/v) acetone, flow rate 1 mL min^{-1}.

Retention times / min: F^-: 2.9, TFA: 3.8, TFMS: 5.4

Another eluent to simultaneously determine PFCAs (C_2-C_8) and fluoride has been used for the IC instrument 881 compact IC Pro. The higher sensitivity of this instrument allowed to dilute the samples to a large extent (1:101) for preventing overload of the column with SO_4^{2-} and $S_2O_8^{2-}$. This eluent was composed as follows: 0.68 mM $NaHCO_3$ and 0.72 mM Na_2CO_3 mixed with 20 % acetonitrile. A sample loop of 20 µL has been used.

This method led to the following retention times (flow rate: 1 mL min^{-1}) / min:

F^-: 4.87, TFA (C_2): 7.05, PFPrA (C_3): 7.01, PFBA (C_4): 8.91, PFPeA (C_5): 10.89, PFHxA (C_6): 13.82, PFHpA (C_7): 18.22, PFOA (C_8): 24.68, sulfate 27.73

8.4 Results and discussion

8.4.1 Mechanistic aspects of the reaction $SO_4^{\bullet-}$ plus PFCAs

A reaction pathway for PFOA degradation by $SO_4^{\bullet-}$ has been proposed as follows (derived from Kutsuna and Hori [25]):

(1) $CF_3(CF_2)_6C(O)O^- + SO_4^{\bullet-} \rightarrow CF_3(CF_2)_6C(O)O^{\bullet} + SO_4^{2-}$

(2) $CF_3(CF_2)_6COO^{\bullet} \rightarrow CF_3(CF_2)_5CF_2^{\bullet} + CO_2$

(3) $CF_3(CF_2)_5CF_2^{\bullet} + O_2 \rightarrow CF_3(CF_2)_5CF_2OO^{\bullet}$

(4) $2\ CF_3(CF_2)_5CFOO^{\bullet} \rightarrow CF_3(CF_2)_5CFOOOOCF(CF_2)_5CF_3$

(5) $CF_3(CF_2)_5CFOOOOCF(CF_2)_5CF_3 \rightarrow 2\ CF_3(CF_2)_5CF_2O^{\bullet} + O_2$

(6) $CF_3(CF_2)_5CF_2O^{\bullet} \rightarrow CF_3(CF_2)_4CF_2^{\bullet} + COF_2$

(7) $COF_2 + H_2O \rightarrow CO_2 + 2HF$

(8) $CF_3(CF_2)_5CF_2O^{\bullet} + HSO_4^- \rightarrow CF_3(CF_2)_5CF_2OH + SO_4^{\bullet-}$

(9) $CF_3(CF_2)_5CF_2OH \rightarrow CF_3(CF_2)_5COF + HF$

(10) $CF_3(CF_2)_5COF + H_2O \rightarrow CF_3(CF_2)_5COO^- + HF + H^+$

It can be deduced from this proposition that the degradation of PFOA is a stepwise elimination of -CF_2 units, leading to shorter-chain PFCAs which are subsequently oxidized by $SO_4^{\bullet-}$ until complete mineralization to CO_2 and HF. This is supported by the experimental findings of arising and subsequent decomposition of short chain PFCAs and a nearly 100% yield of fluoride per CF_2-unit degraded [23]. On the basis of a stepwise degradation of PFCAs a model has been developed and applied on the degradation of PFOA in order to compare the modeled yields of products with the experimental data of Hori et al. [22] (Figure 1).

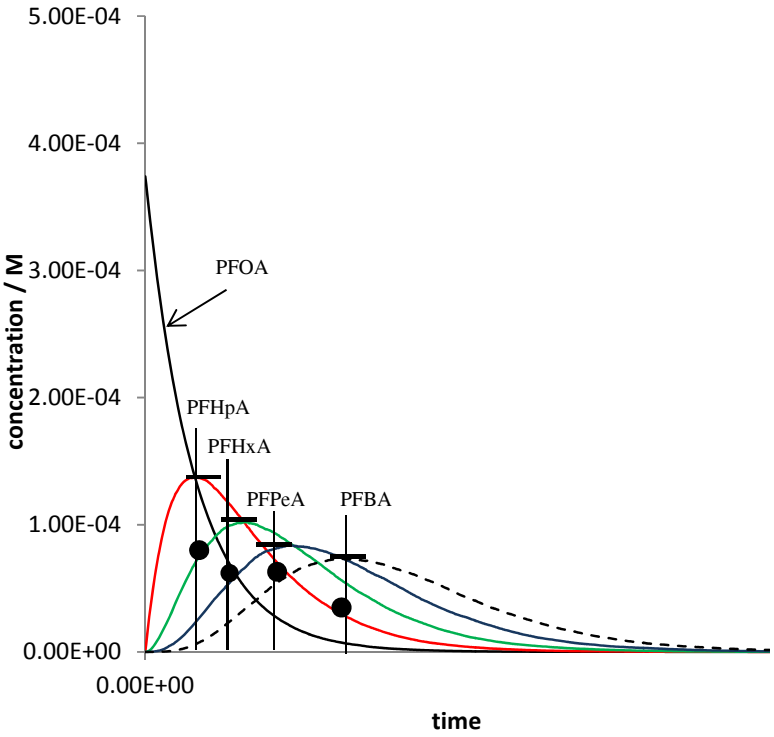

Figure 1: Modeled degradation of PFOA applying the approach of a consecutive formation of PFCAs derived from reaction 1-10; black circles = yields determined experimentally by Hori et al., [22]. Note that the formation rate of $SO_4^{\bullet-}$ in thermal activation of $S_2O_8^{2-}$ is unknown. Thus, the model can only be used to compare the peak concentrations of the PFCAs and no information is given about a reaction time.

The yields fairly match the experimental data supporting the reaction sequence of Kutsuna and Hori [25].

Yet, the presence of perfluoroalkoxyl radicals and oxygen principally enables another pathway which could result in elimination of more than 1 CF_2 unit per $SO_4^{\bullet-}$ attack. The release of carbonyl fluoride (reaction 6) yields a carbon centered radical (shortened by one CF_2-unit) which rapidly adds O_2 (reaction 3). The perfluoroalkylperoxyl radical again gives rise to corresponding perfluoroalkoxyl radicals in its bimolecular decay (reaction 4/5). In presence of sufficient amounts of O_2 these reactions could lead to complete mineralization of PFCAs. However, to account for the observation that PFCAs at different chain lengths are formed, Kutsuna and Hori [25] included reaction 8 to interrupt this reaction cycle. HSO_4^- may be formed in high concentration in corresponding experiments since Hori et al. applied large amounts of $S_2O_8^{2-}$ (e.g., 50 mM; that is > 100 fold excess over PFOA [21, 23]). Thus, the reaction of the perfluoroalkoxyl radicals might be directed into reaction 8.

Indeed, lowering the dosages of $S_2O_8^{2-}$ (i.e., 2 fold excess over PFCAs (10 mM $S_2O_8^{2-}$)) as done in the present study, reveals a very different product pattern, in that different PFCAs formed as products tend to appear simultaneously (Figure 2) instead of being formed sequentially (Figure 1).

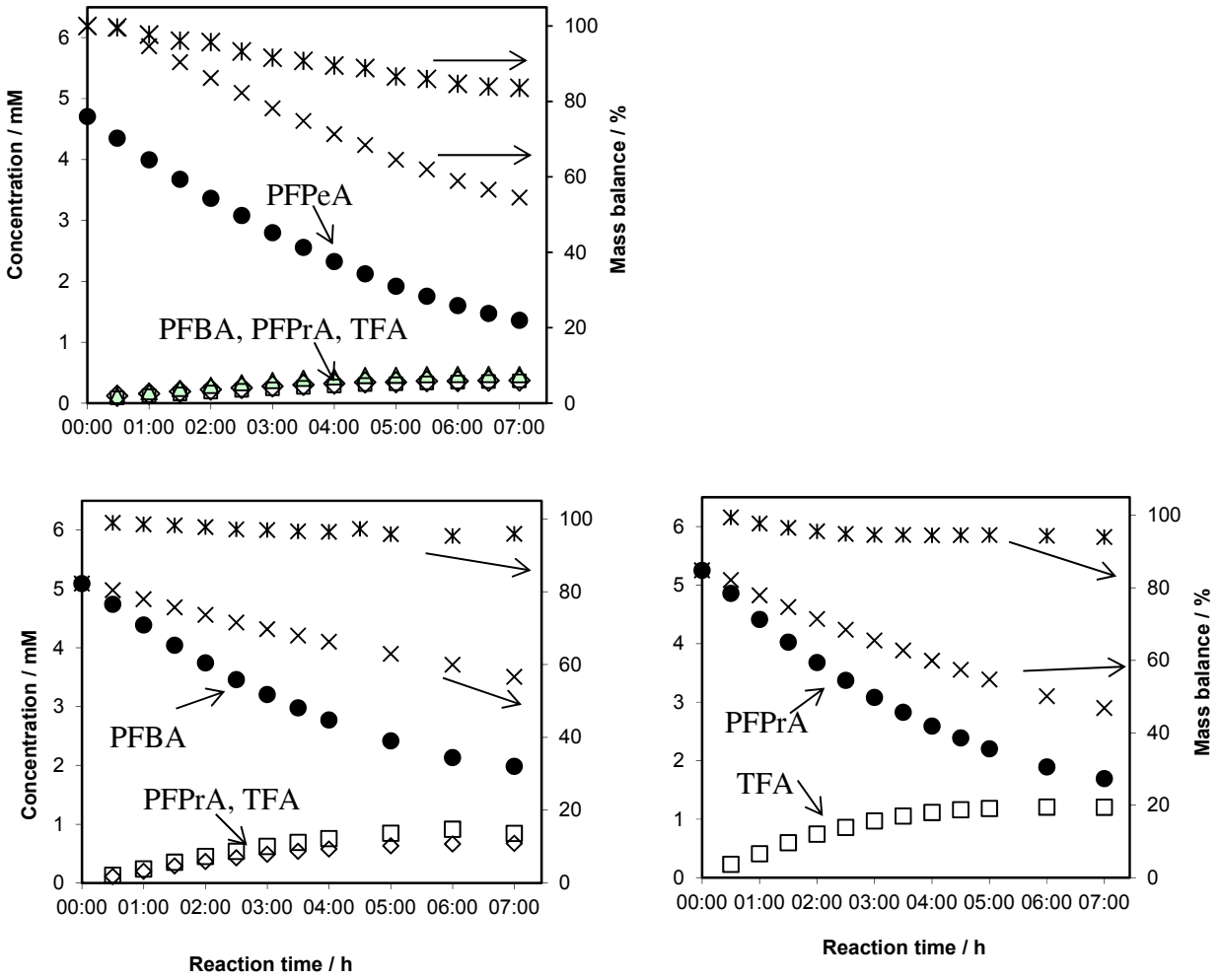

Figure 2: Degradation of PFCAs and product formation; thermal activation of $S_2O_8^{2-}$; stars: fluorine balance, crosses: PFCA-balance, closed circles: precursor PFCA, open symbols PFCAs formed upon degradation of the precursor; $[S_2O_8^{2-}]_0$ = 10 mM, $[PFCAs]_0$ = 5 mM, T= 70°C, pH 2-4

Two observations can be made:

1. A complete mass balance of fluorine is contrasting an incomplete PFCA mass balance
2. Different PFCA-products are formed simultaneously, possibly as primary products

This suggests that reaction 8 is suppressed in the present system due to the low concentration SO_4^{2-}. In that situation Reactions 2-7 may than undergo a chain reaction which may lead to complete mineralization.

In this reaction the perfluoroalkoxyl radicals formed in reaction 5 again undergo β-fragmentation in analogy to reaction 6 yielding another carbon centered radical and carbonyl fluoride without the termination reaction. An analogous reaction has been observed for *tert*-butoxy radicals yielding acetone and methyl radicals [29] (rate of unimolecular decomposition $10^6 – 10^7$ s^{-1} [30]). The carbonyl fluoride is expected to hydrolyze as its chlorinated analogue does (k = 9 s^{-1}, 25 °C) [31]). The carbon centered radical in turn adds oxygen (≈ 10^9 M^{-1} s^{-1} [32]) and yields another peroxylalkoxyl radical (reaction 3-5). The smallest perfluorinated oxyl radical ($F_3C\text{-}O^{\bullet}$) may cleave a fluorine atom as a product of β-fragmentation (reaction 11). Since the fluorine atom rapidly reacts with water yielding HF and $^{\bullet}OH$ (reaction 12), it is removed from the equilibrium, thus increasing the driving force of this reaction.

(11) $F_3C\text{-}O^{\bullet} \rightarrow F^{\bullet} + CF_3{=}O$

(12) $F^{\bullet} + H_2O \rightarrow HF + {}^{\bullet}OH \qquad k = 4 \times 10^{10}\ M^{-1}\ s^{-1}$

As already indicated, this reaction cycle is suppressed by scavenging of perfluorooxyl radicals in other reactions. Beside HSO_4^- (reaction 8) also $S_2O_8^{2-}$ could be a potential scavenger in the present system. For assessing the importance of different competing reactions, corresponding rate constants are key factors. As it stands, information of the reactions of perfluoroalkoxyl radicals is lacking in the literature. Nevertheless, these reactions will be discussed on the basis of thermodynamic data computed by Naumov [33]. Table 1 compiles potential reactions of the perfluorinated alkoxyl radicals occurring in the present reaction system and gives estimates about their kinetics and thermodynamics. The rate of elimination of carbonyl fluoride can be derived from butoxyl radicals which eliminate acetone with a reaction rate of 10^6 s^{-1} [30] (Reaction 20, ΔG = -70 kJ mol^{-1} [33]). Since the driving force in the analogous reaction of perfluorinated alkoxyl radicals is even higher (ΔG = -97 kJ mol^{-1} [33]) it can be concluded that the latter reaction reveals the same if not a faster kinetics (i.e., ≥ 10^6 s^{-1}).

Table 1: Reaction rates and free Gibbs energies of different reactions involving perfluoroalkoxyl radicals and comparison with analogous reactions of *tert*-butoxylradicals and $^{\bullet}OH$

Reaction No.	Reaction	k	ΔG^0 kJ mol^{-1}
8	$CF_3(CF_2)_nCF_2\text{-}O^{\bullet} + HSO_4^- \rightarrow CF_3(CF_2)_nCF_2\text{-}OH + SO_4^{\bullet-}$	$10^6 - 10^7$ M^{-1} s^{-1} Kinetics derived from $^{\bullet}OH$	-61 [33]
13	$^{\bullet}OH + HSO_4^- \rightarrow SO_4^{\bullet-} + H_2O$	$0.7 - 1.7\times 10^6$ M^{-1} s^{-1} [34]	-64 [33]
14	$CF_3(CF_2)_nCF_2\text{-}O^{\bullet} + H_2O \rightarrow CF_3(CF_2)_nCF_2\text{-}OH + {}^{\bullet}OH$	Possibly high driving force due to high concentration of water (55.5 M)	+3 [33]
15	$^{\bullet}OH + S_2O_8^{2-} \rightarrow OH^- + S_2O_8^{\bullet-}$	1.7×10^7 M^{-1} s^{-1} [35]	Not available
16	$CF_3(CF_2)_nCF_2\text{-}O^{\bullet} + S_2O_8^{2-} \rightarrow CF_3(CF_2)_nCF_2\text{-}O^- + S_2O_8^{\bullet-}$	10^7 M^{-1} s^{-1} Kinetics derived from $^{\bullet}OH$	Not available
17	$(CH_3)_3CO^{\bullet} \rightarrow (CH_3)_2O + {}^{\bullet}CH_3$	10^6 s^{-1} [30]	-70 [33]
6	$CF_3(CF_2)_nCF_2O^{\bullet} \rightarrow CF_3(CF_2)_n{}^{\bullet} + CF_2O$	$\geq 10^6$ s^{-1}	-97 [33]

The suggested termination reaction 8 [25] is similar to the corresponding reaction with $^{\bullet}OH$ in that they share the same free energy yield ($k(CF_3(CF_2)_nCF_2\text{-}O^{\bullet})$ = -61 kJ mol^{-1} $k(^{\bullet}OH)$ = -64 kJ mol^{-1} [33]). The same driving forces may indicate that both reactions could reveal the same kinetics ($\approx 10^6$ M^{-1} s^{-1}, Table 1). In the studies of Hori the concentration of $S_2O_8^{2-}$ was ≈ 50 mM [21, 23]. That means maximal 100 mM SO_4^{2-} is formed. This corresponds to 50 mM HSO_4^- and 50 mM SO_4^{2-} since experiments have been conducted in the pH range of 2-3 (pK_a (HSO_4^-) = 1.92 [36]). Thus, the observed reaction rate of perfluoroalkoxyl radicals plus HSO_4^- is probably in the range of 10^4-10^5 s^{-1}. That is at least one order of magnitude below the β-fragmentation rate of perfluoroalkoxyl radicals indicating that the unimolecular decay of perfluorooxyl radicals can hardly be interrupted by reaction 8. However, $S_2O_8^{2-}$ might also be involved in scavenging perfluoroalkoxyl radicals (reactions 16). The reaction with $S_2O_8^{2-}$ is well known in the chemistry of $^{\bullet}OH$ (reaction 15). As shown above $^{\bullet}OH$ reveals some similarities compared to perfluoroalkoxyl radicals, which, thus, could also react with $S_2O_8^{2-}$. Indeed, the deprotonated alcohol formed in reaction 16 is rapidly protonated and removed from the equilibrium. The alcohol itself is removed from the reaction system since it forms a carboxylic acid in presence of water (reactions 9 and 10) which might further accelerate the reaction. Assuming that perfluoroalkoxyl radicals react with $S_2O_8^{2-}$ at a similar rate as $^{\bullet}OH$ may lead to the following interpretation. With 50 mM $S_2O_8^{2-}$ the observed first order kinetics is in the same order of magnitude compared with reaction 6 (i.e., 10^5-10^6 s^{-1}). This implies that even a small decrease in the concentration of $S_2O_8^{2-}$ distinctively diminishes the scavenging of perfluoroalkoxyl radicals and explains why a relatively small change in the concentration of $S_2O_8^{2-}$ (from 50 to 10 mM) already results in considerable differences regarding the product pattern.

Another reaction which might scavenge perfluoroalkoxyl radicals is H-abstraction from water (reaction 14). This reaction is slightly endergonic, but might experience a considerable driving force due to the

high concentration of water (55.5 M). Moreover, the product of reaction 14 is removed from the equilibrium in reactions 9 and 10. Hence, this reaction could also be a feasible competitor for β-fragmentation of the perfluoroalkoxyl radicals (reaction 6).

The scavenging of perfluoroalkoxyl radicals can also be a chain promotor type reaction since $SO_4^{\bullet -}$ are formed. This is obvious in reaction 8 yielding $SO_4^{\bullet -}$ in a primary reaction. However, reaction 14 and 16 could also give rise to $SO_4^{\bullet -}$ in secondary reactions as will be described below. The $^{\bullet}OH$ formed in reaction 14 has a moderate reaction rate towards $S_2O_8^{2-}$ (reaction 18 k = 1.2 × 10^7 M^{-1} s^{-1} [28]), which, however, can become dominant if $S_2O_8^{2-}$ is present in high concentration (e.g., 50 mM). In 1962, House postulated the formation of $SO_4^{\bullet -}$ in the reaction of $^{\bullet}OH$ plus $S_2O_8^{2-}$ (reaction 21).

(18) $^{\bullet}OH + S_2O_8^{2-} \rightarrow HSO_4^- + SO_4^{\bullet -} + ½\ O_2$ [37]

This reaction is initiated by electron transfer yielding OH^- and $S_2O_8^{\bullet -}$. $S_2O_8^{\bullet -}$ than may decompose as follows (note that the stoichiometry of reaction 18 is conserved):

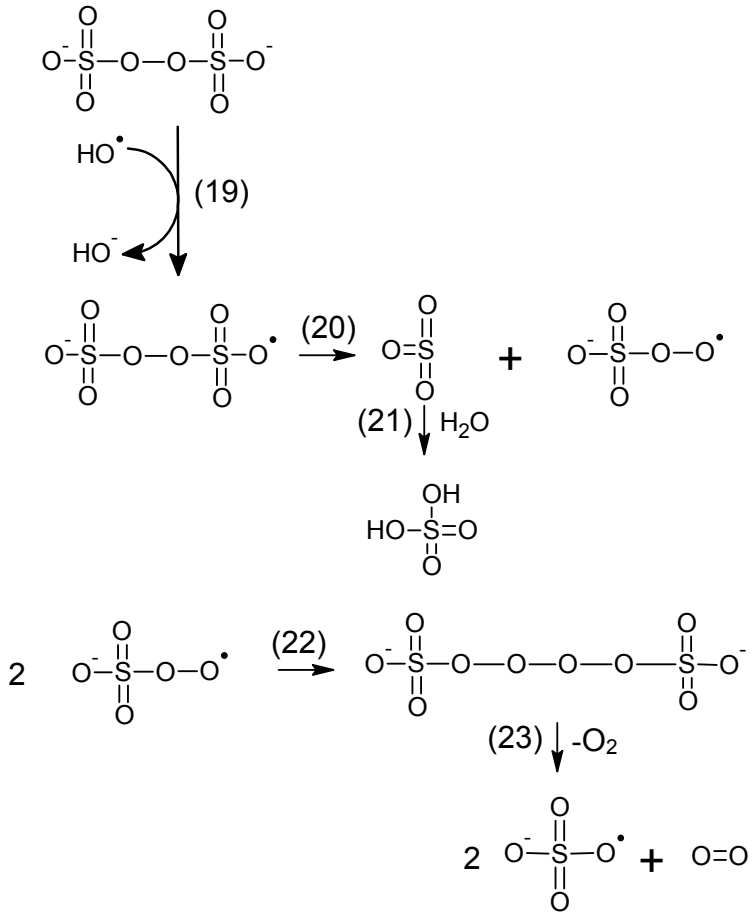

In the reaction of $SO_4^{\bullet-}$ plus $S_2O_8^{2-}$ studied by Mark and von Sonntag [38] a similar pathway has been indicated. Mark and von Sonntag observed the evolvement of O_2 and a drop in pH which might account for the formation of sulfuric acid (reaction 20/21) and elimination of O_2 in a bimolecular type decay of $S_2O_8^{\bullet-}$ (reaction 22). Thus, the reaction of $^{\bullet}OH$ and perfluoroalkoxyl radicals plus $S_2O_8^{2-}$ might yield $SO_4^{\bullet-}$.

Hitherto, the degradation of C_3-C_5 PFCAs has been discussed by means of primary yields of fluoride and PFCA-products (Figure 2). Now, this discussion will be extended for the range of C_2-C_8 PFCAs. Corresponding primary yields of fluoride and fluorine attached to PFCAs which are formed in a primary reaction are depicted in Figure 3.

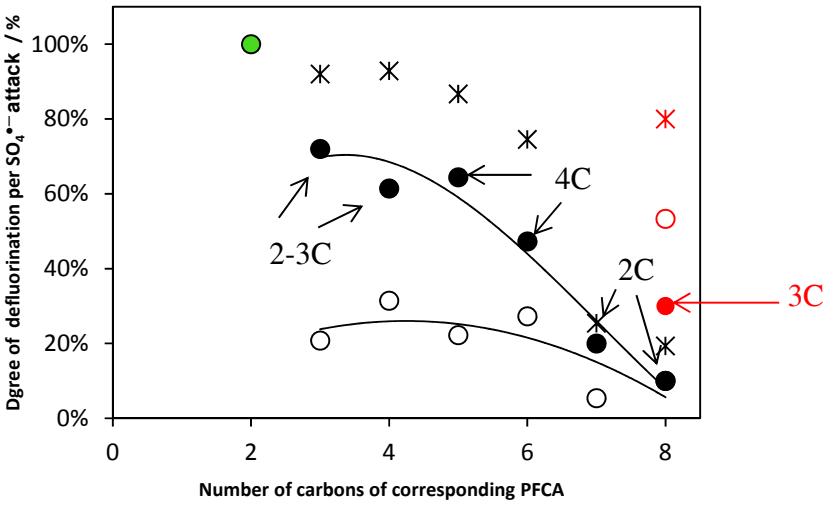

Figure 3: Primary yield of fluorine per $SO_4^{\bullet-}$-attack on different PFCAs (C_2-C_8); open circles = fluorine bound to PFCA products calculated from quantified PFCAs, closed circles = fluoride, stars = fluorine balance, numbers indicate the average amount of carbons potentially converted to CO_2 in a primary reaction (calculated from the primary fluoride yield); pH 2-4, T = 70 °C, $[S_2O_8^{2-}]$ = 10 mM, $[PFCAs]_0$ = 5 mM; red symbols: degradation of PFOA at 80 °C (other experimental parameters see above), green circle: TFA ($SO_4^{\bullet-}$ generated photo-chemically);[TFA] = 1 mM, $[S_2O_8^{2-}]$ = 5-50 mM; pH 2-4, T = 25 °C, Fluence rate (254 nm) ≈ 50 µEinstein m^{-2} s^{-1}

In PFCAs the perfluorinated carbon may be attached to 2 or 3 fluorines (R-CF_2-R and CF_3-R). Hence 2-3 fluorines are cleaved off in the proposed reaction 6/7 and 11. Thus, the primary yield of F^- allows estimating the number of carbons oxidized to CO_2 in a primary reaction (e.g., a primary yield of 4 fluorides in the reaction of PFCAs by $SO_4^{\bullet-}$ indicates that 2 CF_2 units have been oxidized to CO_2 upon

radical attack. However, cleavage of the carboxylic group (reaction 1 and 2) precedes formation of fluoride. That carbon has to be added to the carbons derived from the formation of fluoride to arrive at the total number of carbons oxidized to CO_2. The numbers in Figure 3 indicate the number of carbons cleaved off in a primary reaction derived by the above calculation. Accordingly, 2-4 carbons are oxidized per radical attack indicating that the chain reaction of perfluorinated alkoxylradicals may occur to a certain extend. By that means C_2-C_5-PFCAs are mineralized to 70-80% per radical attack, whereas PFCA of longer chain length display a certain suppression of primary mineralization (< 10% fluoride yield per radical attack (3 carbons were converted to CO_2). In addition, the PFCA- and fluorine-balance of PFCAs with chain length of C_6-C_8 is largely unbalanced indicating that products were formed, which were not detected by IC suggesting that a different reaction pathway set in.

One possible explanation for the loss of organic fluorine is the formation of perfluorinated peroxides upon release of oxygen from the tetroxide (see below).

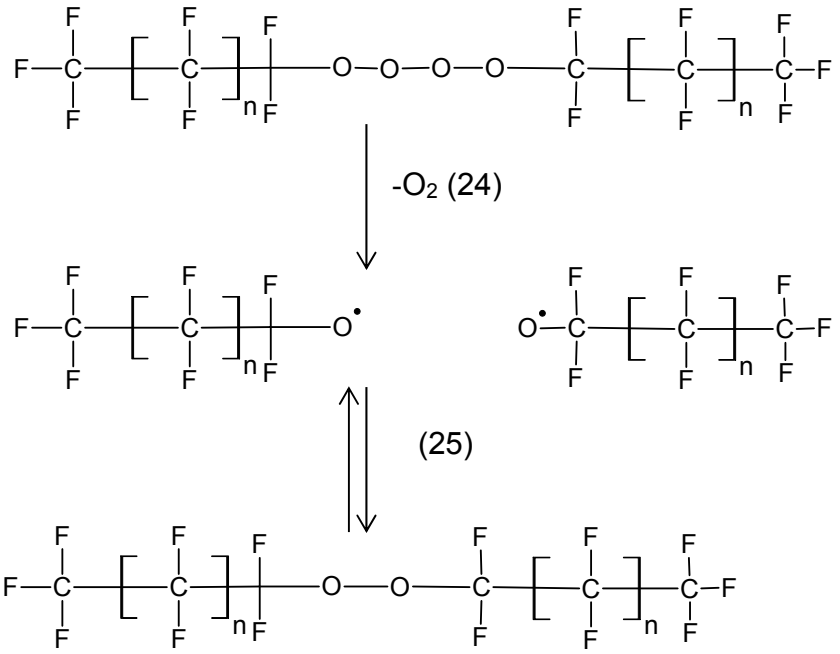

These peroxides may not be reactive towards $SO_4^{\bullet-}$ and thus, represent a sink for fluorine. Self-termination of alkoxylradicals has been observed in the chemistry of $CH_3O^{\bullet}$ albeit in low yields (< 2 %). In that case the self-termination competes with a fast rearrangement of the alkoxylradicals into hydroxymethyl radicals by a 1,2-H shift [32]. Yet, in case of perfluorinated radicals this reaction pathway is not possible and the peroxide yield might be higher. This reaction is thought to happen in the solvent cage upon elimination of oxygen. Thus, self-termination of the perfluoroalkoxyl radicals competes with their escape from the solvent cage for entering the bulk solution. The residence time of

perfluoroalkoxyl radicals in that solvent cage is expected to increase with increasing hydrophobicity (i.e., increasing C-chain length) resulting in an elevated probability of peroxide formation. This would explain the deficient fluorine mass balance especially in case of C_6-C_8-PFCAs.

In another experiment the degradation of PFOA has been determined at higher temperatures (80°C) in presence of $S_2O_8^{2-}$. Figure 3 shows that now the fluorine recovery is close to 80% (red symbols). This leads to the assumption that the organic peroxides could thermally cleave, albeit it is somewhat surprising that 10°C make such a large difference. However, for H_2O_2 the thermal rupture of the peroxide bond has also been reported to happen at ≥ 80 °C [39]. Thus, with increasing temperature equilibrium 25 might be shifted towards the perfluoroalkyloxyl radicals which are available for β-fragmentation (reaction 6) or a reaction with other substances (reaction 8 and Table 1). This explains the higher primary yields of fluoride and PFCAs. Figure 4 shows the detailed product pattern of PFOA degradation at 80°C.

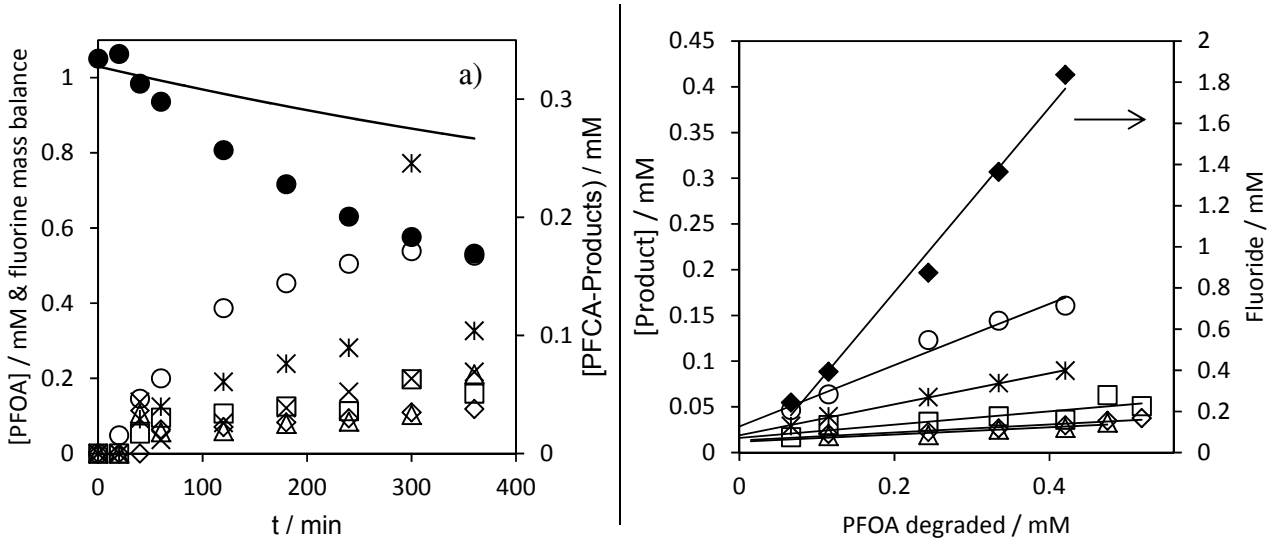

Figure 4: a) degradation of PFOA by $SO_4^{\bullet-}$ and formation of products, b) Yield of products per PFOA (C_8) degraded; thermal activation of $S_2O_8^{2-}$; line in a): fluorine balance, closed circles: PFOA (C_8), open circles: PFHpA (C_7), stars: PFHxA (C_6); crosses: PFPA (C_5), triangles: PFBA (C_4), squares: PFPrA (C_3), diamonds: TFA (C_2), closed diamonds: fluoride; $[S_2O_8^{2-}]_0$ = 2 mM, $[PFOA]_0$ = 1 mM, T= 80 °C, pH 2-4

In analogy to PFCAs with shorter carbon chains (Figure 2), PFCA-products of all chain lengths are formed in a primary reaction of PFOA plus $SO_4^{\bullet-}$. Thereby, the yield of PFCAs formed in this reaction decreases with decreasing of their C-chain length. This can be explained with a consecutive formation of perfluoroalkoxylradicals assuming that the chance of their scavenging is the same for every

perfluoroalkoxyl radical (Table 2). This implies that the chance of collision with a scavenger leading to a reaction has to be squared with every generation of perfluoroalkoxyl radicals formed, which thus becomes smaller. For example: PFHpA is the product of the first generation of oxyl radicals after termination reactions and its yield corresponds to the probability of perfluoroalkoxyl radical scavenging. Squaring this value yields the probability of PFHxA formation etc.. Based on this assumption the yield of PFCA formation was calculated revealing that PFCAs with a carbon chain length of $\leq C_5$ are formed in yields below 10% resembling experimental findings (Table 2). This further indicates that the kinetics of the perfluoroalkoxyl radical scavenging (Table 1) is independent on the chain length of the perfluoroalkoxyl radicals.

Table 2: Primary Product yields in PFOA degradation by $SO_4^{\bullet-}$; $[S_2O_8^{2-}]_0$ = 2 mM, $[PFOA]_0$ = 1 mM, T= 80 °C, pH 2-4

Product	Number of Carbons	Primary yield	Calculated primary yield
PFHpA	C_7	0.34	0.34
PFHxA	C_6	0.17	0.12
PFPeA	C_5	< 0.1	0.04
PFBA	C_4	< 0.1	0.01
PFPrA	C_3	< 0.1	0.00
TFA	C_2	< 0.1	0.00

8.4.2 Behavior of PFCAs and perfluorinated sulfonic acids

The second important group of perfluorinated compounds that is frequently detected in the environment comprises perfluorinated sulfonic acids (PFSAs). The sulfonate group has a much lower electron density than the carboxylic group, thus it can be expected that PFSAs resist the attack of $SO_4^{\bullet-}$ even more than PFCA do. For assessing the degradability of PFSAs the behavior of TFA has been compared with trifluoromethane sulfonic acid (TFMS) in UV/$S_2O_8^{2-}$, a $SO_4^{\bullet-}$ based process which is more related to water treatment than thermal activation of $S_2O_8^{2-}$. In a first step, the photochemical system has been optimized regarding the $S_2O_8^{2-}$ dose for achieving highest possible oxidation strength. Figure 5 shows the degradation of TFA in UV/$S_2O_8^{2-}$ at different concentrations of $S_2O_8^{2-}$.

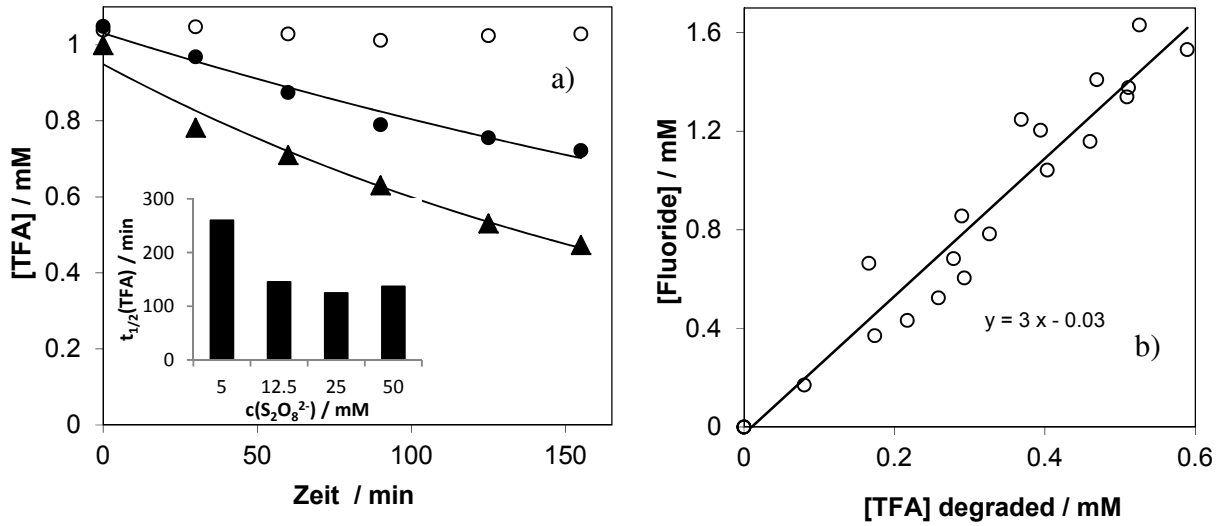

Figure 5: Degradation of TFA in UV/$S_2O_8^{2-}$at different concentrations of $S_2O_8^{2-}$; a) degradation of TFA over time; [$S_2O_8^{2-}$] = 5 mM (closed circles), 50 mM (triangles), absence of $S_2O_8^{2-}$ (open circles); inset half-life time of TFA at different concentrations of $S_2O_8^{2-}$, T = 25°C, pH = 2-3, b) fluoride formation vs. TFA degraded.

The fluorine yield in all experiments is ≈ 3 per TFA degraded, thus each radical attack yields a complete mineralization. TFA is not degraded in absence of $S_2O_8^{2-}$ during the experimental run, thus direct photolysis can be ruled out in the present system. The increase of the $S_2O_8^{2-}$ concentration results in a higher observed TFA degradation rate (Figure 5, inset) to a certain extent as a consequence of increased radical formation rate. However, this tendency reaches a plateau at a $S_2O_8^{2-}$-concentrations of 12.5 mM to 50 mM. Considering, that $S_2O_8^{2-}$ reacts by one order of magnitude faster with $SO_4^{\bullet-}$ than TFA k(TFA = 1.6×10^4 M^{-1} s^{-1} [26]; k($S_2O_8^{2-}$) = 6.3×10^5 M^{-1} s^{-1} [40]) it is remarkable that the degradation of TFA is possible in presence of 10-50 fold excess of $S_2O_8^{2-}$. In fact, comparing the pathways of $SO_4^{\bullet-}$ plus $S_2O_8^{2-}$ with $SO_4^{\bullet-}$ plus TFA reveals that > 98% of the $SO_4^{\bullet-}$ will react with $S_2O_8^{2-}$. This strongly supports the assumption of $SO_4^{\bullet-}$ being formed in the oxidation of $S_2O_8^{2-}$ (see above, note that in analogy to $^{\bullet}OH$, $SO_4^{\bullet-}$ is also capable of oxidizing $S_2O_8^{2-}$).

A $S_2O_8^{2-}$ concentration of 25 mM was chosen for comparing the behavior of TFMS with TFA (Figure 6). In accordance to the previous results TFA is mineralized during UV/$S_2O_8^{2-}$ treatment while TFMS persists both, direct UV-exposure of 300 kJ m^{-2} and $SO_4^{\bullet-}$ radical attack in the present system.

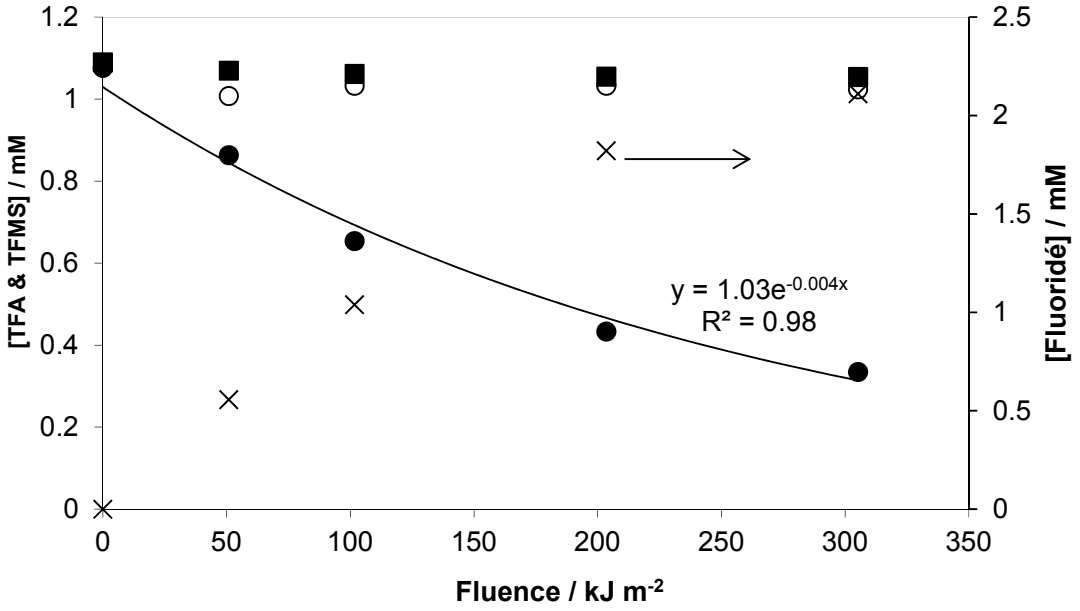

Figure 6: Degradation of TFA and TFMS in UV/$S_2O_8^{2-}$ and UV/H_2O_2; closed circles: TFA, crosses: fluoride, open circles: TFA in absence of $S_2O_8^{2-}$, squares: TFMS in presence of $S_2O_8^{2-}$, open circles: behavior of TFA in UV/H_2O_2; $[TFA]_0 = [TFMS]_0 = 1$ mM, $[S_2O_8^{2-}]_0 = 25$ mM, T = 25°C, initial pH: 3.0-3.1, pH after the reaction time (180 min): 1.7-2.0 (in presence of $S_2O_8^{2-}$), 3.0-3.1 (in absence of $S_2O_8^{2-}$); TFA and TFMS have been investigated in individual batches.

A further increase of $S_2O_8^{2-}$ concentration to 50 mM does also not lead to a significant degradation of TFMS. With these data at hand, it can be postulated that a $SO_4^{\bullet-}$ based pathway of PFSA degradation has no significance for any technical process. Figure 6 also shows, that TFA cannot be degraded by $^{\bullet}OH$ in UV/H_2O_2 (open circles).

8.4.3 Reaction kinetics

The reaction rates of $SO_4^{\bullet-}$ plus different PFCAs (C_8-C_4) (Figure 8) show that the reactivity of PFCAs is independent from their chain length since the average value is in the range of all error bars. This also applies for the reported reaction rate of trifluoroacetic acid plus $SO_4^{\bullet-}$ which hardly differs from the PFCAs under study ($k(SO_4^{\bullet-} + TFA) = 1.6 \times 10^4 \pm 0.1$ M^{-1} s^{-1} [26]). Thus, the assumption that the carboxylic acid function is the only reactive group is further supported.

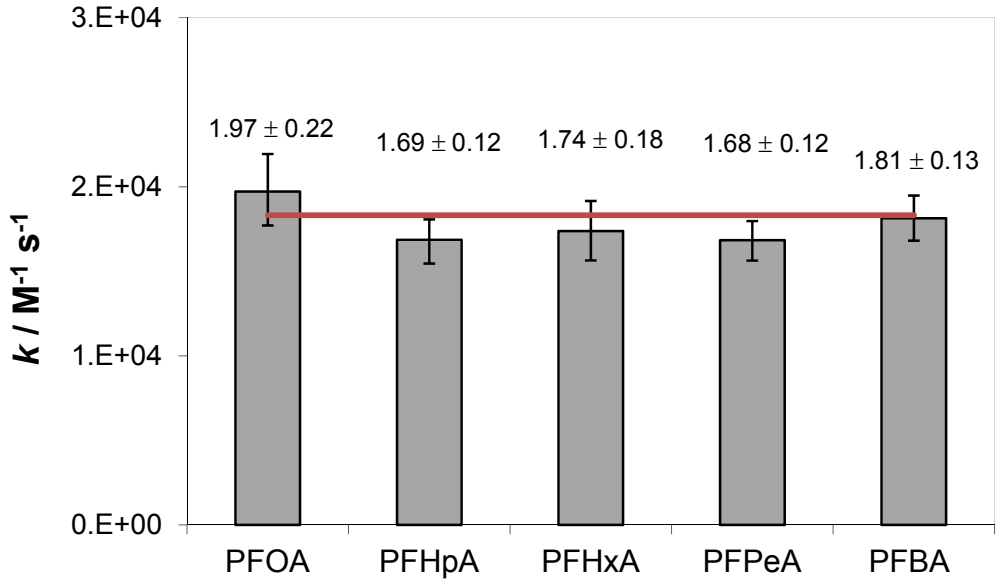

Figure 8: Second order rate constants of the reaction $SO_4^{\bullet-}$ plus PFCAs (C_8-C_4), pH 2-3, [PFCAs] = 1 mM, [$S_2O_8^{2-}$] = 10 mM, T = 70°C; error bars mark the standard deviation derived from the linear regression of the corresponding competition plot (an example of such kind of plot can be found in chapter 3, Figure 3) (α = 0.05). The number of points in the corresponding competition plot has been as follows: PFOA: 54, PFHpA, PFHxA and PFBA: 9 and PFPeA: 27; the line marks the average rate constant

While the number of perfluorinated carbons does not affect the rate constant the degree of halogenation and the type of halogens attached to the carbon chain greatly affects the rate constants (Table 3).

Table 3: Reaction rate constants of $SO_4^{\bullet-}$ and $^{\bullet}OH$ plus acetate and halogenated acetate

Number of halogens attached to acetate	$k(SO_4^{\bullet-})$ / M^{-1} s^{-1}	Reference	$k(^{\bullet}OH)$/ M^{-1} s^{-1}	Reference
0	4.3×10^6	[41]	7.5×10^7	[26]
1 F	$3.4 \pm 0.2 \times 10^6$	[26]	1.2×10^8	
2 F	$8.7 \pm 0.1 \times 10^4$		1.1×10^7	
3 F	$1.6 \pm 0.1 \times 10^4$		$< 1 \times 10^6$	
1 Cl	$4.5 \pm 0.2 \times 10^6$		8.3×10^7	
2 Cl	$2.1 \pm 0.1 \times 10^6$		1×10^8	
3 Cl	2×10^6		6×10^7	

In case of $SO_4^{\bullet-}$ the kinetic data displays a sharp drop in the reaction rate from monofluoro to difluoro acetate by 40 times, whereas di- and trifluoro acetate react within one order of magnitude (i.e., 10^4 M^{-1} s^{-1}). This is in accordance to the observation that the reaction kinetics do not significantly differ between TFA and other perfluorinated acids in spite the number of fluorines attached at the α-carbon is different (TFA: 3 fluorines, PFCAs with larger chain length: 2 fluorines). In case of $^{\bullet}OH$ the reaction rate drastically falls off to inertness in case of perfluorination, whereas the single and double fluorinated derivatives are still moderately reactive towards $^{\bullet}OH$. The lack of any hydrogen disables H-abstraction, thus, the $^{\bullet}OH$ is forced to electron transfer which is hampered by the fluorine driven deactivation of the carboxylic group. Conversely, perchlorinated acetate may still allow electron transfer at the carboxylic group due to the weaker deactivation by the chlorinated alkyl group. The rate upper limit determined for the constant of $k(^{\bullet}OH + TFA < 10^6\ M^{-1}\ s^{-1})$ is two orders of magnitude higher than the kinetics of the reaction $SO_4^{\bullet-}$ plus TFA ($k = 1.6 \times 10^4\ M^{-1}\ s^{-1}$). Thus it would principally be conceivable that $^{\bullet}OH$ react faster with TFA than $SO_4^{\bullet-}$ does. Yet, as shown in above (Figure 6) TFA persists in $^{\bullet}OH$ based systems, whereas it is degraded in presence of $SO_4^{\bullet-}$.

8.4.4 Degradation of perfluorinated compounds in water treatment

The present study has shown that PFCAs can be oxidized by $SO_4^{\bullet-}$, which is not possible in $^{\bullet}OH$ based reactions and that, depending on the boundary conditions (i.e., temperature, HSO_4^- or $S_2O_8^{2-}$) the degradation of PFCAs is prone to an unzipping reaction converting more than one CF_2 unit to CO_2 and F^- per radical attack. However the reaction rate constants of $SO_4^{\bullet-}$ plus PFCAs are very slow ($1\text{-}2 \times 10^4$ M^{-1} s^{-1}) compared to typical reaction rates with other substrates (i.e., $10^7 - 10^8$ M^{-1} s^{-1}). Thus, extremely high oxidant exposures have to be built up to achieve a degradation of PFCAs by $SO_4^{\bullet-}$ (Figure 7, kinetic data taken from [17, 26, 42]).

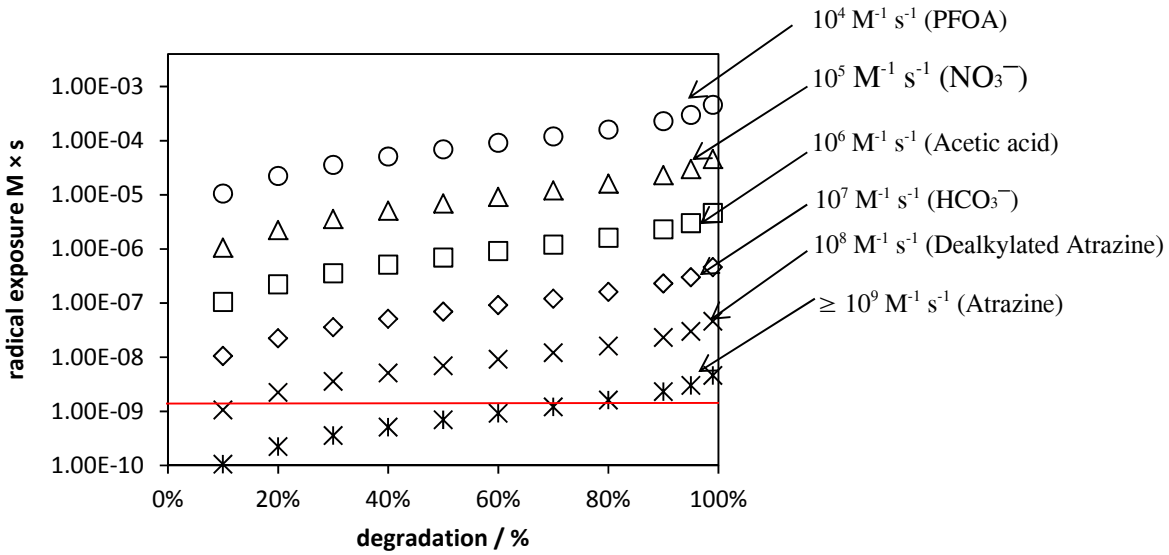

Figure 7: Radical exposures necessary for the degradation of compounds calculated on the basis of second order rate constants; the red line corresponds to the $SO_4^{\bullet-}$ exposure which can be achieved in River Ruhr water in UV/$S_2O_8^{2-}$ applying ≈ 2 kWh m^{-3} and 0.5 mM $S_2O_8^{2-}$

As will be shown below tremendous amounts of energy are required to achieve such exposures.

River Ruhr water represents a typical water which is used for drinking water production. In prior experiments this water has been used for simulating realistic conditions in UV/$S_2O_8^{2-}$ and UV/H_2O_2 (Chapter 6). The steady state concentration of $SO_4^{\bullet-}$ which can typically be achieved during UV/$S_2O_8^{2-}$ in River Ruhr water is ≈ 1×10^{-12} M ([DOC] = 1.9 mg L^{-1}, [HCO_3^-] = 1.6 mM, [$S_2O_8^{2-}$] = 0.5 mM, [Cl^-] = 0.8 mM, pH 7.2, fluence rate 50 µEinstein m^{-2} s^{-1} (254 nm) (note that the this $S_2O_8^{2-}$ dose is optimal with regard to degradation efficiency for atrazine (chapter 6)). In dividing the oxidant exposure required for 10 % degradation of PFOA (i.e., 1×10^{-5} M × s (Figure 7) with the steady state concentration of $SO_4^{\bullet-}$ the time required to build up this exposure can be calculated. Multiplying this time span with the fluence rate gives the corresponding fluence (Equation 1).

Equation (1) $$\frac{\int [SO_4^{\bullet -}]dt}{[SO_4^{\bullet -}]_{steady\ state}} \times E_\lambda = Fluence$$

$\int [SO_4^{\bullet -}]dt$ = Sulfate radical exposure / M × s

$[SO_4^{\bullet -}]_{steady\ state}$ = Sulfate radical steady state concentration / M

E_λ = Fluence rate / Einstein m^{-2} s^{-1}

$Fluence$ = Einstein m^{-2}

With 1 Einstein of photons at 254 nm corresponding to 471 kJ (equation 2) the fluency can be expressed as J m^{-2} s^{-1}.

Equation (2) $$E(photone) = \frac{h \times c}{\lambda} \times N_A$$

$E(photone)$ = Energy of photons / J $Einstein^{-1}$

h = Planck constant / 6.626×10^{-34} J × s

λ = Wave length / m N_A = Avogadro constant / 6.022×10^{-23} mol^{-1}

c = Speed of light/ 2.99792458×10^8 m s^{-1}

Now, the fluency can be converted into energy demand according to Katsoyiannis et al. [43] (Equation 3).

Equation (3) $$ER_{lamp} = \frac{H_\lambda^{'}(10\%)}{l^{avg} \times \eta_{UV}} \times \frac{\text{kWh}}{3.6 \times 10^6 \text{J}}$$

ER_{lamp} = lamp specific energy consumption / kWh m^{-3}

l^{avg} = average path length / m

η_{UV} = Efficiency factor of the radiation source (0.3)

$H_\lambda^{'}$ = Fluence required for 10% degradation of a pollutant

With the present data at hand the required energy for 10% degradation of PFOA is calculated to be 4.6×10^3 kWh m^{-3} (10 cm optical path-length). This is a vast amount of energy and beyond any economic justification (note that the energy demand for 90 % degradation of atrazine in UV/$S_2O_8^{2-}$, UV/H_2O_2 and ozonation in River Ruhr water is < 2 kWh m^{-3} (Chapter 7). It has to be mentioned, that in the above calculations DOC, alkalinity and Cl^- are considered as scavengers for $SO_4^{\bullet -}$. However, nearly all water constituents will compete for $SO_4^{\bullet -}$ against PFCAs and even further decrease the radical exposure

available for PFCAs degradation. In other words, the whole water matrix has to experience $SO_4^{\bullet-}$ radical attack until a surplus of oxidation strength is achieved which eventually leads to a degradation of PFCAs. However, the chemistry which will be initiated in such a situation involves the formation of numerous other reactive agents (e.g., $NO_3^{\bullet}$) with uncertain consequences.

It has to be noted that the electrical energy demand for operating a UV-radiation source can be reduced by increasing the dosage of $S_2O_8^{2-}$. However, even if very high doses of $S_2O_8^{2-}$ are applied, degradation of TFA still requires a very high energy demand as will be described below. Figure 5 illustrated that at a $S_2O_8^{2-}$ dose of 25 mM reveals the highest possible degradation rates of TFA at the present experimental setup. Thereby, the fluence required for 10 % degradation of TFA has been calculated to be 510 kJ m^{-2} s^{-1}. Applying equation 3 the energy demand corresponding to that fluence can be calculated arriving at 47 kWh m^{-3} (assuming a path-length of 10 cm). This energy demand largely exceeds the energy demand in typically applied oxidation options (i.e., ozonation and UV/H_2O_2). Furthermore, such high doses of $S_2O_8^{2-}$ are hardly applicable in water treatment and other matrix constituents (i.e., DOC, Cl^-, HCO_3^-) will further decrease the energy efficiency.

One might now be apt for using the reaction of transition metals (e.g., Fe^{2+}) plus $S_2O_8^{2-}$ as a source for $SO_4^{\bullet-}$, since this reaction does not require a high electrical energy supply. However, in this system the degradation of PFCAs is hampered by the fast reaction of $SO_4^{\bullet-}$ plus Fe^{2+} ($k = 9.9 \times 10^8$ M^{-1} s^{-1} [17]) and it is doubtful if the degradation of PFCAs occurs under such conditions.

Water which is heated up in an industrial process, however, may provide a basis for thermolysis of $S_2O_8^{2-}$ without the necessity of applying extra energy and might allow the degradation of PFCAs as will be explained in the following. The small reaction rate of $SO_4^{\bullet-}$ plus PFCAs suggests a high activation energy and so, the increase of PFCA reaction rates with temperature might be more pronounced than the competing reactions with other solutes and PFCA degradation kinetics might “catch up” the kinetics of competing side reactions.

The present study has shown, that $SO_4^{\bullet-}$ in principle are able to degrade PFCAs. However, the $SO_4^{\bullet-}$ based processes which could be applied require large amounts of energy for degradation of PFCAs. Furthermore, PFSAs cannot be degraded in these processes. Keeping in mind, that other treatment

options currently used to remove both classes of compounds from water (i.e., activated carbon filtration, nano filtration and reverse osmosis) with a much lower energy demand, $SO_4^{\bullet-}$ based processes seem not

to be a feasible alternative (note that perfluorinated surfactants with small carbon chains (< C_4) might not be readily removed by activated carbon filtration but surely by nano filtration or reverse osmosis).

8.5 Literature

1. US-EPA, *Provisional Health Advisories for Perfluorooctanoic Acid (PFOA) and Perfluorooctane Sulfonate (PFOS).* US Environmental Protection Agency, 2009.
2. UBA, *Vorläufige Bewertung von Perfluorierten Tensiden (PFT) im Trinkwasser am Beispiel ihrer Leitsubstanzen Perfluoroctansäure (PFOA) und Perfluoroctansulfonsäure (PFOS), Stellungnahme der Trinkwasserkommission des Bundesministeriums für Gesundheit (BMG) bei Umweltbundesamt vom 21.06.06, überarbeitet am 13.07.06.* 2006.
3. Fujii, S., C. Polprasert, S. Tanaka, N.P.H. Lien, and Y. Qiu, *New POPs in the water environment: Distribution, bioaccumulation and treatment of perfluorinated compounds - A review paper.* Journal of Water Supply: Research and Technology - AQUA, 2007. **56**(5): p. 313-326.
4. Tang, C.Y., Q.S. Fu, A.P. Robertson, C.S. Criddle, and J.O. Leckie, *Use of reverse osmosis membranes to remove perfluorooctane sulfonate (PFOS) from semiconductor wastewater.* Environmental Science and Technology, 2006. **40**(23): p. 7343-7349.
5. Luvarà, G., S. Pickering, I. van der Putte, M. Murín, M.A.J. van Velthoven, and F. Affourtit, *Risk evaluation industrial use of PFOA and PFOS* Report of the RPS Group (Delft, Netherlands), 2010.
6. Boulanger, B., J. Vargo, J.L. Schnoor, and K.C. Hornbuckle, *Detection of perfluorooctane surfactants in Great Lakes water.* Environmental Science and Technology, 2004. **38**(15): p. 4064-4070.
7. De Silva, A.O. and S.A. Mabury, *Isolating isomers of perfluorocarboxylates in polar bears (Ursus maritimus) from two geographical locations.* Environmental Science and Technology, 2004. **38**(24): p. 6538-6545.
8. Ellis, D.A., J.W. Martin, A.O. De Silva, S.A. Mabury, M.D. Hurley, M.P. Sulbaek Andersen, and T.J. Wallington, *Degradation of fluorotelomer alcohols: A likely atmospheric source of perfluorinated carboxylic acids.* Environmental Science and Technology, 2004. **38**(12): p. 3316-3321.
9. Giesy, J.P. and K. Kannan, *Global distribution of perfluorooctane sulfonate in wildlife.* Environmental Science and Technology, 2001. **35**(7): p. 1339-1342.
10. Lange, F.T., C.K. Schmidt, and H.J. Brauch, *Perfluorinated surfactants: The Perfluoroctanesulfonate (PFOS) substitude perfluorobutanesulfonate (PFBS) increasingly affects the raw water quality of rhine waterworks.* Perfluorierte Tenside: Der PFOS (Perfluoroctansulfonat) - Ersatzstoff PFBS (Perfluorbutansulfonat) beeinflusst zunehmend die Rohwasser-qualität von Rheinwasserwerken, 2007. **148**(7-8): p. 510-516.
11. McLachlan, M.S., K.E. Holmstrom, M. Reth, and U. Berger, *Riverine discharge of perfluorinated carboxylates from the European continent.* Environmental Science and Technology, 2007. **41**(21): p. 7260-7265.
12. Moriwaki, H., Y. Takata, and R. Arakawa, *Concentrations of perfluorooctane sulfonate (PFOS) and perfluorooctanoic acid (PFOA) in vacuum cleaner dust collected in Japanese homes.* Journal of Environmental Monitoring, 2003. **5**(5): p. 753-757.
13. Rayne, S. and K. Forest, *Perfluoroalkyl sulfonic and carboxylic acids: A critical review of physicochemical properties, levels and patterns in waters and wastewaters, and treatment methods.* Journal of Environmental Science and Health - Part A Toxic/Hazardous Substances and Environmental Engineering, 2009. **44**(12): p. 1145-1199.
14. Young, C.J., V.I. Furdui, J. Franklin, R.M. Koerner, D.C.G. Muir, and S.A. Mabury, *Perfluorinated acids in arctic snow: New evidence for atmospheric formation.* Environmental Science and Technology, 2007. **41**(10): p. 3455-3461.

15. Rumsby, P.C., C.L. McLaughlin, and T. Hall, *Perfluorooctane sulphonate and perfluorooctanoic acid in drinking and environmental waters.* Philosophical Transactions of the Royal Society A: Mathematical, Physical and Engineering Sciences, 2009. **367**(1904): p. 4119-4136.
16. Schröder, H.F. and R.J.W. Meesters, *Stability of fluorinated surfactants in advanced oxidation processes - A follow up of degradation products using flow injection-mass spectrometry, liquid chromatography-mass spectrometry and liquid chromatography-multiple stage mass spectrometry.* Journal of Chromatography A, 2005. **1082**(1 SPEC. ISS.): p. 110-119.
17. Neta, P., R.E. Huie, and A.B. Ross, *Rate constants for reactions of inorganic radicals in aqueous solution.* Journal of Physical and Chemical Reference Data, 1988. **17**(3): p. 1027 - 1040.
18. Wardman, P., *Reduction potentials of one-electron couples involving free-radicals in aqueous-solution*. Vol. 18 1989. 1637-1755.
19. Liang, C. and C.J. Bruell, *Thermally activated persulfate oxidation of trichloroethylene: Experimental investigation of reaction orders.* Industrial and Engineering Chemistry Research, 2008. **47**(9): p. 2912-2918.
20. Johnson, R.L., P.G. Tratnyek, and R.O. Johnson, *Persulfate persistence under thermal activation conditions.* Environmental Science and Technology, 2008. **42**(24): p. 9350-9356.
21. Hori, H., E. Hayakawa, H. Einaga, S. Kutsuna, K. Koike, T. Ibusuki, H. Kiatagawa, and R. Arakawa, *Decomposition of environmentally persistent perfluorooctanoic acid in water by photochemical approaches.* Environmental Science and Technology, 2004. **38**(22): p. 6118-6124.
22. Hori, H., Y. Nagaoka, M. Murayama, and S. Kutsuna, *Efficient decomposition of perfluorocarboxylic acids and alternative fluorochemical surfactants in hot water.* Environmental Science and Technology, 2008. **42**(19): p. 7438-7443.
23. Hori, H., A. Yamamoto, E. Hayakawa, S. Taniyasu, N. Yamashita, S. Kutsuna, H. Kiatagawa, and R. Arakawa, *Efficient decomposition of environmentally persistent perfluorocarboxylic acids by use of persulfate as a photochemical oxidant.* Environmental Science and Technology, 2005. **39**(7): p. 2383-2388.
24. Hori, H., A. Yamamoto, and S. Kutsuna, *Efficient photochemical decomposition of long-chain perfluorocarboxylic acids by means of an aqueous/liquid CO_2 biphasic system.* Environmental Science and Technology, 2005. **39**(19): p. 7692-7697.
25. Kutsuna, S. and H. Hori, *Rate constants for aqueous-phase reactions of SO_4^- with $C_2F_5C(O)O^-$ and $C_3F_7C(O)O^-$ at 298 K.* International Journal of Chemical Kinetics, 2007. **39**(5): p. 276-288.
26. Maruthamuthu, P., S. Padmaja, and R.E. Huie, *Rate Constants for Some Reactions of Free Radicals with Haloacetates in Aqueous Solution.* International Journal of Chemical Kinetics, 1995. **27**: p. 605-612.
27. Yu, X.Y., Z.C. Bao, and J.R. Barker, *free radical reactions involving Cl, Cl_2^-, and SO_4^- in the 248 nm photolysis of aqueous solutions containing $S_2O_8^{2-}$ and Cl.* Journal of Physical Chemistry A, 2004. **108**(2): p. 295-308.
28. NIST. *National institut of standards and technology - data base of reaction rate constants*. [cited 2013]; Available from: http://kinetics.nist.gov/solution/SearchForm.
29. Erben-Russ, M., C. Michel, W. Bors, and M. Saran, *Absolute rate constants of alkoxyl radical reactions in aqueous solution.* Journal of Physical Chemistry, 1987. **91**(9): p. 2362-2365.
30. Gilbert, B.C., P.D.R. Marshall, R.O.C. Norman, N. Pineda, and P.S. Williams, *Electron spin resonance studies. Part 61. The generation and reactions of the t-butoxyl radical in aqueous solution.* Journal of the Chemical Society, Perkin Transactions 2, 1981(10): p. 1392-1400.
31. Mertens, R., C. Von Sonntag, J. Lind, and G. Merenyi, *A kinetic study of the hydrolysis of phosgene in aqueous solution by pulse radiolysis.* Angewandte Chemie (International Edition in English), 1994. **33**(12): p. 1259-1261.

32. Von Sonntag, C., H.P. Schuchmann, and Z.B. Alfassi, eds. *Peroxyl radicals in aqueous solutions*. 1997, John Wiley & Sons.
33. Naumov, S., *unpublished study* 2011.
34. Buxton, G.V., C.L. Greenstock, W.P. Helman, and A.B. Ross, *Critical review of rate constants for reactions of hydrated electrones, hydrogen-atoms and hydroxyl radicals (•OH/O•-) in aqueous solution.* Journal of Physical and Chemical Reference Data, 1988. **17**(2): p. 513-886.
35. Buxton, G.V., G.A. Salmon, and N.D. Wood, *A pulse-radiolysis study of the chemistry of oxysulfur radicals in aqueous-solution*. Physico-chemical behaviour of atmospheric pollutants, ed. G. Restelli and G. Angeletti. Vol. 23. 1990. 245-250.
36. Mackay, D., W.Y. Shiu, K.-C. Ma, and S.C. Lee, eds. *Handbook of physical-chemical properties and environmental fate for organic chemicals*. 2 ed. 2006.
37. House, D.A., *Kinetics and mechanism of oxidations by peroxydisulfate.* Chemical Reviews, 1962. **62**: p. 185-203.
38. Mark, G., M.N. Schuchmann, H.P. Schuchmann, and C. von Sonntag, *The photolysis of potassium peroxodisulphate in aqueous solution in the presence of tert-butanol: a simple actinometer for 254 nm radiation.* Journal of Photochemistry and Photobiology A, 1990. **55**(2): p. 157-168.
39. von Sonntag, C., *Free-radical-induced DNA damage and its repair- A chemical perpesctive.* Springer Verlag Berlin Heidelberg, ISBN: 3-540-26120-6, 2005.
40. Herrmann, H., A. Reese, and R. Zellner, *Time-resolved UV/VIS diode array radical anions in aqueous solution absorption spectroscopy of SOx -(x=3, 4, 5).* Journal of Molecular Structure, 1995. **348**: p. 183-186.
41. Huie, R.E. and C.L. Clifton, *Temperature dependence of the rate constants for reactions of the sulfate radical, SO_4^-, with anions.* Journal of Physical Chemistry, 1990. **94**(23): p. 8561-8567.
42. Manoj, P., K.P. Prasanthkumar, V.M. Manoj, U.K. Aravind, T.K. Manojkumar, and C.T. Aravindakumar, *Oxidation of substituted triazines by sulfate radical anion ($SO_4^{\bullet-}$) in aqueous medium: A laser flash photolysis and steady state radiolysis study.* Journal of Physical Organic Chemistry, 2007. **20**(2): p. 122-129.
43. Katsoyiannis, I.A., S. Canonica, and U. von Gunten, *Efficiency and energy requirements for the transformation of organic micropollutants by ozone, O_3/H_2O_2 and UV/H_2O_2.* Water Research, 2011. **45**(13): p. 3811-3822.

Chapter 9

-

Concluding remarks & future perspectives

The present study has shown that $SO_4^{\bullet-}$ principally can be used for degradation of pollutants in water treatment. Thereby, the high affinity of $SO_4^{\bullet-}$ to electron transfer enables the degradation of compounds which do not react with $^{\bullet}OH$. Beside the often cited perfluorinated carboxylic acids (PFCAs) also chlorotriazine diamine, a secondary product arising in the degradation of atrazine by $^{\bullet}OH$ and $SO_4^{\bullet-}$, can be oxidized by $SO_4^{\bullet-}$, while both compounds are refractory against $^{\bullet}OH$. This might also apply to other pollutants which do not provide molecular moieties for $^{\bullet}OH$ radical attack. As UV/H_2O_2, UV/$S_2O_8^{2-}$ has no significant tendency to form BrO_3^- in presence of Br^- and natural organic matter. Thus, both processes can be used for purification of source waters containing Br^- in concentrations which would prevent the use of ozonation and ozone based processes due to massive BrO_3^- formation. Furthermore, UV/$S_2O_8^{2-}$ principally has some further advantages over UV/H_2O_2.

1. $S_2O_8^{2-}$ reveals a higher molar absorption (22 M^{-1} cm^{-1}) and quantum yield (1.4 mol $Einstein^{-1}$) than H_2O_2 (molar absorption = 18.6, quantum yield = 1 mol $Einstein^{-1}$) at 254 nm. This results in a higher primary radical formation rate in the photolysis of $S_2O_8^{2-}$ by a factor of 1.6 in case Hg-low pressure lamps are used as radiation source emitting nearly exclusively radiation at 254 nm.
2. The $SO_4^{\bullet-}$ formed react slower with natural organic matter than $^{\bullet}OH$ (factor 2-3), resulting in a weaker scavenging.

As shown in experiments in presence of organic matter both factors can lead to a considerably higher efficiency of pollutant degradation in UV/$S_2O_8^{2-}$ compared with UV/H_2O_2, in case pollutants reveal similar reaction rates with both radicals.

However, Cl^- has far-reaching influences on the reaction system, by converting $SO_4^{\bullet-}$ into $^{\bullet}OH$. This reaction overwhelms the other often cited pathways of $^{\bullet}OH$ formation by $SO_4^{\bullet-}$, i.e., their reaction with OH^- and H_2O. The conversion of $SO_4^{\bullet-}$ into $^{\bullet}OH$, however, can cancel the advantage of the low reaction rate of $SO_4^{\bullet-}$ plus NOM mentioned above. In addition, if HCO_3^- is present, intermediates in the conversion of $SO_4^{\bullet-}$ to $^{\bullet}OH$ ($Cl^{\bullet}$ and $Cl_2^{\bullet-}$) are scavenged in their reaction with HCO_3^-. Hence, with increasing Cl^- and HCO_3^- concentration also the photochemical advantages of $S_2O_8^{2-}$ (higher quantum yield and absorption coefficient compared with H_2O_2) are counterbalanced by shifting the oxidation strength into alkalinity. In fact for a water such as River Ruhr water used in the present study as a model water, both oxidation systems UV/$S_2O_8^{2-}$and UV/H_2O_2 are very similar in their efficiency of pollutant degradation.

Thus, the decision if UV/$S_2O_8^{2-}$ might be preferred over UV/H_2O_2 largely depends on the concentration of dissolved organic matter, Cl^- and HCO_3^- (note that also other aspects have to be considered such as influence of $S_2O_8^{2-}$, SO_4^{2-} or H_2O_2 on subsequent treatment steps). Thereby, the kinetic models

developed in the present study are a useful tool for estimating which major reactive species are present in the reaction system ($^{\bullet}OH$ and/or $SO_4^{\bullet-}$) and how efficient pollutants are degraded in UV/$S_2O_8^{2-}$ compared with UV/H_2O_2.

The reaction of Cl^- plus $SO_4^{\bullet-}$ hampers the degradation of compounds which are refractory against $^{\bullet}OH$. In that regard PFCAs have to be addressed. The degradation of PFCAs by $SO_4^{\bullet-}$ as a potential water treatment option is frequently reported in the literature. However, the reaction rate of $SO_4^{\bullet-}$ plus PFCA is very slow ($\approx 10^4$ M^{-1} s^{-1}). Although at special conditions of water treatment only few radical attacks are sufficient for mineralization of PFCAs, extremely high energy has to be applied for their degradation. In the model water used in the present study (River Ruhr water) the energy demand for UV/$S_2O_8^{2-}$ has been calculated to be within the order of magnitude of 10^3 kWh m^{-3} for 10% degradation of PFOA. This amount of energy by far exceeds that required in alternative processes such as nano-filtration or activated carbon filtration. Note that the energy demand will decrease with the amount of $S_2O_8^{2-}$ added arriving at 47 kWh m^{-3} at 50 mM $S_2O_8^{2-}$ in pure water. However, the high $S_2O_8^{2-}$ dose will result in large $S_2O_8^{2-}$ and SO_4^{2-} concentrations which require additional treatment steps for their removal. Thermal cleavage of the peroxide bond in $S_2O_8^{2-}$, which is possible even at moderate temperatures (i.e., > 40 °C), reveals a certain potential for degradation of PFCAs, though. This becomes in particular apparent in case water is heated up in an industrial process. The excess heat of this water might be used for generation of $SO_4^{\bullet-}$ which could contribute in degrading PFCAs to a certain extent. However, the other large class of perfluorinated chemicals, perfluorinated sulfonic acids, are not degraded by $SO_4^{\bullet-}$.

The information of the present work helps to understand a potential $SO_4^{\bullet-}$ based water treatment option (i.e., UV/$S_2O_8^{2-}$), revealing that the applicability of UV/$S_2O_8^{2-}$ largely depends on the water quality. However, numerous aspects still need further investigation.

While numerous reaction rate constants of the degradation of pollutants by ozone and $^{\bullet}OH$ are available, corresponding reaction rates of $SO_4^{\bullet-}$ are largely lacking. Further studying the reaction kinetics of $SO_4^{\bullet-}$ helps to compare its potential of pollutant control in comparison with $^{\bullet}OH$. The interaction of $SO_4^{\bullet-}$ with Cl^- largely complicates the reaction system by formation of reactive chlorine species such as $Cl^{\bullet}$ and $Cl_2^{\bullet-}$. However reaction rates of these species for reactions related to water treatment are largely lacking such as their reaction rate plus DOC and pollutants (in case of $Cl_2^{\bullet-}$ also the kinetics of its reaction with HCO_3^- and CO_3^{2-} is missing). These data could complete the current

model of the present study for describing pollutant degradation in UV/$S_2O_8^{2-}$ and improve the model calculations for low levels of Cl^-.

Also the reaction of PFCAs plus $SO_4^{\bullet-}$ leaves some gaps. The proposed formation of perfluorinated peroxides could be clarified by their determination and identification e.g., by LC-MS and NMR measurements. Isolation of these compounds would further allow determining some other chemical features such as molar absorption, quantum yields and thermal stability of the peroxide bond. Furthermore, the proposed reaction of perfluorinated alkoxyl radicals plus SO_4^{2-} and $S_2O_8^{2-}$ could be evidenced by investigating if the primary PFCAs and fluoride yields depend on the SO_4^{2-} and $S_2O_8^{2-}$ concentration. A feasibility study on thermal activation of persulfate for degradation of PFCAs in water treatment should be performed. Especially in case of industrial applications where surplus heat is available thermal cleavage of the peroxide bond might be applicable. Additionally, the $SO_4^{\bullet-}$ based degradation of other fluorinated compounds such as fluoro telomeres should be addressed in future work.

Furthermore, there is a certain potential of retrofitting low-tech water treatment options using heat and UV radiation from solar radiation with a $SO_4^{\bullet-}$ based process by addition of $S_2O_8^{2-}$ (e.g., the SODIS project).

One important point is the usage of $S_2O_8^{2-}$ in remediation of contaminated soils and aquifers. The present study has shown that a sufficient concentration of $S_2O_8^{2-}$ lead to substantial acidification in the long term, which may adversely affect the quality of ground water e.g., by mobilization of metals, formation of chlorate and halogenated organic compounds due to the increased steady state concentration of $Cl^{\bullet}$. However, these effects largely depend on the buffer capacity of the contaminated site, which can counter balance acidification. This topic is of particular interest since the tendency of using $S_2O_8^{2-}$ as an oxidizing agent in ground water remediation is currently growing.

Supplement

--

List of abbreviations

List of abbreviations in alphabetic order; Greek follows Latin

AC	Activated carbon
AOP	Advanced Oxidation Processes
A_{λ}	Absorbance at wavelength λ
BDE	Bond dissociation energy
Br^-	Bromide
$Br_2^{\bullet-}$	Dibromine radical
BrO_3^-	Bromate
c	Speed of light
$(CH_3)_2O$	Acetone
$(CH_3)_3CO^{\bullet}$	*tert*-butoxyl radical
$^{\bullet}CH_3$	Methyl radical
$C^{\bullet}R$	Carbon centered radical
$CF_3(CF_2)_n^{\bullet}$	Perfluorinated carbon centered radical
$CF_3(CF_2)_nCF_2\text{-}O^{\bullet}$	Perfluorinated alkoxyl radical
$CF_3(CF_2)_nCF_2\text{-}OH$	Perfluoroalcohol
Cl^-	Chloride
$Cl^{\bullet}$	Chlorine atom
Cl_2	Chlorine
$Cl_2^{\bullet-}$	Dichlorine radical
$ClO^{\bullet}$	Hypochloride radical
ClO_2^-	Chlorite
$ClO_2^{\bullet}$	Chlorine dioxide
ClO_3^-	Chlorate
CN^-	Cyanide
CO_2	Carbon dioxide
$CO_3^{\bullet-}$	Carbonate radical
CO_3^{2-}	Carbonate
COF_2	Carbonyl fluoride
CRISTAL	Combined Reactors Integration a Separation by membranes and Treatment by Adsorption in Liquid
DAD	Dioden-array detector

List of abbreviations in alphabetic order; Greek follows Latin - continued

DEA	Desethyl-atrazine
DEDIA	Desethyl-desisopropyl-atrazine
DET	Desethyl-terbuthylazine
DIA	Desisopropyl-atrazine
DOC	Dissolved organic carbon
DOM	Dissolved organic matter
E_{λ}	Fluence rate
E_{λ}^{avr}	Fluence rate in presence of DOM/NOM
E(photone)	Energy of a photone
ELA	Experimental lakes area
ER_{lamp}	Lamp specific energy consumption
ethyl-imine	Imine at the ethyl group (atrazine)
E_{λ}	Internal fluence rate
E_{λ}^{avg}	Fluence rate in presence of NOM
$E_{\lambda}^{´}$	Fluence required for 10% degradation of a pollutant
F^{-}	Fluoride
Fe^{2+}	Iron(II)
GAC	Granular activated carbon
h	Planck constant
$H_2ClO^{\bullet}$	Chlorine atom complexed by water
H_2O	Water
H_2PO^{4-}	Dihydrogen phosphate
HCN	Hydrogen cyanide
HCO_3^{-}	Bicarbonate
HF	Hydrofluoric acid
HO_2^{-}	Hydrogen peroxide anion
$HO_2^{\bullet}$	Perhydroxyl radical
$HOBr/OBr^{-}$	Hypobromous acid / Hypobromide
HOCl	Hypochloric acid
$HPO_4^{\bullet-}$	Hydrogen phosphate radical
HPO_4^{2-}	Hydrogen phosphate
HSO_4^{-}	Bisulfate
HSO_5^{-}	Caro´s acid, peroxymonosulfuric acid
isopropyl-imine	Imine at the isopropyl group of atrazine
k(photolysis of atrazine)	Rate of atrazine photolysis
k´(atrazine)	First order degradation rate of atrazine
k^{+}(radical)	Radical formation rate
k_{obs}	First order degradation rate

List of abbreviations in alphabetic order; Greek follows Latin - continued

l^{avg}	Average path length
MF	Microfiltration
N_A	Avogadro constant

List of abbreviations in alphabetic order; Greek follows Latin - continued

NF	Nanofiltration
NO_3^-	Nitrate
$NO_3^\bullet$	Nitrate radical
NOM	Natural organic matter
O_2^-	Superoxide
O_2	Oxygen
O_3	Ozone
OCl^-	Hypochloride
$^\bullet OH$	Hydroxyl radikal
P	Pollutant
PAC	Powered activated carbon
pCBA	4-chlorobenzoic acid
[peroxide]	Concentration of H_2O_2 or $S_2O_8^{2-}$
PFBA	Perfluorobutyric acid
PFC	Perfluorinated compound
PFCA	Perfluorinated carboxylic acids
PFHpA	Perfluoroheptanoic acid
PFOA	Perfluorooctane carboxylic acid
PFOS	Perfluorooctane sulfonic acid
PFPeA	Perfluoropentanoic acid
PFPrA	Pentafluoropropionic acid
PFSA	Perfluorosulfonic acid
pNBA	4-Nitrobenzoic acid
$\int$[radical]dt	Radical exposure
$[radical]_{steady\ state}$	Radical steady state concentration
RO	Reverse osmosis
σ	Hammett constants
$S_2O_3^{2-}$	Thiosulfate
$S_2O_8^{2-}$	Peroxodisulfate
$SO_4^{\bullet-}$	Sulfate radical
$\int[SO_4^{\bullet-}]dt$	Sulfate radical exposure
$[SO_4^{\bullet-}]_{staedy\ state}$	Sulfate radical steady state concentration
SO_4^{2-}	Sulfate
S_λ	Morrowitz correction coefficient
t	Time
TFA	Trifluoroacetic acid
TFMS	Trifluoromethane sulfonic acid
TiO_2	Titanium dioxide
UF	Ultrafiltration
UV/H_2O_2	Photolysis of hydrogen peroxide
$UV/S_2O_8^{2-}$	Photolysis of persulfate

List of abbreviations in alphabetic order; Greek follows Latin - continued

UV/TiO_2	Photo excitation of titanium dioxide
ΔG^0	Standard free Gibbs energy
$\varepsilon_{atrazine}$	Molar absorption coefficient of atrazine
$\varepsilon_{peroxide}$	Molar absorption of H_2O_2 or $S_2O_8^{2-}$
η_{uv}	Efficiency factor of the radiation source
λ	Wave length
$\Phi_{atrazine}$	Quantum yield of atrazine
$\Phi_{peroxide}$	Quantum yield of H_2O_2 or $S_2O_8^{2-}$

List of Publications

Book chapter

Lutze, H., Bergmann, A., Panglisch, S. and, Schmidt, T. C. (2012) „Treatment options for the removal and degradation of polyfluorinated chemicals“, The handbook of environmental chemistry, Thomas P. Knepper, Frank T. Lange, 17, S. 103-125

Oral presentations and posters

Lutze, H., Kerlin, N. and Schmidt, T.C.
Oral presentation: *Oxidation of chloride by sulfate radicals;* March 6.-8., 2013, Wasser 2013- Jahrestagung der Wasserchemischen Gesellschaft, Goslar, Germany

Lutze, H.
Oral presentation: *Ozon- und UV-basierte Prozesse der oxidativen Wasseraufbereitung;* October 16., 2013, Forum Wasseraufbereitung, Karlsruhe, Germany

Lutze, H., Bakkour, R., Kerlin, N., von Sonntag, C. and Schmidt, T.C.
Short oral presentation & poster presentation: *Influence of halogens in sulfate radical based oxidation*; May 14. - 16., 2012, Wasser 2012 - Jahrestagung der Wasserchemischen Gesellschaft, Neu-Ulm, Germany

Lutze, H., Bircher, S., von Sonntag, C. and Schmidt, T.C.
Oral presentation: *Degradation of atrazine by sulfate radical anions - Reaction rate constants and mechanistic aspects*; September 4.-7., 2011, Wissenschaftsforum Chemie, Bremen, Germany

Lutze, H., Bircher, S., von Sonntag, C. and Schmidt, T.C.

Oral presentation: *Degradation of Atrazine by Sulfate Radical Anions - Reaction Rate constants and Mechanistic aspects*; May 30. – June 1., 2011, Wasser 2011 - Jahrestagung der Wasserchemischen Gesellschaft, Norderney, Germany

Lutze, H. Peter, A., von Gunten, U., Giger, W., Kaiser, H.P., von Sonntag, C. and Schmidt, T.C.
Poster presentation: *Ozonation of Benzotriazoles*; May 30. – June 1., 2011, Wasser 2011 - Jahrestagung der Wasserchemischen Gesellschaft, Norderney, Deutschland

Lutze, H. Bircher, S., von Sonntag C. and Schmidt, T.C.
Oral presentation: *Degradation of atrazine by sulfate radical anions - Reaction rate constants and mechanistic aspects,* May 23.-25., 2011, Ozone and UV: Leading-edge science and technologies, Paris, France

Lutze, H., Peter, A., Kaiser, H.P. and von Gunten, U.
Short oral presentation & poster: *Oxidation of taste and odor compounds and bromate formation during ozonation and the advanced oxidation process O_3/H_2O_2*, May 23.-25., 2011, Ozone and UV: Leading-edge science and technologies, Paris, France

Lutze, H., Peter, A. von Gunten, U. Giger, W. Kaiser, H.P. von Sonntag, C. and Schmidt, T.C.
Short oral presentation & poster: *Ozonation of benzotriazoles*, May 23.-25., 2011, Ozone and UV: Leading-edge science and technologies, Paris, France

Lutze, H., Ebersbach, I., Kowal, S., Tatzel, A., Bakkour, R., Panglisch, S. and Schmidt, T.C.
Oral Presentation: *Radikalbasierte Oxidation in der Wasseraufbereitung – Grenzfälle innovativer Methoden*, January 12., 2011: Neujahrskolloqium der Fakultät für Chemie und des Ortsverbandes Essen-Duisburg der GDCh, Essen, Germany

Lutze, H., Ebersbach, I. and Schmidt, T.C.

Poster presentation: *Oxidation of trifluoroacetic acid and perfuorooctanoic acid by sulfate radical anions*, June 17.-19, 2010, 2nd International Workshop on Fluorinated Surfactants - New developments: Synthesis – Analysis – Fate – Regulation, Idstein, Germany

Lutze H.,Tatzel A., Ebersbach, I., Kowal S., Panglisch S., Lickes, J.P., Kraus, G. and Schmidt T.C.
Oral presentation: *Pilotierung einer neuen Trinkwasserversorgung einschließlich Ozonung,* March 11., 2010, 23. Mülheimer Wassertechnisches Seminar - Möglichkeiten und Grenzen von oxidativen Prozessen in der Wasserreinhaltung, Mülheim a.d. Ruhr, Germany

Lutze, H., Tatzel, A., Ebersbach, I. Panglisch, S., Krauss, G., Lickes, J.P. and Schmidt, T.C.
Oral presentation: *Oxidative Behandlung von Talsperrenwasser in der Trinkwasseraufbereitung – Vergleich von Vorozonung, intermediärer Ozonung und intermediärem Advanced Oxidation Process O_3/H_2O_2*, May 10.-12., 2010, Wasser 2010 - Jahrestagung der Wasserchemischen Gesellschaft, Bayreuth, Germany

Ebersbach, I., Lutze, H., and Schmidt, T.C.
Poster presentation, *Abbau von Trifluoressigsäure in Gegenwart von Sulfatradikalen*, May 10.-12., 2010, Wasser 2010 - Jahrestagung der Wasserchemischen Gesellschaft, Bayreuth, Germany

Lutze, H., Peter, A. and von Gunten, U.
Poster presentation: *Elimination of Taste and Odor Compounds and Bromate Formation during Ozonation and the AOP O_3/H_2O_2*, May 18. - 20., 2009, Wasser 2009 - Jahrestagung der Wasserchemischen Gesellschaft, Stralsund, Germany

Lutze, H., Peter, A. and von Gunten, U.
Oral presentation: *Elimination of Taste and Odor Compounds and Bromate Formation during Ozonation and the AOP O_3/H_2O_2*, March, 30. - April 2., 2009, 5th International Conference on Oxidation Technologies for Water and Wastewater Treatment, Berlin, Germany

Lutze, H., Peter, A. and von Gunten, U.
Poster presentation: *Elimination of taste and odor compounds and bromate formation during ozonation and the advanced oxidation process O_3/H_2O_2*, March 18.-20., 2009, 42. Essener Tagung, Aachen, Germany

Lutze, H., Peter, A. and von Gunten, U.
Poster presentation: *Elimination of taste and odor compounds and bromate formation during ozonation and the advanced oxidation process O_3/H_2O_2*, March, 2-4, 2009, *enviroWater*, Stellenbosch South Africa

Other publications

Lutze, H. Panglisch, S. and Schmidt, T. C. (2010): *Starke Oxidationsmittel gegen Spurenstoffe*, Umweltmagazin; Technik und Management (4/5); Wasser/Abwasser S. 33/34

Merkel, W., Lutze H. and Schmidt T. C. (2010): *Möglichkeiten und Grenzen oxidativer Verfahren in der Trinkwasseraufbereitung und Abwasserbehandlung*, Vom Wasser (2); S. 41-47

Merkel, W., Lutze H. and Schmidt, T. C. (2010): *Möglichkeiten und Grenzen oxidativer Verfahren in der Trinkwasseraufbereitung und Abwasserbehandlung*, DVGW energie | wasser-praxis (06); S. 20-25

Lutze H., Panglisch S. and Schmidt, T. C. (2011): *Möglichkeiten und Grenzen von oxidativen Aufbereitungsprozessen zur Entfernung von organischen Spurenstoffen*, DVGW energie | wasser-praxis

Lutze, H., Schmidt, T. C. and Panglisch, S. (2009): *Einsatz von oxidierenden Verfahren in Kombination mit Membranen bei der Aufbereitung von Talsperrenwasser*, IWW Journal, 32, S. 6-9

Lutze, H., Schmidt, T. C. and Panglisch, S. (2009): *Advanced Oxidation Process (AOP) – Ein effektives Werkzeug zur Elimination von Spurenstoffen*, IWW Journal, 32, S.10-11

Lutze, H., Peter, A. and von Gunten, U.(2007): *Wenn das Trinkwasser modrig riecht*, Eawag – aquatic research; Jahresbericht, S.47

Contributions in paper reviews

12 Reviews on publications for Environmental Science & Technology and Water Research

Curriculum Vitae

Der Lebenslauf ist in der Online-Version aus Gründen des Datenschutzes nicht enthalten.

Der Lebenslauf ist in der Online-Version aus Gründen des Datenschutzes nicht enthalten.

Der Lebenslauf ist in der Online-Version aus Gründen des Datenschutzes nicht enthalten.

Erklärung

Hiermit versichere ich, dass ich die vorliegende Arbeit mit dem Titel

„ Sulfate radical based oxidation in water treatment”

selbst verfasst und keine außer den angegebenen Hilfsmitteln und Quellen benutzt habe, und dass die Arbeit in dieser oder ähnlicher Form noch bei keiner anderen Universität eingereicht wurde.

Essen, im Juli 2013

Danksagung

Mein größter Dank gilt der Wasserchemischen Gesellschaft, Fachgruppe der GDCh für die großzügige Unterstützung meiner Arbeit durch das Promotionsstipendium.

Ein wesentlicher Faktor für das Gelingen dieser Arbeit war die ausgezeichnete Betreuung meines Doktorvaters Prof. Torsten Schmidt. Besonders schätze ich seine stetige Bereitschaft sowohl in fachlichen wie auch organisatorischen Dingen schnell und effektiv Hilfestellung zu leisten. Die großen Freiräume und die starke wissenschaftliche Vernetzung bot mir eine einzigartige Grundlage zur wissenschaftlichen und persönlichen Entfaltung. Es freut mich sehr zur Weiterentwicklung des Arbeitskreises „Instrumentelle Analytische Chemie“ beigetragen haben zu können.

Ganz herzlich danke ich Prof. Urs von Gunten sowohl für die Übernahme des Co-Referates als auch für die großartige Möglichkeit den Kontakt seit meiner Zeit als Masterstudent in seiner Arbeitsgruppe aufrechterhalten zu dürfen. Die Erfahrungen aus dieser Zeit haben zur Prägung meines wissenschaftlichen Vorgehens beigetragen und sind nach wie vor für mich von unschätzbarem Wert.

Mein großer Dank gilt Herrn Prof. von Sonntag, der mir sowohl als Wissenschaftler als auch als Mensch zum Vorbild geworden ist.

Wunderbar ist die freundliche und inspirierende Atmosphäre in der Arbeitsgruppe „Instrumentelle Analytische Chemie“, für die ich mich bei meinen Kollegen und Freunden herzlich bedanken möchte. Einzigartige Momente gab es sowohl im Institut als auch bei gemeinsamen Ausflügen nach „Draußen“.

Sehr viele studentische Arbeiten prägen den Inhalt dieser Dissertation. Die Arbeit mit den vielen jungen Studenten habe ich sehr genossen und ich bedanke mich ganz herzlich für ihre großartige Mithilfe.

Unvergessliche Momente durfte ich ebenfalls mit meinen Kollegen und Freunden des IWW in gemeinsamen Projekten aber auch bei gemeinschaftlichen Freizeitaktivitäten sammeln.

Ich danke meiner Familie und meinem Freunden für die großartige Unterstützung, Geduld und Toleranz. Dies ermöglichte mir meine Kraft auf die vorliegende Arbeit über die lange Zeit hinweg zu bündeln.

Es gilt mein unendlicher Dank dem wunderbaren Menschen an meiner Seite. Ohne diesen stetigen kühlen Quell von Kraft wäre ich längst im Chaos versunken.

Viele weitere Kollegen und Freunde standen mir auf meinem Weg zur Seite, die vielleicht nicht an dieser Stelle genannt werden. Ihnen möchte hiermit meine tiefste Dankbarkeit aussprechen.